Swansea University
Prifysgol Abertawe

Computational Modelling of Interactions of Marine Mammals and Tidal Stream Turbines

by

Thomas Lake

Submitted to the College of Engineering
in fulfilment of the requirements for the Degree of

Doctor of Philosophy

at

Swansea University

2017

Abstract

Marine renewable energy is a topic of growing interest in academic and commercial contexts, with a number of different devices and technologies under development and in various stages of consenting and deployment. One of the many challenges faced by this emerging industry lies in the understanding of the environment in which these devices are deployed in, both in terms of the physical environment and the local ecology.

This work presents the research, development and testing of a new Individual Based Model (IBM) framework developed to mimic the habitat usage of marine mammals in energetic tidal sites. In particular, the model has been developed with the aim of investigating the potential impacts of tidal stream turbines on harbour porpoise in coastal areas.

The model makes use of existing tidal/coastal models to define a simulation environment within which boids (objects representing the animals being simulated) can be released and their behaviour and motion tracked. This data has been taken from results of simulations carried out using the TELEMAC shallow water model, with the addition of data representing food availability and additional noise levels. Simulations using this IBM have then been carried out to examine the variation in statistical measures of the simulated population based on different sample sizes, and to examine the effect of different model parameters on simulation results.

A case study is presented based on the area around Ramsey Sound, an area where a tidal stream turbine has recently been deployed. The results presented here show a promising initial comparison of simulation outputs against observational data from the site. A final set of results show small but detectable changes in habitat use by the simulated porpoise resulting from the addition of a noise source representing a generic tidal stream device.

Declaration

This work has not previously been accepted in substance for any degree and is not being concurrently submitted in candidature for any degree.

Signed: . . . . . (candidate)

Date: . . . . . .

Statement 1

This thesis is the result of my own investigations, except where otherwise stated. Where correction services have been used, the extent and nature of the correction is clearly marked in a footnote(s).

Other sources are acknowledged by footnotes giving explicit references. A bibliography is appended.

Signed: . . . . . (candidate)

Date: . . . . . .

Statement 2

I hereby give consent for my thesis, if accepted, to be available for photocopying and for inter-library loan, and for the title and summary to be made available to outside organisations.

Signed: . . . . . (candidate)

Date: . . . . . .

Contents

Acknowledgements

I would like to acknowledge the main funding for this project, provided as part of SuperGen UK Centre for Marine Energy Research (UKCMER), which is supported by the Engineering and Physical Sciences Research Council (EPSRC) through grant EP/I027912/1.

The early stages of this project were carried out during the Low Carbon Research Institute Marine Consortium (LCRI Marine), notably in collaboration with members of the Coastal Zone and Marine Environment Studies Research Unit at Pembrokeshire College and Tidal Energy Limited. I would like to thank everyone involved for my introduction to the wildlife side of this project and for access to the sightings data used for the comparisons made in Chapter 7.

I would like to thank my supervisor, Dr Ian Masters, for his advice and support over the duration of this project as well as encouraging me to apply for the project to begin with. The earliest reference to this project landed in my inbox towards the end of my MPhys, containing the phrase “Do you have sea legs, and how interested are you in dolphins?”. This project is the result.

I would also like to thank the other members of the Marine Energy Research Group, both past and present, for their assistance. Particular thanks to Dr Croft, Dr Matt Edmunds and Merin Broudic for their specific contributions.

I also owe thanks to the various members of Swansea University Computer Society and Swansea Hackspace for the programming guidance and discussions over both my PhD and my undergraduate studies - particularly to Justin, Andy, Tim and the other regular inhabitants of Milliways (they know who they are).

To the members of Swansea University Race Engineering: You have been a terrible influence and a welcome distraction. Now get back to the workshop!

To the former occupants of the C2EC office: thank you for the poker games, socials and (possibly) more importantly the discussions and assistance at various points. My thanks to everyone, but in particular Bruce, Hannah, Enayat, Andy, Sean and Mike. And to those yet to submit - good luck!

And at last, and certainly not least, I would like to thank my parents and siblings for putting up with me burying myself in my laptop when simulations needed running and reports needed writing, and for listening to me talk (at length) about the problems, frustrations and work in general. Above all, thank you for supporting and encouraging me to get this far.

- Tom

List of Figures

List of Tables

Nomenclature

In addition to the definitions below, most terms and symbols used throughout this document will also be defined and explained in the accompanying text.

SI Units are used throughout, unless explicitly indicated otherwise. As such, distances are in metres or kilometres [m or km], speeds in metres per second [ms^{-1}].

Angles are given in either degrees - indicated with a superscript circle (e.g. 45°) or in radians (e.g. $\frac{\pi}{4}$) depending on context.

$\boldsymbol{X}$	Vector quantity X, defined in Cartesian components unless otherwise stated
X_x	Component of vector $\boldsymbol{X}$ in the x direction - equivalently X_y and X_z
X_i	The i^{th} value of $\boldsymbol{X}$ - i may be an index or time depending on context
$\bar{X}$	Average of scalar quantity X
$\bar{\boldsymbol{X}}$	Average of vector quantity X
$\hat{\boldsymbol{X}}$	Unit length vector in direction of X
$A_{a,b}$	Projected area in the a, b plane
C_d	Drag coefficient
ρ	Density
$\boldsymbol{F}$	Force (vector)
F_x	Force in the direction of the x axis
$\mathbf{P}$	A porpoise

t	Time
t_i	Timestep i
T_i	Mesh timestep
τ_i	Simulation timestep
$\boldsymbol{v}$	Velocity (vector)
v_x	Velocity in the direction of the x axis

Part I

Background

Chapter 1

Introduction

"Let's work together to make this planet earth environmentally sustainable so that our succeeding generations – children after children – will live peacefully. There is no Plan B because we do not have planet B."

UN Secretary-General Ban Ki-moon, New York, 21 September 2014

1.1 Introduction

In 1984, The World Commission on Environment and Development was established by the United Nations. The commission was appointed as an independent body to report on "environment and the global problématique" [1] for the period to the year 2000 and beyond. The 20th century saw vastly increased technological and industrial development and population growth, but also saw increasing disparity between the rich and poor of the world. This combination led to "grave predictions about the human future becoming commonplace" at the time the commission was established [1].

The commission investigated and reported on ways in which further development could take place in a sustainable manner and emphasised the global and "interlocking" nature of the problems being faced.

The commission's report, adopted by the United Nations in 1987, contains the following definition:

> "Sustainable development is development that meets the needs of the present without compromising the ability of future generations to meet their own needs. It contains within it two key concepts:
>
> - the concept of 'needs', in particular the essential needs of the world's poor, to which overriding priority should be given; and
> - the idea of limitations imposed by the state of technology and social organisation on the environment's ability to meet present and future needs"
>
> *"Our Common Future"* (Bruntland Report) *[1]*

This principle has been adopted and reaffirmed at various levels of governments since the adoption of the initial report. Sustainable development was included among the fundamental values considered to be "essential to international relations in the twenty-first century' in the Millennium Declaration [2]. It has also been recognised, however, that any development must also be carried out with a fundamental "respect for nature" [2].

1.2 Climate Change

One of the many drivers for sustainable development is the impact of climate change. Observed changes in the global climate over the last 60 years show atmospheric and oceanic warming, rising sea levels and continued shrinking of polar ice sheets and glaciers [3, 1.1]. These changes coincide with increased anthropogenic emissions of carbon dioxide and greenhouse gasses. It is "*extremely likely* that more than half of the observed increase in global average surface temperature" over this period is due to anthropogenic causes [3, 1.3.1]. The risks associated with further climate change can be reduced by (among other items) making "substantial cuts" in greenhouse gas emissions [3, 3.2]. One of the routes to lower carbon emissions is to reduce the levels of carbon dioxide emitted in the energy sector by moving to sustainable or renewable energy sources.

The UK has committed to a number of targets aimed at reducing emissions from fossil fuels over the last 30 years, either to reduce emissions associated with climate change or to improve sustainability by reducing emissions associated with other environmental problems such as acid rain. One of the first sets of targets came in 1988 with the European Economic Community Large Combustion Plant Directive, aimed at reducing sulphur and nitrogen dioxide emissions associated with acid rain [4]. In 1997 the UK signed the Kyoto Protocol to the UN Framework Convention on Climate Change [4], which committed the UK to a 12.5% reduction in greenhouse gas emissions by 2008 (relative to 1990 levels). This has been followed by various other national and international targets, with the Climate Change Act 2008 pushing this target to 50% of 1990 levels by 2050.

1.3 Renewable Energy

In an effort to encourage a move away from fossil fuel powered generation, in 1990 electricity generators in the UK had a "Non Fossil Fuel Obligation" imposed upon by the British Government of the time under the Electricity Act 1989. As originally implemented, this led to financial support for nuclear power and was later replaced with the "Renewables Obligation" - a tradeable financial incentive to invest in Renewable Energy sources.

Renewable energy can be defined as energy from sources "that are continually replenished by nature" [5]. The British Government's Department of Energy and Climate Change released the "UK Renewable Energy Roadmap" in 2011 (updated in 2012) which focused on eight main technology areas. Four of these areas are related to electricity generation: onshore and offshore wind, marine energy, and biomass. The remaining four include three alternative sources of heat (biomass, ground source heat pumps and air source heat pumps), with the final technology area being the fairly broad category of "Renewable transport" [6].

Although none of these renewable electricity technologies is a magic bullet that could meet the needs of the UK unaided, they could all contribute to reducing the amount of electricity generated from fossil fuel sources. This in turn will reduce the carbon dioxide and other greenhouse gas emissions released in order to meet the energy needs of a modern developed nation.

In addition to the drive for renewables from a sustainability standpoint, there have also been economic incentives to move away from fossil fuel powered methods of electricity generation. The early 1970s saw substantial increases in wholesale oil prices, providing an incentive to governments around the world to examine alternative sources of electrical generation. This saw an increase in research and development in various renewables technologies, including wave energy research in Edinburgh (in the form of Salter's duck device) [7] and heavy investment in the research and development of wind turbines for electricity generation.

Of current renewables technologies, wind power is the most widely used in a commercial setting. Wind power has been used to power machinery in various forms, historically using windmills to provide mechanical power to operate machinery and then, more recently, as a method of generating electricity in the form of wind turbines. Within the UK, extensive use has been made of the onshore and offshore wind resources, with wind contributing approximately 8% of the UK's electricity generation for 2013. The size of wind turbines being deployed has reached an average of 2.5MW onshore and between 3MW and 5MW for offshore devices, with 7.5GW of installed onshore wind and 3.6GW of installed offshore devices as of 2013 [8]. There is further 11GW of offshore wind consented and due to start supplying electricity to the grid by the early 2020s [9].

1.3.1 Marine Renewable Energy - power from waves and tides

Our oceans, rivers and seas offer potentially large sources of renewable energy [10] that could be harnessed in order to provide significant contributions to the electricity requirements of the UK. For the purposes of electricity generation, there are three main sources of marine renewable energy that can be exploited: tidal streams - the flow of water due to tidal motions, tidal range - the change in water height over a tidal cycle and waves - the oscillatory motion of water in both offshore and coastal areas. These categories represent the main areas of development in the UK to date, each covering a range of specific technologies and device types.

The abundance of energy available in these marine environments also provides for a number of challenges - devices must be designed in a way that allows them to be deployed, tested, operated and maintained in these energetic waters. There are also challenges to be overcome to ensure that these devices can survive in the longer term [11].

As a result of these and other factors, the marine sector is estimated to be 10 to 15 years behind wind power on the road to commercial deployments [12] - but has the potential to make more rapid progress as a result of improved technology and modelling capabilities, and the lessons learnt from the wind industry has it has grown [13].

A number of different wave energy and tidal stream devices have been deployed and tested around the UK, including a number of grid connected deployments [12, 14]. Alongside a number of independently sited and located devices (40 sites were licensed by The Crown Estate for wave and tidal devices between 2010 and 2012, although many of these sites have yet to be developed [11]), test sites were established to provide easier access to suitable wave and tidal resources for developers.

According to data from 2014, there were 10 active marine energy generating sites around the UK [8]. There were also other projects under development, including the Tidal Energy Ltd. DeltaStream^{TM} device at Ramsey Sound, Wales (400kW deployed) [15] and phase 1 of the MeyGen tidal array development in the Pentland Firth in Scotland (86MW planned) [16].

Of the three sources of marine renewable energy mentioned, it is worth noting the substantial amounts of power that tidal range schemes can generate given suitable locations

- the Hafren Power proposal for a Cardiff - Weston-Super-Mare barrage could have provided 5% of the UK's electricity supply on its own [17]. As with wave and tidal stream schemes, the environmental benefit of a tidal range project in terms of reduced carbon emissions has to be offset against the loss of (and changes to) habitats. The area affected by physical changes associated with the project is large in comparison to single wave and tidal stream devices (both in terms of the device construction, but also the area which will be subject to an altered tidal cycle and range), this in turn changes the scale of the potential impact of these projects on the environment.

1.4 Challenges, risks, and opportunities for the marine renewable energy sector

Focusing on the marine renewable energy industry, it can be seen that there are a number of obstacles that must be overcome in order to develop a commercially viable device capable of supplying electricity to the grid. Some of these challenges are related to the resource itself, such as predicting how much energy can be extracted from a given location and the conditions that a device will have to survive. Other challenges are more closely linked to the mechanics and control of the device - devices must be developed to allow for cost-effective methods of manufacture, installation, and maintenance while ensuring that the devices will still operate reliably and efficiently over their lifetime [11, 12].

1.4.1 Design, Manufacture and Development

One route to ensuring devices can meet these criteria is to enable developers to conduct trials of devices in an easier manner, without incurring the full cost of deploying an independent device. One of the first areas set up for this purpose is The European Marine Energy Centre in Orkney, Scotland which opened in August 2004 [18] and provides berths for wave and tidal energy developers to deploy full scale grid connected or independent prototype devices. The provision of a grid connection and associated infrastructure reduces the outlay required for developers to conduct device testing, and also allows developers to be paid for electricity generated and fed to the National Grid [18].

In 2014, an estimated 500 full time equivalent jobs were attributed to the growing marine renewable energy sector in Scotland, with half of that figure concentrated in Orkney

- due to the presence of EMEC. EMEC is also notable for transitioning from an organisation founded and run entirely on public funds at opening in 2003/4 to self sufficiency by 2010, contributing nearly £150m to the surrounding economy between 2003 and 2012 [11]. The development of a marine energy industry in the UK in both public and private sectors has lead to both devices and expertise being exported around the globe.

As well as providing access to testing facilities, funding has also been provided to universities to carry out generic research into marine energy, which includes the funding for this work through the SuperGen UK Centre for Marine Energy Research (UKCMER). The first aim of UKCMER is to "Conduct world-class fundamental and applied research that assists the marine energy sector to accelerate deployment and ensure growth in generating capacity through 2020 targets" [19].

1.4.2 Environmental Impacts

An area for potential conflict in the case for marine renewables concerns the interactions of any marine energy device with its environment. Any marine energy device, regardless of the specific technologies used, by definition must have an impact on its local environment - it is extracting energy. This is the fundamental function of such devices, to remove energy from a marine environment and transform it into electrical energy for further use. This has potential for environmental benefits in the form of reducing global carbon emissions as discussed above, but also has the potential for impact on the local ecology (which could be positive or negative) [20].

Coastal waters are valuable habitats, home to a large variety of species. Some of these areas are protected under law, either because of their nature (e.g. estuaries, lagoons, reefs) or because of the presence of certain species [21]. In particular, areas with known populations of marine mammals (such as seals, porpoise and dolphins) are protected habitats under the relevant legislation [21]. This conflict between the need to reduce carbon dioxide (and other pollutant) emissions as part of our electricity generation process and the need to ensure that this is done without long term negative impacts on the environment is one of the many challenges for the emerging marine renewables sector.

As a result, developers planning to deploy a device in the UK are required to consider the impact of their devices on the environment as part of the consenting process [22,23], with similar obligations applying elsewhere in the European Union [24, 25]. Typically

these reports (Environmental Impact Assessments or EIAs) are required to detail how the development will effect the local wildlife in both the short- and long-term. This is a significant part of the consenting process, typically requiring significant investment of both time and funds to complete - typically the site will be subject to surveys and observation for years prior to a device being deployed.

An Environmental Impact Assessment must contain "A description of the aspects of the environment likely to be significantly affected by the development, including, in particular, population, fauna, flora, soil, water, air, climatic factors, material assets, including the architectural and archaeological heritage, landscape and the interrelationship between the above factors" [22].

This would usually include animal observation data, with two years of observational data generally considered sufficient for long lived animal populations [26]. This data can be used to provide a baseline set of data allowing the behaviour of a population before and after device deployment to be compared. Reducing the burden of these surveys and studies on developers could be of benefit to the industry.

1.5 Project Motivations and Aims

In the context of a new and growing marine energy industry, it is clear that one of the main challenges and uncertainties involved with developing a device for deployment at sea and commercialisation can be found in the potential for environmental impacts from a device.

Equally, the industry has embraced computer modelling as a tool for both structural and material concerns as well as to investigate device deployment sites using hydrodynamic and tidal models. Computer models of a different variety could provide tools to investigate some of these environmental concerns, and possibly to predict the potential impact of these devices on a habitat [27, 28].

This project aims to develop a computational model that can be used to simulate the fine scale movement of harbour porpoise (*Phocoena phocoena*), based on individual/agent based modelling. Harbour porpoise are a protected cetacean species present in many coastal areas around the UK. They have been chosen as a species of interest for this study due to their presence within Ramsey Sound [29–31] - an area in south west

Wales that contains a licensed deployment site for a prototype tidal stream turbine and which has been the subject of a number of recent studies [32, 33]. The computer model that will be described in the remainder of this thesis aims to provide a simulated representation of the movement of these animals which could be used to investigate both potential changes to their movement and presence within an area and investigate how these changes might appear in observational data.

The model will use existing tidal data to provide a simulated environment, and combine this with representations of the food and noise within the area. This information will then be combined with a set of behaviour rules that define the interactions between a given individual and these environmental factors. The resulting group movements can then be examined and investigated.

An implementation of this computer model will then be described and some example results discussed. A set of simulations will be carried out using data based on the existing study site of Ramsey sound and presented alongside available data for the presence of porpoise in the area in order to illustrate potential uses of the model.

1.6 Thesis Layout

In order to meet the above aims and place this work in its proper context, this thesis has been split into the following chapters:

A review of available literature is given in **Chapter 2**, covering some of the known information and behaviours of harbour porpoise and methods that can and have been used to study wildlife and their behaviours. Methods of simulating this behaviour are examined, and these two items are placed in context with a brief examination of marine energy technology.

Chapter 3 provides an overview of the computational model, including the inputs required and the various processes applied before and during the simulation. A standard methodology for describing behavioural models of this type is the ODD protocol [34, 35], which is provided in **Section 3.8** and summarises the model design.

Building on these descriptions and outline, the details of the implementation of this model are discussed in **Chapter 4**. This includes the specifications for the configuration

files used, the software components that make up the model and some of the steps taken to improve the performance and efficiency of the model over the course of its creation.

Chapters 5 and 6 give results of test cases carried out using the computational model to simulate harbour porpoise movement in an example environment. The statistical response of simulations of these results to variations in simulated population size are explored in **Chapter 5**. This is followed in **Chapter 6** with an investigation into the ways the different model parameters can affect the patterns of behaviour observed in simulations.

The final set of results are presented in **Chapter 7**, and detail the simulations carried out in Ramsey Sound and comparisons to available data from the site.

This document concludes in **Chapter 8**, with a summary of results and recommendations for future work.

Chapter 2

Literature Review

"Aziraphale collected books. If he were totally honest with himself he would have to have admitted that his bookshop was simply somewhere to store them."

Terry Pratchett and Neil Gaiman - Good Omens (1990)

2.1 Introduction

In order to develop a model of animal behaviour that can be applied to marine energy projects, it is necessary to understand modelling techniques, the environment and the animals being simulated. In addition, an understanding of the current/usual methods used within the marine energy sector for site surveys and environmental assessment need to be understood if the outputs of the model are to be used alongside these existing and understood methods.

2.2 Generating power from the sea

In order to take advantage of renewable energy sources, they need to be accessible in sufficient quantity to make energy extraction viable. Fortunately, the UK has access to the best wind, wave and tidal energy resources in Europe [6], with theoretical wave and tidal resources of 69TWh/year for wave energy and 95TWh/year for tidal stream. Tidal range solutions are potentially able to provide up to 25TWh/year from lagoons and 96TWh/year from barrages [10]. These figures are not independent of each other, however, as the areas open to exploitation by these technologies overlap. In context, the annual electricity consumption for the UK stood at 317TWh (for 2013), with existing renewables providing 48.97TWh - a large proportion of which came from wind farms (23.83TWh) [36].

Figure 2.1 shows the peak flow speeds for a spring tide around the UK coast, and is reproduced from [37, 38] (which gives details regarding the methods used to generate this image and the data used). It show the number of areas around the coast of the UK and in the surrounding waters that are exposed to high tidal flows and provides an indication of the energy available for extraction using tidal stream devices. It can also be seen that the available tidal stream resource is not uniformly distributed around the coast, with distinct patches of higher resource in the Bristol Channel, North and South West Wales, Orkney and the Pentland Firth and East Anglia.

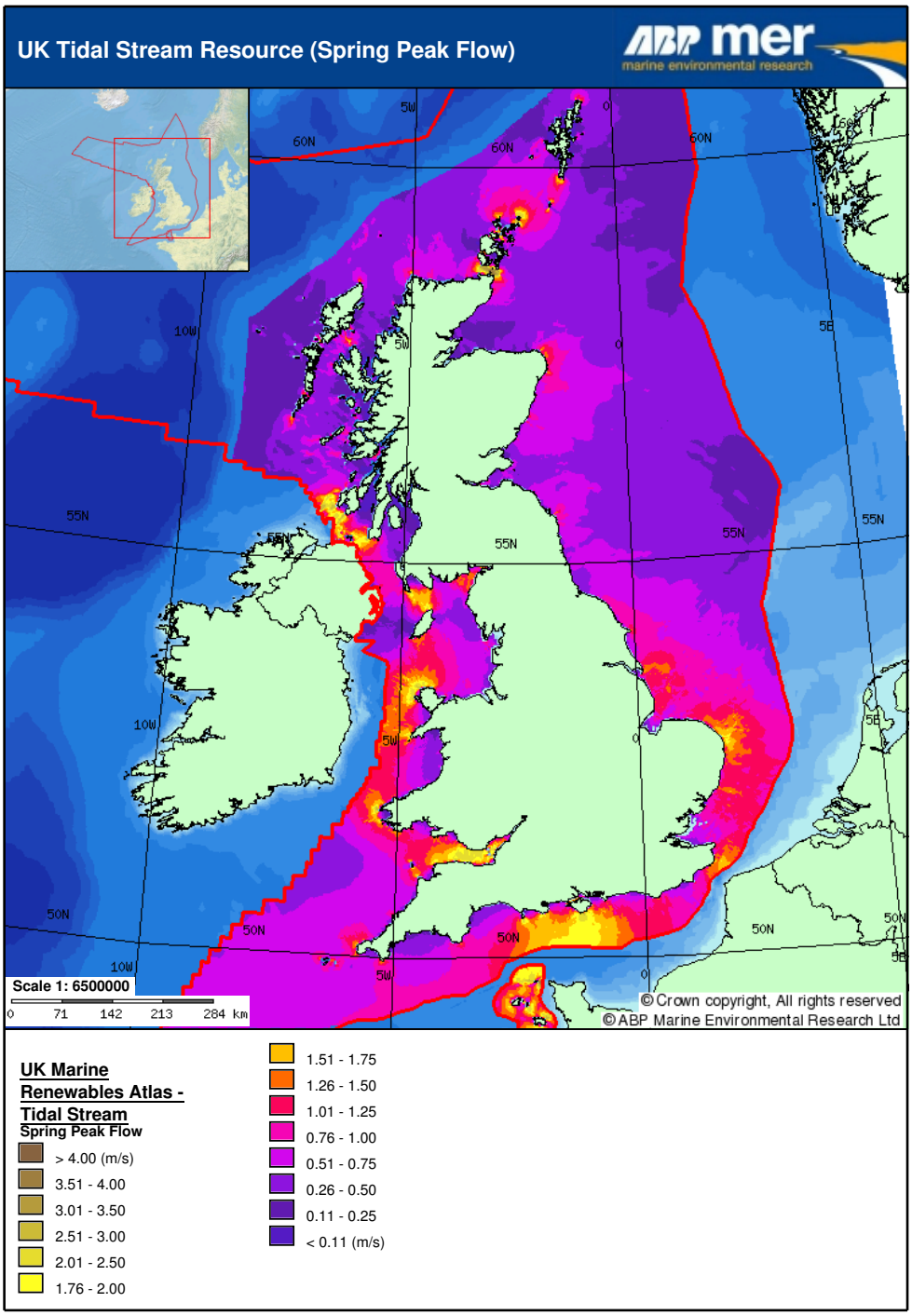

Figure 2.1: UK Tidal Stream Resource (Spring Peak Flow)

2.2.1 Energy extraction methods

Although a range of different technologies exist that are potentially able to extract energy from the seas, the three main classes of device of consideration in the UK are those that depend on wave energy, those that depend on the tidal stream and those that depend on tidal range [10]. These can be subdivided further based on device characteristics (e.g. methods of energy absorption in wave devices, the types of power conversion used or the foundations and moorings used) if required.

Wave energy devices extract energy directly or indirectly from the motion of the water surface or the motion further down the water column induced by these surface movements. Devices can use the motion of the water to move the device (or some component of the device) and extract energy from this movement (flaps, floats etc.) or use the motion to drive a working fluid to move a mechanism indirectly (e.g. an enclosed column of water driving air through a turbine [Oscillating Water Columns]) [7, 12].

Tidal range devices take advantage of the rise and fall of the tide to generate a situation where a height (head) difference exists between two volumes of water. This height difference generates a pressure difference which can be used to drive turbines. Typical examples of this would be a barrage project, where an estuary is blocked and the water held behind the barrage until a suitable height difference allows for electricity generation [8, 17]. On a smaller scale, a wall can be constructed to impound a smaller area of water rather than an entire estuary. The smaller enclosed area reduces both the potential environmental impact and the amount of power that could be generated [8, 39]

Tidal stream devices convert the kinetic energy of tidal flows into electricity, using the flow of water over and through the device to create motion that can then (directly or indirectly) drive a generator. A typical example would be horizontal axis tidal stream turbines ([27,32,40]), which utilise flow over lifting blades to drive rotation in a similar manner to wind turbines.

2.3 Analysing Animal Behaviour

In order to predict changes in the behaviour of marine mammals in the vicinity of marine energy devices, we need to understand their existing behaviours. This understanding is typically driven by observations and recordings of animal movements and behaviours. Examining the recorded behaviours that correlate with those of other individuals and the surrounding environmental condition allows factors to be identified to incorporate into behavioural models [41].

2.3.1 Data Acquisition

Recording the behaviour of animals can be a challenging task, particularly in a marine environment. Capturing behavioural data can be split into tag based methods (which require a device to be attached to the animal being studied) and tagless methods such as sonar, radar, passive acoustic monitors, photography or visual observations.

Recordings based on tagging animals can often give longer term information about the movement of an individual animal [42], but requires the live capture and release of the animals in order to fit the devices to them. Tagless methods may allow the fine scale movement and behaviour of a number of individuals in an area to be recorded, at the expense of information about the movement of any given individual over a longer period, or outside the area under observation.

Animal tagging

Tag based methods (at least in terms of electronic data logging/transmission type tags) require a device to be attached to the animal being observed, and as such are limited to animals which can have a tag fitted without harm - either by capture and release or other suitable method. Additionally, it must be possible to attach the tags securely without causing problems for the animal should the device get stuck or caught on an obstacle, or if the animal is not able to be recaptured to remove the device. The tags must also be designed to minimise the effect the tags have on the animal's behaviour - both in terms of the tag design [43] and placement [44]. Tags can be designed to upload data over GSM networks [42] or via satellite [45], or designed to record data to internal storage for processing once the tag has been recovered [46, 47].

The use of these electronic tags attached to the animals allows the movement of a specific animal to be tracked over a longer term (in some cases tracking of an individual can be maintained for 6 months [48]), and the inclusion of additional sensors can allow information about the environmental conditions surrounding the animal to be recorded [47].

It should be noted that techniques such as photo ID can provide information about an individual over a span of many years (or even decades), subject to the ability to identify a given individual between photos based on markings (either natural or artificial, e.g. bird rings). This differs from electronic tagging where data can be acquired for periods where (for logging type tags) the individual was out of sight/range of observers for a period provided the device can (eventually) be retrieved or return within range of a suitable receiver.

Passive Acoustic Monitoring

Passive acoustic monitoring is a technique which allows animals which vocalise, such as cetaceans, to be monitored and located passively. This minimises the disturbance to the animals and allows for monitoring over longer study periods. Passive acoustic monitoring involves using hydrophones to detect the vocalisations made by the animals, such as the distinctive clicks made by cetaceans such as harbour porpoise. Logging the time and amplitude of these clicks and/or the audio itself allows an animal to be located within a given radius of a particular device. Classification of detected signal as a porpoise click is often done by comparing the signal in a suitable frequency band (e.g. 115-145 kHz [49]) and the signal in one or more control bands located outside the range designated for porpoise detection, due to the narrow band of frequencies in which harbour porpoise clicks are emitted [49–51].

Monitoring can be conducted using static [50], drifting [52,53] or towed hydrophones/detectors [49]. Static moored devices have the advantage of a confined location, although care must be taken to account for the movement of the device within the range of its mooring due to local flow conditions [54]. Drifting devices will follow the currents from their deployment location, which requires measurement/recording of the position of the device during its deployment. Drifting devices are, however, easy to deploy and can cover larger areas in a relatively short time and a less susceptible to interference

from flow noise generated by water flowing over the hydrophone due to the reduced relative flow velocity [53, 54]

Visual observations

Visual observations (recordings of an animal's surface position and behaviour based on reports from trained observers) are subject to a number of limitations based on the available number of observers, weather and (for marine mammals in particular) the sea state [55]. These observations can be shore based [31] or vessel based (where "vessel" here includes vehicles of both nautical and aerial varieties [56]). Vessel based observations can be further split into surveys conducted by vessels dedicated to that task and following a predetermined survey pattern and platform of opportunity surveys making use of vessels in an area for other purposes such as ferries or tourist boats [41].

A typical visual observation method will involve scanning an area for a given period of time and noting the presence/absence of animals and a way of determining their position relative to the observation point. This would normally be recorded as a bearing and distance, with the absolute position being calculated later [30, 31]. Ideally the effect of distance on the rate at which the presence of the animals are correctly detected should also be included, but calculating this effect is not always practical [55]. This data forms an important part of many studies and, in combination with expert opinion and analysis, is accepted by regulators when examining potential impacts of a development [28, 30]

Data can also be acquired from other sources, including bycatch data from fisheries [57, 58] and strandings and rescue data from sources such as the UK Cetaceans Strandings Investigation Programme [59]. Although this data can be quite sparse, much like data obtained from opportunistic sources as mentioned above, it can provide information from areas that would otherwise be out of scope for a particular survey series.

2.3.2 Data Analysis

Once information about animal movements and distribution has been recorded, it is necessary to analyse in order to work out whether the recorded behaviour corresponds to identifiable environmental factors. There are a number of methods that can be used to identify the statistical correlation between factors and the available data, or between results from models based on combinations of factors and the original data.

This often includes showing the spatial extent of the data, either as plots showing sightings or the number of sightings in given locations [41, 49, 60], tracks [45, 61] or as a density or other derived quantity [30, 48]. Data can also be presented as a statistical analysis, giving measured and derived quantities [46, 48, 60, 62]. Many of these methods can be carried out on data generated from a simulation, allowing for comparison between simulated and real data.

Different survey methods, techniques and technologies impose different limitations on the subsequent analysis and interpretation of the information recorded. Positional data will have an uncertainty associated with it, either limited by the quality of the received signal [45] or by the conditions, survey platform and experience of the observers [55]. This uncertainty should be considered when analysing data in order to consider the reliability and limitations of the information it contains. Where animals are observed or detected from a fixed location, the range of coverage in both space and time needs to be considered [30] - this allows the results to be analysed within the context of the survey effort expended, and any variation in that effort compensated for. In previous work carried out in conjunction with colleagues at Pembrokeshire College under the Low Carbon Research Institute project [30], raw sightings data for harbour porpoise was corrected based on the hours of effort expended, accounting for overlapping periods and areas of observation from a limited number of fixed observation locations.

2.4 Harbour porpoise

Harbour porpoise, *Phocoena phocoena* (Linnaeus, 1758), are a small species of "odontocete cetaceans" [48] (toothed whales) found in coastal waters throughout much of the northern hemisphere [45, 48, 64]. They are known to inhabit regions with high tidal flows, including areas under consideration for marine renewable energy deployments [29–31, 54].

Harbour porpoise are rated as of "Least Concern" internationally in the IUCN Red List [64], although they are considered "Vulnerable" within Europe [65]. The increased European concern is related to the status of specific populations - such as the Baltic Sea region and the Mediterranean [66].

Harbour porpoise are a protected species within the European Union under the auspices

of the Habitats Directive [21], making it an offence to unduly disturb any population of harbour porpoise in the region and requiring regular reports on their conservation status to be made by EU member states. This status also places obligations on developers looking to install marine energy devices in these areas [22, 24, 25].

2.4.1 Physiology

Harbour porpoise are small cetaceans, with males ranging up to 1.5m long and females 1.6m long and typical weights up to 65kg (although a few larger examples have been found) [45, 67]. Although mammals, they spend relatively little time on the surface - one set of estimates ranges from $3 \pm 1\%$ to $7 \pm 4\%$ - and are more likely to be found diving and swimming at depth. Calves are born between May and July, depending on location, and are approximately 0.7m long at birth [45, 68, 69].

The animals are capable of covering large distances in a day ($\sim$ 50km d^{-1} [50]), and can have relatively large "home" ranges [45]. Typical swimming speeds for healthy specimens are estimated to be up to 7.5km h^{-1} ($\sim$ 2ms^{-1}) cruising speed with a burst speed between 16km h^{-1} and 22km h^{-1} (4.6ms^{-1} and 6.1ms^{-1} respectively) [45,50,70].

Despite the potentially large "home" ranges, there is also evidence for locally consistent patterns of harbour porpoise movement and behaviour observable over many years [30, 31, 45]. It is not possible to say for certainty whether or not these patterns are due to individuals remaining within an area or whether the observed patterns are due to independent individuals taking advantage of the local conditions in similar ways. In either case, it suggests that there is some underlying property of the local area that correlates with this pattern, and could be used to drive a simulation to produce similar movements.

Harbour porpoise are sensitive to noises in a wide range of frequencies, with a hearing bandwidth wider than many other animals [71–73]. An audiogram for harbour porpoise is presented in [71], which shows a peak sensitivity above the 100kHz region, with a reduced sensitivity to sounds in lower frequencies.

2.4.2 Locations and Habitat

Harbour porpoise are typically found in coastal areas around the northern hemisphere [45, 48], and are most prevalent in deeper areas within the continental shelf. They are typically found in waters less than 200m in depth [45], and are more likely to be found in areas with between 50m and 150m depth [45, 49, 74, 75]. Previous studies have found a strong avoidance for areas of shallow water [41, 49, 74, 75], although the depth specified varies between 8m [75] and 60m [74] depending on the study in question.

In addition to this, harbour porpoise have also been found to prefer areas of high vorticity [48] and areas of higher velocities [54].

2.4.3 Foraging and feeding

The movement and habitat usage of harbour porpoise is considered to be primarily motivated by the availability and movement of their various prey species [30, 48]. Harbour porpoise are known to feed on species such as herring, hake and sprat [29, 48, 69, 76]. The exact mix and species varies both seasonally and spatially depending on the presence and abundance of the different prey species available [64, 76]. These prey can be characterised as “demersal” or “pelagic” species - they can be found in deeper waters above the seabed (as opposed to shallow coastal waters or on the seabed itself) [77]. Harbour porpoise tend to ingest larger numbers of smaller individuals, and feed nearly continuously [78].

Harbour porpoise use echolocation for both navigation and feeding [49, 54, 73, 78], with the rate of echolocation clicks varying based on activity and concluding with a distinctive “buzz” when feeding [73, 78]. The echolocation frequency used lies in the 120-130kHz range [51, 71, 75], which (perhaps unsurprisingly) corresponds to their peak hearing sensitivity [71]. These clicks and buzzes can be detected using passive acoustic techniques as mentioned in subsection 2.3.1.

2.5 Individual Based Models (IBMs)

There exists a range of techniques that can be and have been used to model ecological systems, ranging from analytical equation based modelling through various simplified computer models to 'full' individual based models. Each of these methods have different strengths and weaknesses [79]. Analytical methods describe a situation with a set of equations that can be solved in order to obtain a solution for a given set of parameter values. These models (often built around differential equations) can be used to model population dynamics and energy flow through an area or population and solved either to give an equilibrium state or iteratively in order to produce a timeseries showing the change in population state over time [80]. Differential equation models can be of particular use for scenarios with a homogeneous population and environment, but may struggle to represent a situation where the environment or individuals within it are too widely varied [80].

Individual Based Models (IBMs), present a method which allows a range of behaviours and variation between individuals to be captured in a way that is difficult to express in a classical, equation based formulation. Individual Based Models, sometimes also known as Agent Based Models, simulate the actions of individual members of a population in a given environment. The individual members of the population are given a set of rules that define their behaviour, with the behaviour of each simulated individual being determined on a case by case basis based on the state of the simulated population and/or environment [80, 81].

The aggregate behaviours of individuals in this model are potentially able to provide insight into the behaviour of intelligent actors, given a suitable set of rules. The exact requirements for a model to be counted as "individual based" have been the subject of some discussion [79, 82], but a common requirement is that the model represents individuals in a countable fashion and includes some explicit representation of the underlying resources in terms of spatial or temporal distribution.

It should be noted that in the computational contexts, the term "population" is used in the statistical sense meaning "group" rather than the stricter biological definition.

For completeness, use of the word "population" can be considered to fit the following definition from the *Oxford English Dictionary*:

> A (real or hypothetical) totality of objects or individuals under consideration, of which the statistical attributes may be estimated by the study of a sample or samples drawn from it. [83]

IBMs are able to provide for a 'bottom-up' description of the situation they describe - the final, high level,results emerge from the independent, locally motivated behaviours of the the simulated individuals [84–86]. This can allow for field observations to be more closely mapped to model properties [80]. Ultimately, any model can never be a complete description of a system due to the limitations of the available data and our understanding of it. They can, however, be used as a investigative tools, examining how changes in an environment may change the patterns of behaviour observed and producing testable hypotheses based on the simplified versions of nature that they encompass [84, 87, 88]. IBMs have been used as surrogate experimental systems in this way, albeit with success limited by the input data and the constraints of the rules used [86], but are acknowledged as being "powerful tools" [79], and able to capture the properties of a more varied and heterogeneous environment than analytical approaches [79,80,82].

One of the early applications for IBMs did not arise from ecological studies, but from a computer graphics approach. The technique allowed realistic looking animations of flocks of birds to be produced, without the need to specify the precise movement of each individual in the flock [89]. This class of model has since also been used in ecological models to evaluate the interaction of animals with the environment around them [81, 90]. An individual based model contains a description or simulation of the environment, and behavioural rules and properties of the individuals being simulated, as shown in Figure 2.2.

In its simplest implementation individuals (also referred to as "agents" or "boids" [89]) use information about other the world and individuals around them to make decisions regarding their movement [80, 89]. This basic simulation can be built upon to incorporate a simulated environment and more realistic representations of senses. The boids can also be designed to react differently to stimuli depending on their current behavioural state [91], and to incorporate simple memory models to allow them to map the areas that they have visited [92]. The wide range of possible modelling approaches encompassed here presents a great deal of flexibility when considering a problem, but

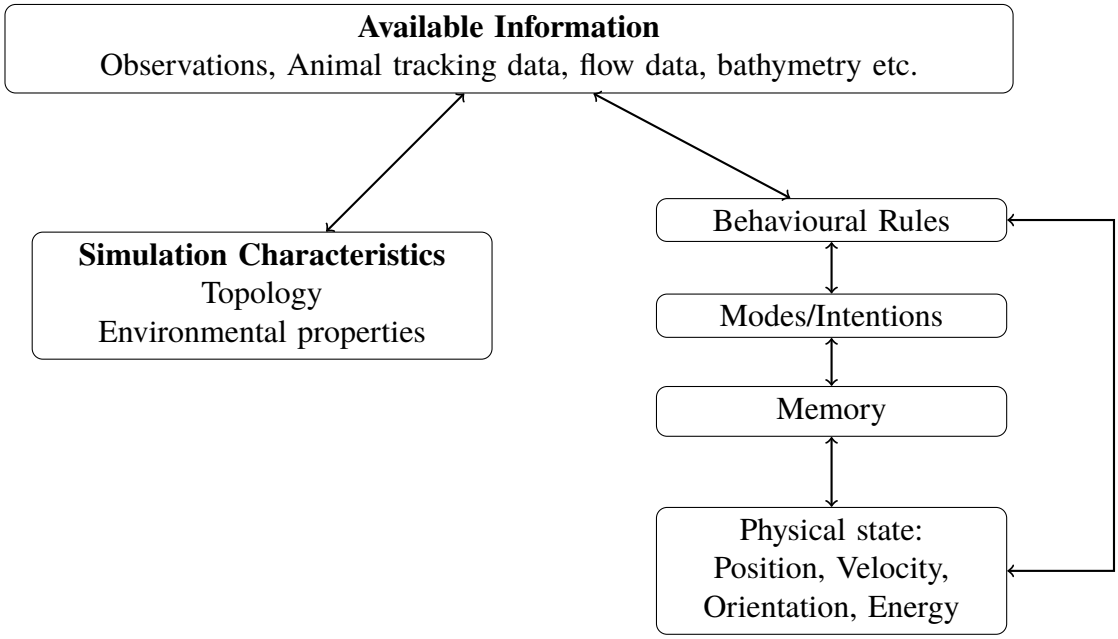

Figure 2.2: Concepts of an individual based model

presents its own difficulties - a more detailed model may produce results that more closely fit the real behaviours observed, but will have a higher computational cost. Detailed models require a greater understanding of both the animals concerned and location being simulated, both of which can be particularly challenging in a Marine environment.

2.5.1 Basic Methodology

A simple individual based model can be described as an iterative process [80, 93]:

1. For each boid in the population:
   (a) Get information (other boids, environment etc.)
   (b) Make decision about movement
   (c) Update velocity/orientation/position
2. Record positions
3. Advance simulation clock
4. Repeat from 1 for next time step

The behavioural rules defined in the model are used in step 1b to determine how each individual will move, which typically involves consulting the list of nearby boids. Realistic looking behaviour does not necessarily require a complex set of rules to be put in place. As an example, flocking behaviour of birds which "correspond[ed] to the observer's intuitive notion of what constitutes 'flock-like' motion." [89] can be generated with 3 simple rules governing each boids position, velocity and orientation relative to the rest of the simulated flock.

2.5.2 Representing boids and boid movements

Before looking in more detail at the additional features that can be incorporated into individual based models, it is necessary to consider how the boids themselves will be modelled. This has an impact on how the movement of the boids is handled.

The simplest representation of a boid is that of a point particle, followed closely by orientable point particles as in [89]. Under these representations the position of each boid is marked by a set of coordinates and orientation indicated by a vector in two or three dimensions. Alternatively, a skeletal model of the animal represented by the boid can be implemented as in [91]. This approach allows more physically realistic motion to be obtained, and allows the effect of currents on the orientation and manoeuvrability of the animal to be modelled by the boids. This also allows for detailed outputs showing the physical movement simulated by the boid, although this level of detail may be more useful in the field of computer animation [89, 91] than for ecological studies looking at the usage of a larger habitat.

The next consideration concerns the spatial movement of the boids, and is dependent on both the representation of the boid discussed above and the way in which behavioural rules are to be implemented. A simple model might use a single rule to set a velocity for the boid, which is then combined with the timestep duration to calculate the position of the boid. If the boid is being represented by a skeletal model as in [91] then it may be more appropriate to calculate the acceleration due to the forces acting on or exerted by the different portions of the boid. This also allows the orientation of the boid to be altered by external forces as well as its own intended movements. For simpler representations, these accelerations may be set directly by the behavioural rules rather than due to forces arising from changes in the shape of the boid.

In other cases the precise movement of an individual may not be considered important, and only the area of the simulation occupied by a boid needs to be recorded. The simulated environment in that instance is divided into a number of cells, with boids moving directly from cell to cell with destination cells selected by their behaviour rules as in [94]. This can reduce the complexity of the model while still capturing useful information. This assumes that the smallest significant movement is on the same order as the cell sizes, and adds constraints on the minimum timestep unless a minimum dwell time per cell is imposed on the boids via their behavioural rules. This discretisation of the simulated environment can also simplify how environmental information is represented in the simulation, which will be discussed further below. In the context of harbour porpoise, a small number of individuals are interacting with a continuously variable vector field data set (velocity) and tracking the exact position in space and time appears to be sensible.

Intentions, goals and modes

Under the simple model outlined above in Section 2.5.1 a boid will react based on the information available to it at that instant - the decisions made by a boid in any particular timestep are not directly influenced by its decisions in previous timesteps. This is the sort of decision making seen in a number of models, such as those given in [89, 95, 96]. An alternative model is to set a short term goal, or intention, that determines how the boid will react to a given set of inputs until the next event which causes that intention to change. This is implemented in the model given in [91] which assigns each boid an 'intention'. The model implemented in [92] takes a slightly different route, and has different behaviours that are chosen based on the boid's internal state.

This modification to the basic concept allows for the simulation of different individual behaviours, as well as simulating movement. For the fish boids in [91] this included avoid (collision avoidance), escape (evade predator), school (join or remain in a school), eat, mate, leave (leave current school) and wander. Each of these intentions resulted in different movements and reactions to the environment, with the current intention being stored with each boid to enable intentions to be carried over between timesteps. This allows behaviours to persist over longer time frames and allows for conditions to be defined which determine when a particular intention or mode will yield to different modes.

2.5.3 Memory models

In addition to tracking any current intentions between timesteps, boids can be constructed with an ability to memorise information. An example of this can be seen in [92], where the boids (representing moose) remembered the state of areas of the environment that they had visited and used this when deciding where to move. This was implemented in such a way that each boid only had access to the state at the time it left each of the areas, such that a boid could travel to an area and find it no longer suitable to satisfy the boid's intentions. Boid memories could be extended in any way thought suitable for a model. This might be to remember whether they have encountered another boid before, to store the location of particular features of the environment or locations where a boid has successfully fed. This may be useful if a species being modelled is thought to habitually return to certain areas.

A memory of previously visited locations was implemented in [94], allowing the boids (representing panthers) to prefer moving to familiar territory and causing them to establish home ranges. This memory of previously visited locations could be queried by other boids, allowing a boid to 'track' other boids that had recently passed its location. This could be considered analogous to tracking the scent of an individual through the environment. This model only stored a list of coordinates and the time at which they were visited, as the environment was modelled as a static set of information rather than as areas with dynamically changeable properties.

2.5.4 Environmental properties

The simulated environment in an IBM need not be a simple, homogeneous environment. The simulation can include environmental data, either generated to represent a generic environment or taken from measurements of a real site. For a real site, the available data is likely to be available in different formats and at different resolutions which will need to be reconciled. In the model implemented in [94], the environment was divided into a grid of 30m $\times$ 30m cells. Each of these cells (which they referred to as 'pixels') was assigned a value for each of a number of properties, including land cover, deer population density, road presence and human population density among other factors. Where the data was available at a lower resolution, the same value was assigned to all 30m cells within the areas defined in the lower resolution data. When

each boid in the model made a movement decision, the environmental values for each were then combined with a familiarity weighting based on the boid's memory as discussed above, with the most favourable resulting nearby cell chosen as the destination for that boid. This method is simple to implement for properties that can be represented as scalar fields (For this purpose, a text label applied to an area can be considered as a scalar). If a vector field can sensibly be averaged over a cell then these can also be applied in a similar manner.The properties associated with areas of the simulation need not be confined to descriptions of the physical environment, the local ecology can also be included this way. Food sources and fauna can also be modelled by tracking the quantity within each area, which can be used by boids as part of their decision making process. These quantities need not be static - they can be increased or reduced as appropriate based on the presence of boids as in [92], or altered over time to reflect seasonal variations. These properties can even include prey if the boids being simulated are not thought to cause migration of the prey over the simulated timescales.

2.5.5 Boid interactions

One of the features of individual based models is the ability of the models to develop emergent behaviours that can mimic flocking and schooling behaviours observed in nature. It was observed in [89] that simple rules governing the interactions between boids could give rise to 'Plausible looking' behaviours, and this concept can be used to try and mimic the observed behaviour and movement in real species. In addition to flocking and schooling type behaviours and usage patterns, mating behaviours and predator/prey interactions can be investigated, as described in [91, 94].

Interactions create additional computational demands on the model, as each of the boids in the simulation needs to check the positions of all other boids in order to determine its neighbours (Step 1a of the simple model given in subsection 2.5.1). For a simulation containing N boids, the time required for the simulation in a naive implementation scales according to N^2. This reduces to scaling linearly with N if the boids do not interact with each other. For cases where the boids interact with one another, the computational cost can be reduced by decreasing the number of boids which must be checked to calculate the interactions between neighbours. One approach to this is to split the simulated environment into a number of different areas (partitions) and maintain a list

of boids in each partition. This reduces the cost of searching for neighbours, as each boid need only consult the list of other boids in its partition (local area) in most cases. Boids that are approaching or crossing the boundary between partitions will need to consult the list of neighbouring partitions, but this can be minimised by periodically rearranging the partitions to reflect the changing distributions of boids.

Alternatively, the state and properties of the other boids in the model can be used to reduce the tracking burden. As well as the position and velocity of the target boid (for flocking and schooling behaviours), other properties such as species, gender, age or size could be used. The model used in [94] used gender as a factor to allow simulated males to track simulated females while avoiding other males, while the model detailed in [91] featured both mating behaviours based on gender and predator/prey dynamics based on the species of the simulated boids.

Any approach that allows the population to be split also permits parallelisation - computing operations on the population in parallel across multiple processors in order to reduce the total time required to complete that operation. If the population is split (partitioned) based on the influences between individuals (such as splitting by area as described above) then this parallelisation can be done without sacrificing the influence of the other individuals within the simulation. In the case of spatial partitioning of the population, the number of boids in each partition should be periodically rebalanced to minimise boids near borders and should also attempt to balance the number of boids in each partition in order to keep the processing time similar for all partitions. This partitioning process can be fulfilled by a number of different algorithms, as explored in [97], with the aim of splitting the simulated environment into an appropriate number of partitions as quickly and consistently as possible in order to minimise overheads.

2.5.6 Device representations

In order to examine the potential effects of marine energy devices such as tidal stream turbines or wave energy devices on a population, it is necessary to incorporate the effects of the device into the simulated environment. If the simulation permits free movement of boids and detailed bathymetry then it may be appropriate to include a full 3D model of the device and any support structures, and their corresponding effects on local wave climate and currents. If the simulation has been designed around a grid with

simplified environmental properties, such as in [92, 94] then the effects of the device can be incorporated into those area based properties in the appropriate locations.

The effects of a device can include both near- and far-field effects on a number of environmental properties, including noise propagating from the device and changes to upstream and downstream velocities and pressures. Changes to these properties can also cause changes to other aspects of the environment, such as transported sediment [98], which may need to be incorporated if the animals being simulated depend on these properties. This represents a computationally simpler method, but doesn't necessarily take into account the physical obstacle represented by the device, which may be particularly relevant for tidal range type devices or marine energy devices with significant support structures.

As an alternative to the above extremes, it may be possible to incorporate aspects of the two into a larger model by splitting the simulation into a number of domains. Domains further from the device(s) can be represented in the simplified, cell based representation discussed, with boids then migrating to/from a full 3D model in the vicinity of the device area. This could be considered analogous to mesh refinement in the vicinity of a solid part in CFD type simulations.

When deciding on device representations, the physical effects on the species represented by the boids should be considered and this can be used to guide the representation used. Considering the example of tidal stream turbines and adult Killer Whales, work done in [99] showed that in the unlikely event that a head on collision occurs between the whale and the turbine design discussed there is a chance of significant injury. Conversely, work investigating the effects of a turbine transit on fish shows that fish transiting a turbine disk can be subject to rapid changes in pressure which may have an effect on the swim bladder, which presents a chance for injury - likelihood and severity of which depends on the species and turbine design [100]. Initial work looking at pressure transients experienced by fish travelling through a tidal stream turbine shows that the transients are of relatively small magnitude [101].

2.6 Ramsey Sound, DeltaStream and Harbour porpoise

Ramsey Sound is a tidal channel in south west Wales that separates Ramsey Island from the mainland. The sound is approximately 3km long, and is used by a number of species - including grey seals (*Halichoerus Grypus*) [102] and harbour porpoise (*Phocoena phocoena*) [30].

The Sound is an highly energetic site with peak tidal flows up to $4ms^{-1}$ and a 5m vertical tidal range [52, 103]. The Sound features a number of distinctive bathymetric features including deep water, shallow reefs and surface piercing rock features. These features generate complex flows with significant flow asymmetry. These features are described and examined in more detail in [104] and [103], with more detailed simulation work carried out on a smaller area of the sound presented in [105]. All three of these papers identify the area as having complex variable flow features, which complicate attempts to model the area.

The DeltaStream™ device developed by Tidal Energy Ltd is licensed for a deployment in Ramsey Sound [15, 32]. The device is a 3 bladed, 12m diameter horizontal axis tidal stream turbine generating up to 400kW in flows of $2.6ms^{-1}$ [15]. The location of the device has previously been subject to study by Swansea University and other academic partners under the Low Carbon Research Institute project, largely in order to understand the tidal flow and physical conditions of the region [33, 52, 53, 103–106].

Understanding the interactions between animals and marine energy devices (in general, and not just DeltaStream in particular) is an integral part of increasing our understanding of the environmental effects that these new and emerging technologies may have [28]. The planned deployment of a tidal stream turbine, combined with the availability of existing knowledge, data and experience of the area within the Marine Energy Research Group at Swansea University provided a useful opportunity to examine animal movement models in a marine energy context. Given the spatial and temporal variability of the area, an Individual Based Model offers a method that could be used based on the existing data. Existing information about the movement of harbour porpoise and seals in the region suggested that grey seals were likely to be too individually variable to capture in a first attempt at such a model, prompting the selection of harbour porpoise as the target species for this work [30, 42, 102].

2.6.1 An existing harbour porpoise IBM

During the initial research and development phase of this project, there did not appear to be any existing IBMs for marine mammals. A selection of models had been published (as referenced above) for terrestrial mammals and fish (c.f. [81] and others listed above), but nothing directly applied to porpoise. A description of a harbour porpoise IBM published after the beginning of this project can be found in [107] and [87]. This model considered the effect of anthropogenic noise and bycatch on the harbour porpoise population. This model examined the effect of these factors on population sizes and properties over a wide area (240km x 400km) and long timescales (40 years), and examined the effect of different combinations of parameters on the resulting population. The duration of the simulation allowed the lifecycle of the animals to be investigated, and included mortality, births and distinguished between calves and adult porpoise.

The models do have some differences in terms of application as well as the simulated time scales involved. The model presented in [87] considers the movement and development of a group of porpoise over the longer term (40 years at half hour intervals), including the impact of disturbances in their environment on population size. The work presented further in this document aims to look at shorter term differences in movement that may be visible in field observations of a given site, with the simulated duration running up to 60 days with individual simulation steps at <1 minute intervals.

2.6.2 Behaviour Influences

The new harbour porpoise IBM that will be implemented and discussed in the remainder of this document will be based around a small set of environmental factors that may affect the behaviour and fine scale movement of the animals. Four factors were selected to incorporate into the model - food availability, noise, water flow and water depth. As discussed above, it is known that harbour porpoise are foraging animals that eat “almost continually” [78], while noise has been selected repeatedly as a potential environmental impact (e.g. [28, 52, 53]). Harbour porpoise are also known to have hearing range that spans a wide range of frequencies [71, 72]. The final influence of depth and flow speed were selected based on information in [41, 74, 75], with the depth constraint also being used to keep porpoise within ‘wet’ areas of the modelled environment. This is described in more detail in Chapters 3 and 4.

2.7 Summary

Marine energy is a developing industry, with a great deal of potential power that could be extracted from the waters around the British Isles. These coastal waters are also important habitats for species such as harbour porpoise and it is important to understand how these creatures behave currently and how those behaviours might be affected by the presence of marine energy devices.

Individual Based Modelling covers a wide range of complexities and possible options that could be explored, at the cost of computational time and the detailed data required to validate and run a model. The technique has seen use for ecological simulations in a range of settings, and can produce plausible looking results based on comparatively simple results. As such, a suitable IBM may be able to mimic harbour porpoise behaviour (as shown in [87]) and allow investigation of the potential impacts of a marine energy device deployment and changing environmental conditions on their habitat usage.

The design and development of such a model follows in Chapter 3, with implementation details in Chapter 4. The characteristics and results of the model are then explored in the remaining chapters.

Part II

Modelling

Chapter 3

Computational Theory and Model Development

"I checked it very thoroughly," said the computer, "and that quite definitely is the answer. I think the problem, to be quite honest with you, is that you've never actually known what the question is."

Douglas Adams - The Hitchhiker's Guide to the Galaxy (1979)

3.1 Introduction

The preceding chapters have introduced the growing need to generate electricity from renewable energy sources and the motivations behind a computational model that could be used to investigate how these new sources of energy could impact on animals in these habitats. Some of these existing models and the concepts behind their operation have been discussed in the preceding chapters, alongside some background information on both tidal stream devices and harbour porpoise.

This chapter will take the information and concepts from these sources and apply them in the context of a model for the behaviour of marine mammals in the vicinity of anthropogenic disturbances that can then be used to model the potential interactions between harbour porpoise and tidal stream turbines.

3.2 Model Aims

The aim of this project is to develop a set of tools that will allow us to investigate the movement and behaviour of harbour porpoise in a tidal environment, and to then simulate the potential impact of tidal stream turbines on that behaviour and set of movements. This movement varies naturally over time, so it will be advantageous to have a set of tools allowing the simulation of movement over a range of periods. In a typical device development scenario, hydrodynamic data for the proposed site will have been obtained, allowing for tidal models to be developed if they have not already been used to inform the device design and placement constraints. Tidal models and other site data can then be coupled with a behavioural model to investigate the response of simulated animals within the area.

3.2.1 Behaviour Modelling

In order to model the behaviour of a simulated population of animals, an Individual Based Model (IBM) will be implemented. This class of model has been used successfully across a range of fields, including computer graphics, economics, and political sciences in addition to ecological and environmental modelling [34, 81, 89, 97]. This will allow the population to be simulated as a collection of autonomous individuals, each responding to their surroundings according to a common set of behaviours but with independent freedom of movement.

3.3 Model Inputs

The model being developed here is intended to be a transient model - generating a series of results corresponding to a period of time rather than a single result at one specified time. Any such model can only ever be as accurate as the data that is used as its inputs. A 'perfect' simulation of harbour porpoise movement over a given period would require information on every possible influence on the behaviour of the individual animals. It would also require a detailed understanding of not only the individual motivations and responses of animals, but also their prey and the environment around them. To acquire data at this level of detail is, unfortunately, not an achievable goal. It should, however, be possible to generate approximate results based on factors for which data can be acquired more readily.

Rather than aiming to capture accurate simulation of any given individual, the model aims to simulate a variety of individuals in order to provide a response that, on average, matches the average behaviours observed in the wild. This is achieved by simulating a small number of influences thought to dominate the observed behaviour and adding random noise to the movement and properties of the animals to increase the variation in the simulation. Based on the information considered in Chapter 2, the model will simulate a 3D tidal environment, with representations of noise and food for the simulated animals to respond to.

The basis of the model will be a representation of the space that the simulated creatures can inhabit. Harbour porpoise are marine mammals, and spend their lives in water. Previous work (such as [41], [29] and [31]) has identified that both the tidal flow and water depth correlate with observed harbour porpoise movements, so should be included in any representation of the environment used.

Closely following the physical environment is the movement of the food supply for these animals, which is also a known factor in their movement and behaviour [30, 48]. This should include some measure of the location and size of the food sources and the variation in these factors over time. This could be also be modelled under an IBM framework, but would introduce more computational overhead and complexity into the simulation. Verifying the individual behaviours of both species and the coupling between them would also be a substantially more challenging than a single species simulation.

In addition, it will be necessary to include data on the changes that will be introduced into the environment. One such factor is additional noise, which may be both useful (in preventing animals approaching too closely), but could also cause harm if levels are high and the area cannot be avoided. This is a known effect that has been observed in other studies [72, 108], and is used in other industries to deter cetaceans and other animals from areas [71].

3.4 Defining a domain: Meshes

Physics and engineering feature many problems which, despite involving complex processes, can be represented as simple mathematical equations. These equations can often, in theory, be solved for arbitrarily complicated situations - the important words here being "in theory". In practice we often cannot create exact solutions for these equations and must make some sort of approximation - sacrificing precision in order to obtain an answer in order to obtain an answer in a timely fashion. In many engineering problems - including solid mechanics and fluid dynamics - this approximation involves splitting the problem into smaller, simpler pieces which turns the problem from a difficult, continuous equation into a set of simpler, easier to solve discrete problems [109]. For a problem being solved over a spatial area or volume, it is normally this space itself which is split into smaller pieces, with these pieces being (in the general case) 'elements' and the discretised space formed from these elements is then referred to as a 'mesh'.

In mechanics, the problems to be solved may involve physical objects which can be simplified by treating them as a collection of smaller, simpler, connected shapes. Conversely, in fluid mechanics problems it is often the fluid filled space around an object that is of interest, and this space can be split into smaller sections in a similar manner, as shown in Figure 3.1. For a particular problem, the equations of interest can be solved in a number of ways, including finite difference, finite volume and finite element methods [109]. Each has its own advantages, disadvantages and requirements - the specific details of which are outside the scope of the model developed here.

3.4.1 TELEMAC

For this work, the simulation domain has been defined by the output of TELEMAC models. TELEMAC (also known as openTELEMAC or TELEMAC-MASCARET) is a set of simulation tools initially developed by Laboratoire National D'Hydralique et Environnement and now maintained by a consortium of institutions[1]. TELEMAC uses finite element and finite volume techniques to solve hydrodynamic equations (De Saint-Venant or Navier-Stokes) and is commonly used for hydrodynamic simulations, including simulation of large, tidal areas [110].

TELEMAC represents the simulated domain using meshes formed from a limited set of linear element types: triangles and quadrilaterals in two dimensions and prisms/wedges in three dimensions, as shown in Figure 3.2. The 3D meshes used in TELEMAC are formed from layers of 2D triangular meshes, yielding the prismatic elements shown in 3.2c. This mesh can be used to define the domain within which the simulated animals can move, as well as providing the depth and fluid flow information needed to represent the tides.

Although results from TELEMAC models have been used as the primary source of data for this project, any source which can be converted to a suitable form could be used in its place.

[1] See http://www.opentelemac.org for more information about the software and the consortium

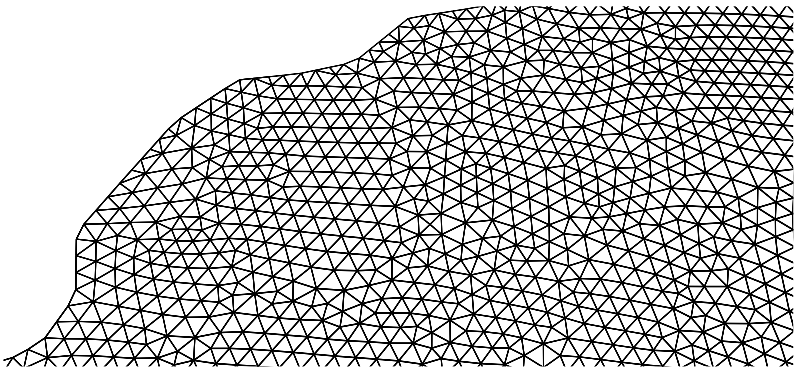

Figure 3.1: A section of mesh for a tidal model

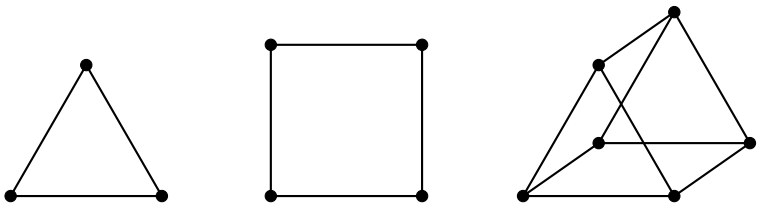

(a) Triangles **(b)** Quadrilaterals **(c)** Prisms/Wedges

Figure 3.2: Element types used in 2D and 3D TELEMAC meshes

3.5 Model Overview

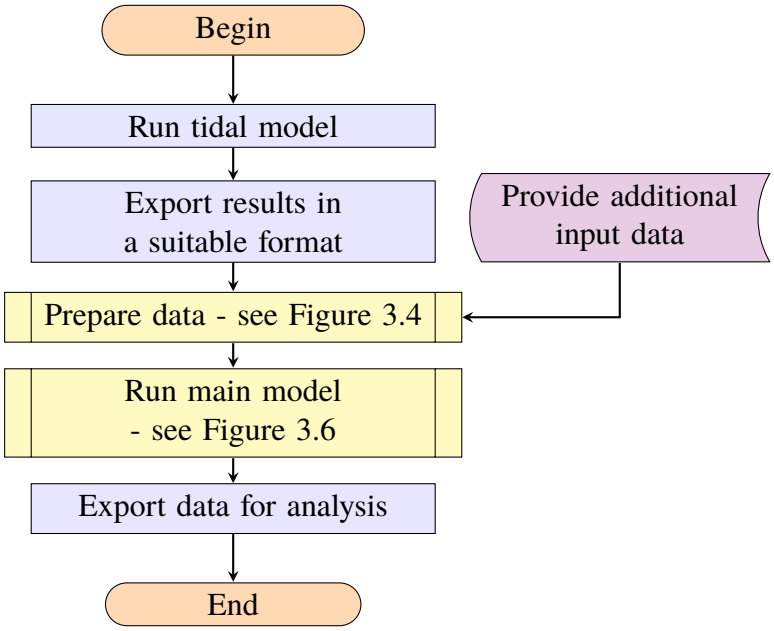

Figure 3.3: Flowchart showing use of model components

Figure 3.3 shows the different steps required to generate results from the IBM. This starts with external data from a tidal model, which must be converted into a suitable input format, and any pre-processing steps required to make the data available to the model. These are discussed further below and illustrated in Figure 3.4. The model itself can then be run, and the different processes that define the main model are shown in Figure 3.6. The generated data can then be exported for display, measurement and further analysis.

The output of TELEMAC fulfils the “tidal model” section of Figure 3.3, with tools

developed as part of this work able to export the model results into a format suitable for input into the main model.

3.6 Pre-processing: Data Preparation

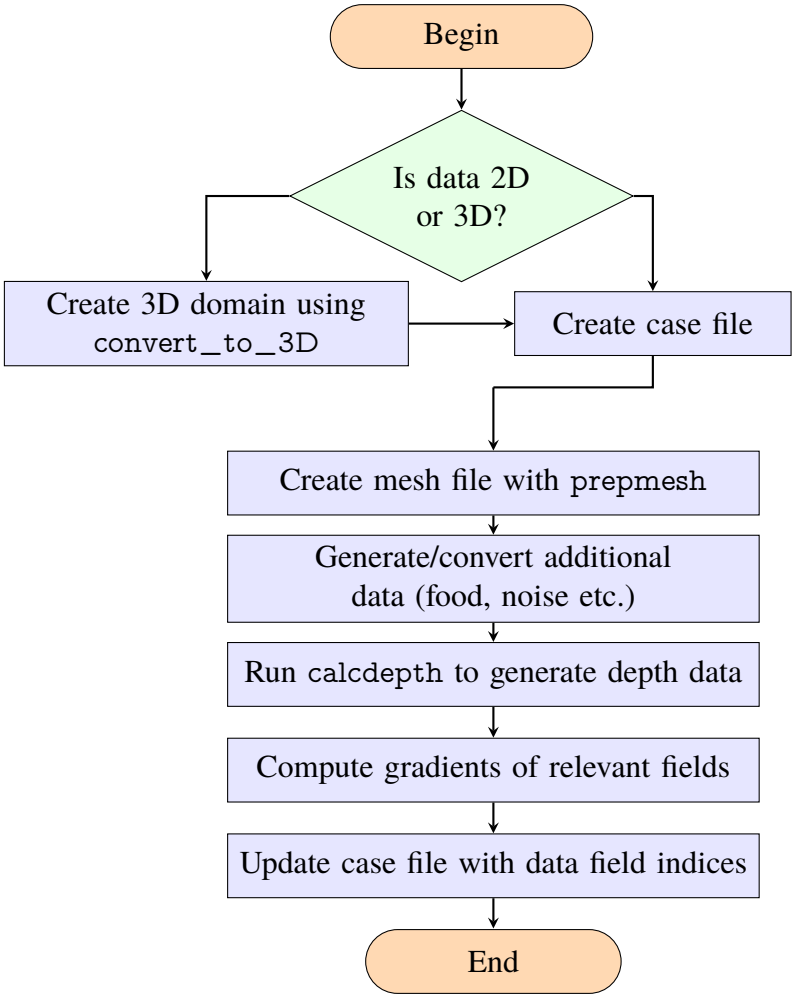

Figure 3.4: Flowchart showing data preparation steps

Before a simulation can be run, data must be collated and converted into a common format that the model can understand. The format used is defined and discussed in Appendix A. The various steps involved are shown in flowchart form in Figure 3.4. The general procedure is to convert the tidal model into a suitable (3D) format, then add additional data (representing influences on the simulated individuals) to the domain defined by the tidal model.

3.6.1 Creating a 3D domain from 2D data

In some cases, the tidal models available in an area may be 2D, depth averaged models. A 2D unstructured mesh can be converted to a 3D by duplicating the existing mesh 2 or more times, joining the layers vertically to form prisms. The height of each layer can then be set to a fraction of the water depth at each point. This yields a mesh equivalent to the native TELEMAC 3D meshes, similar to the extract shown in Figure 3.5, where the layers follow the contours of the domain bottom.

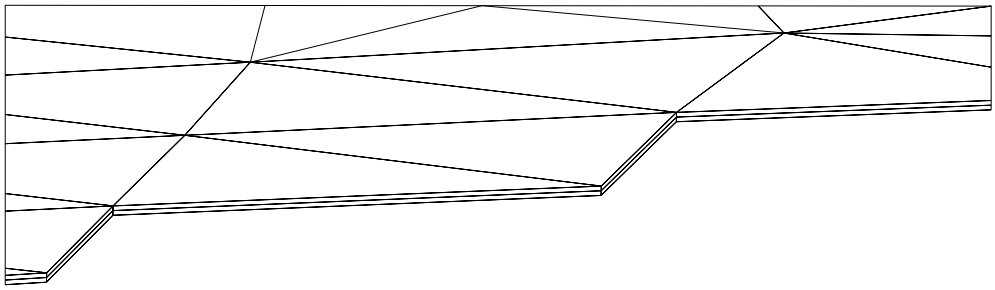

Figure 3.5: Slice through an example TELEMAC mesh, showing the prism shaped elements formed from a stacked 2D mesh

Handling the data at each point requires a little more care. In a simple case, the only variables initially available may be depth (which is used to set the z coordinates) and the 2D depth averaged velocity components, which need to be scaled according to a suitable vertical profile and distributed through the water column

A typical vertical profile used in these cases is a "$\frac{1}{7}^{th}$ power law" [111, 112], giving the velocity v at a height h as:

$$\boldsymbol{v}(h) = \bar{\boldsymbol{v}} \left(\frac{h}{z_0} \right)^{\frac{1}{7}} \tag{3.1}$$

where z_0 is a suitable reference height [112]. Given a depth averaged velocity, $\bar{\boldsymbol{v}}$, an expression for the reference height z_0 can be calculated analytically in order to yield an expression for the depth dependent velocity $\boldsymbol{v}(z)$.

If a $\frac{1}{7}^{th}$ power law is assumed, the reference height used should be just under 40% of the water depth at that point, based on the derivation on the following page.

$$\text{Let } \boldsymbol{v}(z) = \boldsymbol{v}_{ref}\left(\frac{z}{z_{ref}}\right)^{\frac{1}{7}} \tag{3.2}$$

$$\begin{aligned}
\bar{\boldsymbol{v}} &= \frac{1}{Z}\int_0^Z \boldsymbol{v}_{ref}\left(\frac{z}{z_{ref}}\right)^{\frac{1}{7}} \mathrm{d}z \\
&= \frac{\boldsymbol{v}_{ref}}{Z}\left[\frac{7z}{8}\left(\frac{z}{z_{ref}}\right)^{\frac{1}{7}}\right]_0^Z \\
&= \frac{7}{8}\,\boldsymbol{v}_{ref}\left(\frac{Z}{z_{ref}}\right)^{\frac{1}{7}}
\end{aligned}$$

$$\bar{\boldsymbol{v}}^7 = \left(\frac{7}{8}\boldsymbol{v}_{ref}\right)^7 \frac{Z}{z_{ref}} \tag{3.3}$$

$$z_{ref} = \left(\frac{7}{8}\boldsymbol{v}_{ref}\right)^7 \frac{Z}{\bar{\boldsymbol{v}}^7} \tag{3.4}$$

$$z_{ref} = Z\,\frac{7}{8}\frac{\boldsymbol{v}_{ref}}{\bar{\boldsymbol{v}}} \tag{3.5}$$

If $\boldsymbol{v}_{ref} = \boldsymbol{v}\left(z_{ref}\right)$:

$$z_{ref} = \left(\frac{7}{8}\right)^7 Z \tag{3.6}$$

This gives a final expression for $v(z)$, for depth Z and the depth averaged velocity $\bar{v}$:

$$\boldsymbol{v}(z) = \bar{\boldsymbol{v}}\left(\frac{z}{\left(\frac{7}{8}\right)^7 Z}\right)^{\frac{1}{7}} \tag{3.7}$$

This yields an appropriate vertical profile for $\boldsymbol{v}$, while retaining the flow direction. It should be noted that this approach does not introduce any vertical component into the velocities. The scaling factor applied to the water depth is calculated here analytically, but is equivalent to the "bed roughness parameter" used in hydrodynamic modelling and is in agreement with recent work in [112].

3.6.2 Representing behavioural influences

Although a tidal model provides a suitable domain in which to simulate harbour porpoise movement, it is necessary to import additional information (as mentioned in section 3.3) in order to provide stimuli against which the simulated animals can react. The three main influences that act on the simulated porpoise in this model are food availability, additional environmental noise and the water depth.

A fully realistic representation of food availability or propagation of additional noise within the domain may require extensive modelling and development, which is beyond the scope of this project. Instead, a simplified representation was implemented based on a field of values derived from independent sources which represent the food availability or additional noise[2] throughout the domain. Implementing these as precomputed variables[3] allows them to be replaced with more detailed representations should these become available.

Source Contributions

Both food and noise sources are represented using the same basic mechanism - a 'field' created from the combined effect of a number of sources. Each source is defined with a position in the x, y plane and a given strength a. The model assigns no special meaning to the value of a, allowing it to represent a quantity with arbitrary units. Defining the 2D distance between a source and a given location as:

$$d = \sqrt{\Delta x^2 + \Delta y^2} \tag{3.8}$$

with Δx and Δy representing the distance to the source in x and y respectively, the contribution of each source n to the field at a given location is then given by:

$$\phi_n = \frac{k.a}{d^b} \tag{3.9}$$

[2] Represented as sources of sound with a specified mean square pressure value
[3] For implementation details, see chapter 4

with k being an additional multiplier value specified when the field is created and b controlling how the value due to that source should decay with distance. These factors control the spatial propagation of the value due to a particular source.

As an additional effect, sources can be defined to have a particular radius, r. In this instance, the value is redefined as:

$$\phi_n = \begin{cases} \frac{k.a}{d^b} & d > r, \text{ and} \\ k.a & \text{for } d \leq r \end{cases} \tag{3.10}$$

For a field of N different sources, the value of the field at a given point can then be expressed as:

$$\Phi = \sum_{n=0}^{N} \phi_n \tag{3.11}$$

For each model, the food availability and additional noise can then be represented by defining the location, size (radius) and strength (value) of a suitable number of sources. The value of Φ can then be calculated and used when determining the behavioural response of a porpoise at a given location and time.

3.6.3 How deep is the water?

The depth of water has been shown to correlate strongly with the likelihood of observing harbour porpoise in a given location [41]. For the sake of clarity, *depth* refers to the vertical distance between the free surface and the sea bed/bottom at a given point. This can be contrasted to height or elevation derived from the underlying flow model which refers to the distance in the vertical axis (z) between a point and a given reference (datum) point, and as such can be a positive or negative quantity.

Referring back to section 3.4, recall that the domains used for this model are formed from stacked layers of a 2D unstructured mesh. The free surface is defined by the uppermost layer of the mesh and the bed by the lowermost, as defined by the z component

of the node coordinates. The difference in the z coordinates gives the water depth at that point at that time.

Symbolically, we can express the calculation of water depth, D as follows:

$$\begin{aligned} \forall\, n \in Nodes : & \\ C &= \{j : j_x = n_x \text{ and } j_y = n_y \forall\, j \in Nodes \neq n\} \\ D &= \max(j_z \;\forall\, j \in C) - \min(j_z \;\forall\, j \in C) \end{aligned}$$

Where *Nodes* contains all of the nodes forming the domain.

From this it should be noted that all vertically connected nodes will have the same value for 'depth', but will (in general) have different z coordinates.

3.6.4 Data interpolation

Using a mesh to define the model domain provides spatially (and temporally) varying values for environmental properties, but only at a finite number of discrete locations and times.

Temporal interpolation

Tidal models are able to provide much of the data required for this model, but typically only make data available at relatively coarse intervals - tens of minutes or even hours. In order to permit finer grained simulation of animal movement within the model, each of these input *mesh timesteps* (T_i) can be subdivided into a number of smaller *simulation timesteps* (τ_i). This allows motions to be calculated and represented at an appropriate timescale, but requires valid data to be present at each of these simulation timesteps. To do this, the available data from each mesh timestep can be interpolated.

Assuming the input data to be linear between timesteps, the value of some variable g can be calculated as follows:

Assume each mesh timestep is divided into f simulation timesteps:

$$m = \left\lfloor \frac{\tau_s}{f} \right\rfloor \tag{3.12}$$

$$\delta = \frac{\tau_s}{f} - \mathsf{T}_m \tag{3.13}$$

$$g_s(\tau_s) = (1-\delta) \cdot g_m(\mathsf{T}_m) + \delta \cdot g_m(\mathsf{T}_{m+1}) \tag{3.14}$$

where g_s represents the value of g in simulation time and g_m represents its values in mesh time.

Spatial Interpolation: Mean Value Coordinates

As mentioned above, the input data is discretised in space as well as time. In this case, data is stored based on node locations - i.e. the value of each variable at each node location is stored. The distance between adjacent nodes varies significantly depending on the axis - in shallow water areas the vertical (z) distances can range from zero to tens of meters, while the horizontal separation (x, y plane) can be several kilometres. For two of the meshes used in this work (detailed in Chapters 5 and 6), the horizontal node separations varied between 461m and 1683m in one case and between 6m and 5250m in the other. This level of variation reflects one of the useful properties of unstructured meshes - the ability to vary the resolution around features of interest.

In order to allow porpoise to be located at any arbitrary point within the domain, it is necessary to interpolate the data in space in addition to the temporal interpolation above.

In this model, the data is interpolated using mean value coordinates, as described in [113]. The mean value interpolant as defined in [113] yields smooth, well defined values for convex planar polygons and can be expressed in a piece-wise linear form, allowing for shapes to be defined as a series of linear edges. As the domain used is defined as a set of elements formed of planar faces, each element of the mesh can be represented as a series of edges joining the nodes of that element. The value of each variable at the nodes is then obtained using the linear temporal interpolation described above.

3.6.5 Gradients

With the exception of water velocity, all of the data mentioned so far has been composed of scalar values. In terms of behaviour, it is useful to know in which direction a porpoise should move to increase or decrease the values it experiences - for example, which direction to swim in order to place itself in an area with increased food availability. This direction could be obtained by trial and error on the part of the animal, adding additional complexity to both the implementation and another layer of complexity to the potential behaviours. This would further complicate calibration of the model, but would allow more scope for individual behaviour variation. Alternatively, the gradient of the values can be computed and used to represent the knowledge the animals would have acquired through this process.

3.7 Calculating animal movement and behaviour

Once all of the required data has been collated and prepared, the next stage is to examine the main model itself. An overview of the processes involved in the model is shown as a flowchart in Figure 3.6. After reading and verifying the initial data and set up for a given simulation, the model runs through two nested loops. The first (outer) loop iterates over the mesh timesteps ($\{\mathsf{T}\}$), with the second (inner) loop iterating over the simulation timesteps ($\{\tau\}$) within each mesh timestep.

Within each simulation timestep, the vertical positions of nodes within the mesh are updated (to account for changing water levels). The positions of the porpoise are then checked for validity and adjusted to take into account the new water levels before the behaviour and movement of each porpoise is calculated. After saving the simulation state, the model continues these iterations until all porpoise have left the domain or the end of the input data is reached.

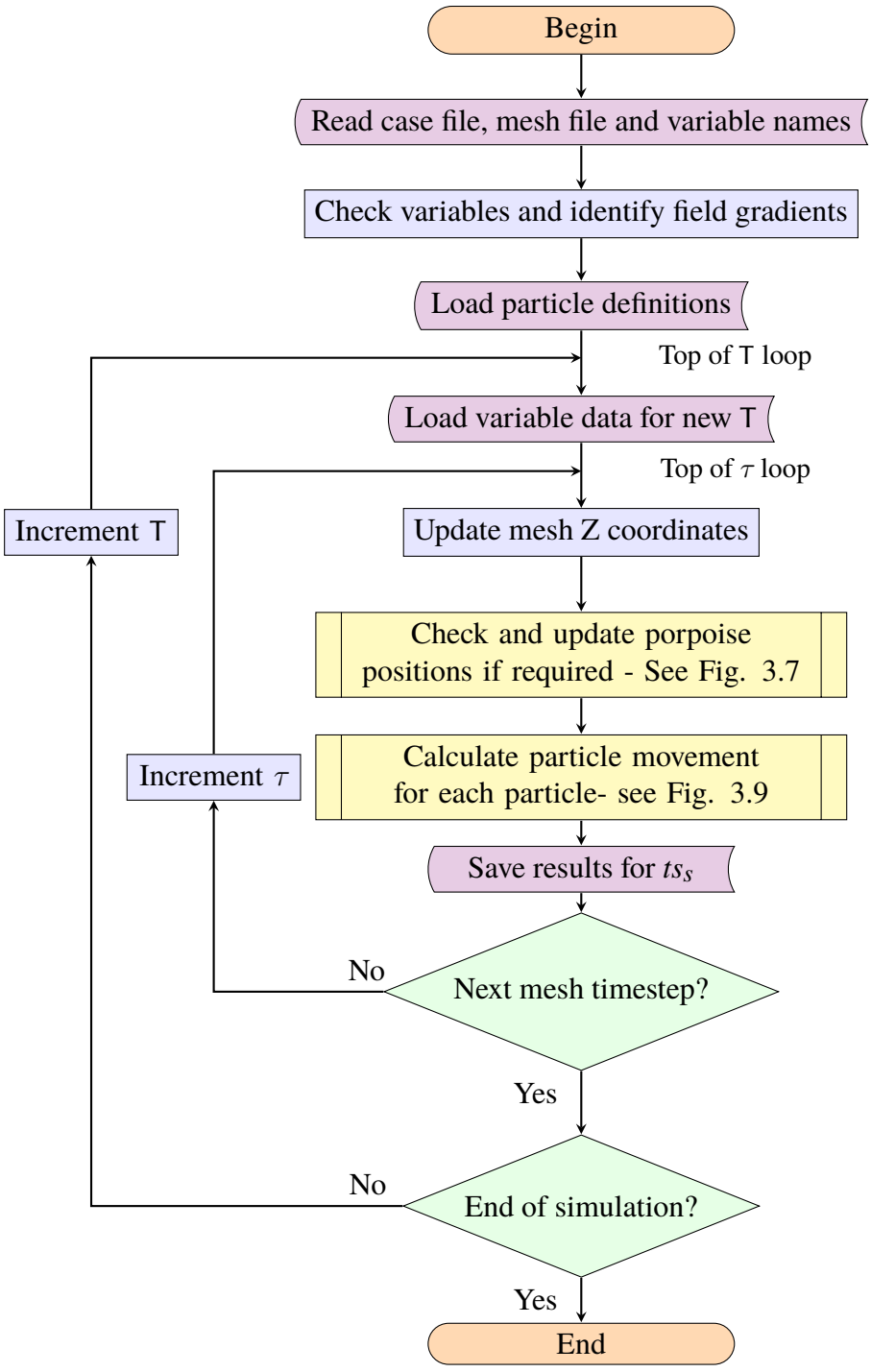

Figure 3.6: Flowchart showing the main model process

3.7.1 Time varying meshes

The mesh used in the model represents a tidal area, split into layers of elements as previously described. The mesh moves over time to represent the change in water level as the tide rises and falls - this is implemented by providing the vertical coordinates of each node as a time varying quantity that must be read in and used to update the nodes during a simulation. The x and y coordinates of nodes are fixed over time, so all motion is constrained to the vertical (z) axis.

As a consequence of this constrained motion, some elements may be reduced to zero height at various times during any given simulation - these represent areas of land which are exposed as the tide recedes. The behavioural rules implemented within the model should ensure that the simulated animals avoid these areas naturally, but care must still be taken within the simulation to handle any wayward creatures that stray on to dry land. This is done by re-validating the position of each porpoise during the simulation - a process that is already necessary in order to account for mesh movement, as described below.

The changing size and position of the elements also mean that a porpoise can move from one element to another between timesteps (typically vertically), so the position of each of the simulated animals must be checked in order to determine whether or not it remains in the domain, and to update its position and properties appropriately. The algorithm used is outlined in Figure 3.7, and either updates the last known element of the simulated animal, or marks it as having left the domain due to the movement of the mesh.

Boundary classification

When the movement of a porpoise would take the porpoise out of the domain, it is necessary to examine the type of boundary it would cross. A typical tidal model will have several external boundaries - these will be the seabed, free surface of the water in the domain and edges which either border land or open water. There may also be internal boundaries representing islands within the domain. In the absence of information in the input file, it is necessary to classify the domain boundaries to ensure that behaviour rules can be implemented to deal with them appropriately. This process is illustrated in Figure 3.8.

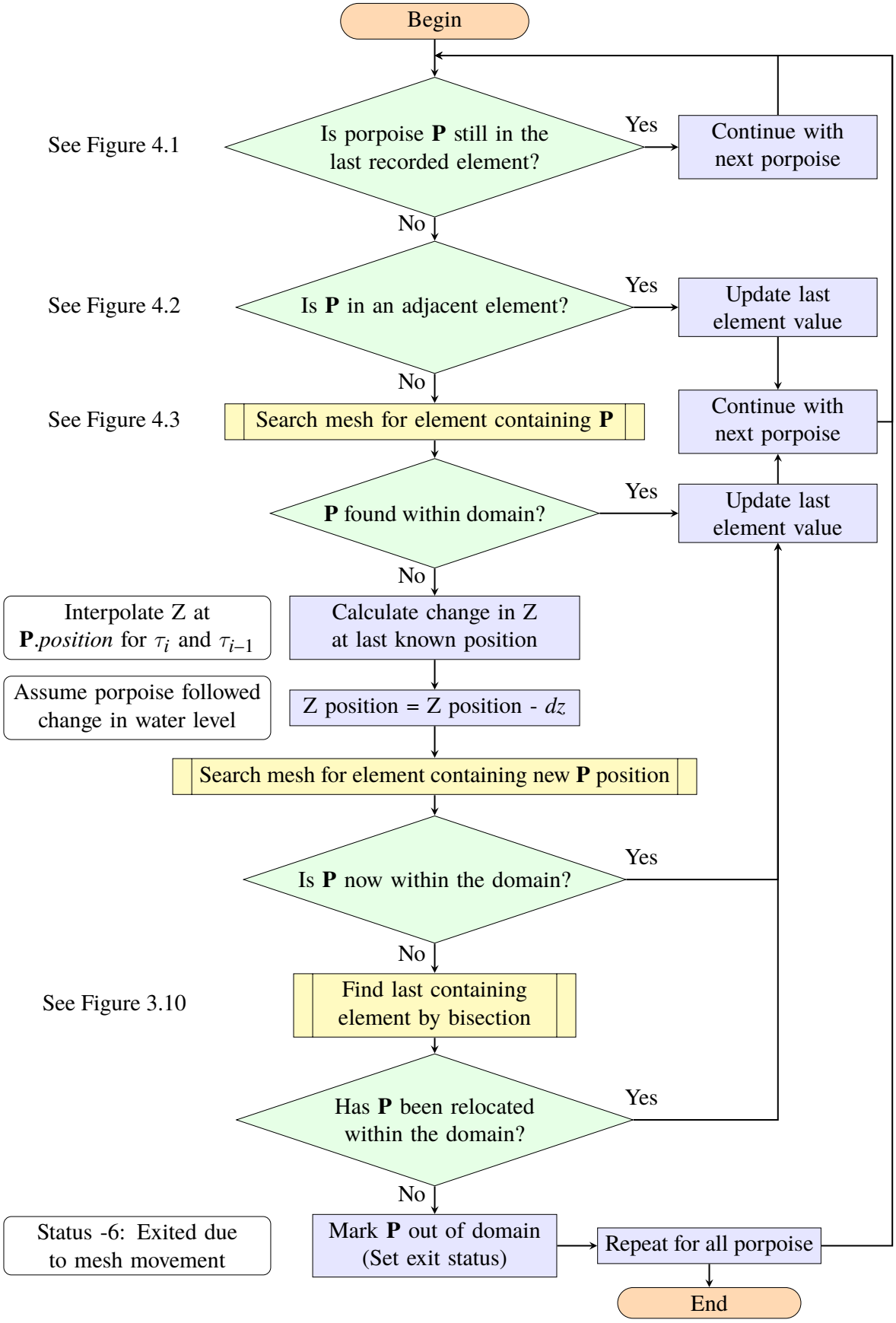

Figure 3.7: Porpoise position check and update algorithm. Used after mesh movement

The faces are classified as being vertical or horizontal based on the angle formed between the z axis and the normal vector for each face. This angle is represented by the quantity dp shown in Figure 3.8. This is calculated as:

$$dp = \hat{\boldsymbol{f_n}}.\hat{z} \tag{3.15}$$

where $\hat{\boldsymbol{f_n}}$ is the outward pointing unit normal of a given face and $\hat{z}$ is a unit normal in the z direction.

This quantity dp can be expressed equivalently as:

$$dp = \left|\hat{\boldsymbol{f_n}}\right| \left|\hat{z}\right| \cos(\theta) \tag{3.16}$$

$$= \cos(\theta) \tag{3.17}$$

From this, it can be seen that dp is equivalent to the cosine of the angle between the face normal and the z axis. The value of dp ranges between +1 (if the face normal is parallel to $\hat{z}$) and -1 (if the face normal is anti-parallel to $\hat{z}$). Threshold values of ± 0.9 are used within the code to allow for the natural skew of the surfaces - neither the sea bed or surface are perfectly flat planes in any realistic scenario. This corresponds to approximately $\pm 26^{\circ}$ allowable deviation from vertical, and lead to correct boundary classification of the meshes used.

There are four distinct boundary types used within the model, each assigned a type number:

- -1 represents an internal domain boundary (e.g. an island)
- -2 represents an external domain boundary
- -3 represents free surface boundaries
- -4 represents domain bottom/seabed boundaries

These type numbers are then used in behaviour and movement rules to handle porpoise movement throughout the simulation domain. In order to distinguish between internal and external domain walls (islands vs open sea or coastlines), all wall boundaries are initially marked as internal. The 4 corners of the domain are identified and any wall

boundary faces connected to those points are marked as external. Any wall faces connected to those faces are then inspected and marked, and so on. This ensures that any wall face that can be reached from the 4 extremes of the domain are marked as external, with internal closed loops being left marked as internal boundaries.

3.7.2 Behaviour processing

Building upon the processes described so far, a simple behaviour model can now be implemented. Based on the information available from the literature review (see Chapter 2), a model with three behaviours was implemented. These behaviours are simplified responses to the environmental parameters, and are not expected to represent the full range of behaviours that could be observed in real porpoise.

The three behaviours implemented in this model were:

- Shallow Water avoidance:
  If the depth of water available at a given location falls below a specified threshold, swim towards deeper water.
- Noise avoidance:
  If the local (additional) noise rises above a specified threshold, swim towards quieter waters.
- A "default" behaviour:
  In this mode, porpoise follow a compromise between adopting drag minimisation and swimming towards sources of food.

Each of these behaviours has an associated mean swimming velocity, which forms the centre of a normal distribution with a given standard deviation, which is also specified for each behaviour. In addition to this, the yaw angle calculated for the default behaviour is also subject to an additional random offset, with a mean offset of zero. The standard deviation for this yaw offset is also adjustable in the model.

Using shallow water avoidance as an example, the velocity $\boldsymbol{v}$ and yaw angle α can be written as follows:

$$\boldsymbol{v} = \left(N\left(v_{depth}, r_{depth}\right), 0, 0\right) \tag{3.18}$$

$$\alpha = \arctan\left(\frac{\delta depth}{\delta y}, \frac{\delta depth}{\delta x}\right) \tag{3.19}$$

with $N(\bar{a}, \sigma)$ representing a random number taken from a normal distribution with mean

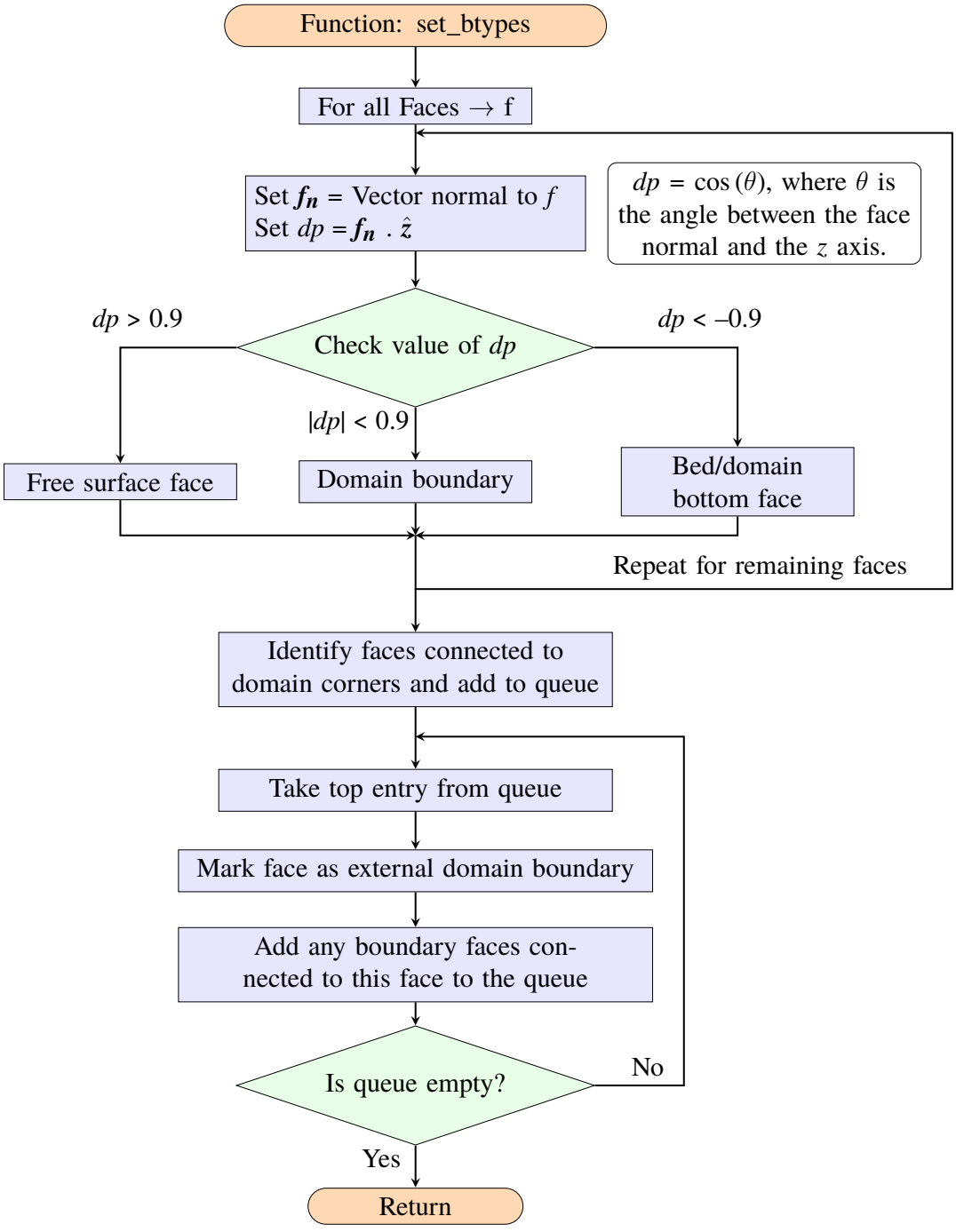

Figure 3.8: Boundary classification process

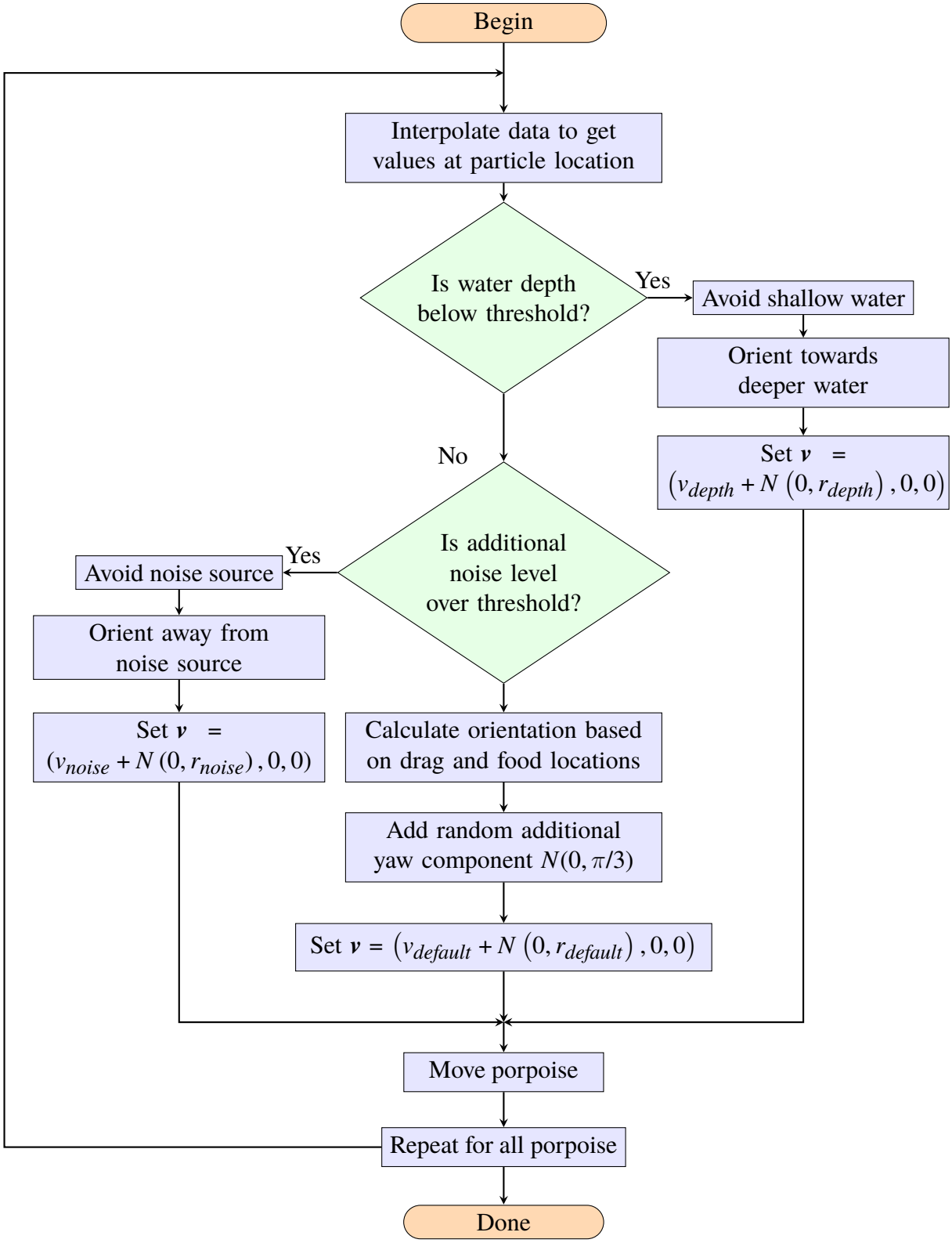

Figure 3.9: Flowchart showing details of the particle movement loop

value $\bar{a}$ and standard deviation σ, *depth* meaning the water column depth as explained in subsection 3.6.3 and v_{depth} and r_{depth} being the adjustable parameters. The expressions for noise avoidance take the same form.

The equivalent expressions for the default case take a slightly different form:

$$\boldsymbol{v} = \left(N\left(v_{default}, r_{default}\right), 0, 0\right) \tag{3.20}$$

$$\alpha = \alpha_{target} + N\left(0, r_{\alpha}\right) \tag{3.21}$$

with r_{α} being an additional adjustable parameter for the random yaw offset and α_{target} being the calculated target heading.

This target heading (α_{target}) is calculated as:

$$\boldsymbol{\xi} = \omega \cdot food \cdot \nabla\left(food\right) + \boldsymbol{\eta} \tag{3.22}$$

$$\alpha_{target} = \arctan\left(\xi_y, \xi_x\right) \tag{3.23}$$

where, $\boldsymbol{\eta}$ represents a unit vector pointing at the lowest drag orientation found by iterative search about the porpoise's current orientation, ω represents a configurable weighting parameter and *food* represents the food availability at the porpoise's current location. $\boldsymbol{\xi}$ is a temporary quantity used only as part of these calculations, then discarded. It should be noted that there is no attempt here to model the actual mechanism behind harbour porpoise hunting, and that it is acknowledged that this would be an area for future improvement.

3.7.3 Exiting the domain: Recapturing porpoise

When porpoise end up outside the domain, it is necessary to determine the type of boundary the porpoise has passed through. Boundaries are categorised as described in subsubsection 3.7.1, and each of these needs to be treated differently.

In this context, the porpoise is known to lie on a line between it's current and last known positions - bisecting this path allows the last element the porpoise passed through to be determined, and from there the type of boundary. In cases where the movement would be impossible (e.g. into the seabed) or beyond the scope of the model (leaping into the air through the free surface), the motion of the porpoise is restrained - equivalent to the

porpoise stopping short of exiting the water into mid-air or onto dry land, and making only part of its expected movement for that timestep. The bisection process is also used when the mesh positions are updated at the beginning of each simulation timestep, and returns any porpoise stranded outside their domain to an appropriate position within the (updated) domain. The process is shown in flowchart form in Figure 3.10.

3.7.4 Representing drag on simulated porpoise

In order to model the movement and behaviour of animals within the fluid domain, it is necessary to define a physical representation for the animals within the model. It can be assumed that the animals are small enough to have no significant influence on the flow of fluid through the domain. The reverse however, is not true - the hydrodynamics of an area can have very significant effects on the movement and behaviour of the animals.

Given that porpoise are not uniformly dense spheres, some approximate shape is required to allow calculation of the effect of hydrodynamic forces on the animals. It is recognised that results of this approach are, as a consequence, also approximations of the real drag forces exerted on the animals, but are expected to provide results in a suitable range to illustrate the concepts and provide a suitable behavioural input.

Each animal is modelled as a cuboid, as shown in Figure 3.11b, with three planar areas ($A_{x,y}$, $A_{x,z}$ and $A_{y,z}$) at a given position in space with a known orientation. The three areas are taken to be the projected area of a typical porpoise in top, side and front views respectively. The orientation of each animal is stored as yaw, pitch and roll angles (α, β, γ) as shown in Figure 3.11a. This allows the forces in the local frame to be calculated using the local flow velocities, resolved into three components normal to each of the areas, or in the global frame by rotating the cuboid appropriately and calculating the new effective areas. In either case, the approximate drag force is then calculated as:

$$\boldsymbol{F} = \begin{pmatrix} F_x \\ F_y \\ F_z \end{pmatrix} = \frac{1}{2}\rho \begin{pmatrix} C_{d_x} A_{y,z} v_x^2 \\ C_{d_y} A_{x,z} v_y^2 \\ C_{d_z} A_{x,y} v_z^2 \end{pmatrix} \tag{3.24}$$

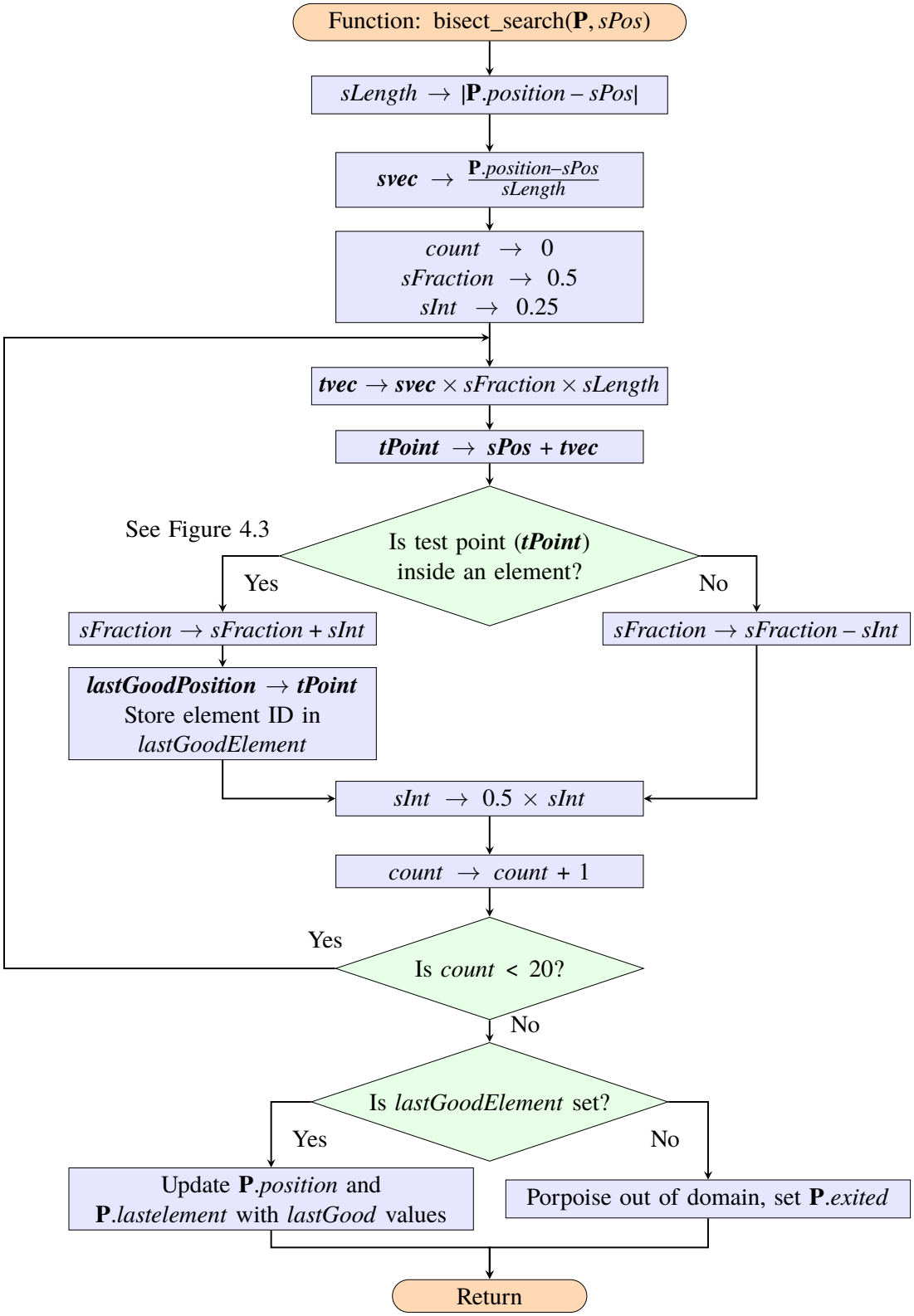

Figure 3.10: bisect_search: Determine exit location or containing element by bisection

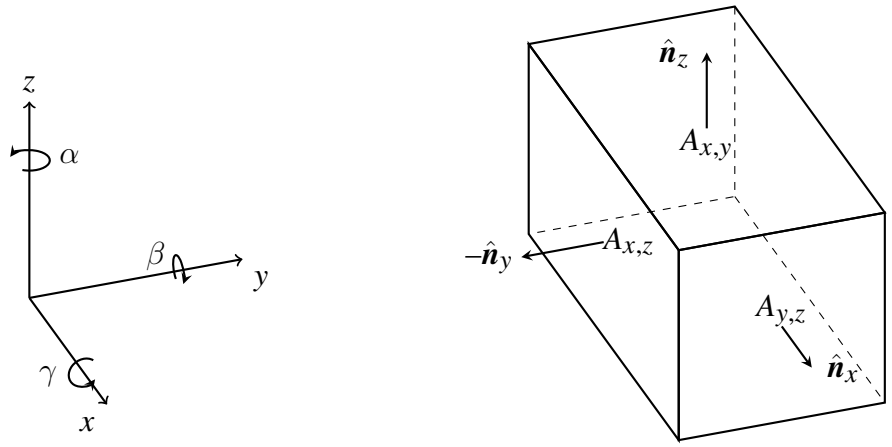

(a) Cartesian axes, with corresponding rotation angles labelled

(b) Cuboid volume with face areas and volumes labelled. Note the sign of $\hat{n}_y$

Figure 3.11: Standard reference axes and terms for general coordinates and face/area definitions for drag calculations

Where C_{d_i} are the drag coefficients applicable in each direction, $A_{i,j}$ the reference areas in the i, j plane and v_i are the velocity components in each axis.

The drag force is calculated based on the relative velocity of the porpoise to the surrounding flow and used to calculate an acceleration to be applied to the porpoise over the duration of that simulation timestep.

3.8 ODD protocol

The ODD (Overview, Design Concepts, Details) protocol is a standardised method for describing the mechanics and properties of individual/agent based models, originally described by Grimm et al. in [34] and later reviewed and revised by a subset of the original authors in [35]. IBMs can vary in many ways between different uses and implementations, one of the aims of the ODD protocol is to provide a consistent description of IBMs to aid understanding and replication. A description for this model is provided below, using the ODD protocol. Some sections replicate information provided elsewhere in this document, but are included here for completeness - in line with the recommendations in [34] and [35].

3.8.1 Overview

Purpose

The aim of the model is to simulate the fine scale movement of harbour porpoise (*Phocoena phocoena*) in tidal waters in a manner consistent with available observational data, with a view to exploring the potential impact of tidal stream turbine installation and operation on the habitat usage of these creatures. The model is deliberately simplified, and does not attempt to model energy use or the life cycle of the animals.

Entities, State variables and Scales

The model consists of two main classes of entity: porpoise and mesh components, defining the simulated individuals and the simulation environment (or domain) respectively.

The simulation domain is modelled as a finite element mesh, with the data provided by this mesh stored at the nodes. These nodes then form elements to create the fluid domain representing the tidal environment. The vertical position of the nodes varies over time, providing the variation in water depth due to tidal motion. In coastal and estuarine areas, some of the elements are reduced to zero or near-zero heights at various times throughout the simulation as a result of this motion - these represent dry areas and, as such, represent areas where porpoise should not be found at those times.

Within the model, the mesh is represented as a single main object, with properties as listed in Table 3.1, with nodes, edges, faces and elements listed in the following tables. The main mesh object refers to lists (technically, arrays) of nodes, edges, faces and elements that make up the mesh itself as well as holding other global data such as the times represented by each timestep. Within these tables, types including a number in square brackets (e.g. integer[3]) represent an array with specified length. Types specified as type[...] represent arrays of variable length, typically sized according to other properties of each object.

As implemented, faces and edges are stored in a particular orientation - typically the orientation when first constructed. This presents a problem in cases where the orientation of these items effects calculation results. To permit these objects to be reused (and information to be easily shared within the model), elements have a “mask” field

Variable	Type	Table	Description
Nodes	point[...]	3.2	Array of points (nodes)
Edges	edge[...]	3.3	Array of edges of faces
Faces	face[...]	3.4	Array of faces within mesh
Elements	element[...]	3.5	Array of elements
Dimensions	integer	-	Indicates whether mesh is 2 or 3 dimensional
NPoin	integer	-	Number of points (nodes) in mesh.nodes
NEdges	integer	-	Number of edges in mesh.edges
NFaces	integer	-	Number of faces in mesh.faces
NElem	integer	-	Number of elements in mesh.elements
Nt	integer	-	Number of timesteps defined for the mesh in mesh.times
Times	double[...]	-	Time (in seconds) represented by each timestep. Not required to start at 0.
Bounding Box	double[6]	-	Bounding box coordinates {x,y,z},{X,Y,Z} such that x < X, y < Y, z < Z

Table 3.1: Properties of the mesh object within the model

Variable	Type	Description
ID	integer	ID number
Position, $\boldsymbol{x}$	double[3]	Position vector (coordinates in x, y and z) [m]
Edge IDs	integer[...]	List of edge IDs that begin or end at this point

Table 3.2: Properties of the node objects within the model

Variable	Type	Description
ID	integer	ID number
Node IDs	integer[2]	Node IDs for each end of the edge
Face IDs	integer[...]	List of face IDs that contain this edge. Negative values represent boundaries - see subsubsection 3.7.1

Table 3.3: Properties of the edge objects within the model

Variable	Type	Description
ID	integer	ID number
NDP	integer	Number of points per face. Valid values are 3 (triangles) or 4 (quadrilaterals)
Edge IDs	integer[4]	List of edge IDs that form this face
Edge Mask	integer[4]	± 1 or 0, indicating whether edge direction needs to be reversed.
Element IDs	integer[2]	List of element IDs that are bounded by this face
Node IDs	integer[4]	List of node IDs used to create the face

Table 3.4: Properties of the face objects within the model

Variable	Type	Description
ID	integer	ID number
NFaces	integer	Number of faces forming this element. Currently the only valid value for this is 5
Face IDs	integer[...]	List of IDs for faces that form this element
Face Mask	integer[...]	± 1 or 0, indicating whether face direction needs to be reversed.
Node IDs	integer[...]	List of node IDs used to create the element
The following items are not requirements of the model		
Z-Pairs	integer[...]	For each node, this contains the ID of the node above/below it, if one exists.
Bounding Box	double[6]	Bounding box coordinates {x,y,z},{X,Y,Z} such that x < X, y < Y, z < Z
min(dZ)	double	Minimum Z-clearance between nodes

Table 3.5: Properties of the element objects within the model

which notes whether each face is used in its default orientation or whether it should be reversed (see Face Mask in Table 3.5). Similarly, each face has a corresponding mask for edges. This is important for data handling and determining which element contains porpoise at any given time, as it effects the direction of the normals used in 4.4.1.

The porpoise are represented as orientable point particles, with drag calculated on the basis of 3 mutually orthogonal reference areas and corresponding drag coefficients. Each porpoise maintains its own internal state, as described in Table 3.6. Some of the properties included in the list were added for ease of debugging and visualisation, and are not required to implement an independent version of the model.

Variable	**Symbol**	**Type**	**Description**
ID	-	integer	ID number
Position	$\boldsymbol{x}$	double[3]	Position vector (coordinates in x, y and z) [m]
Velocity	$\boldsymbol{v}$	double[3]	Velocity vector [m]
Orientation	(α, β, γ)	double[3]	Yaw, pitch and roll angles
Drag Coefficients	C_{d_i}	double[3]	Drag coefficients in x, y and z - See note
Area	A_i	double[3]	Reference areas in x, y and z - See note [m^2]
Mass	m	double	Mass of the porpoise [kg]
Transient variables - track porpoise state during simulation			
State	-	integer	Behaviour mode for current timestep
Last Element	-	integer	Face (2D) or element (3D) containing the porpoise at the end of the timestep
Exited	-	integer	Timestep that particle exited domain
Exit Status	-	integer	Records type of boundary crossed on exit
Force	$\boldsymbol{F}$	double[3]	Force (vector) acting on porpoise for current timestep
Stored for export + debugging, not required by model			
Local Velocity	-	double[3]	Local fluid velocity
Target Vector	-	double[3]	Target vector used by behaviour rule (if any)
Orientation Fuzz	-	double	Random variations added to orientation value (if any)
Velocity Fuzz	-	double	Random variations added to velocity (if any)

Note: "Area in x" refers to the reference area in the plane normal to $\hat{\boldsymbol{x}}$ - the (y, z) plane. Similarly for y - (z, x) and z - (x, y). Drag coefficients are stored in the same order

Table 3.6: Properties of a porpoise object within the model

Process Overview and Scheduling

After the initial simulation setup is complete, the model iterates through each simulation timestep. A "simulation timestep" is one of four related measures of time used within the model:

- Mesh timestep (integer, T):
  Represents the steps of the input data, and is typically much coarser than the simulation requires.
- Simulation time (double):
  A floating point number between zero and max (T). Represents simulation progress relative to the mesh timesteps.
- Simulation Timestep (integer, τ):
  Each mesh timestep is subdivided into smaller increments - typically there will be hundreds of simulation timesteps for each mesh timestep.
- Clock time (double):
  Each mesh timestep represents a specific period of real time - for some simulations this can be cast to a specific instance in time (full date/time value). The clock time allows the duration of each simulation timestep to be calculated for both simulation physics and display purposes.

All behaviours and movements are modelled on a discrete basis, calculated at each simulation timestep. The mesh movement and variation in input data is assumed to be linear in space and time, and is interpolated linearly between mesh timesteps. Spatial interpolation is carried out using mean value coordinates, discussed in subsection 3.6.4.

The model runs from the initial timestep until either the final mesh timestep or until all porpoise have left the domain, whichever occurs first.

At each simulation timestep, the following processes take place:

1. Update mesh positions
   - loading fresh data from disk if required)
2. Check porpoise locations are valid and correct as required (See Figure 3.7)

3. For each porpoise:
   (a) Interpolate mesh data to get local values
   (b) Select behaviour response
   (c) Update porpoise states
   (d) Check if porpoise has exited an element, update "last element" state as appropriate
4. Write snapshot to file
5. Loop

The steps listed under step 3 above are also shown in a flowchart in Figure 3.9

The model can also be run in a parallel mode, which splits processing across multiple threads to take advantage of multiple processors/cores available on a typical desktop machine. In this mode, operations carried out over a range of items are split into n portions, with each of n threads processing $\frac{1}{n}^{th}$ of the total load[4]. The parallel computation mode splits the mesh update step into two distinct phases: Node position updates and element bounding box updates. These phases are run in that order, and each completes before the next begins. Each thread updates a continuous range of node or elements respectively, designated by ID number. Any contiguous range of ID numbers maps to a contiguous region of system memory. A similar process happens for the porpoise, with step 3 in the above list being executed independently for each porpoise. The porpoise are distributed between threads based on ID number, which is determined by the input file ordering.

3.8.2 Design Concepts

Basic principles

Referring back to the aims given in section 3.2, this model focuses on the movement of harbour porpoise within a tidal environment and their potential response to a tidal stream device in that area. Other models exist which examine the longer term movement and behaviour of these animals, and include more details relating to their lifecycle and development (such as [87]).

[4]Not everything divides equally across the number of threads, which leaves 1 thread to process up to an additional $n - 1$ items

This model examines smaller scale movements and periods, so does not aim to replicate these aspects of the animals' life. Of the shorter list of behaviours implemented, it has been assumed that avoiding harm or injury takes precedence over resting/default behaviour. This resting/default behaviour has been implemented as a balance between minimum effort motion and swimming towards food sources.

Emergence

"What results are expected to vary in complex and perhaps unpredictable ways when particular characteristics of individuals or their environment change?" [35]

The key results emerging from the behaviour of the simulated animals will be in the patterns of habitat use and any significant change in these patterns based on the presence, absence, scaling or movement of noise and food sources. It is expected that the coupling between these factors would make predicting these patterns *a priori* significantly more challenging. Although the movement patterns of given individuals are expected to be of interest, the statistical usage of an area is likely to hold greater value for measurement and comparison purposes - both between models and between the model and observational data, such as that gathered in [30, 31].

Adaptation and objectives

No variation in behaviour priorities or threshold values is currently permitted for porpoise within a given simulation. As such, the behaviour of a porpoise at a particular location is solely governed by the instantaneous conditions at that point in space and time. The resulting motion is then a combination of that behavioural response and the physical state properties of the porpoise (e.g. orientation and velocity).

Similarly, the simulated animals have no concept of a long term objective, and act entirely based on their current behaviour mode and respond based on the instantaneous local conditions.

Learning and prediction

In the current implementation of the model, the animals do not directly learn from past history or attempt to predict future conditions. These are both options for future expansion, and would allow the "default" behaviour mode to be improved.

Sensing

The model implementation exposes the local interpolated value of all variables associated with the mesh to the animals. Under the current implementation, the local water velocity is used along with water depth, noise level, food availability and the associated gradients of these variables[5]. The noise and food values are time varying quantities, based on the distance to the respective sources, and will tend to zero over sufficient distances, dependent on the values and weightings used. There is no explicit distance cap imposed on the position of each animal relative to any individual source of food or noise.

The implementation of food did not attempt to mimic any particular biological mechanism for detection. It could be argued that the implementation of food within the model (specifically the gradient of the field) represents a combination of sensed information and memory, but this is not explored or refined further. This is another area where the model could be improved in future works.

Interaction

Each individual represented within the model is assumed to represent approximately 1 real individual. Based on data available in [30] and [31] for the Ramsey Sound area and [50] for Baltic waters, this is the most frequent group size during observational surveys. As the breeding and development of these animals is not included within the model there was no obvious requirement for explicitly modelling interactions between individuals. On this basis, it was neglected to improve computational performance.

[5]Gradients were precomputed and treated as separate variables to improve computation times

Stochasticity

Although no specific events or processes are modelled as entirely random in their nature, there are stochastic elements used within the model. The velocity magnitude of each animal at each timestep has a random offset applied taken from a pseudo-random number generator with a Gaussian distribution with a mean value of 0 and a standard deviation of $\pm 1 \text{ms}^{-1}$ in the noise avoidance and shallow water avoidance cases and $\pm 0.5 \text{ms}^{-1}$ in the default case. The default behaviour also includes a random heading offset which is taken from a Gaussian distribution with a mean of 0 and a standard deviation of $\frac{\pi}{3}$.

Collectives

Collectives of individuals form spontaneously within the model, based on the hydrodynamics and environmental conditions present leading to areas of preferred habitat. These collectives are entirely emergent in nature, and play no part in the modelled behaviour. As mentioned above, the interactions between individuals are neglected, so there is no benefit or detriment to any given individual for their position relative to any clusters or collectives that form. Results presented below will show examples of collectives that form in different circumstances, along with preferred travel routes between locations. The formation of these structures may be of interest when investigating individual locations, but can also be an artefact of the input data and require careful evaluation on that basis.

Observation

The model supports two levels of data export - a full format which includes the full internal state (described in Table 3.6) of every porpoise at each timestep and a reduced mode which outputs position, state, and exit time and status (if applicable). Either format can be used for further analysis, depending on the variables of interest. Analysis methods and measurements used are discussed further below, but include an effort normalised grid analysis that is similar to methods used in [30] which is presented and discussed in Chapter 7.

3.8.3 Details

Initialisation and Input

The initial state of the world is determined by the first timestep of the imported mesh - the state of the tide and extent of the domain are defined as part of the TELEMAC simulation and are not subject to control by this model. The initial state of the porpoise is read from a separate file, which defines the overall properties of the population and any individual variations. Typically these files define a generic porpoise at the origin as the default state, then set the position of each porpoise in the simulation according to a desired distribution. Other properties of each porpoise could also be varied in this file, although that has not been done for results presented here.

The simulation domain is updated at each mesh timestep according to the next set of input files, with all input variables able to vary over time.

The file formats and naming conventions are detailed in Appendix A.

Submodels

Three behaviour modes are implemented in this model, with each selected based on the instantaneous conditions around the porpoise at that point in the simulation. The three behaviours are shallow water avoidance, noise avoidance and a "default" behaviour.

The shallow water and noise avoidance behaviours use the depth and additional noise fields and are triggered based on threshold values (depth less than threshold and additional noise above a given threshold respectively). In each instance the porpoise yaw to face deeper or quieter water and then swim in that direction. The speed is modulated by a random offset as described above, with the mean speed and standard deviation of the noise being configurable parameters as described above.

The default behaviour in deep enough and quiet enough waters is a balance between swimming effort and food seeking. This is modelled based on a weighted average of the best orientation for low drag and the nearest available food sources. The weighting is controlled by the strength of the food availability field supplied as input and a configurable weighting factor, which is discussed further in chapter 6. The swimming speed is modulated as above, with the heading modulated with an additional noise component.

3.9 Summary

This chapter has examined the aims of the model, the inputs required and has introduced and discussed many of the underpinning concepts required to develop the model. The model has also been described using the standardised ODD protocol, providing a general overview of the representations and behaviours used. The following chapter will detail how these principles have been implemented to form a suite of software responsible for preprocessing, running, exporting and analysing the results produced by the model.

Chapter 4

Model Implementation

"Why? What do you mean, Why?
Because racecar.
That's why. "

Matt Brown - Racecar: Searching for the Limit in Formula SAE (2011)

4.1 Introduction

Previous chapters have introduced the theoretical basis and justifications behind the model, as well as some of the limitations and considerations required to develop the model into a practical solution. This chapter will introduce the software components produced to implement the model, as well as illustrating their usage and the general processes required to run a simulation.

4.2 Components

The software implementation of this model has largely been written in C, with some Python scripts and modules and a small number of supplementary scripts written for use with Bash. The C code used has been compiled and tested using various versions of GCC (up to 5.3.1), and has been written to C99 standards [1].

The software makes use of the following third party components:

- inih - © 2009 Brush Technology
  `http://code.google.com/p/inih/`
  Used to read input files in INI format [New BSD license]
- libxml2 - from the GNOME project
  `http://www.xmlsoft.org`
  Used by post-processors to write VTK compatible files [MIT licensed]
- libb64 - Chris Venter
  Base64 Encoding/Decoding routines required to write VTK format outputs [Public Domain]
- zlib - © 1995-2013 Jean-loup Gailly and Mark Adler
  `http://www.zlib.net/`
  Used to (optionally) compress some output files

Copies of the required code for inih and libb64 are included verbatim with the software, while libxml2 and zlib must be obtained and installed separately.

[1] Although code can be compiled with the `-std=c99` option to gcc, it has mainly been compiled and tested using `-std=gnu99`

For the purposes of this chapter a "component" of this implementation is any generalised executable or script. Libraries, shared code and most debugging and utility scripts are not discussed here. The components can be split into 4 broad groups: Preprocessing tools, the main model, and the post-processing and analysis tools.

There are various file formats used by the different components of this project, some of which will be discussed in the text below. Appendix A contains the full details of all input and output formats used by the model.

4.2.1 Case files

The vast majority of the components described below use a common settings file to ensure consistent transfer and treatment of data. This file defines the input and output paths, assigns meaning to different variables and sets the values of various simulation parameters. These files are plain text (ASCII) files, using the INI format. An excerpt from one of these files is shown below:

```
[paths]
basename = /home/tom/NorthSea/processed/r3snsNk001Cor.slf
output = /home/tom/NorthSea/outputs/
particles = /home/tom/NorthSea/NSPorp1.txt

[settings]
dimensions = 3
particle_steps = 800

[indexes]
fish = 8
```

The file is split into several sections, delimited by a section name enclosed in square brackets, e.g. `[paths]`. Within each section, parameters are specified in the format `name = value`. Parameters names are only recognised and interpreted when present in the correct section of the file. Valid sections, parameter names and their meanings are listed in Table 4.1. Values listed as "float" or "integer" should be positive, and variable numbers should match those listed in the corresponding `basename.vars.txt` file or the output of `varinfo`.

Name	Values	Meaning
Section: paths		
basename	string	Path and prefix for input files, typically generated with `telemac-parse`
particles	string	Path to porpoise definition file
output	string	Path to output folder
Section: settings		
dimensions	2, 3	Define a 2D or 3D simulation
particle_steps	integer	Number of simulation timesteps per mesh timestep
prefix	string	Gradient variable prefix - for auto-detection of pre-computed gradients
threshold	float	Minimum acceptable depth
noise_threshold	float	Maximum acceptable additional noise threshold
food_weight	float	Weighting applied for food weighting
longoutput	true, false	Specify long/full output format. Defaults to false
foodrule	0, 1	Specify food rule variant. Defaults to 0
Section: indexes		
z	variable	Variable number for Z coordinates
u	variable	Variable number for velocity component in x
v	variable	Variable number for velocity component in y
w	variable	Variable number for velocity component in z
noise	variable	Variable number for additional environmental noise
fish	variable	Variable number for food availability data
depth	variable	Variable number for precomputed depth data
Section: scaling		
fish	float, float[3]	Scaling value for food availability gradient. Either a single value or a vector of scaling factors for each Cartesian component
Section: speeds		
default	float	Default mean swimming speed, in ms^{-1}
defaultrange	float	Standard deviation of noise applied to default speed
ydamping	float	Y velocity damping factor
noise	float	Mean swimming speed for noise avoidance behaviour
noiserange	float	Standard deviation of noise applied during noise avoidance
depth	float	Mean swimming speed for shallow water avoidance behaviour
depthrange	float	Standard deviation of noise applied during shallow water avoidance

Table 4.1: Simulation case file parameter descriptions

4.2.2 Pre-processing

The pre-processing tools are responsible for converting and preparing input data for use with the main model. Not all of the components in this section are required in all cases.

telemac-parse (Part of tawe-telemac-utils)

`telemac-parse` is responsible for converting 2D or 3D TELEMAC data into the flat file formats used by this software. `telemac-parse` is part of a set of related utilities that have been made publicly available as `tawe-telemac-utils` on GitHub[2]. The folder of files produced by `telemac-parse` are prefixed with the name of the input TELEMAC file, and this path and prefix become the `basename` property of a simulation case file. The format and naming convention for these files is given in section A.1 of Appendix A.

Importing a 2D mesh: `convert_to_3D`

When a 2D TELEMAC mesh is used as input, it is necessary to "upgrade" the mesh to 3D based on the depth averaged velocity and water depth. This is done using `convert_to_3D`, which stacks a 2D triangular mesh to form a number of depth conforming layers of prismatic elements. The 2D depth averaged velocity components u and v are scaled to provide a vertical profile fitting a $\frac{1}{7}^{\text{th}}$ power law with no vertical motion.

Cached mesh data

In order to improve performance of the model, the mesh connectivity and generated data structures are stored on disk for access by the various other processes. This file is generated by the `prepmesh` utility, which must be run before any tools other than initial data import (such as `telemac-parse` and `convert_to_3D`).

Precomputing water depth: `calcdepth`

In order to improve the run-time performance of the model, the water depth at each point in the domain is calculated and stored as an additional variable. This removes the need to traverse the mesh at each timestep to calculate the depth when determining which behaviour rule to follow. Some input data may include a suitable variable already, or as a consequence of being converted to 3D using `convert_to_3D` - in these cases there is no need to calculate another separate depth value.

[2] https://github.com/tswsl1989/tawe-telemac-utils

In all cases, the variable number corresponding to the calculated or imported depth need to be supplied in the simulation case file.

Adding new information

In order for the animals within the model to react to food availability and additional noise, it is necessary to add that information to the simulation. There are currently three tools provided to create additional variables based on discrete sources and a spatially varying strength. The fields are calculated based on the equations and explanation given in Section 3.6.2. The variation with 2D distance d is referred to below, but the preceding chapter should be referred to for more detail.

- `datafill.py`
  `datafill.py` can produce a new variable based on either random values at each node or as the sum of the effect of discrete point sources. The value of the field around each point source is constant at all depths (no vertical variation) and proportional to $\frac{1}{d}$. The point sources are defined by a value and their Cartesian coordinates.

- `lldataconvert.py`
  As with `datafill.py`, `lldataconvert.py` produces a variable that is the sum of a number of discrete point sources. It differs slightly in that the input points can also be specified using latitude, longitude and a strength value. The lat,lon position is converted to Universal Transverse Mercator coordinates, then the combined effect of each point source at each node is calculated. The value of each point source is proportional to $\frac{1}{d^b}$, where b is variable.

  Both of these python scripts produce static fields with respect to time - the position and strength of the defined sources cannot vary over time.

- `fielddata`
  Unlike the other two options, `fielddata` is able to produce time varying fields. A series of files containing positions and values need to be prepared, with one file for each mesh timestep. These files are then used to calculate the value of the field at each node at each mesh timestep. The field strength at each point is proportional to $\frac{k}{d^b}$, with k being an additional multiplier value specified when creating the field and all other terms defined as above and as described in Section 3.6.2.

Unlike the two python scripts, the sources defined using `fielddata` here have a finite radius which is specified when creating the field. Any node lying within the radius of a source has it's contribution from that source set to the source value, independent of where within the radius it falls.

Defining porpoise

In addition to defining the simulation environment, it is necessary to define the properties and initial states of the porpoise to be simulated. The full list of properties can be found in Table 3.6, although only some of these can be defined from input.

Similar to the use of case files described in subsection 4.2.1, the properties of the porpoise are defined in an INI format file. This is the file referenced in the `particles` property of the case file. The file starts with an `[info]` section containing the number of porpoise and an optional comment, then optional `[defaults]` section, followed by a section for each porpoise, sequentially numbered starting from zero - i.e. `[0]`, `[1]`, `[2]`. The properties that can be set in each section of the file are listed in Table 4.2.

Name	**Values**	**Meaning**
Section: info		
comment	string	Descriptive text displayed at run time
np	integer	Number of porpoise to include in the simulation
Section: defaults or **id**		
position	float[3]	Porpoise release coordinates
velocity	float[3]	Initial release velocity (ms^{-1})
orientation	float[3]	Initial orientation angles (α, β, γ)
drag	float[3]	Drag coefficients
area	float[3]	Reference areas

Table 4.2: Porpoise definition file parameters

The `generate_particles.py` script is an interactive utility which prompts for values and allowable ranges for position, orientation and velocity and values for mass, drag coefficients and reference areas. A population is then generated with randomised parameters based on the values and ranges provided. No checks are made to determine whether the generated positions are valid, so some adjustment is typically needed after the file is generated.

4.2.3 Main model

The main model, `simulation`, uses the information provided in the case file to locate the particle definition file, mesh cache and input and output folders. Optional arguments allow a simulation to be resumed from a checkpoint file, early termination of a simulation (rather than using the time defined in the input data) and control over logging output and the number of processes used.

The simulation output is placed into a text file containing the position and full or partial state of each porpoise at each simulation timestep, depending on the options supplied in the case file.

4.2.4 Post-processing

Post-processing tools developed alongside the implementation can be split into 3 main categories: Extraction, Rendering and Analysis

Extraction tools

The extraction tools are designed to partition output data, reducing the files to a more manageable size.

- `track_converter.py`
  Take a track file and convert it to a series of CSV files - one file per simulation timestep.
- `extractparticle`
  Extracts position and state of a specified porpoise at every simulation timestep into a single text file.

Render tools

The rendering tools provided allow results to be viewed and inspected graphically, either as 2D plots/graphs or as 3D graphics files using Paraview [114] - an open source visualisation tool that can import and export data from a variety of formats.

The main tools for export to Paraview[3] are `vtkparticles` and `vtkexport`. These tools

[3] Strictly speaking the tools output to VTK format files, which are compatible with a range of software including Paraview. Only Paraview was used or tested.

take a case file as input, and allow the export of one or more timesteps at specified intervals. In order to provide information regarding the clock time of each simulation timestep, a wrapper PVD file is created, referencing the individual VTK format files. This allows Paraview to (optionally) display the correct time as an annotation and as part of the interface.

In addition to Paraview, a number of Python scripts have been used to plot smaller meshes and extracted data. These scripts make use of the following 3rd party libraries:

- Matplotlib [115]
  http://www.matplotlib.org
- NumPy
  http://www.numpy.org/
- Seaborn
  https://stanford.edu/~mwaskom/software/seaborn/, and
- Pandas
  http://pandas.pydata.org/

These libraries are use to plot, visualise and analyse the available data, and have been used to generate many of the figures in this thesis.

There are three main Python scripts used to visualise results:

- `plot_particle_set.py` - Plots a 2D overview of multiple porpoise tracks
- `plot_combined.py` - Plots 2D or 3D mesh data, optionally including particle start and end points.
- `plot_extracted_particle.py` - Takes data for a single porpoise extracted by `extractparticle` and plots state variables against time.

Analysis

In addition to rendering the results graphically for visual inspection and interpretation, numerical and statistical results can also be extracted from the simulations. These are generated by two tools, `particlestats` and `trackstats`.

- `particlestats` - generates summary statistics (min/max/mean/standard deviation) for position and velocity of all porpoise at each timestep.
- `trackstats` - generates summary statistics for position and velocity of all porpoise over all timesteps.

Both tools can also operate on subsets of the simulated population, allowing the population to be sampled for comparisons. This is used and discussed further in chapter 5.

The scripts and programs described above provide the building blocks for carrying out a simulation based investigation into harbour porpoise behaviours in tidal sites, and allow the results to be examined in a number of ways. To illustrate their use, an example case is illustrated below.

4.3 Process Overview

The general procedure for creating and running a simulation is shown in Figure 3.3, with the data preparation steps broken out into Figure 3.4. These processes are typically only required once for any given environment, unless changes need to be made to the additional noise sources or prey locations. There is no explicit limit to the number of fields that can be added to a given simulation, although each additional variable does require additional processing time when the simulation is run.

Taking a 2D TELEMAC file as the basis of a simulation, the steps in Figure 3.3 and Figure 3.4 become the following commands:

```
telemac-parse -o ../RS2D -b ../RS_basecase.slf
convert_to_3D -bBv -n 5 -d 2 -U 0 -V 1 ../RS2D/RS_basecase.slf
prepmesh -b RS3D.ini
calcdepth -v -o 7 RS3D.ini
fielddata -vfo 8 RS3D.ini fish.fp.ini
fielddata -v -o 9 RS3D.ini noise.fp.ini
precomputegrads -i 7 -o 10 -v RS3D.ini
precomputegrads -i 8 -o 13 -v RS3D.ini
precomputegrads -i 9 -o 16 -v RS3D.ini
```

These commands, in order, import data from TELEMAC, convert it from 2D depth averaged to 3D, cache the mesh information and calculate the water depth throughout the domain. The fields representing fish/food and noise are calculated and the gradients of the depth, food and noise variables are computed and stored in order to improve the speed of the main simulation.

This set of commands would typically only be required once for a given scenario, with multiple simulations being run from this prepared data set. After this data preparation has been completed, the main simulation would be run as described in subsection 4.2.3.

4.4 Speed and efficiency

Over the course of developing the model and its associated tools, a number of measures were taken to increase the efficiency of the code - decreasing the time taken for simulations and other operations to be completed. Some of these improvements were made to the algorithms implemented within the code, while others included changes to data storage and workflows.

4.4.1 Efficient searches

In order to efficiently manage particles throughout the domain, it is necessary to have a method to determine which element contains a given point in space. Once the containing element is known, the properties of that element can be used to determine the relevant environmental properties for the area immediately surrounding the particle.

In order to determine within which element a given set of coordinates lie, they are checked using a series of algorithms based around a function $\mathrm{D_f}$, described in [116] and shown in Equation 4.1.

$$\mathrm{D_f}\,(\boldsymbol{p},f) \quad = \quad (\boldsymbol{f_c} - \boldsymbol{p})\,.\hat{\boldsymbol{n}}_f \tag{4.1}$$

where f_c are the coordinates of the face centroid and $\hat{\boldsymbol{n}}_f$ the outward pointing normal unit vector for f.

Given a point $\boldsymbol{p}$ and a face f, the value returned by this function indicates in which direction the point lies, relative to the outward pointing normal vector of the face. A positive value of $\mathrm{D_f}$ indicates that a point lies somewhere beyond the external side of

that face (i.e. in the direction of the positive normal), while a negative value means that the point lies somewhere beyond the internal side of that face.

This can be extended to determine whether or not a point lies within a given volume, bounded by a known set of faces, as described below.

Single element search

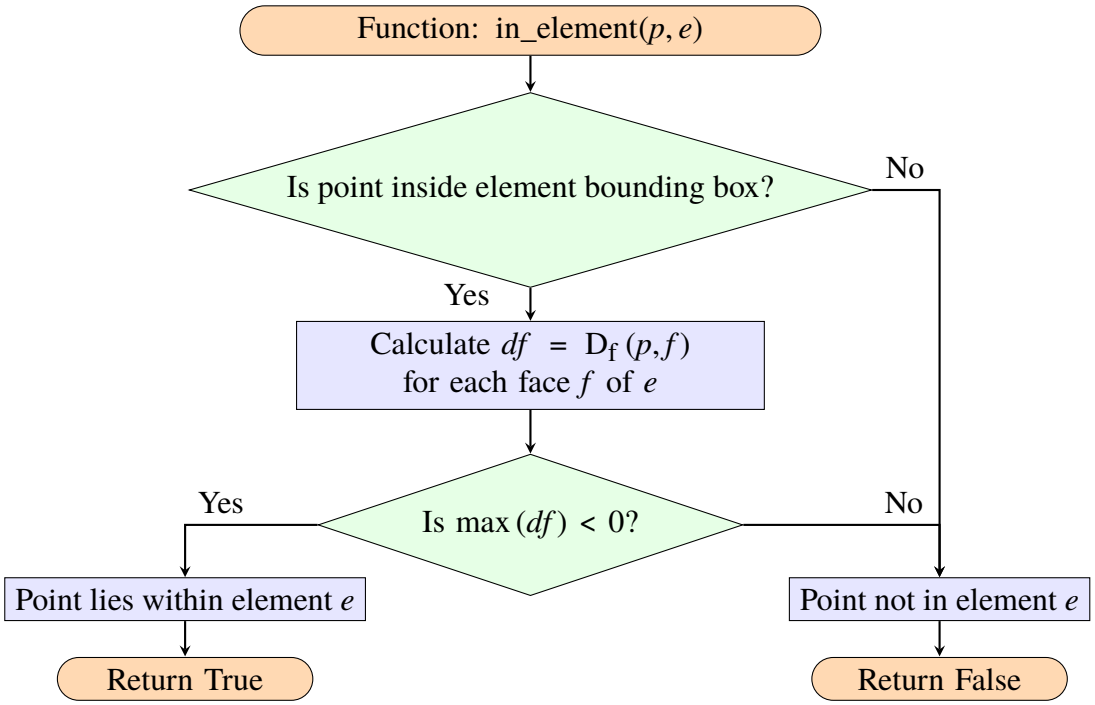

Figure 4.1: in_element: Test if point p lies within element e

The algorithm used to test whether a point lies within a given element is outlined in Figure 4.1. It calculates D_f for all faces as described above, after first checking whether the coordinates of the point lie within a cuboid defined by the minimum and maximum x, y and z coordinates of the element. This bounding box is computed in advance, and provides a fast method of excluding the vast majority of points before continuing with the more complex D_f calculations.

Given the behaviour of D_f (discussed above), if D_f is negative for all faces then the point p must lie within the element, assuming that the element is convex and has a non-zero volume. The first assumption is guaranteed for the elements described in Figure 3.2, as all are convex shapes with planar faces. Due to the dynamically changing height of

elements due to the motion of tide during the simulation , the second assumption is not guaranteed, but can be easily checked at runtime.

Neighbouring element searches

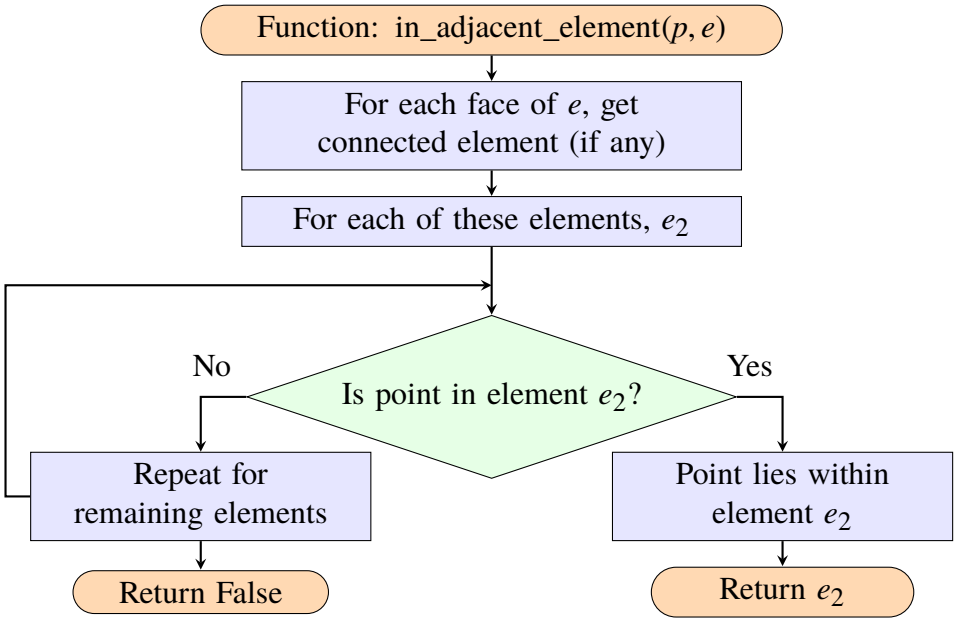

Figure 4.2: in_adjacent_element: Search for point p in elements adjacent to e

One of the complications of dealing with a moving mesh is that a set of coordinates are not guaranteed to lie within a given element for the entire duration of a simulation. In this instance, if a point is no longer contained within the element it occupied at the start of the previous timestep then it is likely to be contained within one of the adjacent elements. This is a relatively simple check, as outlined in Figure 4.2.

For a given element e, the adjacent elements can be defined as the set of elements that share one of the faces of e. For each of these elements, in_element (Figure 4.1) can be called in order to quickly determine whether the point lies within that element. The search ends when the point is successfully located or when all immediately adjacent elements have been checked.

Checking adjacent elements before resorting to brute force methods allows the majority of these cases to be handled in a more computationally efficient manner. In a similar manner, the animals moving through the simulation will move between elements, with

the previously occupied element providing a starting point for locating its new home within the mesh.

Brute force searching

If no previous element is available as a starting point, or where a nearest neighbour search has failed, the simulation falls back on testing every element within the domain to determine whether the search location is contained within it. In a similar manner to the element check outlined in 4.1, the algorithm initially checks whether a point lies within the bounding box of the mesh as a whole before continuing in order to easily discard any points which cannot possibly lie within any elements of the mesh.

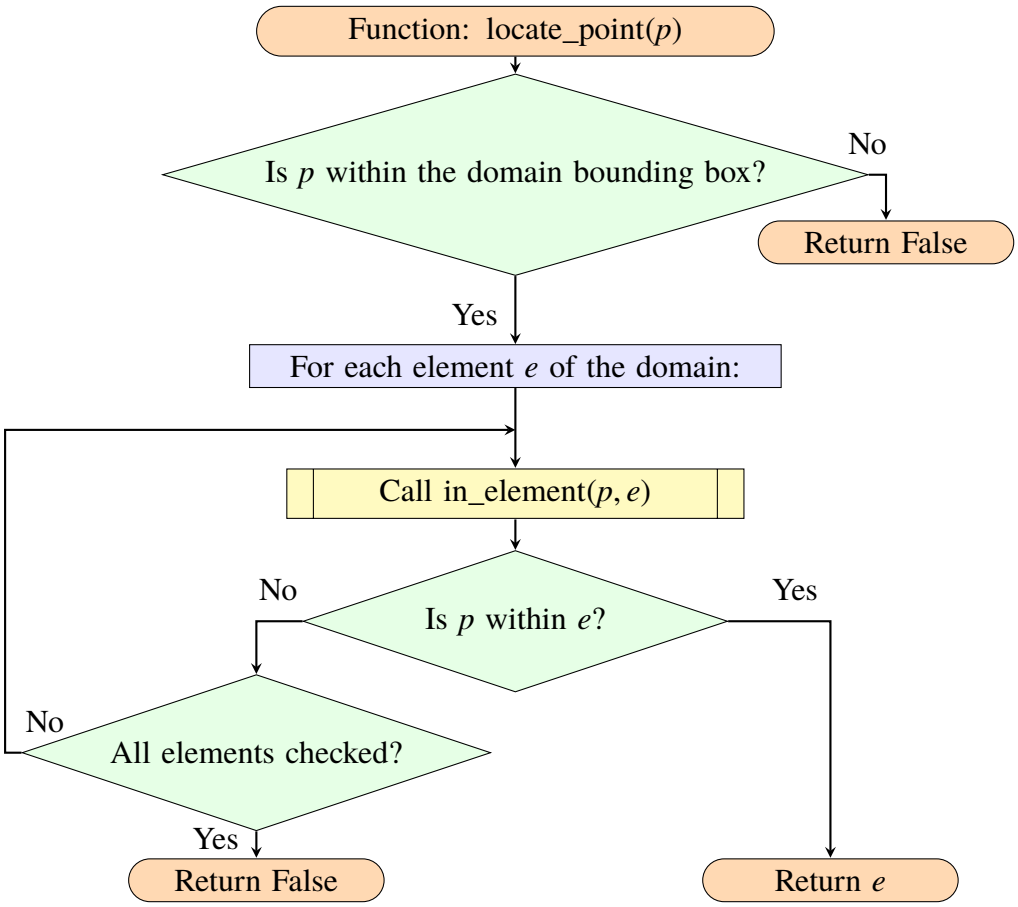

Figure 4.3: locate_point: Locate element containing a point, p

4.4.2 Mesh building and caching

The input format used describes a mesh in sufficient detail to allow a computational representation of that mesh to be generated. In this implementation, each point, edge, face and element exists as a data structure held in memory, cross referenced to one another for ease of reference. These data structures are built from the node coordinates read from file and their associated connectivity data - an ordered list of points forming each element. The full file format details are listed in Appendix A.

The mesh is built in phases, described below for a three dimensional mesh:

1. Read node coordinates from file
2. Read connectivity data from file. For each element:
    (a) Initialise new element
    (b) Set XY bounding box
    (c) Create template edges from nodes given
    (d) For each template edge:
        i. Get a list of existing edges connected to its nodes
        ii. If an existing edge matches, store its ID for later
        iii. If no matches, allocate a new edge and store its ID. Update connected nodes with new edge ID.
    (e) Collect edges (existing or allocated) and create template faces
    (f) For each template face:
        i. Get a list of existing faces connected to edges
        ii. If an existing face matches, store its ID
        iii. If no matches, allocate new face and store its ID. Update connected edges with new face ID
    (g) Store face IDs and directions
    (h) Update faces with element ID
3. Read timestamps from files and store in mesh object
4. Classify boundaries using process described in 3.8

Test Case	Elements	Naive (s)	Improved (s)	Speedup	File Size
r3d_tide	43580	809.48	0.47	190	15MB
NorthSea [Note 1]	344412	56452.59	2.55	22138.27	191MB

Note 1: Test case used in Chapters 5 and 6

Table 4.3: Test case run times for mesh building using naive iterative approach and improved algorithm described in Section 4.4.2

Initially, the process was carried out by searching all existing edges/faces rather than only checking those connected to nodes forming part of the face/element under construction. In order to further improve performance of the overall simulation, this mesh data structure is cached on disk for use by repeated simulations and export tools.

Moving from the original naive implementation to the version described reduced the computational time required by a factor of 190 for the initial test case (see Table 4.3), or by a factor of over 22000 on a real dataset. The generated mesh file is saved, requiring some additional disk space. This additional space (stated in Table 4.3) is negligible compared to the output data, which can require several gigabytes of disk space for storage and post-processing. All performance figures were generated on the same hardware, which is detailed in Appendix B.

4.4.3 Precomputation

Two other processes occur during the main simulation loop that were moved to preprocessing steps - calculating water column depth and calculating field gradients using the tools `calcdepth` and `precomputegrads` respectively. These quantities both require the collection of data from adjacent elements - either determining the vertically connected elements in order to calculate depth or from neighbouring nodes in order to calculate gradients.

Computing the values once and storing them as variables on disk allows the values to be calculated once per dataset rather than on a per simulation basis. The trade off is increased disk space requirements and higher I/O loads during a simulation.

4.4.4 Parallelisation - multi-threaded implementation

In the initial, single threaded, implementation of this project each simulation was effectively constrained by the speed of the processor on which it was running. This is not an issue unique to IBMs, but has been recognised as a limiting factor in previous works - particularly when inter-individual interactions have been simulated [97, 117].

A profiling tool was used to identify the most heavily used function calls within the simulation, an example of which is shown in Figure 4.4. The two areas highlighted were the main behaviour loop and the function responsible for resetting the mesh z coordinates at the start of each timestep. These functions are purely computational, with no disk accesses required, making them suitable candidates for parallelisation.

A thread pool (also known as a "Manager/Worker" model [118, p. 98] was implemented to handle the parallel computation aspects of the model. A number of threads are initialised at the start of the simulation (a “pool” of threads) which remain idle until a task is assigned to them.

In this implementation, all threads are assigned a portion of the total work to be completed, and the main thread waits for all of the worker threads to finish their task before continuing. This setup avoids the overhead of creating new threads at each point where parallel functionality is required. The improvement in execution time varies with the number of threads and the specific cases tested, but was found to be between 4% and 24% in simple tests, with a test case using 8 threads completing in 63 minutes compared to 82 minutes for the same case run in single threaded mode. Tests were conducted on a 4 core Intel i7 with HyperThreading enabled to give 8 logical cores - further specifications for the computer used are given in Appendix B. Further improvement in runtime is constrained by other factors, such as time spent reading and writing data from storage, that can be considered for future work.

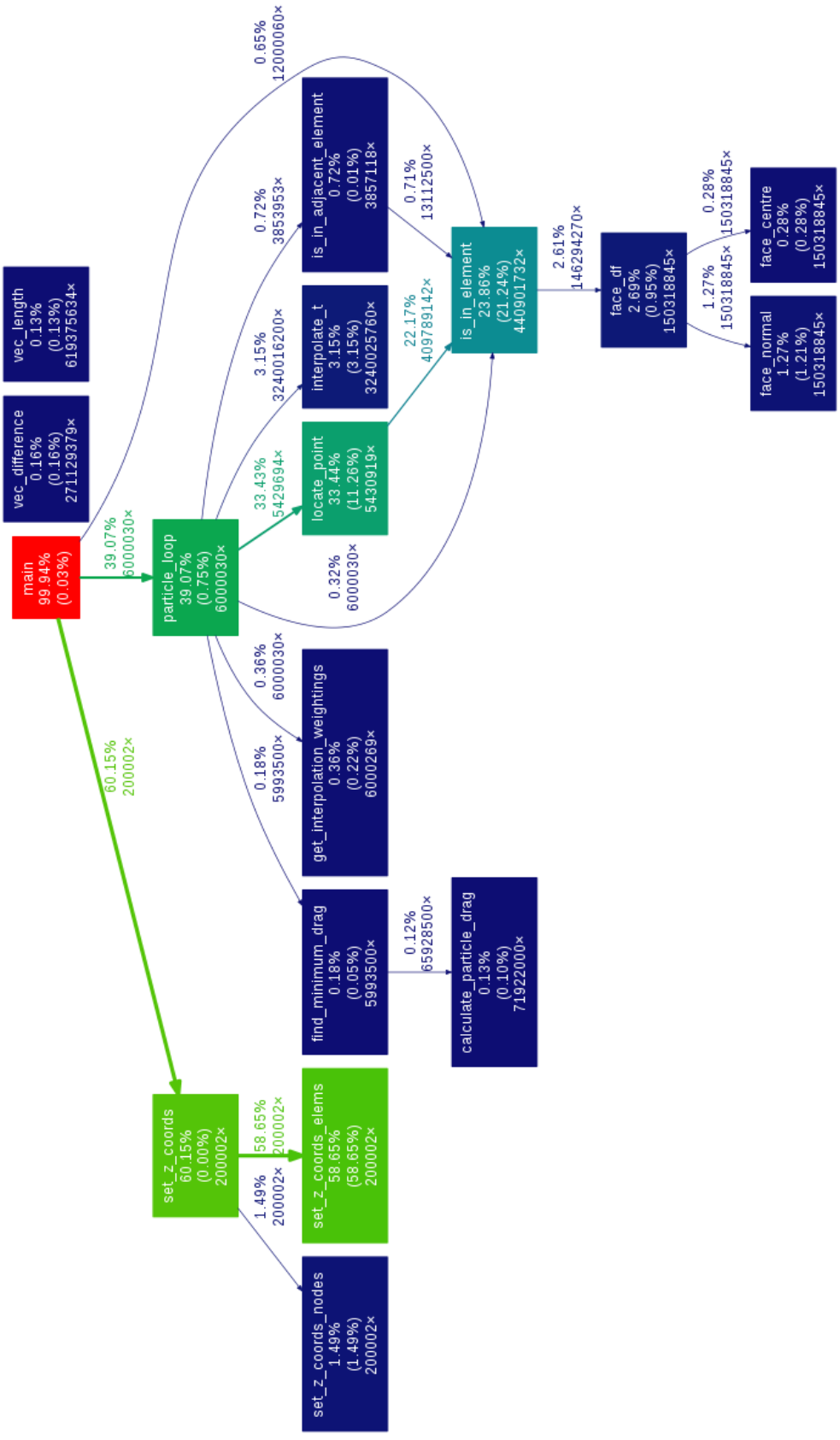

Figure 4.4: Call profile for the main simulation showing proportion of runtime spent in each function for a single threaded run.

4.5 Model Outputs

The main output of the model is a track file, giving the position of each porpoise at every timestep in the simulation. There are two levels of detail that can be selected: short or long. The short output mode saves the position, last occupied element, behaviour state, and exit time and status. The long output saves the full state of every porpoise at every timestep, along with the local value of other variables used primarily for debugging and development.

The file formats are specified fully in Appendix A (section A.5). A single timestep of the long format is also saved periodically for use resuming the simulation if interrupted - detailed in section A.6.

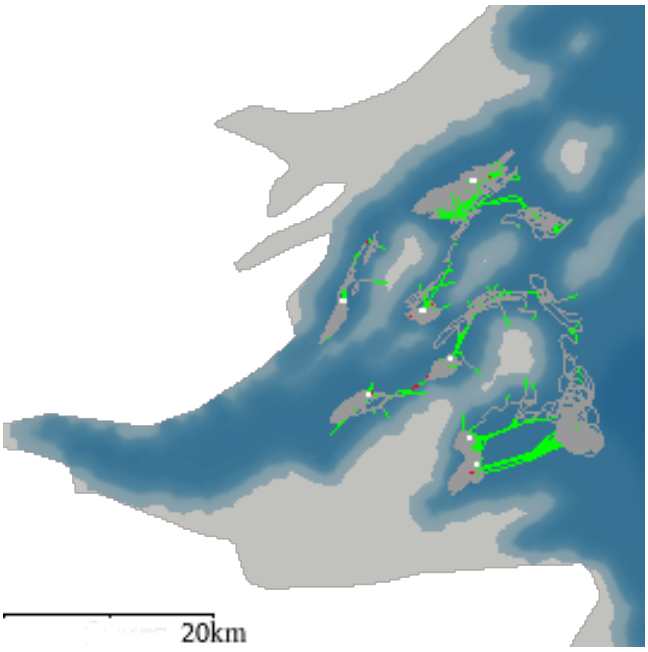

Figure 4.5: Example output showing porpoise tracks in the Thames estuary, taken from a larger simulation of the North Sea

These outputs can then be post-processed to allow the results to be analysed. The track data itself is analogous to position data obtained from tagging/tracking studies carried out on real animals, although the simulated data is typically generated at a far higher frequency than is practical for tagging exercises and does not (currently) account for the diving/surfacing behaviour.

Track renders

An example rendering of this data is shown in Figure 4.5, which shows trails formed from the recorded positions of each porpoise, coloured by the behaviour state at that timestep. These renderings can be generated the full dataset, or (as in the example shown in Figure 4.5) from a sample taken every n timesteps. The colouring of the background domain and the tracks themselves can be varied, but unless otherwise stated the domain will be coloured to show water depth (from grey (0m) to dark blue) and the tracks will be coloured grey for default behaviour, red for noise avoidance and green for shallow water avoidance.

Grid analysis

Another method of analysing animal position data is to consider the presence or absence of animals within a given area over time. This has previously been done based on animal sightings in the Ramsey Sound area as part of a study carried out between 2009 and 2012 [30].

In the study reported in [30], the area was surveyed visually from 3 fixed vantage points. The visual surveys were divided into 5 minute blocks (survey scans), with the range and bearing of any porpoise sighted during those 5 minute blocks recorded along with the vantage point in use and other environmental information.

When analysing this data, the survey area was divided into cells using a grid of 50m squares. The total number of sightings in each cell over the study period was counted and recorded. To account for the different amounts of time spent at each vantage point, the total number of survey scans made from each point (with or without sightings) were counted and used to calculate the amount of time each 50m square spent under observation.

The number of sightings in each cell was then divided by the total time under observation:

$$\text{Sightings per hour in cell}_i = \frac{\sum \text{Sightings in cell}_i}{\sum \text{Time spent observing cell}_i} \tag{4.2}$$

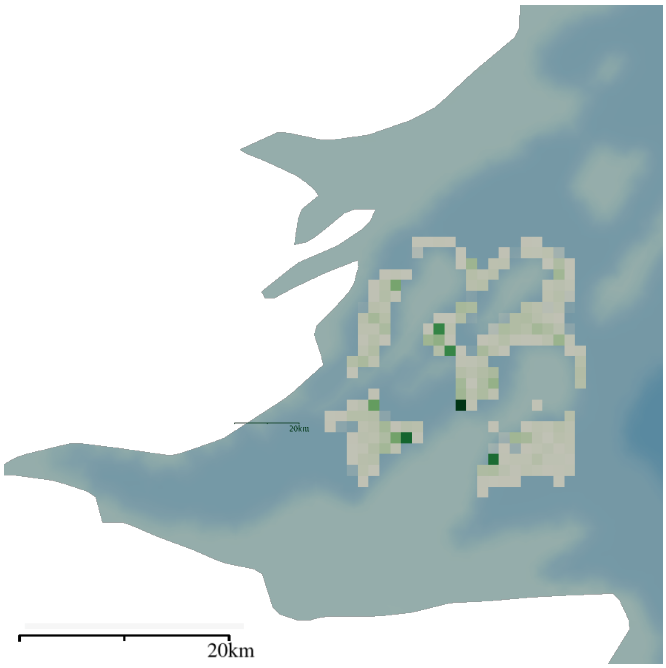

Figure 4.6: Example of grid analysed results, showing porpoise presence within 1km grid cells based on 5 minute scans over 1 hour

In the study in question, this was done for the entire dataset as well as for specific subsets of the data based on month, season and tidal state in order to investigate the relationship between these factors and the "sightings per hour" quantity.

Adapting this for application to simulated data, snapshots of the track data can be taken at specified intervals (e.g. 5 minutes) to represent the survey scans. If the domain is divided into cells as described above, the number of porpoise in each cell can be counted for each of these snapshots. This "sighting" data can then be aggregated over a given period of the simulation and divided by the length of the period. As the "survey" time in this instance is uniform across the domain, the counts in each cell can be scaled uniformly.

An example plot of this data is shown in Figure 4.6. This can then be compared (visually or numerically) to equivalent field survey data.

4.6 A simple example

To put this in context, a simple simulation has been run with and without food and noise present in order to show how the rules take effect. The tracks corresponding to these results are rendered in Figure 4.7.

The simulation consists of a 200m $\times$ 200m $\times$ 22.5m cuboid domain, divided into 96 elements (3 layers of 32). The boundaries of the elements on the top surface of the domain can be seen in Figure 4.7 as the black triangular outlines. The domain was uniformly deep, with a current flowing in the Y direction (vertically upwards as shown in images presented here). The flow imposed had an depth averaged value of 1ms^{-1} and a $\frac{1}{7}^{\text{th}}$ power law vertical profile applied. A single point source was added to the centre of the domain, and the strength of this field is illustrated by the colour gradient in the background of the plots. The units on this field are arbitrary for the purposes of this simulation. The same data is used for both food and noise when present, effectively presenting both sources at the same location.

4.6.1 Tracks

The tracks taken by the simulated porpoise are shown in Figures 4.7a-4.7d. All porpoise start the simulation distributed randomly along the bottom edge of the domain as shown, with the same starting locations used for all simulations. Starting with Figure 4.7a, we can see that the porpoise follow the water flow in the absence of any other influence. With no incentive to remain within the domain, all porpoise leave via the top of the domain as shown after 103 timesteps (309 seconds - just over 5 minutes).

Figure 4.7b shows the threshold effect of the noise response, with porpoise heading radially away from the point source once they reach an area where the value of the noise source exceeds the defined threshold (1 unit in this instance). The small timestep (3 seconds) leads to porpoise alternating between this noise avoidance (red marks) and their default behaviour (grey). It should be noted that the green segments shown in the image are the result of interpolation by the visualisation software used and do not represent actual depth avoidance behaviour within the model. The alternating headings taken by the porpoise lead to movement which follows the edge of the noise contour until it can be avoided, leading to the concentration of tracks either side of the noise

Simulation	$\Delta\tau$	$\Delta\bar{x}$	$\Delta\bar{y}$	$\Delta\sigma_x$	$\Delta\sigma_y$
Food and Noise	185	1.20	201.13	9.88	1.78
Food only	248	-1.86	199.17	-3.70	1.56
Noise only	279	2.22	201.22	11.12	1.09
No Food, No Noise	103	3.50	200.75	0.35	1.10

Table 4.4: Results of a simple simulation to illustrate impact of the behaviour rules
See Section 4.6.2 for further explanation of column headings

source. Once clear of the influence of the noise source the porpoise continue out of the domain as per the behaviour in Figure 4.7a.

The results shown in Figure 4.7c show the simulation with food response enabled (but noise response left disabled). Comparing the tracks visually with those in Figure 4.7a it can be seen that there is an increased presence of porpoise in the central region of the domain, with tracks generally deviating towards the centre. Given that the food response is not a threshold based response (it varies based on the value of the food availability at the porpoise's current location as described in Section 3.7.2), it does not show the same 'hard edge' response given in the noise response case shown in Figure 4.7b.

The final image in this set (Figure 4.7d) shows results of a simulation with both responses enabled. The same source data was used for both, so this image represents a co-located source of food and noise. Elements of both behaviours can be observed, with tracks initially deviating towards the domain centre until the noise threshold is encountered, where this then takes priority and the animals skirt the edges of the source until reaching the left or right most edge of the 1 unit limit. In the upper half of the image, it can be seen that the porpoise tracks are more dispersed than in Figure 4.7b, due to the influence of the food source.

4.6.2 Statistical measures

Taking the data behind the images shown in Figure 4.7, we can measure the mean and standard deviation of the position of the porpoise and examine how these quantities differ based on the behaviour rules in use. The figures in Table 4.4 show the change in the mean X position ($\Delta\bar{x}$), mean Y position ($\Delta\bar{y}$), standard deviation in X ($\Delta\sigma_x$), and standard deviation in Y ($\Delta\sigma_y$) between the beginning and end of each simulation. These give some information about the change in position of the simulated population,

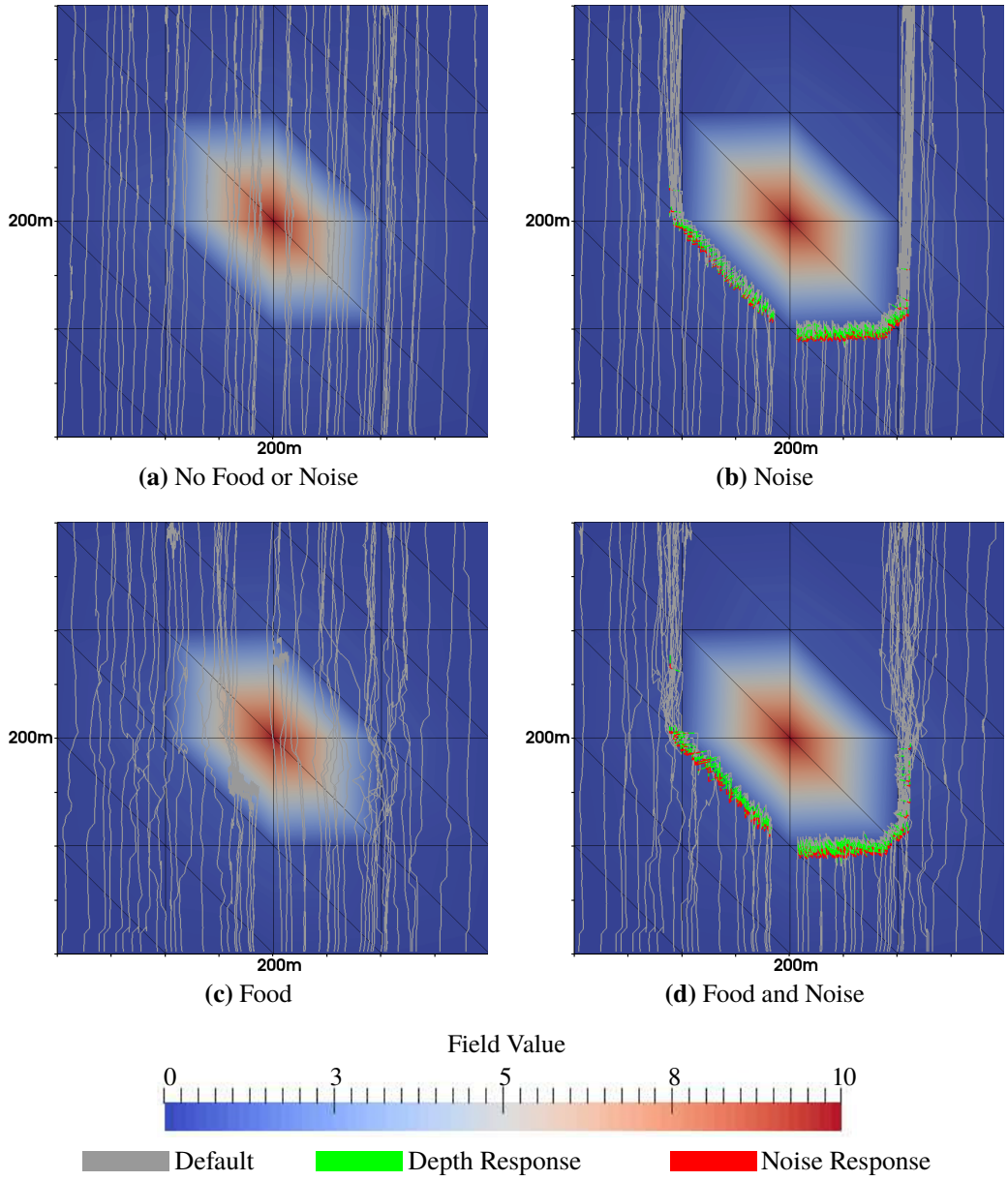

(a) No Food or Noise

(b) Noise

(c) Food

(d) Food and Noise

Figure 4.7: Simple simulation results

as well whether the group has moved closer together or further apart in each axis over the course of each simulation.

Looking at the first two columns of Table 4.4, it can be seen that in this instance there is little difference in the change in mean position between the 4 simulations. This is consistent with all porpoise leaving the domain through the top edge (y = 200), with small variations in $\Delta\bar{x}$ reflecting the lateral movements of the porpoise.

The change in standard deviation gives a better illustration of changes between the four simulations. Looking at $\Delta\sigma_x$, we can see that the effect of noise is to increase the standard deviation in x and the effect of the food response decreases it - this is consistent with attempts to avoid and move towards the centre of the domain and with the tracks shown in Figure 4.7. The combined response value lies between the two individual responses. The values for $\Delta\sigma_y$ show no substantial difference between the four simulations in this instance, but this is consistent with all porpoise exiting the domain past y = 200 as mentioned above.

4.7 Summary

Building upon the concepts and framework introduced in Chapter 3, this Chapter has introduced the architecture of the Individual Based Model that has been developed as well as illustrating how these components fit together to produce simulations. It has also shown some example outputs and analysis options as well as describing some of the improvements made to the speed and efficiency of the model during its implementation.

The following chapters present the results of investigations into the statistical behaviour of the model (Chapter 5) and its sensitivity to parameter changes (Chapter 6) before moving to a case study of porpoise behaviour at an example site (Chapter 7).

Chapter 5

Statistical Measures

"HOLMES: How often have I said to you that when you have eliminated the impossible whatever remains, however improbable, must be the truth? "

Arthur Conan Doyle - The Sign of Four (1890)

5.1 Introduction

The previous chapters have described the background and implementation of the model and provided example data demonstrating the behaviours that are implemented. The amount of data produced is significant (Each of the 3 simulations discussed in this chapter produced approximately 90GB of raw output data), and needs to be examined and analysed in order to produce outputs that can be used to compare results between simulations and to other data.

Some simple information that should begin characterising the simulated population[1] would be the spatial location and extent of the population within the model. Two of the easiest measurements that can provide those details are the mean and standard deviation of the population's position respectively. The change in those two measures over the course of the simulation provides a measure of the impact of the behaviour rules on the population, relative to the original characteristics of the population.

Given that these measures are based on the movement of the population, it is also important to determine the impact of population size on these measures. This can be done by conducting a number of simulations at different sizes and comparing the results, or by analysing smaller samples of a larger simulated population. The latter approach has been taken here, allowing multiple samples of a given size to be compared against each other as well as allowing the results to be obtained with fewer simulation runs. Determining a suitable number of individuals to provide statistically robust measurements will allow further simulations to be run with a population sufficient to generate good quality data, without running to excess and using unnecessary resources.

5.2 Model Environment

The simulated environment used is taken from a 60 day TELEMAC tidal model of the North Sea, provided by Violeta Moloney[2] of the Zienkiewicz Centre for Computational Engineering at Swansea University. The model domain measures 488km in the x direction (East-West) and 368km in the y direction (North-South), with depths of up to 78m.

[1] The simulated group of animals. This is not necessarily equivalent to the use of the term 'population' in a biology text.

[2] 716469@swansea.ac.uk

The model uses a Cartesian coordinate system, with the origin (SW corner) sitting at (+282742, +5638386) in the x, y plane. This domain has been split into a 3D mesh of prismatic elements, formed from from 3 unstructured triangular mesh layers, with edge lengths ranging from 460m to 1700m in the x, y plane and 0 to 40m in the z axis. This yields a total of 344,412 elements. The full domain at τ_0 is shown in figure 5.1, with the colouring representing water depth. Most figures used will crop (at least) the easternmost section of the domain to provide a more compact view of the results, but the full domain is used for all computations unless explicitly noted otherwise.

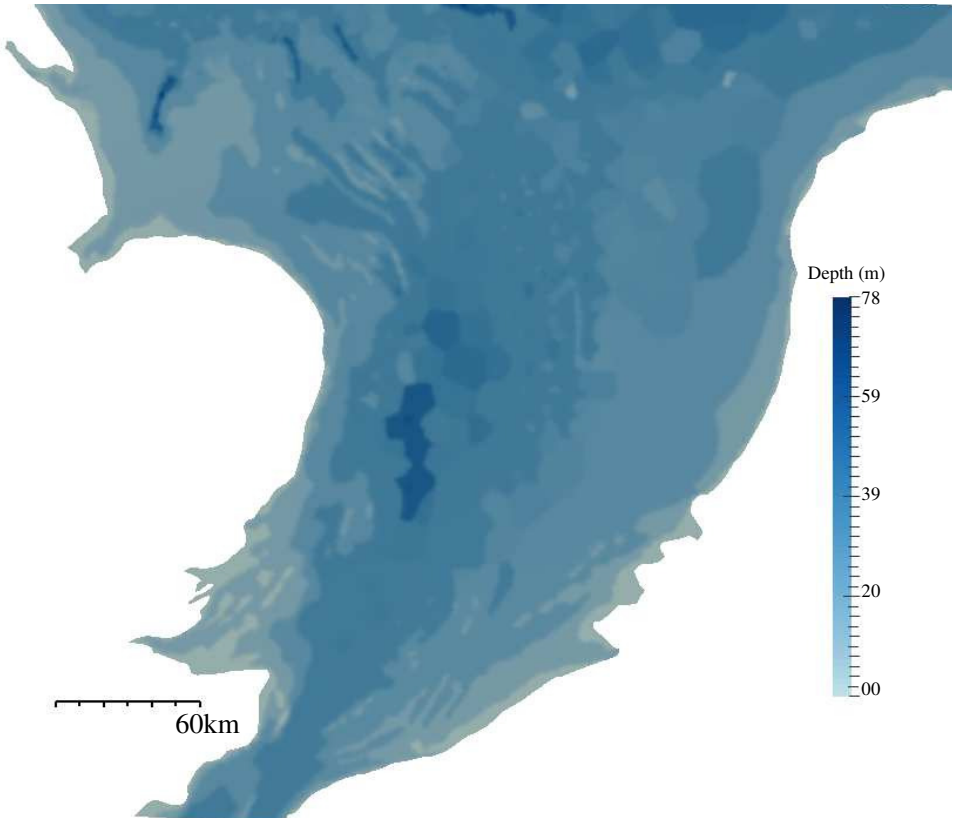

Figure 5.1: North Sea model domain, coloured by depth

The model data provided contains hourly snapshots of the model for the entire 60 day duration. These snapshots (mesh timesteps) have been split into 400 smaller intervals (simulation timesteps) as described in subsection 3.6.4, with each simulation timestep representing 9 seconds of simulated time.

5.2.1 Food Sources

In addition to the flow and depth information provided by the tidal model, it is also necessary to provide sources of food and noise for the simulated porpoise to react to. For this model, 6 food sources were defined within the Thames estuary area. Each food source was assigned an arbitrary value of 9000 to represent the strength of that source. Each food source was treated as a point source at the specified coordinates, with the value of the food 'field' in inverse proportion to the two dimensional distance to the source. The total contribution of each source at each node was then summed to give the availability of food at that location, with the gradient of the field providing directional information. The locations of each source are shown in Figure 5.2a, with contours showing variation in food availability resulting from the combined effect of the sources.

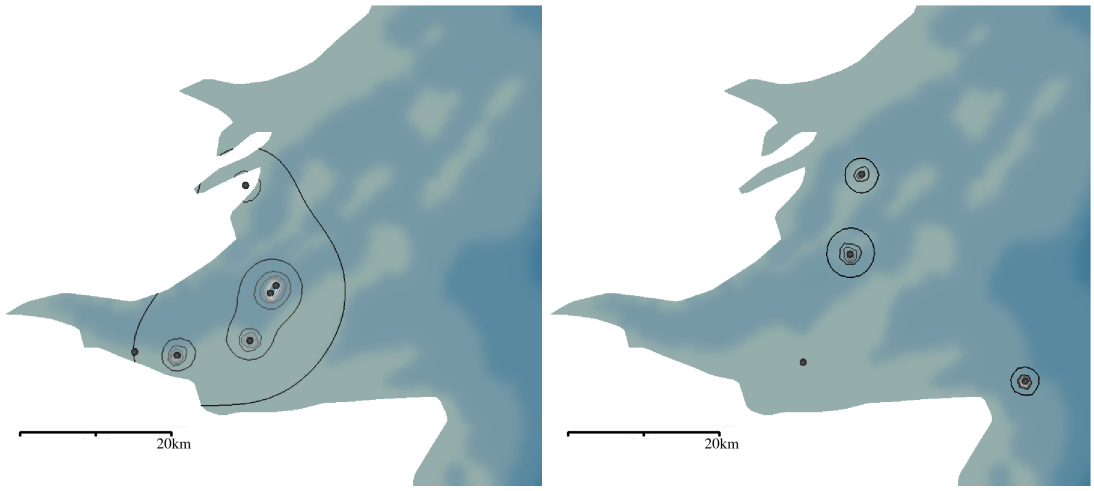

(a) Food sources **(b)** Additional Noise Sources

Figure 5.2: Location of point sources of food and noise within the Thames Estuary area of the model

5.2.2 Noise Sources

Noise sources for the model were implemented in a similar manner to the food sources described above, and were located as shown in Figure 5.2b. The value of each source was set at 6000 (arbitrary units), with a similar decay with respect to distance as described above. Figure 5.2b includes contours showing the combined effect of each noise source.

5.3 Parameter Space

Three simulations were run in order to obtain statistics covering varying model behaviours. The three simulations selected were chosen from a series of 25 different simulations carried out as part of the parametric exploration of the model that is described in Chapter 6. The three simulations presented in this chapter were selected based on the variety of results shown in a parametric exploration of the model's response to varying control parameters - specifically the threshold for noise avoidance behaviour and the weighting applied to food seeking behaviour.

The three simulations used are designated A-A-HP5MM, C-C-HP5MM, and E-E-HP5MM. The letters represent different multipliers for the food weighting and noise threshold respectively, which are discussed in more detail in Chapter 6. Simulations A-A-HP5MM and E-E-HP5MM represent two extremes of behaviour - no tolerance to additional noise and no interest in food (A-A-HP5MM) and high tolerance to additional noise and high weighting for food (E-E-HP5MM). The remaining simulation (C-C-HP5MM) represents an intermediate case, with a medium tolerance to additional noise and medium weighting on food behaviours.

		Noise Threshold Multiplier				
		A	B	C	D	E
Food weighting	A	**A-A-HP5**	A-B-HP5	A-C-HP5	A-D-HP5	A-E-HP5
	B	B-A-HP5	B-B-HP5	B-C-HP5	B-D-HP5	B-E-HP5
	C	C-A-HP5	C-B-HP5	**C-C-HP5**	C-D-HP5	C-E-HP5
	D	D-A-HP5	D-B-HP5	D-C-HP5	D-D-HP5	D-E-HP5
	E	E-A-HP5	E-B-HP5	E-C-HP5	E-D-HP5	**E-E-HP5**

Table 5.1: Subset of simulation ID codes, identifying the parameter values and distributions used. See Table 6.1 for corresponding values and Table 6.3 for the full table

Distribution	HP5	HP5MM
Release Coordinates (m)	378800, 5724500, –1	
Release Range (m)	$\pm$10000, $\pm$10000, $\pm$0.75	$\pm$10000, $\pm$10000, $\pm$0.75
Mean Coordinates (m)	382875, 5724900, –0.919	379840, 5722968, –0.909
Std. Deviation (m)	6351.27, 5671.47, 0.307	6055.90, 5941.85, 0.464

Table 5.2: Summary statistics for the HP5 and HP5MM porpoise distributions

The final part of each simulation ID defines the porpoise starting distribution, and is the same in all three cases. The distribution used is designated as HP5MM and was initialised using the same parameters as the smaller HP5 distribution used in other simulations (including the parametric exploration results), but expanded to include 2000 simulated individuals. This is shown in Figure 5.3 and detailed in Table 5.2 with the corresponding details of the HP5 distribution provided for comparison.

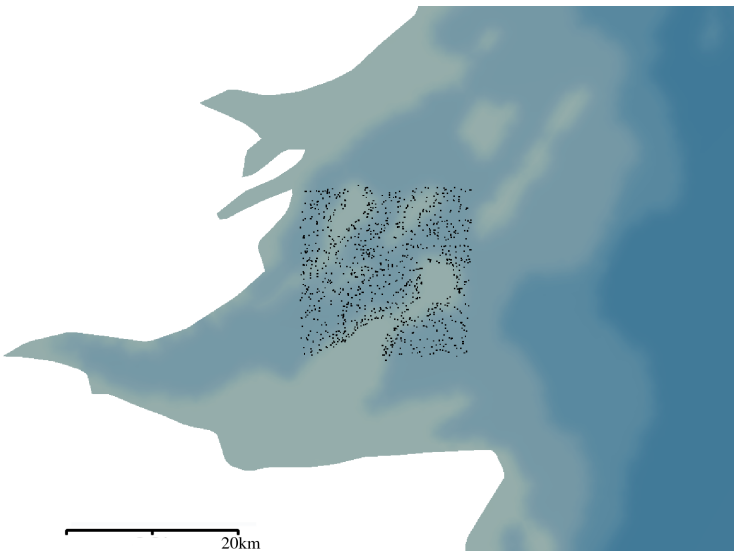

Figure 5.3: Starting porpoise distribution HP5MM, containing 2000 simulated porpoise.

Each simulation was run for the full duration (60 days) using 400 simulation timesteps per hourly mesh timestep (9 second timestep). The porpoise positions at each timestep were recorded at each step for analysis.

5.4 Measurements

In order to summarise the movement of the simulated population, three numerical measures have been selected. These are the mean population position, the standard deviation of the population positions and the displacement of the mean population position.

5.4.1 Mean Position

The mean position of the population is calculated over the whole population as:

$$\bar{\boldsymbol{x}} = \frac{1}{N}\sum_{i}^{N} \boldsymbol{x_i} \tag{5.1}$$

where N is the population size.

This can be expressed more verbosely as:

$$\begin{pmatrix} \bar{x} \\ \bar{y} \\ \bar{z} \end{pmatrix} = \frac{1}{N}\sum_{i}^{N} \begin{pmatrix} x_i \\ y_i \\ z_i \end{pmatrix} \tag{5.2}$$

The mean position is trivial to compute, and provides an indication of the position of the population within the model domain. It can be calculated as an average over the entire simulation, but is used here as calculated at a single timestep.

5.4.2 Standard Deviation of position

The mean position and displacement of the mean position provide ways of measuring where the centre of the population is located in a simple and easy to measure manner. In terms of the spatial properties of a population, another property to consider is the spread of that population - is the group all very closely located to the mean position or dispersed over a wider area, with the mean being located far from any particular individual or cluster of individuals?

This can, in part, be answered by looking at the standard deviation of position, and the change in standard deviation over time.

The standard deviation of position is given as:

$$\sigma = \sqrt{\frac{1}{N}\sum_{i}^{N} (\boldsymbol{x}_i - \bar{\boldsymbol{x}})^2} \tag{5.3}$$

where N is the sample size, $\boldsymbol{x}_i$ the position of an individual within that sample and $\bar{\boldsymbol{x}}$ the mean position of the sample, calculated as shown in Equation 5.1.

5.4.3 Net effects

The two measures previously describe the spatial position and spread of the population as it stands at a particular snapshot in time, but give no information about how the population has changed over time. A full description could be given as a timeseries showing the values of both the mean and standard deviation of position at each timestep, or alternatively the net change in each quantity could be examined.

Displacement of mean position

The change in the mean position of the population over the course of the simulation provides a measure of the cumulative effect of the behaviour of the animals over the duration of the simulation independent of the coordinate system used. This change, hereafter referred to as the displacement of the mean position, is calculated as the difference between the mean position at the final timestep ($\bar{\boldsymbol{x}}_f$) and mean position at the initial timesteps ($\bar{\boldsymbol{x}}_0$).

This quantity is calculated as shown in Equation 5.4.

$$\Delta\bar{\boldsymbol{x}} = \left| \begin{pmatrix} \bar{x}_f \\ \bar{y}_f \\ \bar{z}_f \end{pmatrix} - \begin{pmatrix} \bar{x}_0 \\ \bar{y}_0 \\ \bar{z}_0 \end{pmatrix} \right| \tag{5.4}$$

Change in standard deviation

Similarly, the change in standard deviation provides a measure of whether the population has moved closer together or dispersed over the course of the simulation. The change is calculated as shown in Equation 5.5, with σ_0 and σ_f representing the standard deviation of position for the initial and final timesteps respectively.

$$\Delta\sigma = \sigma_f - \sigma_0 \tag{5.5}$$

5.4.4 Relative Error

In order to compare these measures between simulations, it is helpful to define another measure that describes how closely a pair of results match in a manner independent of the units or scale of the original quantities. One such measure is the relative error between a value and a given reference, calculated as shown below in Equation 5.6.

$$\varepsilon = \frac{\left|X_{ref} - X\right|}{\left|X_{ref}\right|} \tag{5.6}$$

The relative error, denoted here as ε, is the error relative to a known quantity - denoted here as X_{ref} for an arbitrary quantity X. If the real or actual value for a quantity is known, that could be used for X_{ref}.

In the scenarios described here there is no known value for the quantities measured, so a reference must be specified. For each of the measures above, the reference value used will be the equivalent value from the 2000 porpoise result.

As an example, the relative error in mean position in x for a sample size i would be calculated as:

$$\varepsilon = \frac{\left|\bar{x_i}_{2000} - \bar{x_i}\right|}{\left|x_{2000}\right|} \tag{5.7}$$

This defines the relative error for the 2000 porpoise results as zero.

5.5 Results and sensitivity study

The three simulations were analysed by calculating the measures described previously for each timestep, over the full population of 2000 individuals. In order to investigate the dependence of each measure on the population size, each of the measures described has also been calculated for different subsets of the overall population for each of the three simulations. Where multiple independent sets of a given size can be split from the main population, each measure has been calculated for each of those sets - e.g. 20 measurements for different 100 porpoise subsets of the overall population, 10 measurements for 200 porpoise, 5 measurements for 400 porpoise and so on.

These sets were drawn sequentially from the population, such that the first five samples

of 10 porpoise represent the same population as the first sample of 50 and so on. The samples were drawn in this fashion in order to guarantee no overlap between different samples of the same population size while allowing the calculation process to be carried out in a more efficient manner. The initial population were generated with random coordinates (from a uniform distribution) within the release area, and as such there is no correlation between ID number and position. This means that sequential populations drawn from the main population also contain randomly distributed porpoise.

To illustrate these results, Figure 5.4 shows the pathlines formed by a small population of porpoise under the conditions used in simulation A-A-HP5MM. A series of results presented in this manner are discussed and analysed further in Chapter 6.

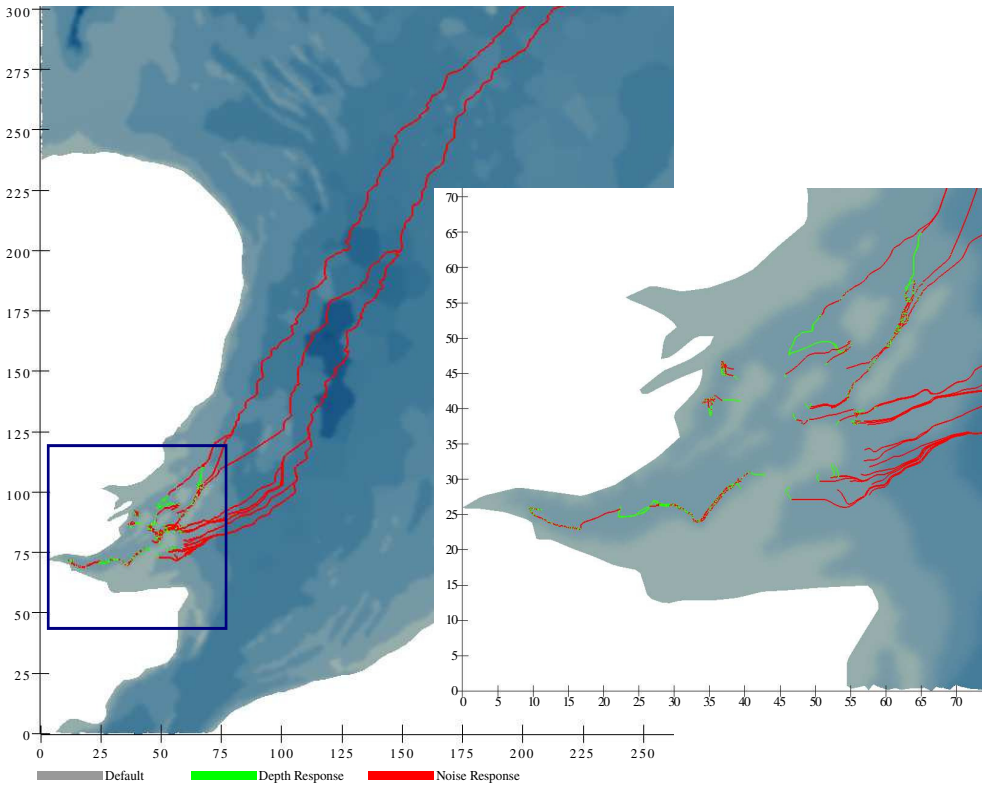

Figure 5.4: Example output, based on a subset of simulation A-A-HP5.
See Chapter 6 for discussion of results in this form

The results in the remainder of this chapter are plotted as graphs, showing the measurements described above for the different population samples. The results from equally sized samples appear as vertically aligned results. The mean value for each sample size has also been calculated where relevant, and is indicated on the corresponding plots using a black triangle.

5.5.1 Mean position

The mean population position was calculated as described in subsection 5.4.1 for the final timestep of each simulation. The mean population position in the X and Y axis is shown in Figure 5.5 and Figure 5.6 respectively, as calculated for various size samples of the population. The mean position in the Z axis is not discussed, as it is constrained by local bathymetry and not explicitly adjusted as part of the simulated behaviours and would provide little additional information about the populations.

The variation in results between samples reduces as the sample size increases, converging towards the full population mean position. The mean position in X shown in Figure 5.5a converges to a value around 530000m, and appears to reaches this value consistently for sample sizes of 400 or more individuals, with an anomalous pair of values for samples of 700 individuals.

Looking at the results for simulation C-C-HP5MM (Figure 5.5b), the results converge to a lower value around 373900m, with the results being visually consistent from 500 individuals onward. It should be noted that the range of values is also much lower than for the A-A-HP5MM results. The results for E-E-HP5MM shown in Figure 5.5c show a similar pattern and scale as the results for C-C-HP5MM, but with slightly more variation until sample sizes around 800.

Moving to the equivalent plots for mean Y position (Figure 5.6), the same trends are evident in all three cases, with convergence to a value around 5900000 by a population size of 500 porpoise for simulation A-A-HP5MM (Figure 5.6a), bar an anomalous increase in variation seen at the 700 porpoise sample size, as exhibited in the X axis results.

The results for simulations C-C-HP5MM and E-E-HP5MM (Figures 5.6b and 5.6c) are similar to their X position equivalents. Unlike the X position data, there are more notable outlying values for the position at some sample sizes - notably for the data returned for a population of 600 porpoise. There is no explanation available from this data for these particular outlying values, but the variations seen are still smaller than those observed in the A-A-HP5MM case.

As well as examining the trends in mean X and Y position, the relative error between the mean for each sample and the mean of the full population can be calculated, as described in subsection 5.4.4 and shown in Equation 5.6.

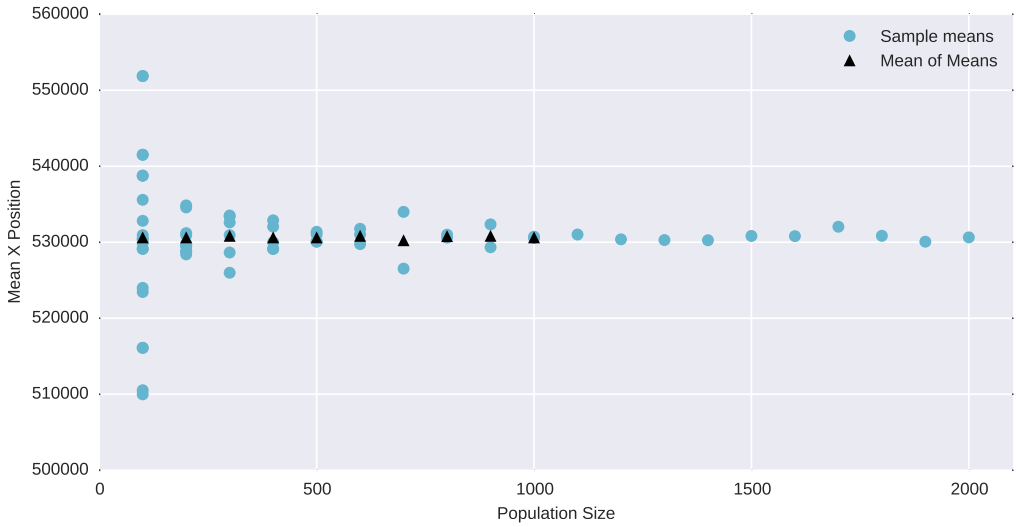

(a) Mean X positions for A-A-HP5MM

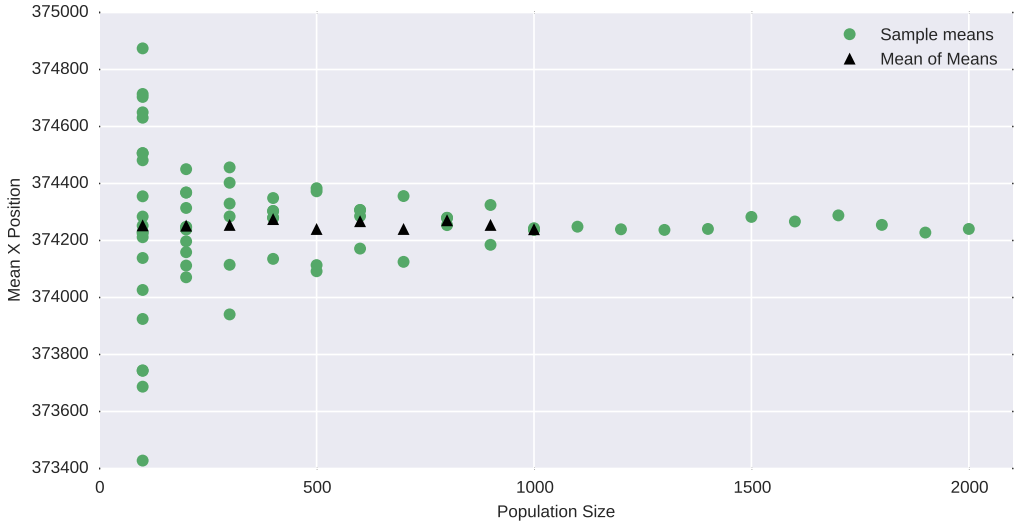

(b) Mean X positions for C-C-HP5MM

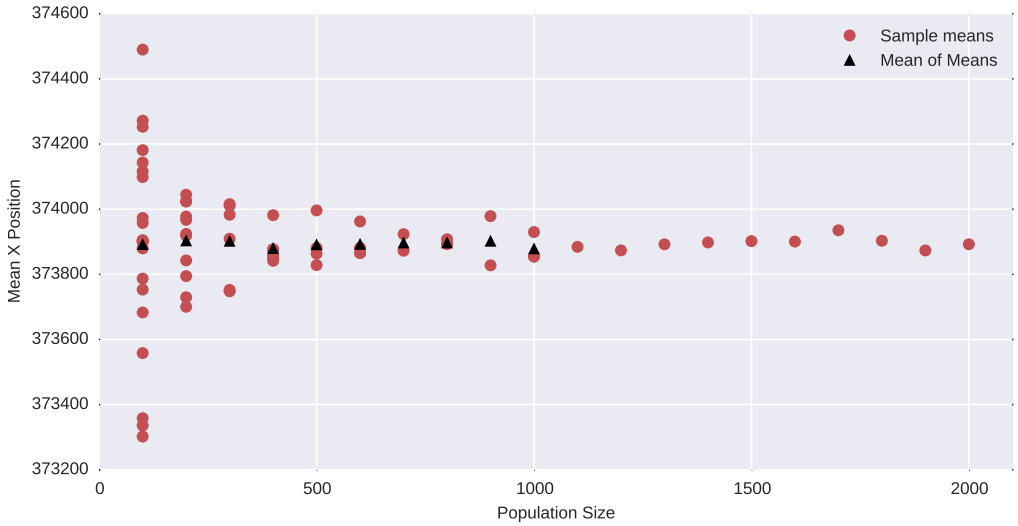

(c) Mean X positions for E-E-HP5MM

Figure 5.5: Mean X positions against sample size

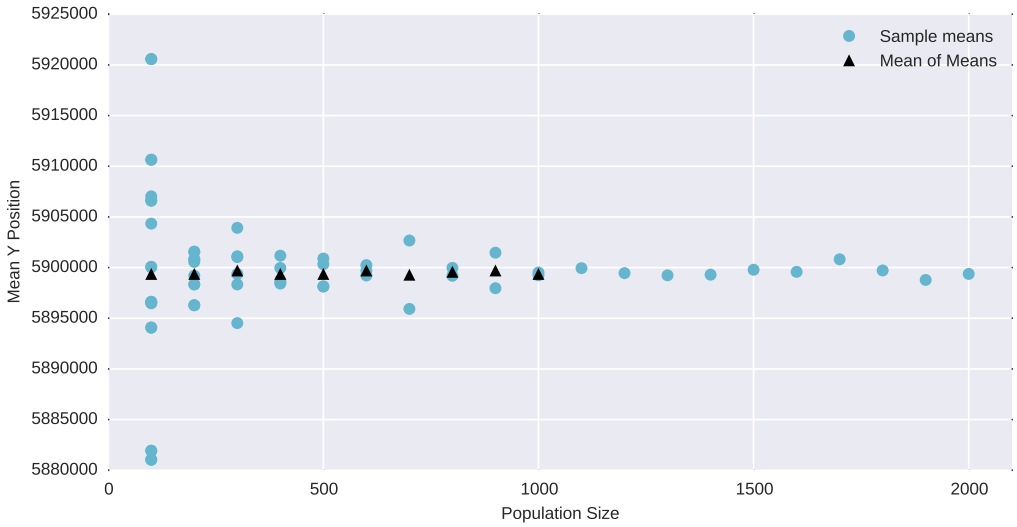

(a) Mean Y positions for A-A-HP5MM

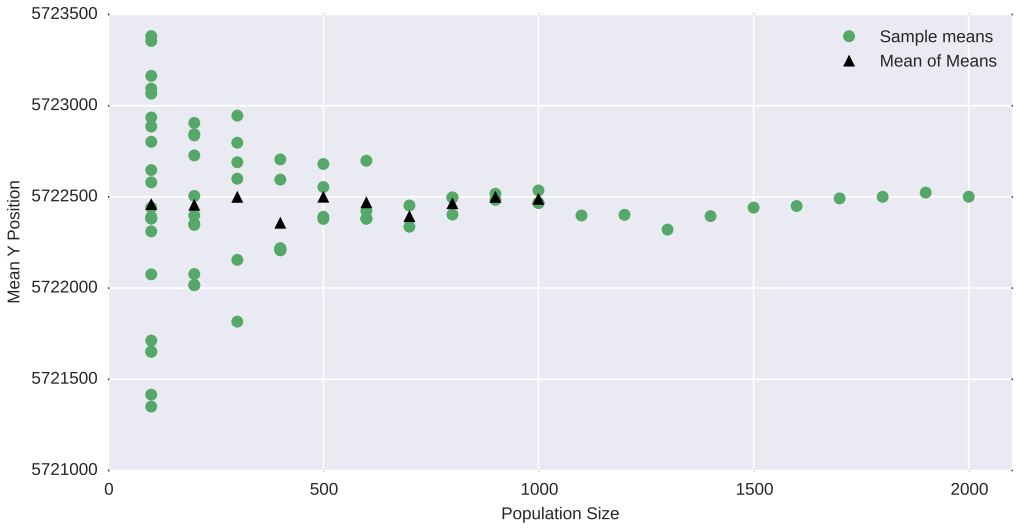

(b) Mean Y positions for C-C-HP5MM

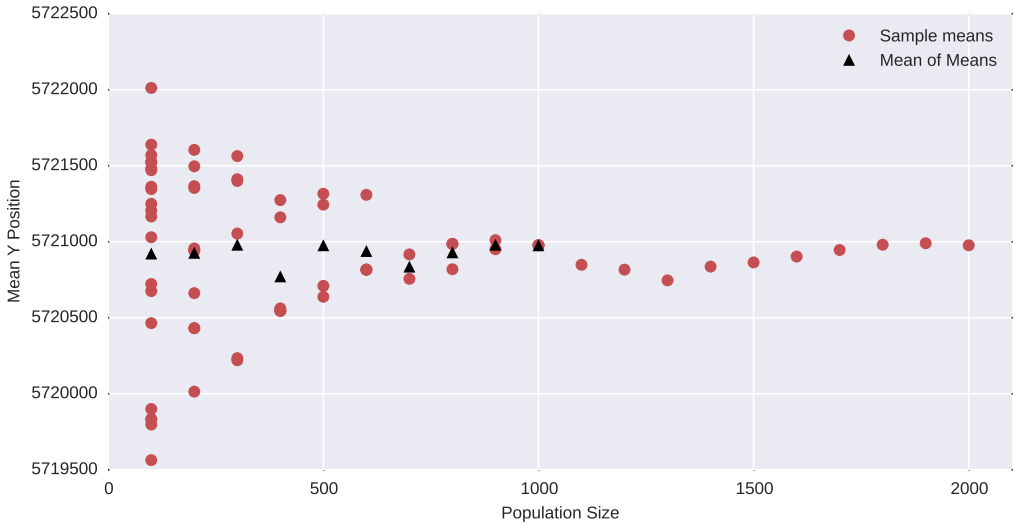

(c) Mean Y positions for E-E-HP5MM

Figure 5.6: Mean Y position against sample size

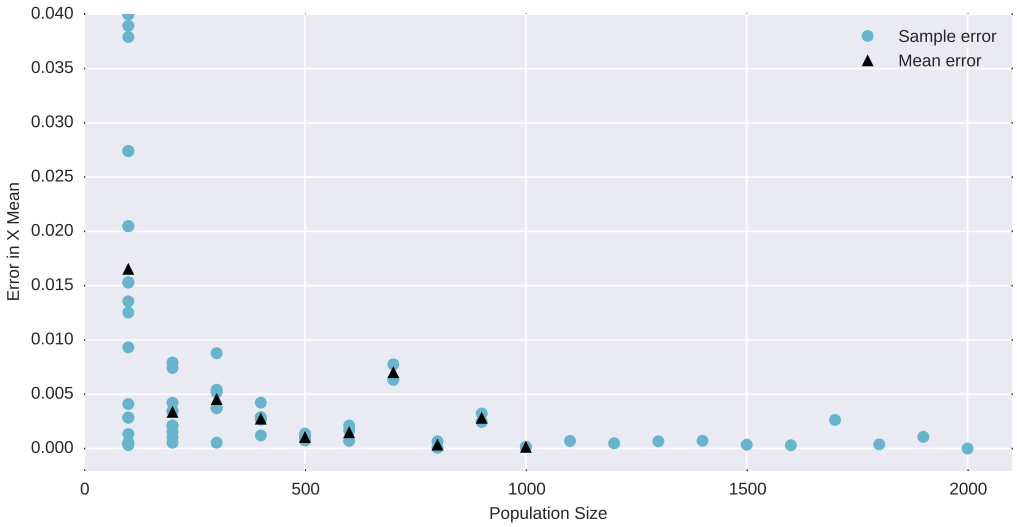

(a) Error in mean X position for A-A-HP5MM

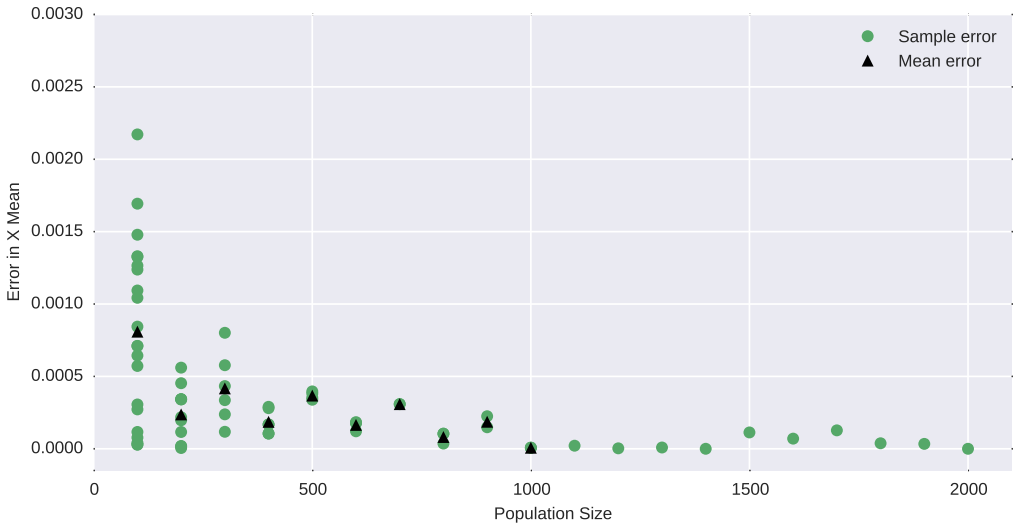

(b) Error in mean X position for C-C-HP5MM

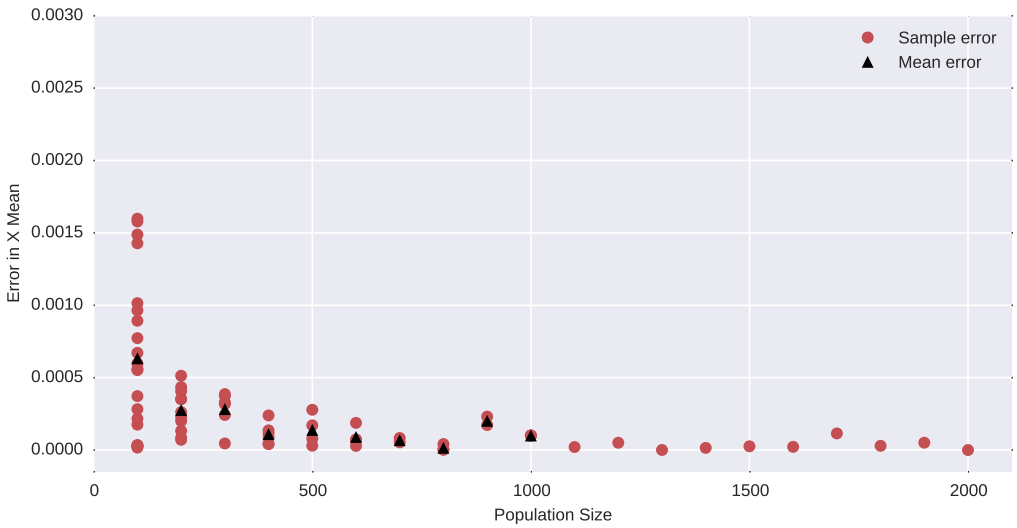

(c) Error in mean X position for E-E-HP5MM

Figure 5.7: Error in mean X position against population size

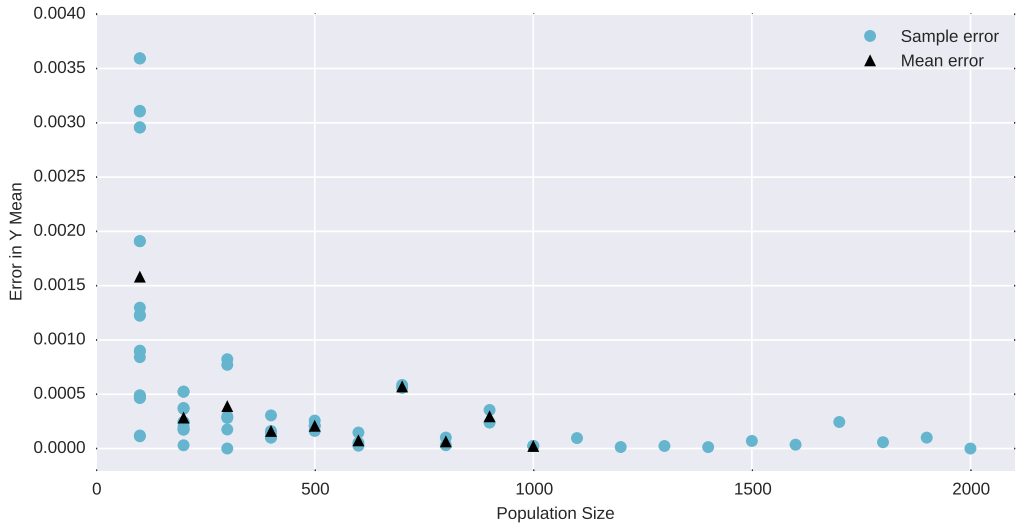

(a) Error in mean Y position for A-A-HP5MM

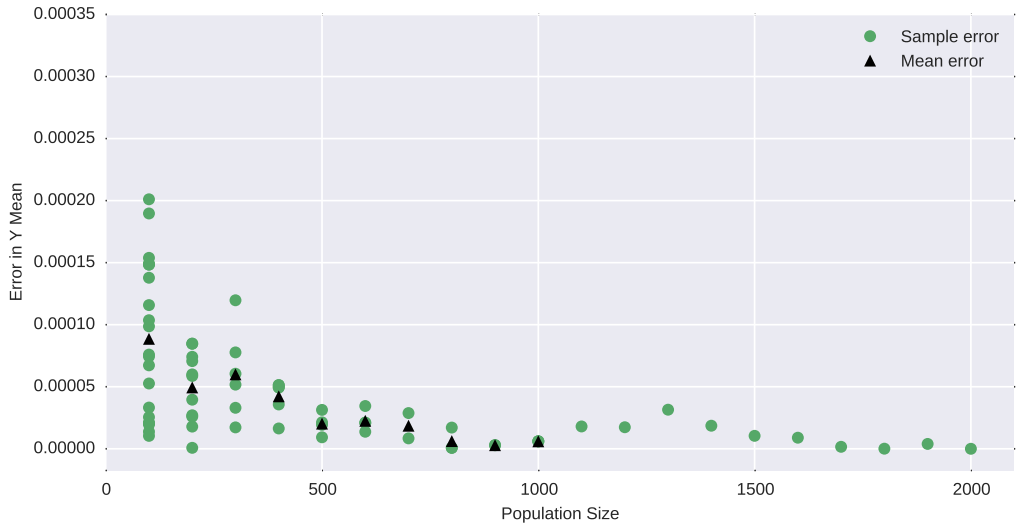

(b) Error in mean Y position for C-C-HP5MM

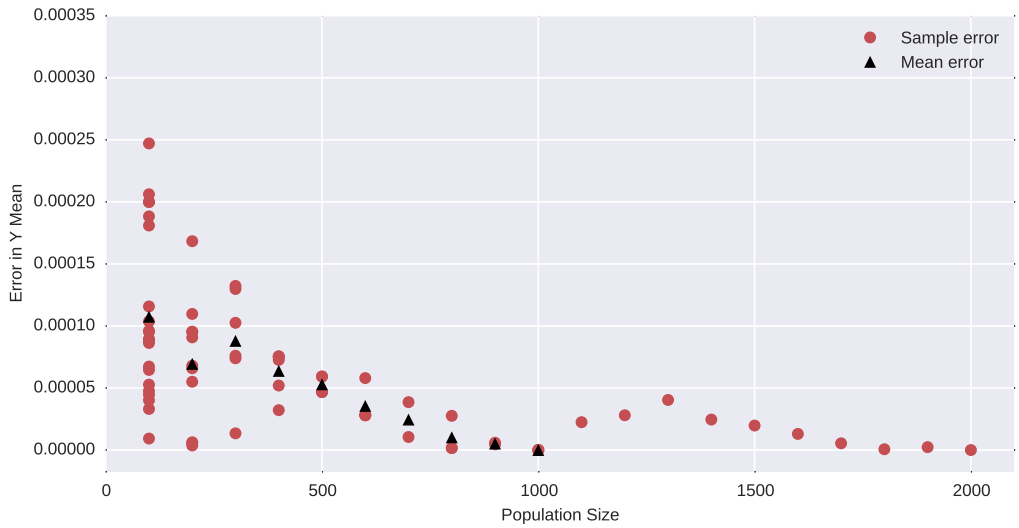

(c) Error in mean Y position for E-E-HP5MM

Figure 5.8: Error in mean Y position against population size

Examining the error in the X positions (Figure 5.7), it can be seen that results split cleanly into two ranges - one for A-A-HP5MM (Figure 5.7a) and one for simulations C-C-HP5MM and E-E-HP5MM (Figures 5.7b and 5.7c). The same pattern is seen in each of the three cases, with little improvement in relative error for increases in sample size beyond 800 individuals. In the case of A-A-HP5MM this yields a relative error below 0.005, with the relative error being below 0.0005 for the remaining two cases.

Moving to the relative error in mean Y position, shown in Figure 5.8, the same split in values and general trends can be seen. The relative error for the mean Y position is an order of magnitude lower than the corresponding cases for the mean X position, largely due to the order of magnitude difference in the coordinates used - as described in section 5.2. This can be improved by examining the change in position over time, accounting for the initial positions.

5.5.2 Displacement of mean position

The displacement of the population mean position has been calculated as described in subsection 5.4.3 for the same simulations (and samples) as the mean position results above. The displacement in X is shown in Figure 5.9 and Figure 5.10 shows the corresponding displacement in Y. These show similar patterns to the mean position data discussed above.

Comparing Figure 5.9a to Figure 5.5a, the overall trends are very similar, with samples of 800 porpoise and above yielding results consistent with the 2000 porpoise case. If the 700 porpoise samples are excluded, the results are consistent for samples of 400 porpoise and above. The pattern is similar for simulations C-C-HP5MM and E-E-HP5MM (Figures 5.9b and 5.9c), although the variation is at a much lower scale than the A-A-HP5MM case (Approximately $\pm$2000m for samples of 100 individuals in C-C-HP5MM and E-E-HP5MM, compared to $\pm$40000m in the A-A-HP5MM case).

Figure 5.10 presents a very similar picture for the displacement in the Y axis, although there is a more obvious variability in values shown in Figures 5.10b and5.10c compared to the X axis counterparts. It should be noted that the total range of results for the Y mean displacement in the C-C-HP5MM and E-E-HP5MM cases is approximately $\pm$1300m (for comparison, the domain measures 368km in the y axis), exaggerating the appearance of the variation in the results presented.

The relative error of the mean displacements was calculated using the same approach as described above for mean positions, substituting $\Delta\bar{x}$ for x in Equation 5.6. The mean displacement for the full population was used as the reference value.

Plots showing the relative error in mean X displacement are shown in figure 5.11. The highest relative error in X is 0.22 and occurs for a sample of 100 porpoise in simulation C-C-HP5MM (Figure 5.11b), with the highest values in A-A-HP5MM and E-E-HP5MM being 0.13 and 0.20 respectively.

For all three simulations, the relative error drops below 0.1 for samples of 400 or more animals, and falls below 0.05 after 600 porpoise. The pattern of results is similar again for the mean Y displacements shown in Figure 5.12, but the values involved are a little higher. The initial relative error reaches just over 0.3 for one sample of 100 porpoise in the C-C-HP5MM simulation (Figure 5.12b). The relative error for all three simulations falls below 0.05 for samples of 800 porpoise or more.

Calculating the displacement of the mean in component form also allows us to visualise the change in XY position of the population mean position by plotting the change in Y against the change in X. This is shown in Figure 5.13a, with each point coloured to indicate which simulation it was drawn from. The results for simulations C-C-HP5MM and E-E-HP5MM are shown in greater detail in Figure 5.13b.

Although these plots contain no new information, they does show that each simulation yields measurably different results, particularly for A-A-HP5MM. The lack of additional noise tolerance applied to the individuals in the A-A-HP5MM simulation means that these individuals travel much further through the domain than in either of the other two simulations. Figure 5.13b also illustrates the impact of the different behaviour weightings on the population positions, with the mean positions of each population forming distinct clusters - even at small sample sizes.

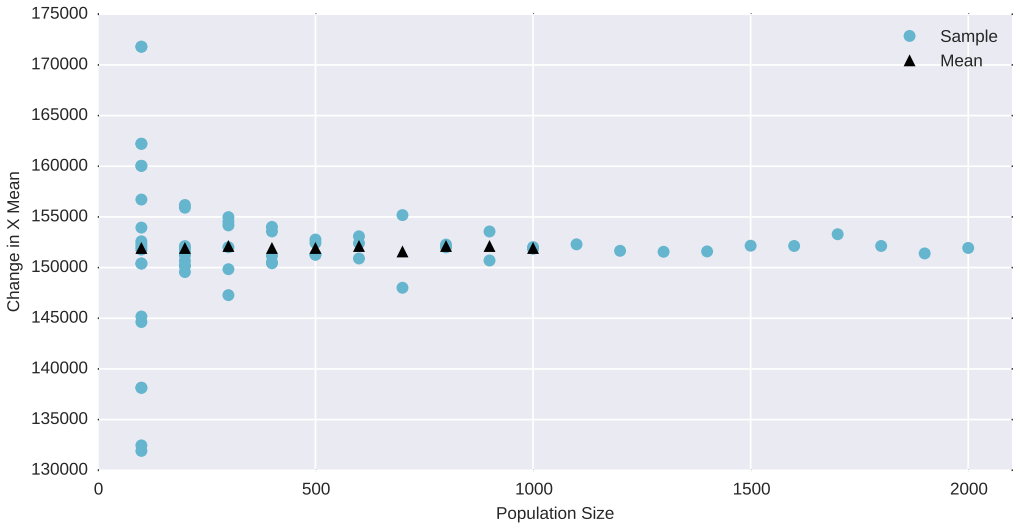

(a) Mean X displacement for A-A-HP5MM

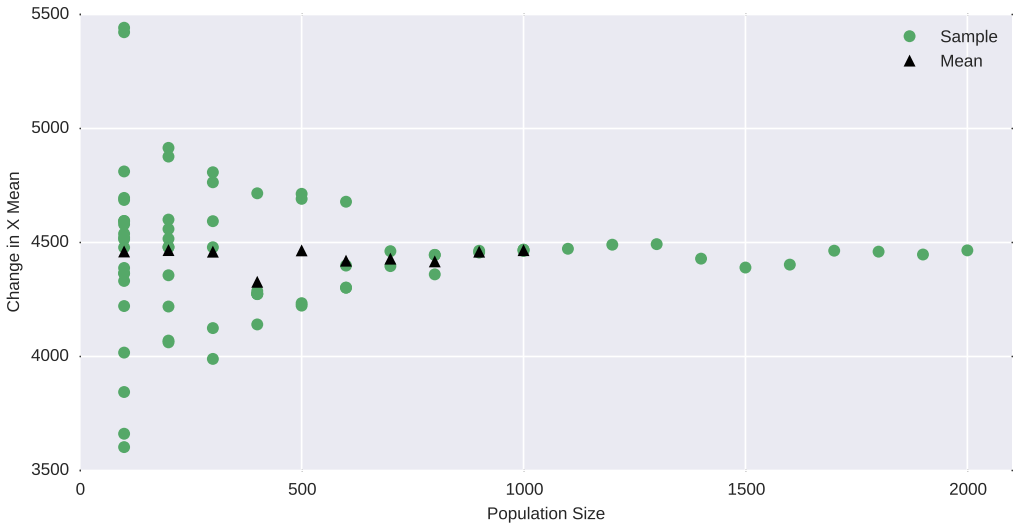

(b) Mean X displacement for C-C-HP5MM

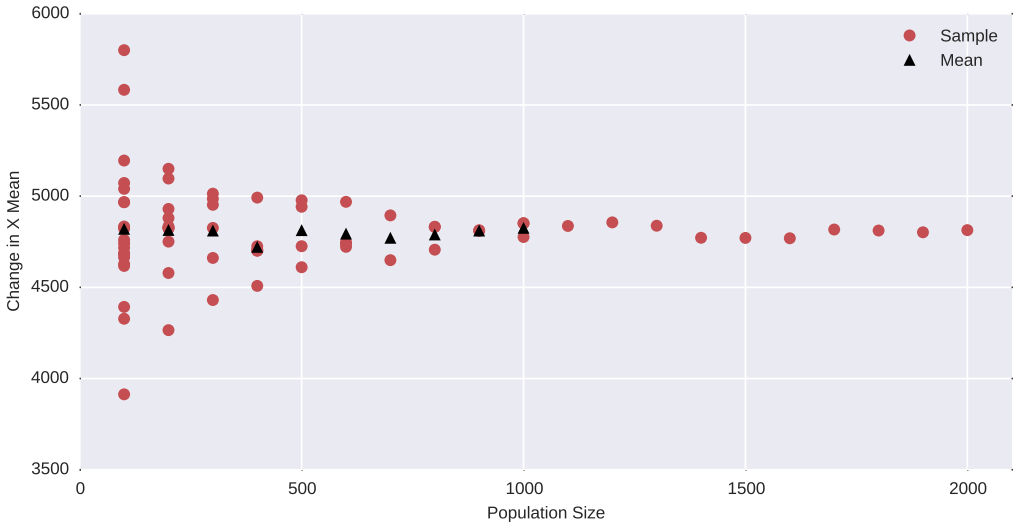

(c) Mean X displacement for E-E-HP5MM

Figure 5.9: Mean X displacement for varying population sizes

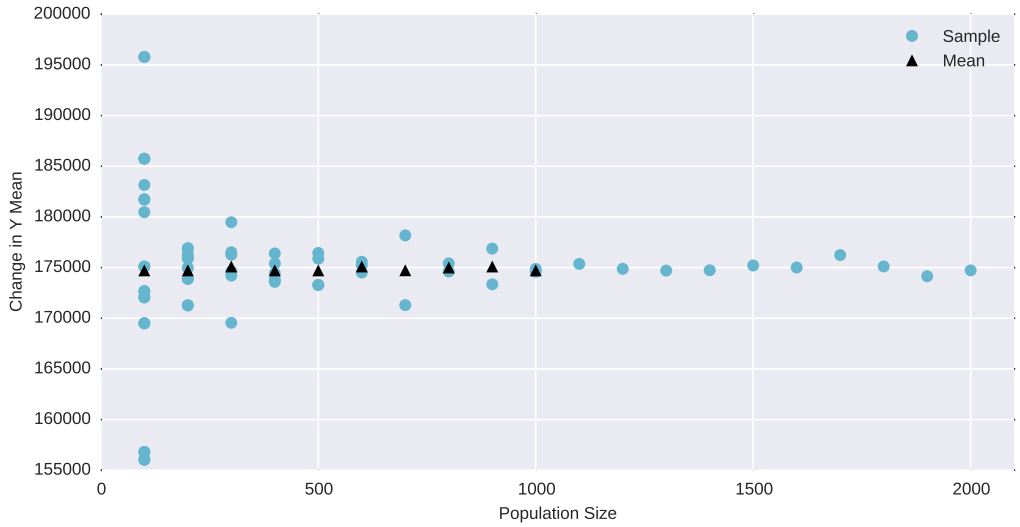

(a) Mean Y displacement for A-A-HP5MM

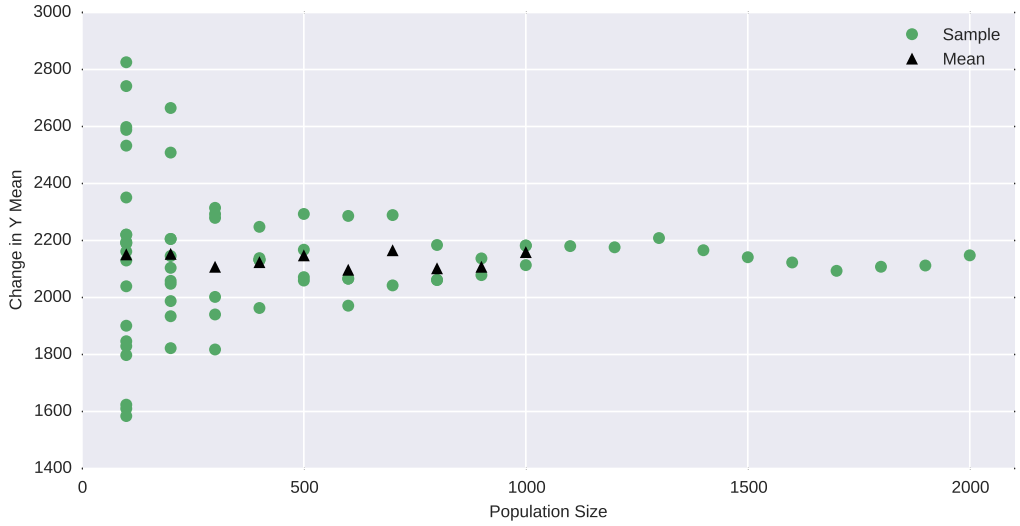

(b) Mean Y displacement for C-C-HP5MM

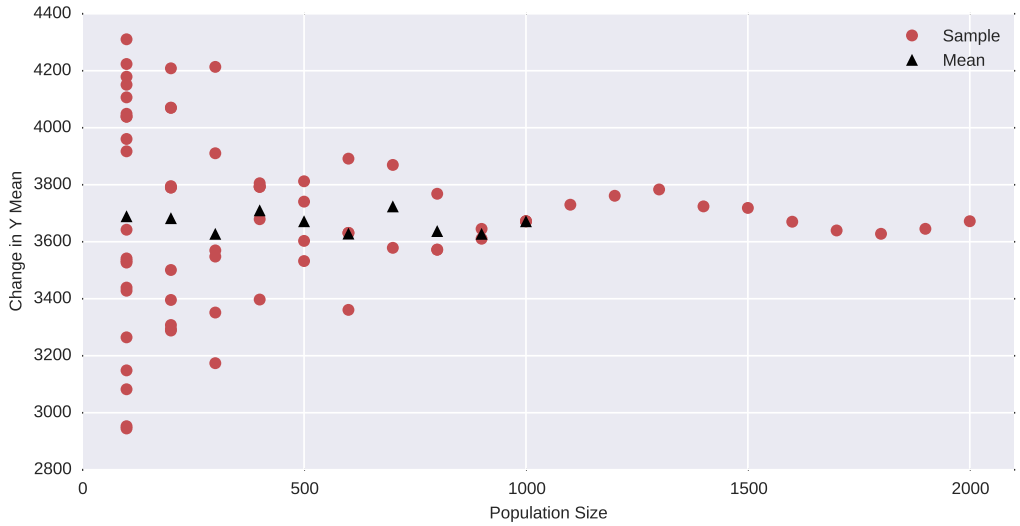

(c) Mean Y displacement for E-E-HP5MM

Figure 5.10: Mean Y displacement against sample size

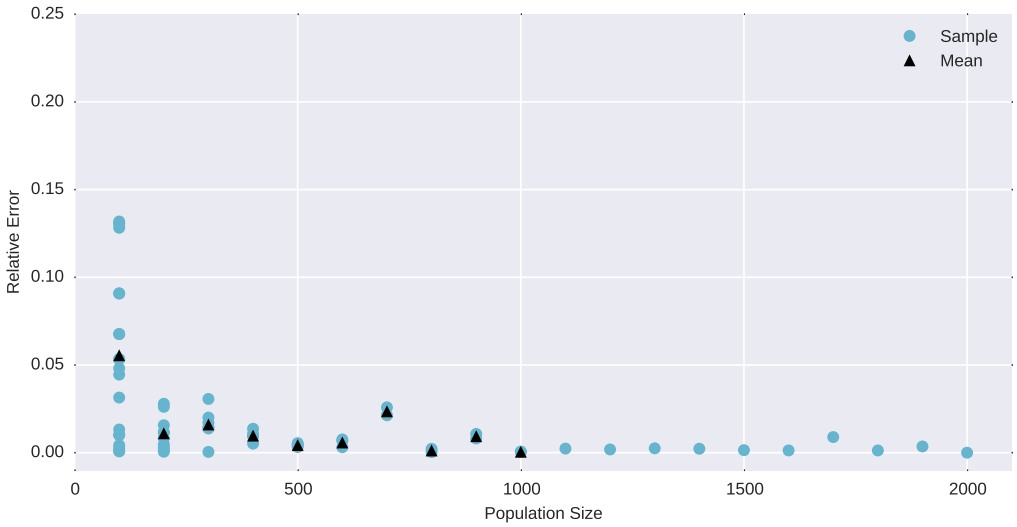

(a) Error in mean X displacement for A-A-HP5MM

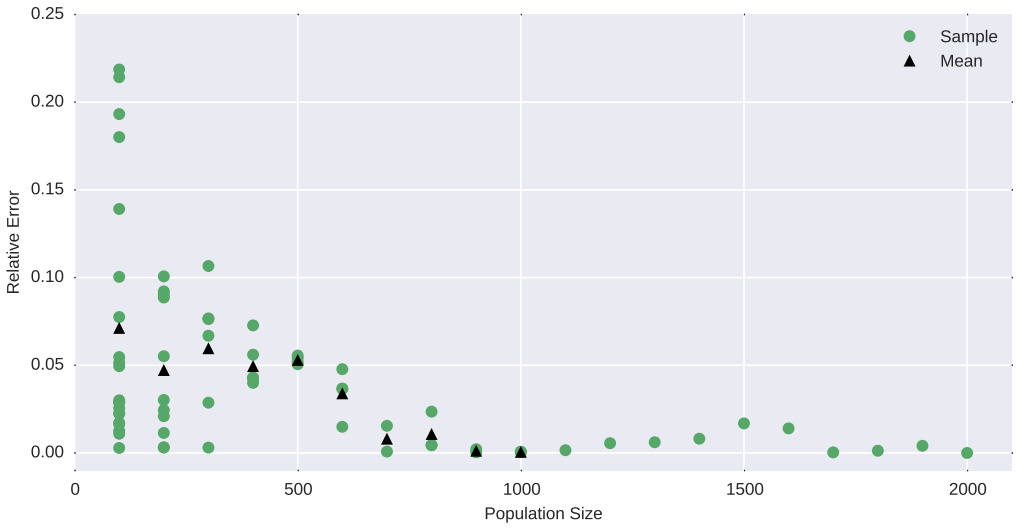

(b) Error in mean X displacement for C-C-HP5MM

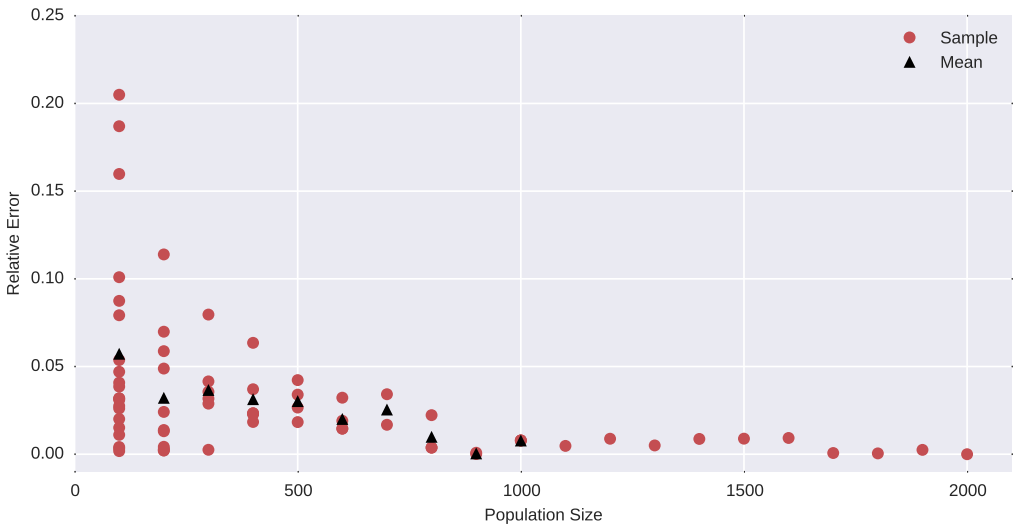

(c) Error in mean X displacement for E-E-HP5MM

Figure 5.11: Error in mean X displacement against population size

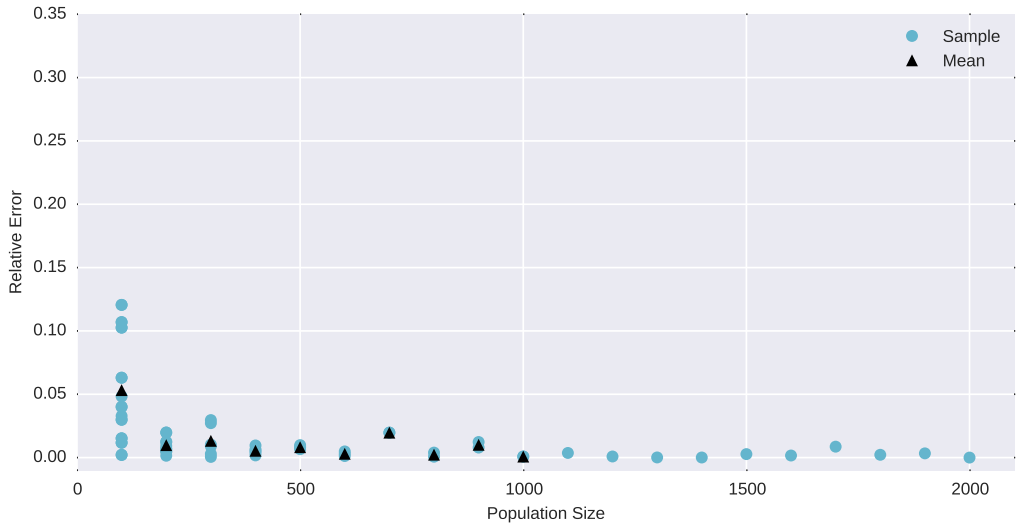

(a) Error in mean Y displacement for A-A-HP5MM

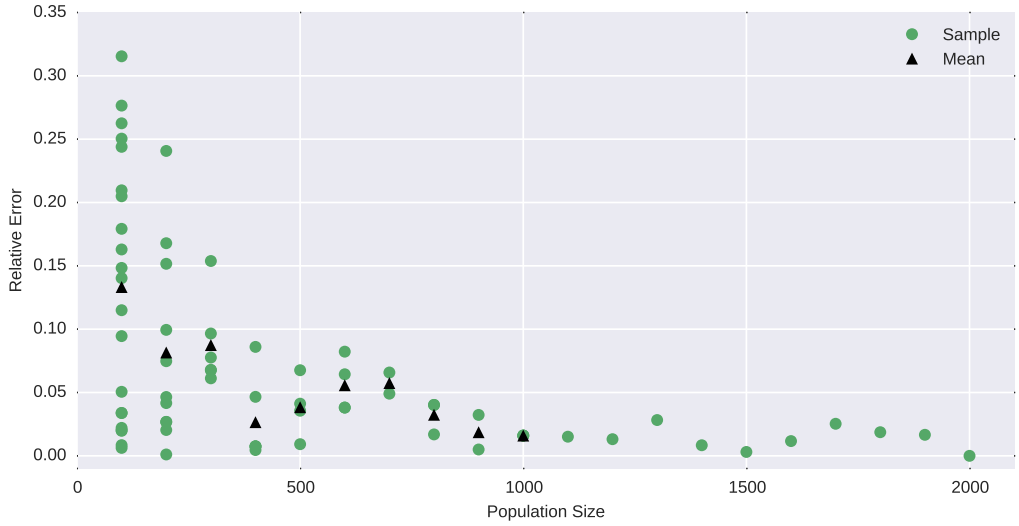

(b) Error in mean Y displacement for C-C-HP5MM

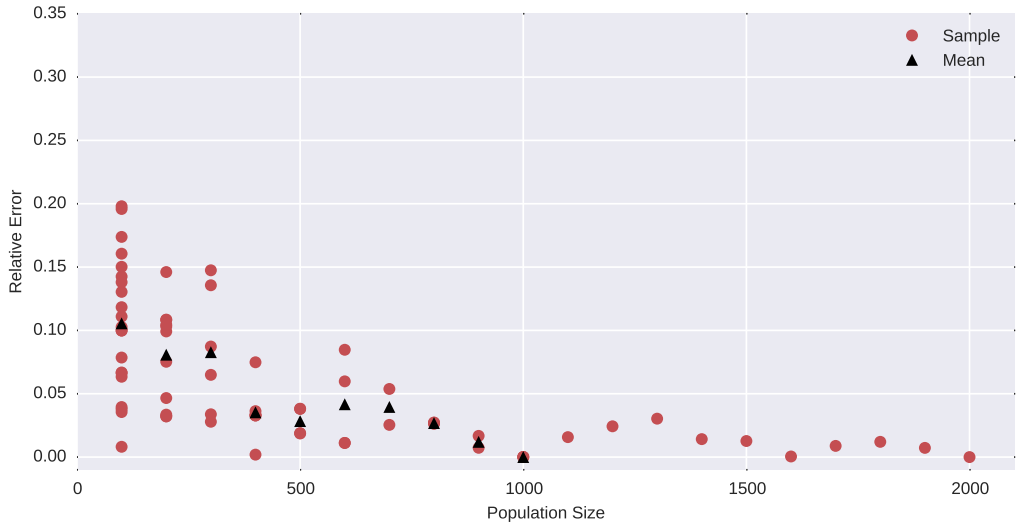

(c) Error in mean Y displacement for E-E-HP5MM

Figure 5.12: Error in mean Y displacement against population size

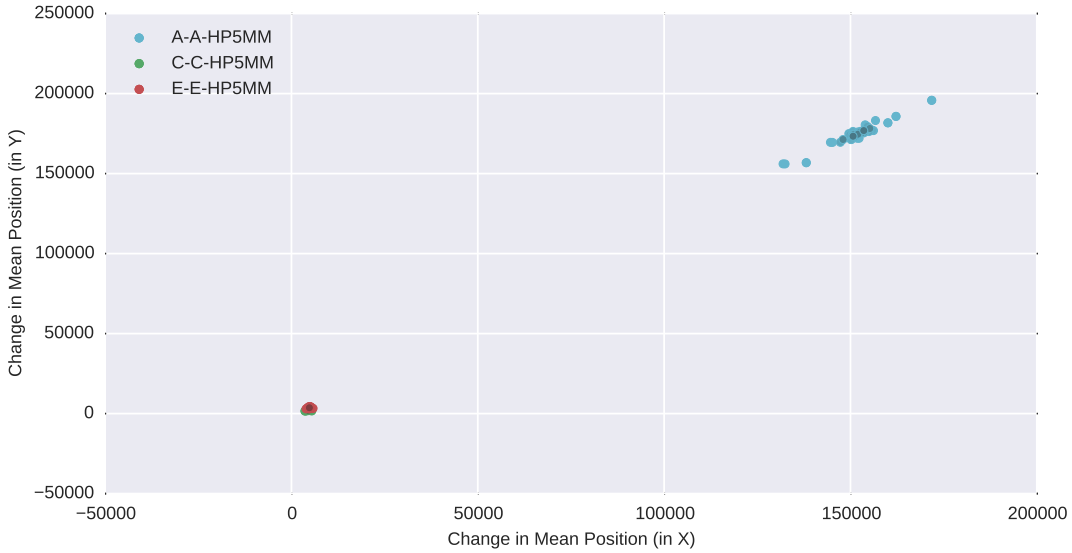

(a) Displacement of mean for all three simulations

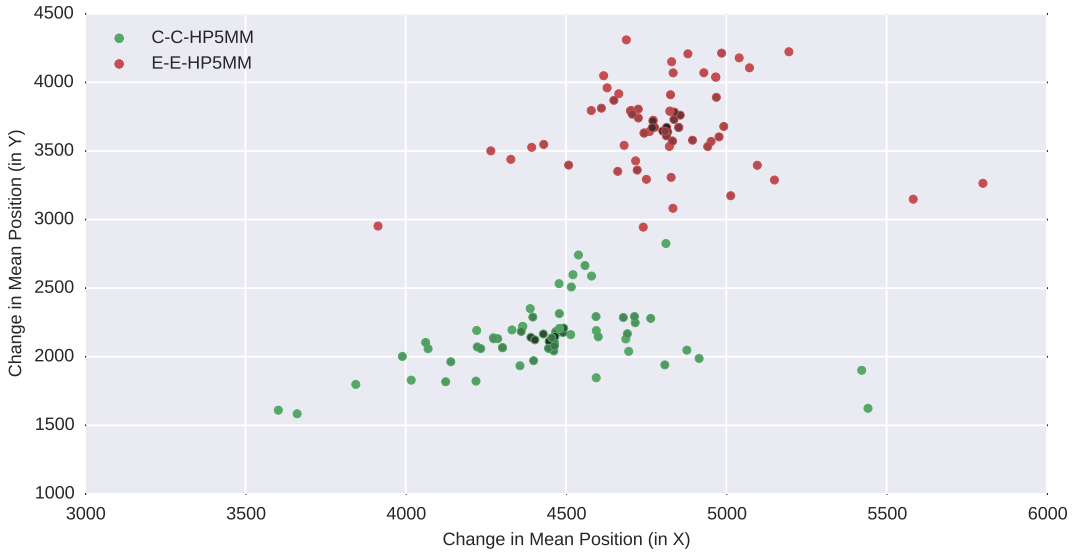

(b) More detailed view of C-C-HP5MM and E-E-HP5MM

Figure 5.13: XY plot showing the displacement of the mean position for simulations A-A-HP5MM (cyan), C-C-HP5MM (green) and E-E-HP5MM (red). Darker markers represent larger samples

5.5.3 Population spread

As described in Section 5.4.2, the standard deviation of position can be calculated in each axis as a measure of the population spread. The standard deviation has been calculated across the same samples as above, and is shown in Figure 5.14 (Standard deviation of X position) and Figure 5.15 (Standard deviation of Y position).

Little of note is present in the 6 graphs shown, with the same general trends present as discussed in Sections 5.5.1 and 5.5.2, with most plots showing stable numerical results for populations of 700 or 800 porpoise.

The sole notable exception to this is the standard deviation in the X axis for simulation E-E-HP5MM, shown in Figure 5.14c. This graph exhibits two distinct "branches" up to and including the 1000 porpoise cases, with one branch centred around 4850m and the other centred loosely around 4725m before trending up, towards the final value of 4800m at 2000 porpoise. This is likely to be due to outlying individuals in the population that are not included in the sample populations forming the upper "branch" of the results.

Plotting the relative error in the standard deviation in X (Figure 5.16) and Y (Figure 5.17) shows the same general trends as before, with the relative error in Y being slightly larger than in X.

Despite the bifurcated behaviour observed in the plots of standard deviation in X for the E-E-HP5MM results (Figure 5.14c), the relative error plot shows only a slight elevation. The slight elevation observed does mean that the relative error remains above 0.01 until the 1000 porpoise samples.

A second notable deviation from the general trend is the relative error in standard deviation in Y for E-E-HP5MM, shown in Figure 5.17c. This converges to a relative error below 0.02, in line with the Y component for the other two simulations, but then "spikes" at 1300 porpoise with a relative error of 0.03. A similar, but far less pronounced, spike can be seen in the other two simulations but cannot be consistently identified in the X data.

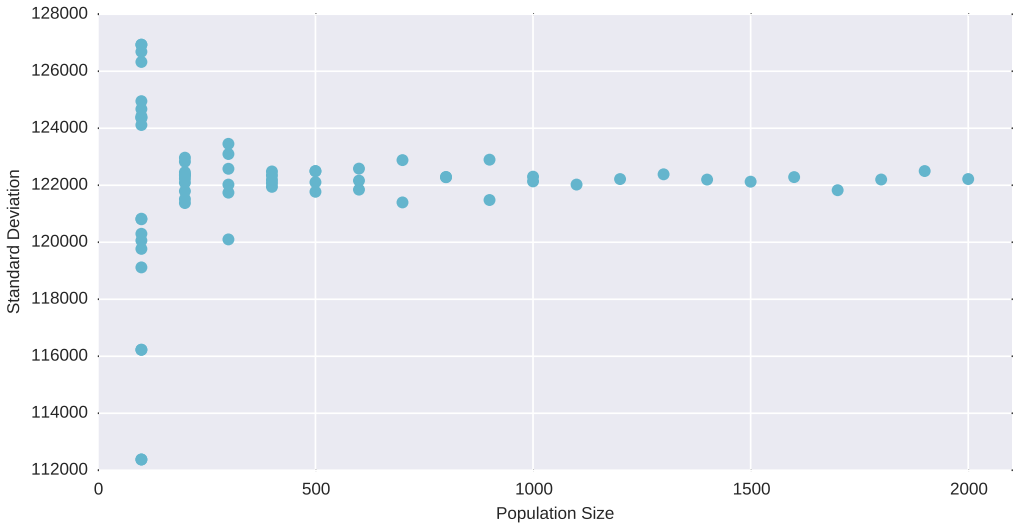

(a) Standard deviation in X for A-A-HP5MM

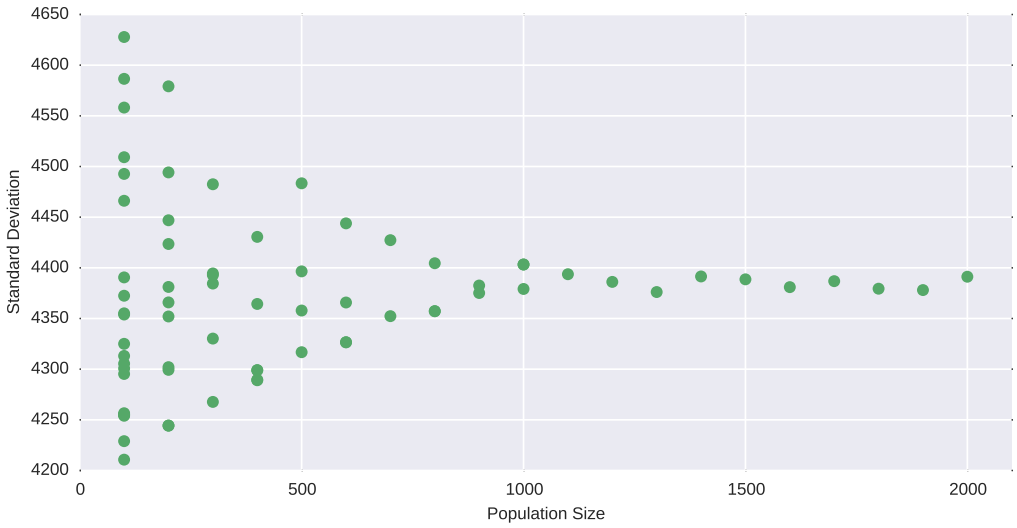

(b) Standard deviation in X for C-C-HP5MM

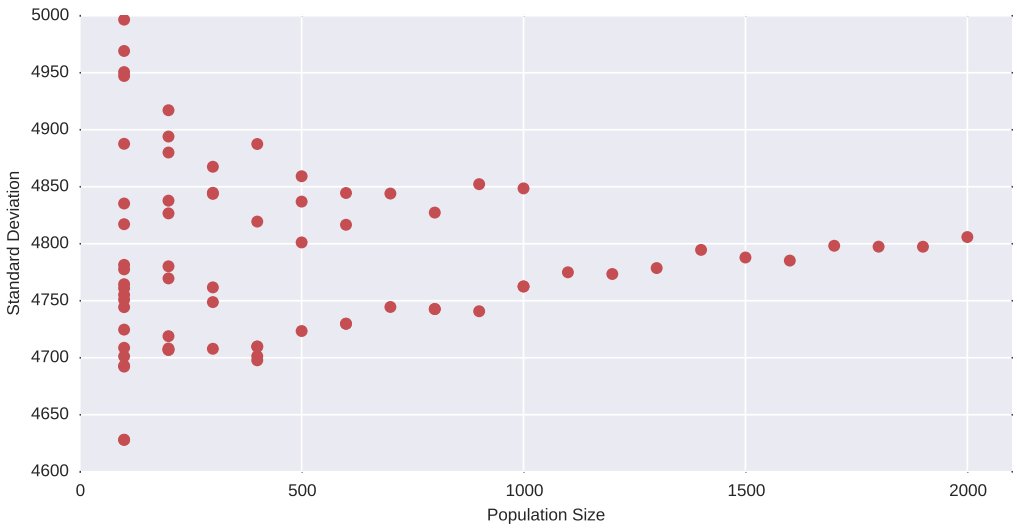

(c) Standard deviation in X for E-E-HP5MM

Figure 5.14: Standard deviation of position in X against sample size

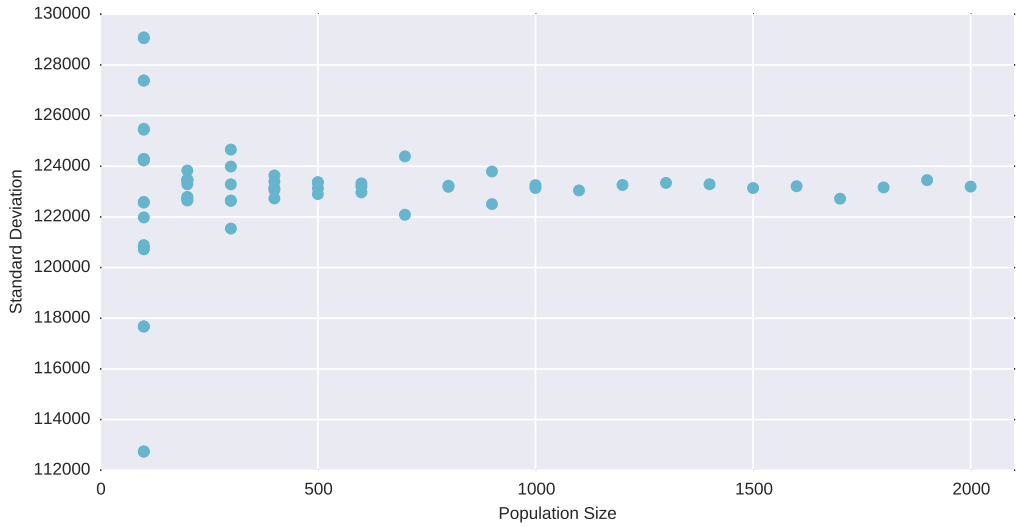

(a) Standard deviation in Y for A-A-HP5MM

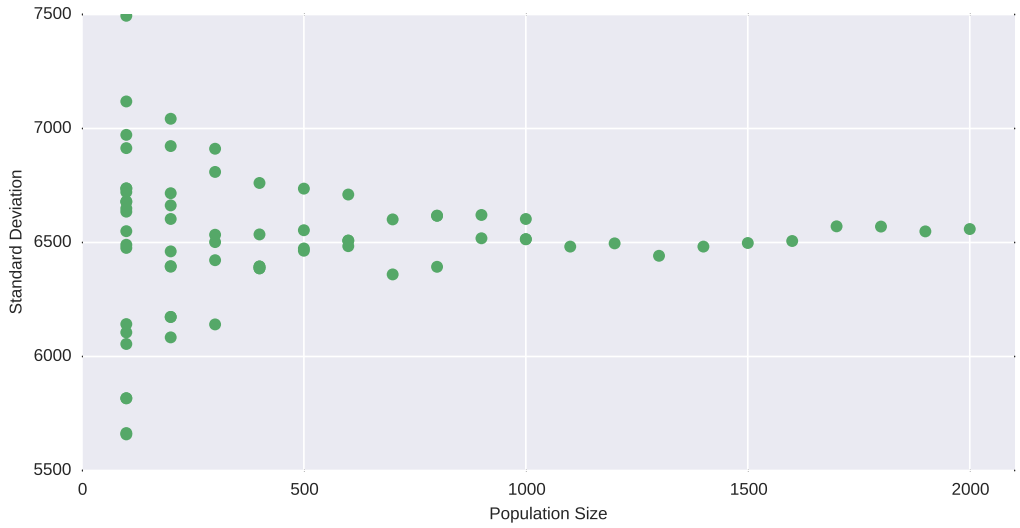

(b) Standard deviation in Y for C-C-HP5MM

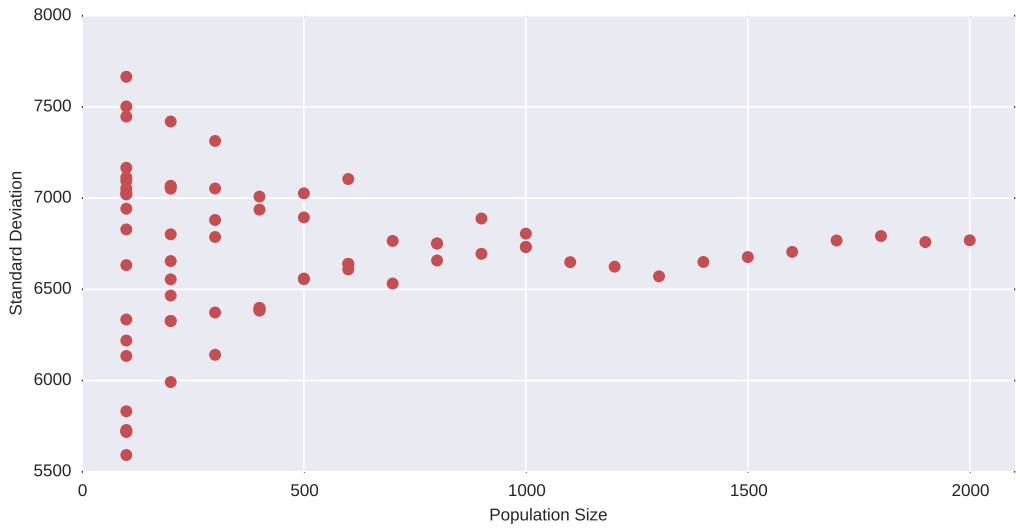

(c) Standard deviation in Y for E-E-HP5MM

Figure 5.15: Standard deviation of position in Y for varying population sizes

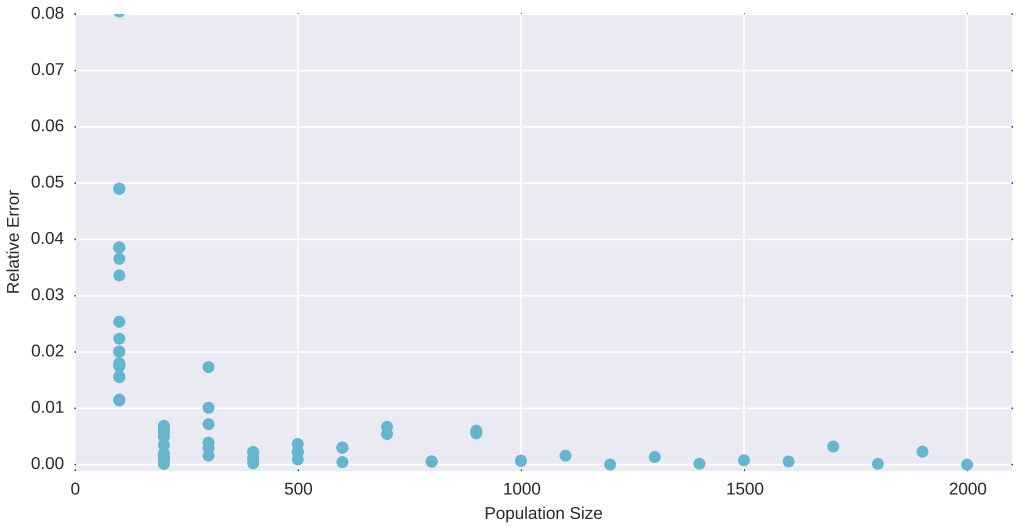

(a) Error in standard deviation in X for A-A-HP5MM

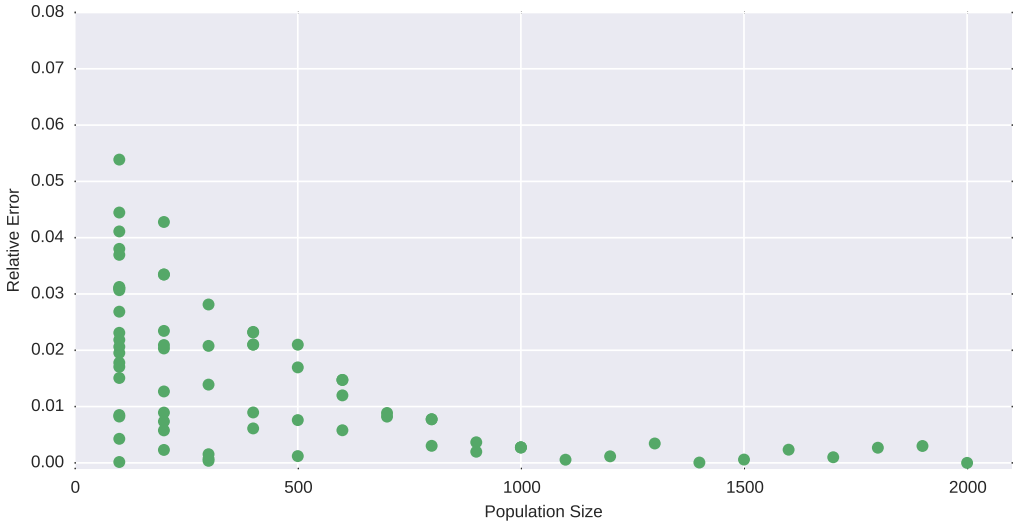

(b) Error in standard deviation in X for C-C-HP5MM

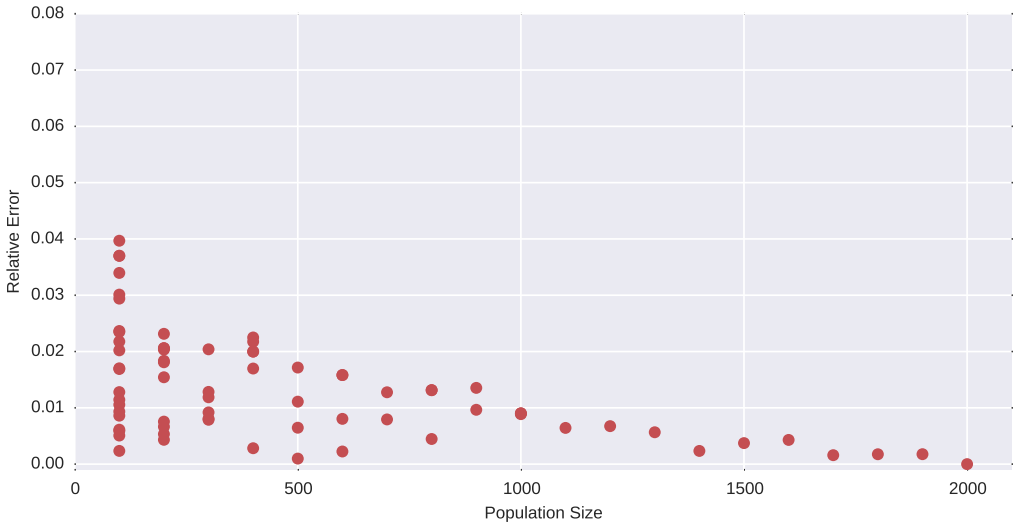

(c) Error in standard deviation in X for E-E-HP5MM

Figure 5.16: Error in standard deviation of position in X against sample size

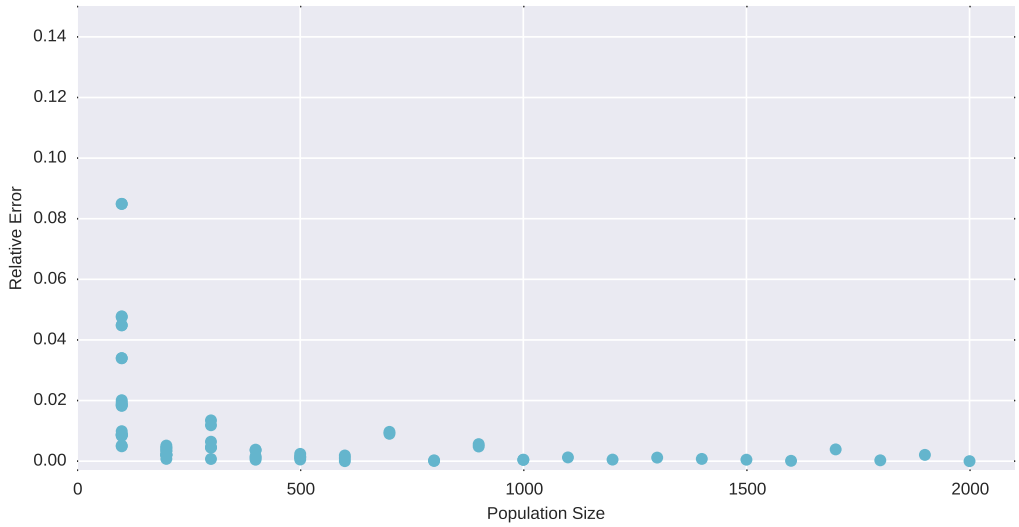

(a) Error in standard deviation in Y for A-A-HP5MM

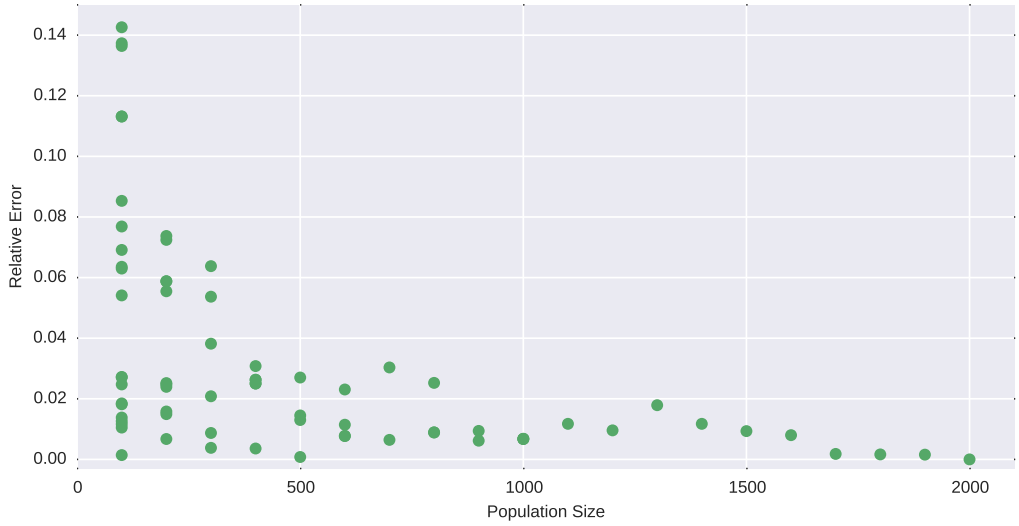

(b) Error in standard deviation in Y for C-C-HP5MM

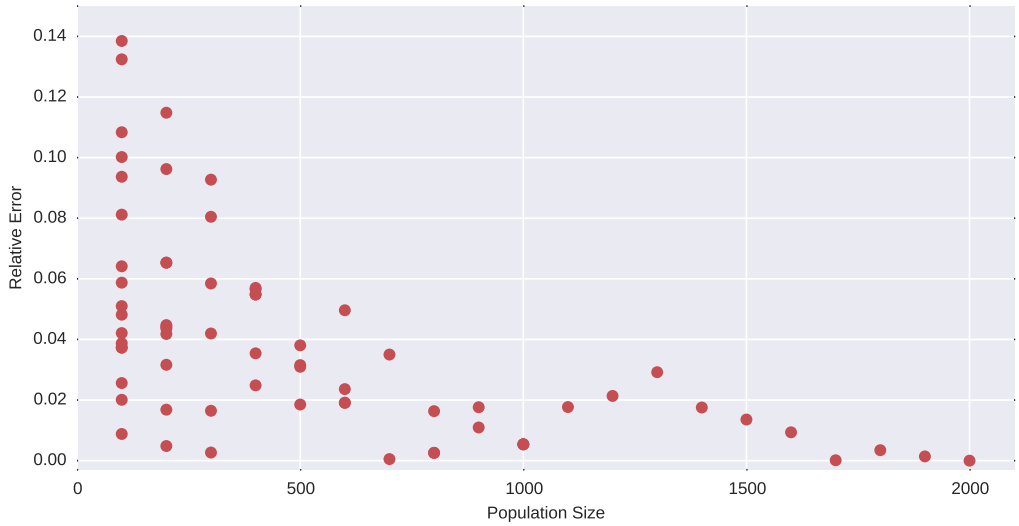

(c) Error in standard deviation in Y for E-E-HP5MM

Figure 5.17: Error in standard deviation of position in Y against sample size

Change in Standard Deviation

The change in standard deviation is calculated as described in Section 5.4.3, and plots of these results are shown in Figures 5.18 and 5.19.

The initial starting population for the model had a standard deviation of 6056m in X and 5942m in Y, however in order to represent the data consistently, the standard deviation of each batch was subtracted from its own initial value rather than the global population standard deviation.

Starting with the change in standard deviation in X, it can be seen that A-A-HP5MM (Figure 5.18a) represents a large dispersion of the group, with the standard deviation increasing by more than 116km (the initial standard deviation being $\sim$ 6km). The other two simulations shown in Figure 5.18 show a population that has clustered together relative to the initial distribution, with both simulations yielding a negative value for the change in standard deviation (-1362m and -946m for C-C-HP5MM and E-E-HP5MM respectively).

The change in standard deviation in Y is positive for all simulations shown in Figure 5.19, representing populations which have dispersed along the Y axis relative to the initial starting population. The change in standard deviation in Y is 118km for A-A-HP5MM, 878m for C-C-HP5MM and 1088m for E-E-HP5MM. The substantially larger value for A-A-HP5MM (in both axis) is expected due to widely diverging final positions of the individuals in that population, with individual animals reaching or in close vicinity to the western and northern boundaries of the domain. It is also consistent with the change in mean population position shown in Figure 5.13a. The values for the remaining two simulations suggest that, although the population is more closely spaced in the X axis, the individuals are spread slightly further in the Y axis - transforming the initial rectangular population distribution into something along the lines of an ellipse with the major axis closer to the Y axis (North-South) than the X axis (East-West).

The differences between each simulation can be seen more clearly in Figure 5.20a, which shows the change in standard deviation for each simulation and sample size in a similar manner to the change in mean position illustrated in Figure 5.13a. Simulation A-A-HP5MM immediately stands apart from the other two, showing the large change in both axis. Figure 5.20b shows simulations C-C-HP5MM and E-E-HP5MM in closer

detail. Although the two simulations do occupy distinct clusters on the graph, there is more overlap between the results than in the change in mean case. This suggests a similar net effect on population spread between the two simulations, despite the very different combination of behavioural rules implemented in each simulation.

5.5.4 Population Positions

To visualise the overall behaviour of each of the 3 simulations, the mean position over time can be plotted as shown in Figure 5.21. In the overall plot (Figure 5.21a), the movement of the mean position of population A-A-HP5 dominates as it moves towards the domain boundary due to the porpoise exiting the domain to the north east in that simulation. If these results are excluded and the two remaining simulations plotted separately (Figure 5.21b), then the tidal influence of the motion can clearly be seen. Each simulation moves from the initial mean position (triangles, top right corner of Figure) towards the South West before settling into a pattern of movement resembling a tidal ellipse. This is consistent with the majority behaviour of the individuals being in the "default" mode - combining food seeking and effort minimisation behaviours. Notably, the two sets of behaviour do show a different mean position at the final timestep (Figures 5.5 and 5.6) as well as the different longer term pattern of movement displayed in Figure 5.21b.

5.6 Conclusions

In the above sections, the results of a number of measures have been presented and their dependence on population sample size discussed. Looking at the relative errors for each variable, the suitable minimum batch size can be determined by selecting the maximum tolerable relative error. The required sample size to reduce all relative errors below 0.5, 0.1 and 0.01 were investigated and are shown in Table 5.3. The "Constraint" column represents the field which was the last to converge below the specified limit - in all instances this was the relative error in the change in standard deviation in the Y axis. If this field is excluded then the population required to converge on a relative error below 0.05 is reduced to 1000 individuals, constrained by the relative error of the displacement of the mean position in the X axis.

[3]The 2000 porpoise cases all have relative error of zero, by definition

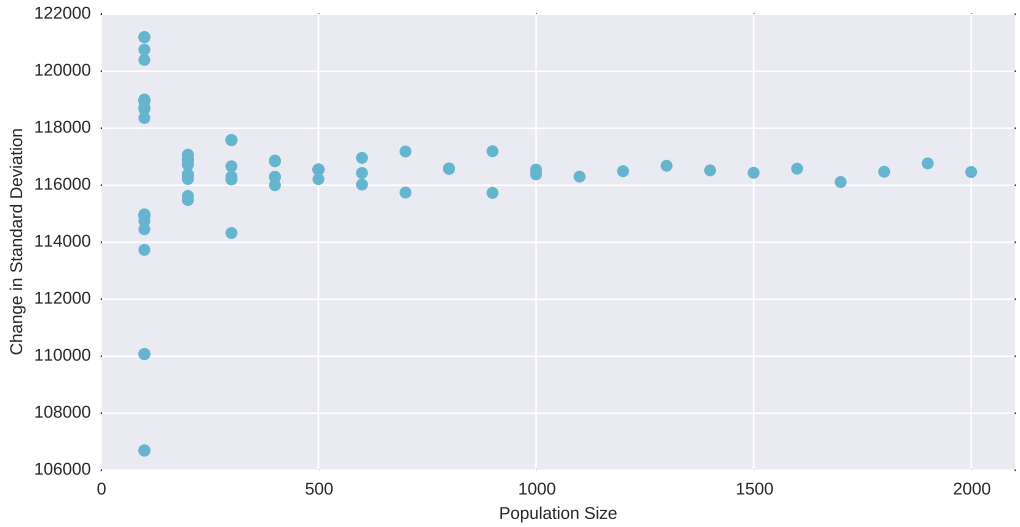

(a) Change in standard deviation in X for A-A-HP5MM

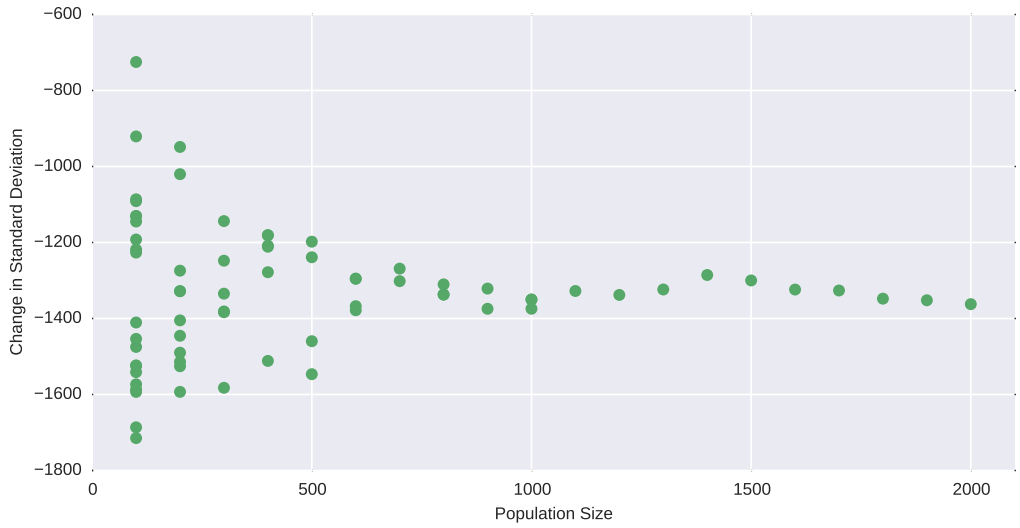

(b) Change in standard deviation in X for C-C-HP5MM

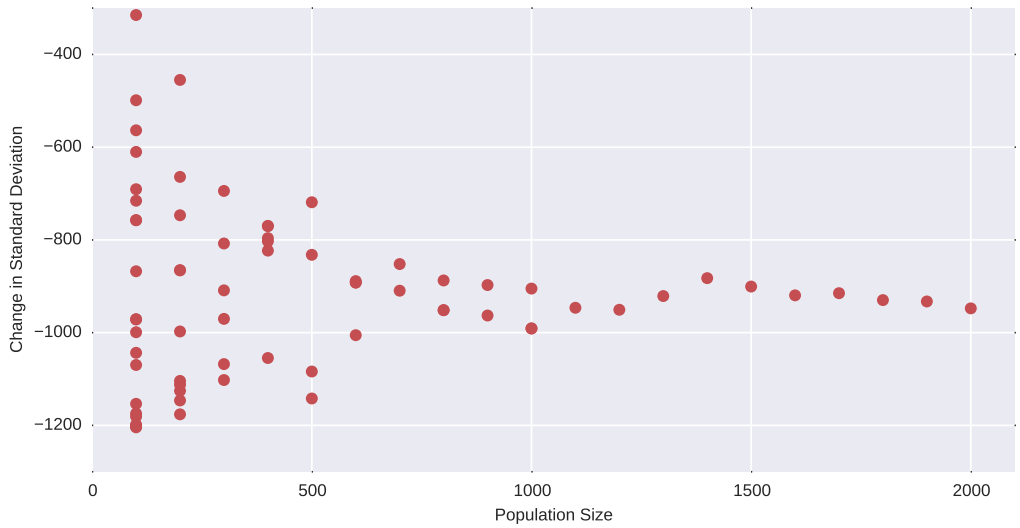

(c) Change in standard deviation in X for E-E-HP5MM

Figure 5.18: Change in standard deviation of position in X against sample size

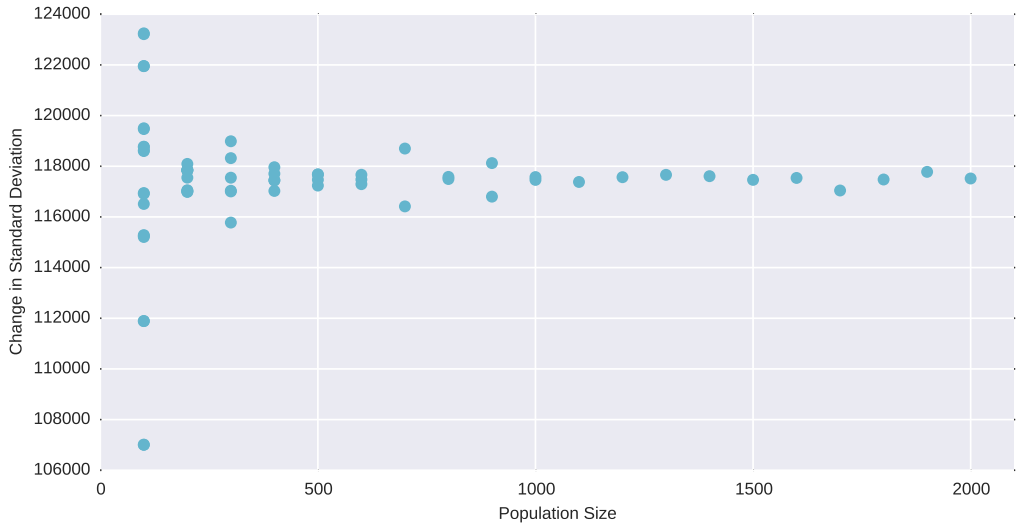

(a) Change in standard deviation in Y for A-A-HP5MM

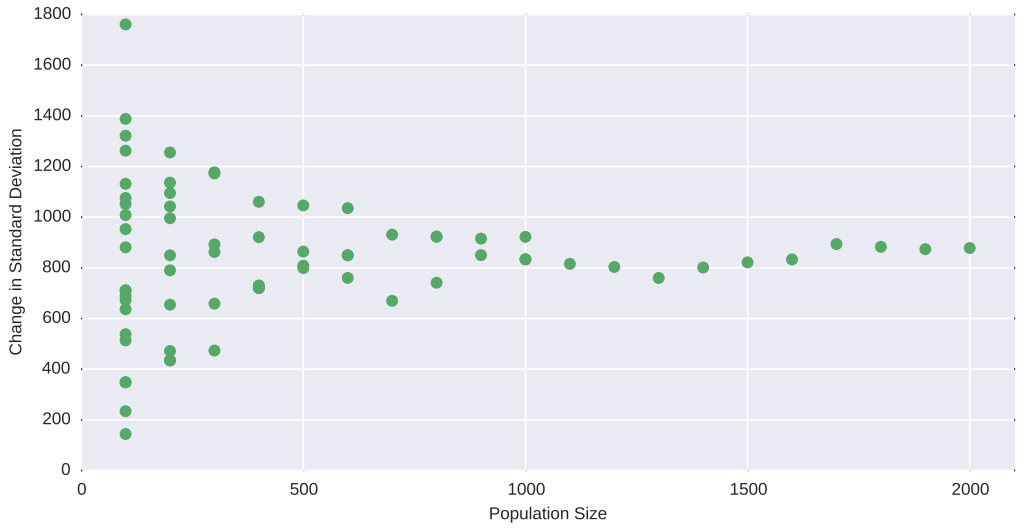

(b) Change in standard deviation in Y for C-C-HP5MM

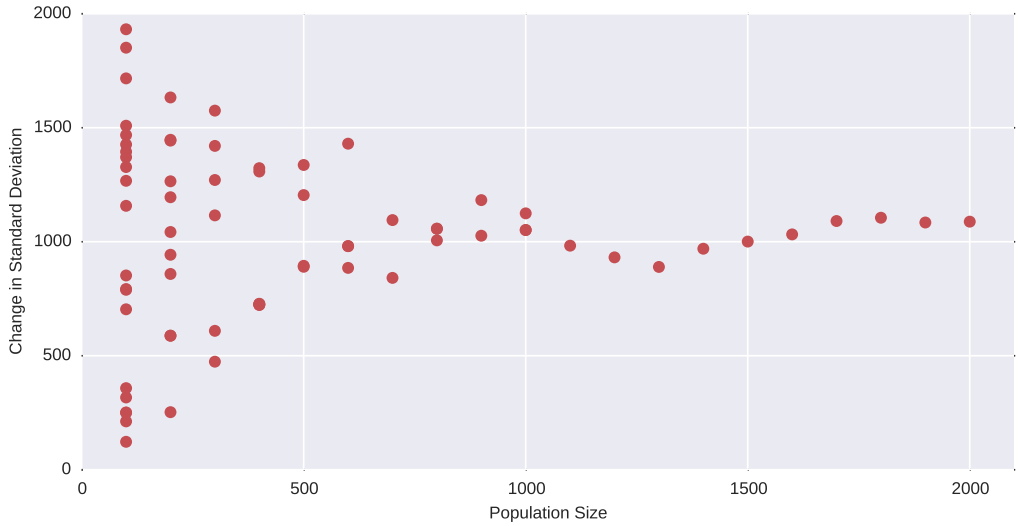

(c) Change in standard deviation in Y for E-E-HP5MM

Figure 5.19: Change in standard deviation of position in Y against sample size

Max(error)	Sample Size	Constraint
0.5	400	Change in standard deviation (Y)
0.1	900	Change in standard deviation (Y)
0.05	1700	Change in standard deviation (Y)
0.01	Not possible[3]	Change in mean position (Y) and change in standard deviation (X)

Table 5.3: Sample sizes required to achieve a given relative error

Based on the values discussed, populations of 1700 individuals should be considered the minimum useful population size where measures of the population spread are required. If simulations are to be run that only consider the mean position values, then this requirement can be relaxed to 1000 individuals. This should provide results with a relative error against the 2000 porpoise reference cases that is 5% or below.

These results are, however, based around a single scenario, with features of interest grouped into a small area in the south west of the domain, and do not take into account the effect of input data limitations such as timestep size and mesh density. In addition, no effort has been made to relate the statistical measures to the underlying tidal model or to account for the residual tide when measuring positions. These may be worth consideration in future work.

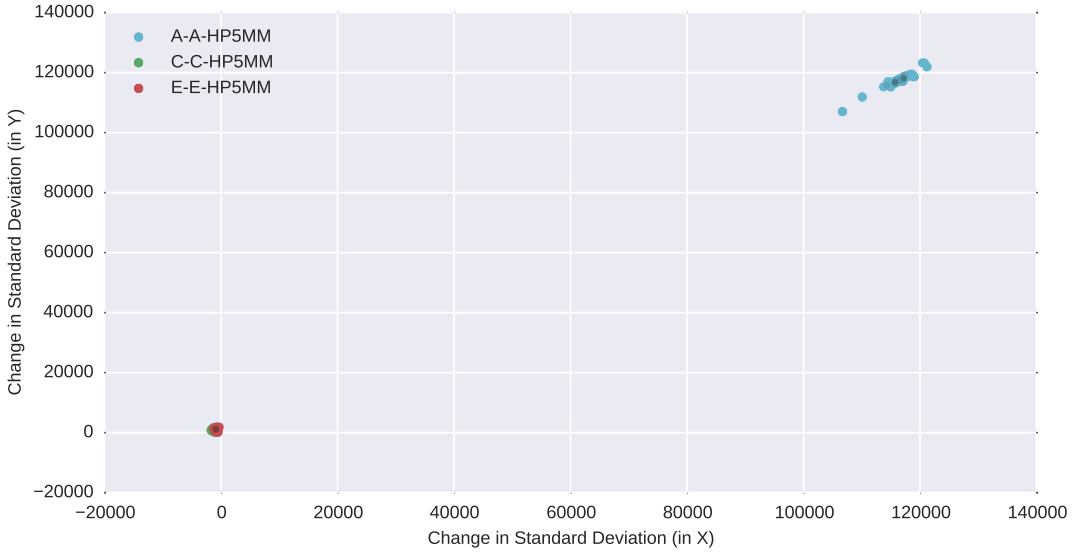

(a) Change in standard deviation for all three simulations

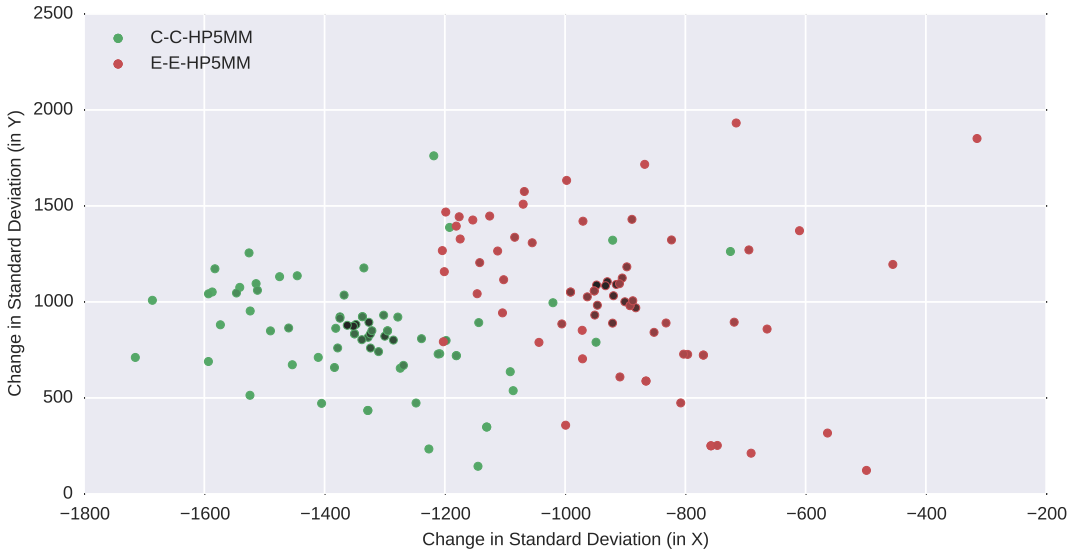

(b) More detailed plot of C-C-HP5MM and E-E-HP5MM

Figure 5.20: XY plot showing the change in standard deviation position for different size samples of three simulations: A-A-HP5MM (cyan), C-C-HP5MM (green) and E-E-HP5MM (red). Darker markers represent larger samples

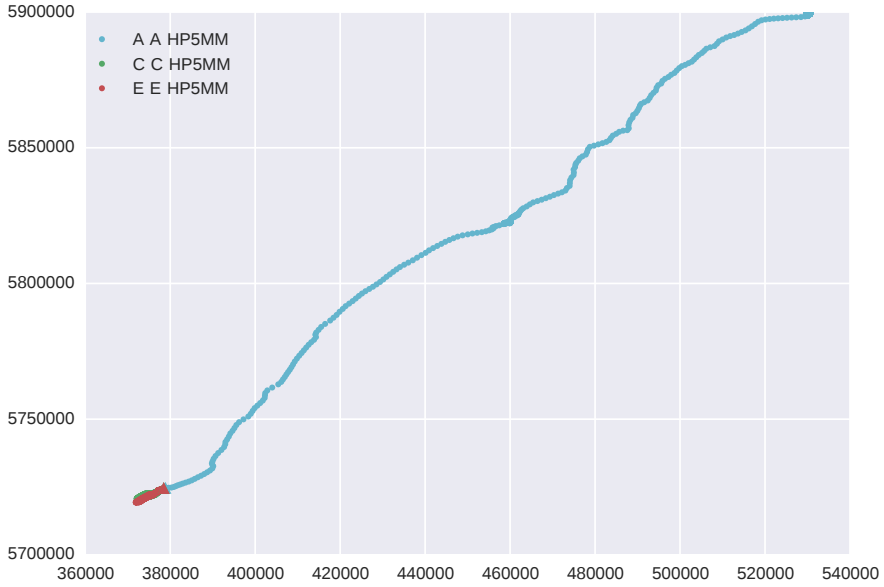

(a) Population mean position over 60 days

(b) Population mean position over 60 days for C-C-HP5MM and E-E-HP5MM

Figure 5.21: XY plot showing population mean position for 2000 porpoise over 60 days at 30 minute intervals

Chapter 6

Parametric Exploration

"If it looks like a duck, and quacks like a duck, we have at least to consider the possibility that we have a small aquatic bird of the family Anatidae *on our hands. "*

Douglas Adams - Dirk Gently's Holistic Detective Agency (1987)

6.1 Introduction

One of the design aims of the model and its associated tools has been to provide a simple, baseline set of behaviours that can be easily adjusted to match behavioural responses in an observed population. The general background and internal layout of the model have been presented in previous chapters, as well as different ways to measure the model outputs and the sensitivity of those outputs to different population sizes. In order to allow the behaviours to be easily adjusted, the model has a number of free parameters that can be supplied at runtime in simulation case files and affect the response of individuals to their surrounding environmental conditions at every step of the simulation. This can then lead to substantially different population level responses to the same environmental conditions.

In order to demonstrate these effects, and to provide some detail on how sensitive the population level responses to these parameters can be, 50 simulations have been run using a range of values for the parameters. The outputs of these simulations can then be used to provide a guide to both the range of behavioural patterns that can be observed from the simulations, but also some reference values and considerations to take into account when setting up and developing simulations in the future.

The simulations presented here are a purely theoretical exercise, exploring the variation in model outputs based on varying the input parameters. Some of the parameters used are deliberately unrealistic in order to show the variation in possible model outputs.

6.2 Model Environment

This study makes use of the same 60 day North Sea TELEMAC model used in the previous chapter, described in Section 5.2. The domain mesh and timesteps are identical, and each (hourly) mesh timestep is split into 400 simulation timesteps - giving each simulation timestep a duration of 9 seconds.

The food and noise sources used were also retained with the same positions and values as shown in Figures 5.2a and 5.2b. These values are arbitrary and unitless, which should be taken into consideration when viewing the results in terms of the parameter values stated. This does, however, allow for similarly arbitrary combinations of data to be

used provided that the noise threshold and multiplier and the food weightings are set appropriately.

6.3 Parameter Space

The three main free parameters available in the model are the Food vector weighting, a noise threshold multiplier and the initial starting positions of the simulated porpoise. There are additional parameters that can be adjusted - including the depth threshold for the shallow water behaviour rules and the raw value of the noise threshold, as well as other initial properties of the porpoise population such as orientation and initial velocity. The three main parameters chosen give rise to the main variations in behaviours, so constraining the parameters explored to these three permitted a greater range of values to be explored. Any parameters not discussed were fixed constant throughout the simulations discussed in this chapter.

6.3.1 Environmental parameters

The food vector weighting and noise threshold multiplier (environmental parameters) for each simulation were taken to be one of 5 different values: 0, 0.1, 1, 10 or 100. These values were chosen to cover a wide range of options in order to identify broad changes in behaviour with a view to conducting more specific exploration of narrower parameter ranges if required. For ease of reference, each of these values was assigned to a letter (see Table 6.1), which are then used to refer the different simulations as discussed below (Section 6.3.3).

Letter	A	B	C	D	E
Value	0	0.1	1	10	100

Table 6.1: Parameter values and corresponding code letters

6.3.2 Porpoise Distributions

For the purposes of this study, two sets of porpoise starting positions were used. These were labelled HP4 and HP5, as continuations of distributions examined during earlier tests. These two distributions consist of 40 simulated harbour porpoise, seeded randomly within an square region with 8km (HP4) or 20km (HP5) edges. The vertical position of each porpoise was randomly set between -0.5m and -1.5m for the HP4 dis-

tribution and between -0.25m and -1.75m in HP5. These depths were kept shallow in order to minimise manual adjustment to the generated positions, and were constrained by shallow areas within the release region. The other properties of the simulated porpoise remain constant - both between individuals in a set and between the two distributions. The starting parameters are summarised in Table 6.2 and shown in Figure 6.1.

Distribution	HP4	HP5
Release Coordinates (m)	378800, 5724500, –1	
Release Range (m)	$\pm$4000, $\pm$4000, $\pm$0.5	$\pm$10000, $\pm$10000, $\pm$0.75
Mean Coordinates (m)	378871, 5724550, –0.972	382875, 5724900, –0.919
Std. Deviation (m)	2486.24, 2431.31, 0.295	6351.27, 5671.47, 0.307

Table 6.2: Porpoise start location description

A disadvantage of using a random seeding process to set the initial porpoise positions is that the water depth at t_0 is not taken into account, leading to porpoise occupying invalid locations at the beginning of the simulation. This is caught by the model and prevents the simulation from continuing based on invalid initial data. In order to allow the simulation to proceed with the correct population size, any porpoise located at invalid positions were manually relocated to the closest area of water with sufficient depth in the initial timestep. This can be seen in 6.1b, where individuals have been moved clear of the shallowest areas within the release region. The relocation was performed incrementally, aiming for the smallest possible deviation between the initial seeded position and the nearest valid position. For the HP5 distribution, the adjustments lead to the mean position moving a total distance of 45m, with a change in standard deviation of 42m, -35m and +1.7mm in the X, Y and Z axis respectively. Equivalent Figures were not recorded for the HP4 distribution, but are expected to have been comparable.

6.3.3 Simulations

Combining the information from the previous sections yields 50 unique simulations, covering 25 combinations of noise thresholds and food weightings for each of two different starting distributions. The IDs for these simulations are created using the letter codes given in Table 6.1, with the food weighting first, followed by the noise threshold multiplier. The initial population distribution is then appended, giving the codes shown in full in Table 6.3. When presented in tabular form, results will be laid out in the same manner, with the results for the HP4 distributions shown above the result for

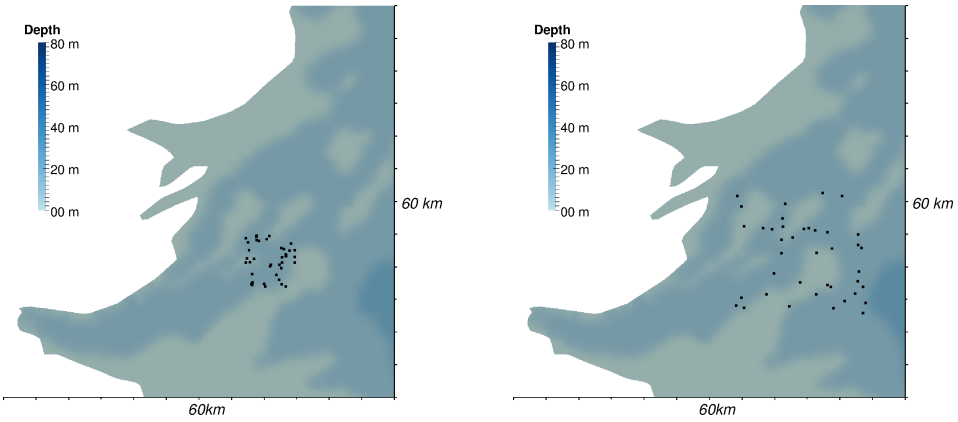

(a) HP4 - 8km × 8km release area **(b)** HP5 - 20km × 20km release area

Figure 6.1: A view of the Thames estuary area, showing the two initial porpoise distributions used in this study.

the equivalent HP5 simulation. Graphical results will be labelled with the simulations depicted.

		Noise Threshold Multiplier				
		A	B	C	D	E
Food weighting	A	A-A-HP4 A-A-HP5	A-B-HP4 A-B-HP5	A-C-HP4 A-C-HP5	A-D-HP4 A-D-HP5	A-E-HP4 A-E-HP5
	B	B-A-HP4 B-A-HP5	B-B-HP4 B-B-HP5	B-C-HP4 B-C-HP5	B-D-HP4 B-D-HP5	B-E-HP4 B-E-HP5
	C	C-A-HP4 C-A-HP5	C-B-HP4 C-B-HP5	C-C-HP4 C-C-HP5	C-D-HP4 C-D-HP5	C-E-HP4 C-E-HP5
	D	D-A-HP4 D-A-HP5	D-B-HP4 D-B-HP5	D-C-HP4 D-C-HP5	D-D-HP4 D-D-HP5	D-E-HP4 D-E-HP5
	E	E-A-HP4 E-A-HP5	E-B-HP4 E-B-HP5	E-C-HP4 E-C-HP5	E-D-HP4 E-D-HP5	E-E-HP4 E-E-HP5

Table 6.3: Simulation ID codes, identifying the parameter values and distributions used. See Table 6.1 for corresponding values

6.4 Model Outputs

The simulation outputs include the position and internal behaviour state of each porpoise at each timestep, as with the simulations discussed in Chapter 5. This information can be measured and analysed statistically as previously discussed, but can also be plotted to allow qualitative analysis of each scenario. The positions can be presented in a number of ways, the first and simplest of which is to plot the position and state of the porpoise as pathlines showing the motion of the animals over time. This allows the behaviour of individuals for the full simulation to be observed, and permits discussion of the behaviour of the population and comparison to the patterns observed with the statistical measures established previously.

The images shown in Sections 6.4.1 and 6.4.2 show the pathlines for the porpoise in each simulation. The paths are coloured by the internal state of the animal, reflecting the behaviour rule in effect at that point - grey showing default behaviour, red showing noise avoidance and green showing shallow water avoidance. It should be noted that the results shown are based on a subset of the total data used, with the position and state sampled once every 100 timesteps, equivalent to every 900 seconds. This has been done due to practical limitations associated with the software used. All other plots and numerical results use either data from single timesteps or the full, unsampled, set of data unless otherwise indicated.

The background shown in the figures in the following sections show the simulation domain, coloured by water depth at $t = 0$. The water depth throughout the domain does vary over time, with a spring tidal range within the estuary of 4m, but the main variations in depth are evident in the $t = 0$ snapshot used.

Each of the simulations presented here generated an average of 4GB in raw output data, with additional output data of up to 10GB produced during post-processing. Due to the text based output format used, the raw output files can be compressed to an average of 2.5GB using `gzip`.

6.4.1 Example output

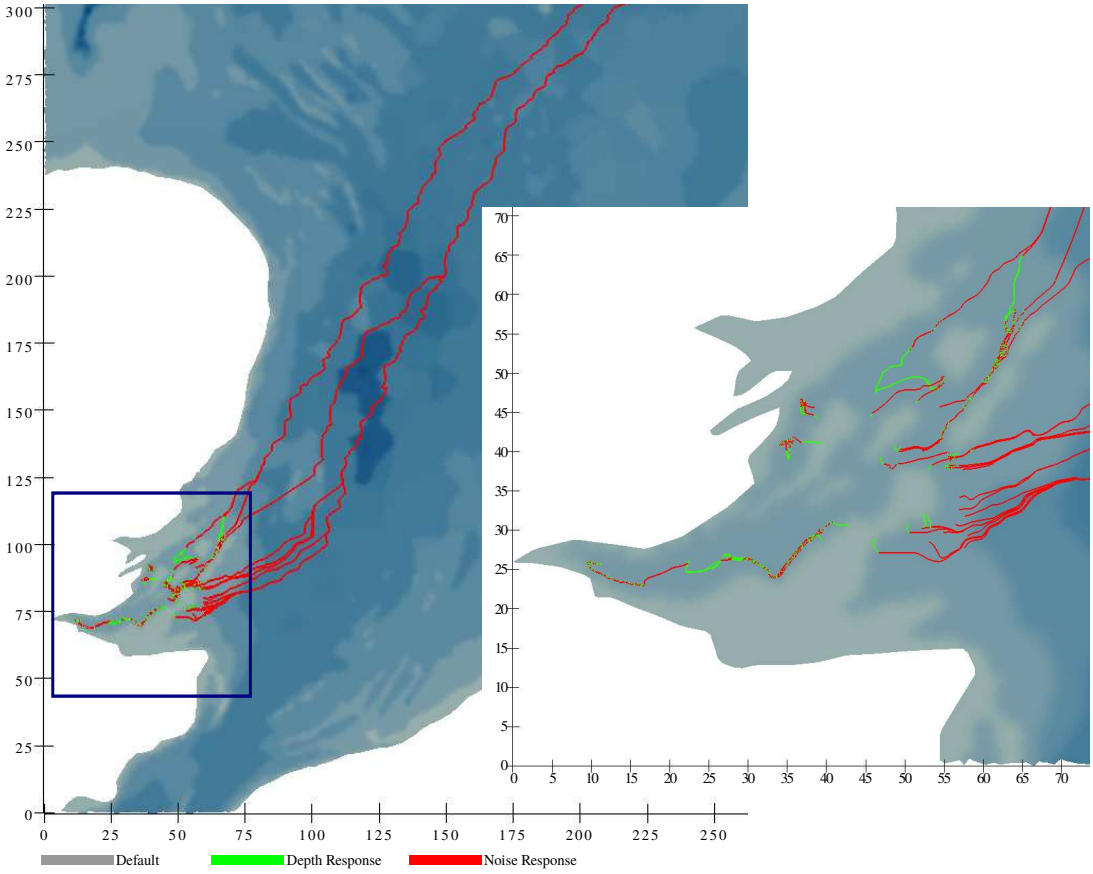

Figure 6.2: Example simulation output, showing porpoise tracks for simulation A-A-HP5. Grid scales in km

An example of the tracks output by the model is shown in Figure 6.2. This shows the pathlines corresponding to movement of each individual in simulation A-A-HP5 over the entire duration of the simulation.

In this simulation, the porpoise have no tolerance for any additional noise, so head for the domain boundaries - predominantly following a series of “escape routes” towards the North East corner of the domain.

In this simulation, the additional noise tolerance is set to zero (multiplier A - see Table 6.1). Under this condition, any value of the additional noise field that is non-zero will cause the porpoise to react accordingly unless overridden by their shallow water avoid-

ance response. It should be noted that, were this a real scenario, the animals present in the inner Thames area would likely have suffered permanent hearing threshold shift - this effect is not included in the model.

If the estuary area is examined (Inset of Figure 6.2), a mix of behaviours can be seen. To the south west of the image (within the estuary), there are areas where the porpoise are taking action to avoid shallow water - shown green. Under this behavioural rule, the porpoise will swim towards a noise source if required in order to reach sufficiently deep areas of the domain.

Some trails can be seen to alternate rapidly between red (noise avoidance) and green (shallow water avoidance) along their length within this region. This indicates areas where the water only meets the minimum depth requirements at certain points of the tide. As the water depth falls in these locations, the simulated porpoise in this simulation switch from noise avoidance to shallow water avoidance. Once the water level rises again, they switch back to noise avoidance. In reality, the response in this scenario may have involved a trade off between short term exposure to increased noise levels in order to find a quieter area in the longer term - this trade off process is not incorporated into the simple response process used in the model.

Moving east from the estuary, the majority of the porpoise head North East away from the additional noise sources. The routes taken converge to form three main “escape routes” through the domain, with two of these merging together (shown adjacent to the top left corner of the inset image in Figure 6.2). This escape behaviour is shown in more detail in Figure 6.3.

Starting from the edge of the estuary (lower left of Figure 6.3), the porpoise are all travelling towards the upper edge of the image. It can be seen that a shallow sandbank area splits the routes taken at this point, with one group of individuals following this shallow patch (red and green trails, lower left) and others taking a more easterly route. The individuals that pass south east of the shallows are joined by other individuals that enter this image from the bottom edge of the frame, and the tracks for all of these individuals eventually merge together under the combined influence of the local noise field (and their response to it) and the effect of the tides. Returning to the group that passed to the North West of the shallows, these individuals move North, where some of

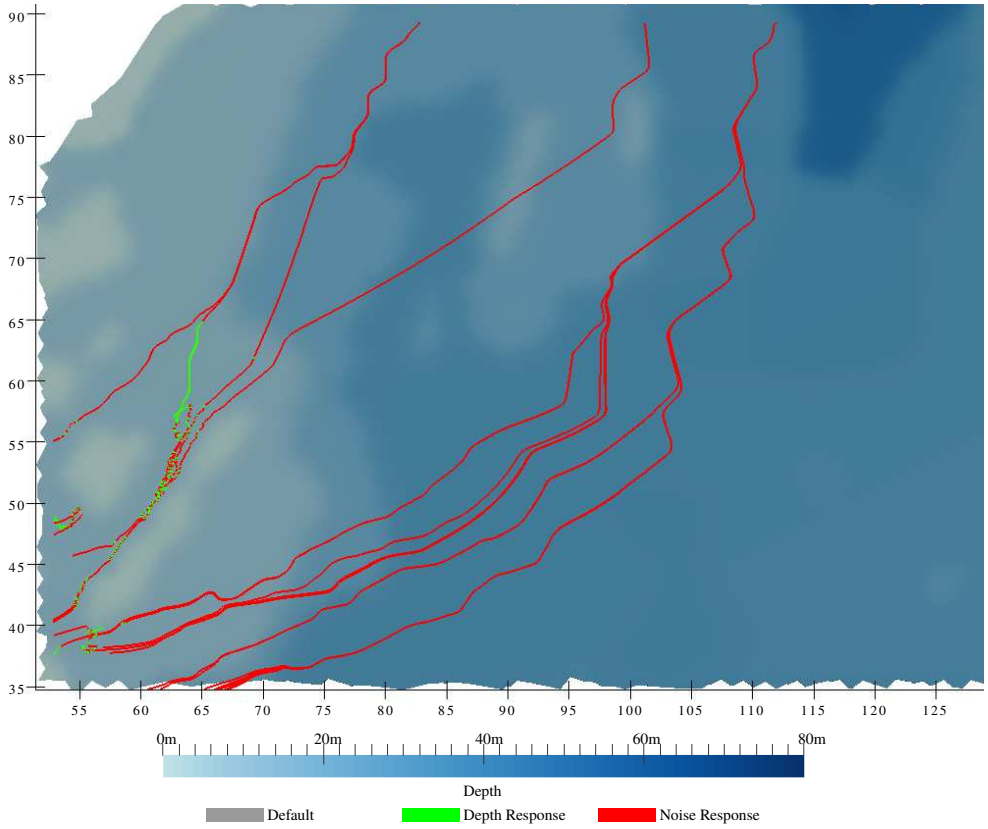

Figure 6.3: Detailed view of the Eastern edge of the Thames estuary area, showing "escape routes" forming

the tracks diverge - likely due to the individuals traversing the region at different times and encountering different water depths - and either continue North, merging into the tracks of other individuals entering from the left side of the frame, or form the thicker escape route shown in the centre of the domain.

6.4.2 General trends and patterns

Figure 6.4 shows the pathlines drawn for porpoise positions over the duration of two simulations using the HP4 initial population distribution. The tracks are coloured by the behavioural state of the porpoise at that point in time, with grey representing the default behaviour, red representing noise avoidance and green representing shallow water avoidance. These two simulations (A-A-HP4 and E-E-HP4) represent very different behaviours, with results for the latter simulation hard to distinguish when shown on the same scale as the former. The remaining results have been split into two groups,

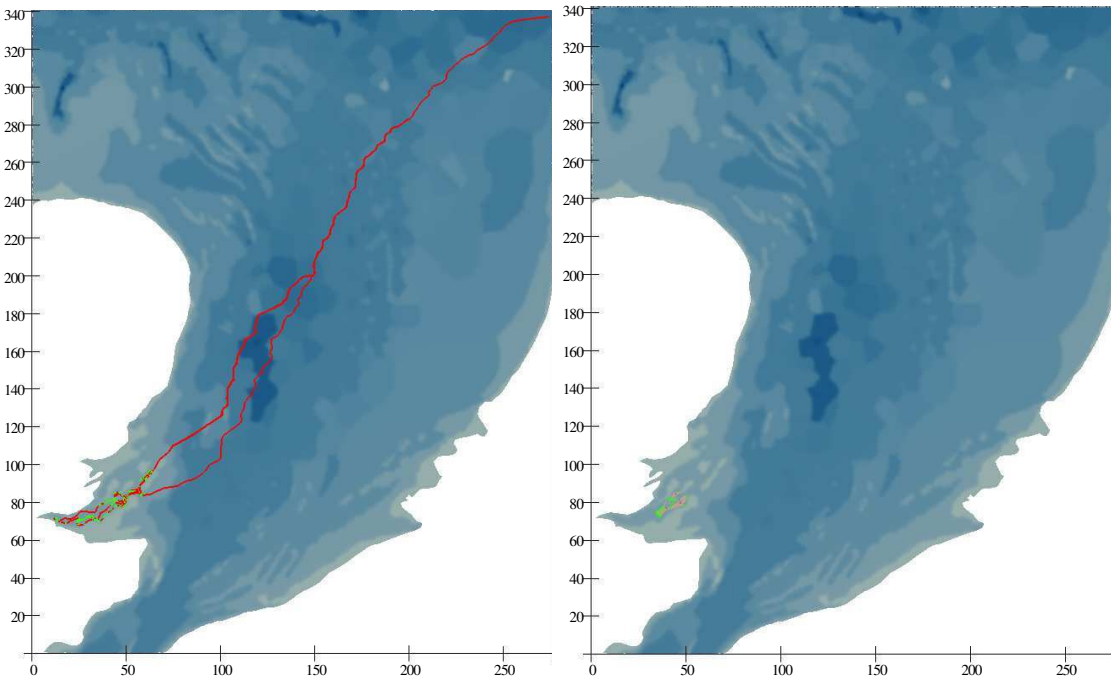

Figure 6.4: Two examples of simulation output from the parametric study.

presented in Figures 6.5 and 6.6. The two groups are shown at different spatial scales, but all images in each group represent the same area of the domain. The images in each figure are grouped such that all simulations with a given noise threshold are in columns, with rows corresponding to the food weightings used. The values can be cross referenced using the ID under each image, as described in Section 6.3.3.

Examining the images shown in Figures 6.5 and 6.6, we can split the results into three sets exhibiting different patterns of motion - those in the first column of Figure 6.5 (Noise threshold A), those in the second column of Figure 6.5 (Noise threshold B) and the remaining results shown in Figure 6.6 (Noise thresholds C, D, and E). All of the results shown in the first column (X-A-HP4) exhibit noise avoidance behaviour (shown in red) throughout the domain, with porpoise pathlines extending to the domain boundary. The majority of the population moves towards the North East, with a smaller section of the population moving West, up the estuary. In a real scenario, this could be a significant impact as the porpoise are driven inland to shallow, congested waters although it is likely that more realistic and complex responses to the situation would lead to a

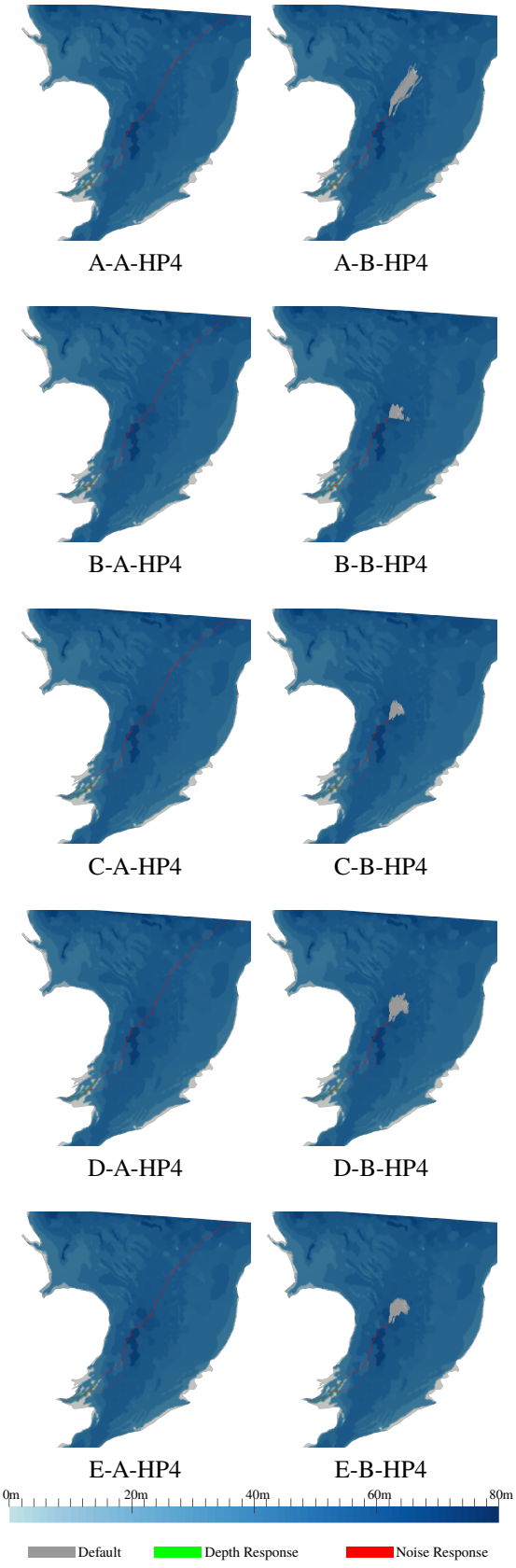

Figure 6.5: Porpoise tracks for HP4 simulations for noise thresholds A and B

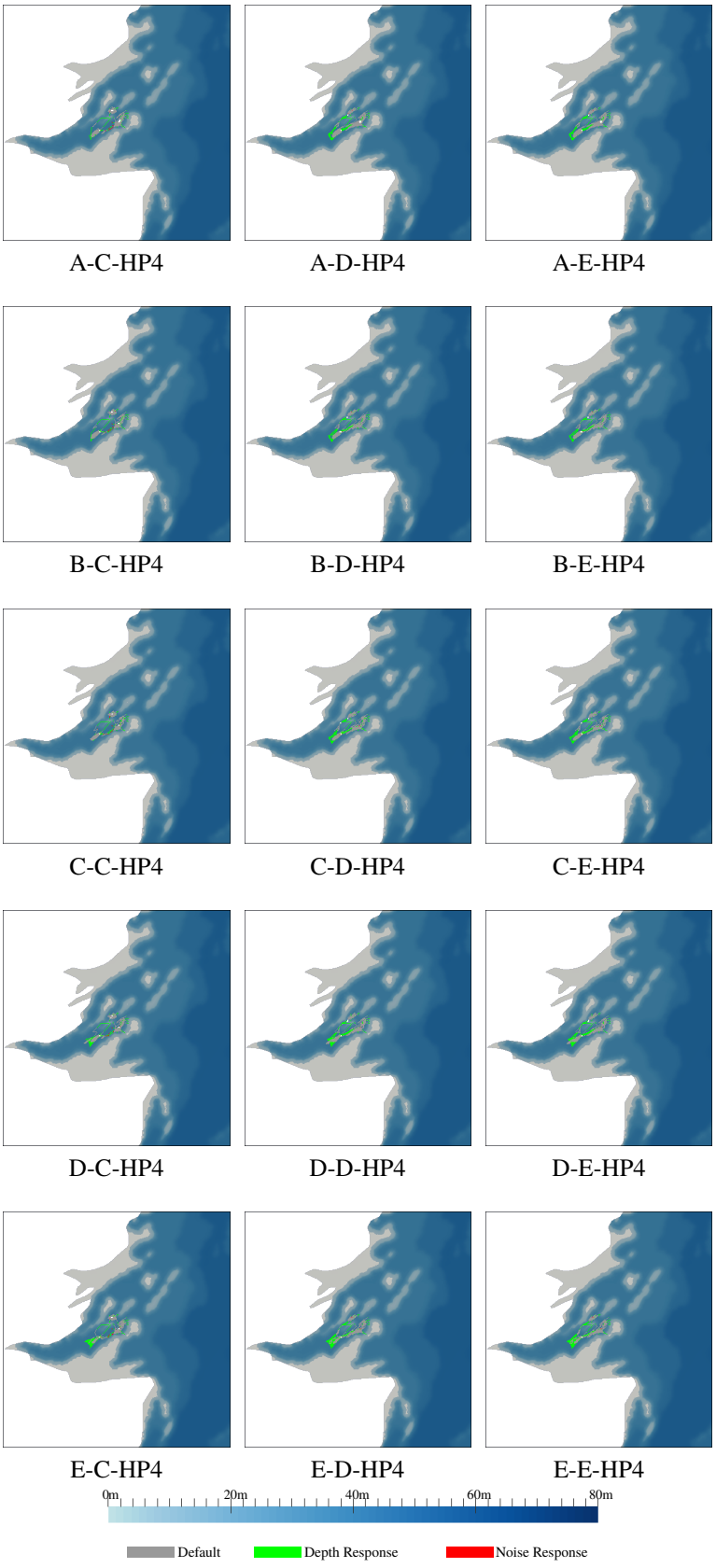

Figure 6.6: Porpoise tracks for HP4 simulations for noise thresholds C, D and E

different outcome. Porpoise that transit to the boundary are assumed to leave the simulation, and are not simulated further. This is consistent with the noise threshold used - 0 - which represents a scenario where any additional noise is intolerable.

Looking at the next group of results (2nd column, with noise threshold B), noise avoidance behaviour is again observed, with porpoise travelling both up estuary (West) and out to sea (North East). The results in this column differ from the previous set discussed (1st column, noise threshold A) in the appearance of a grey "tail" in the middle of the domain. These tracks represent tidally mediated motion of the porpoise once they reach an area of the domain where the additional noise level is low enough not to trigger that behavioural response. The shape and size of this tail varies down the column as the food weighting value increases, altering the position of the individuals and their exposure and reaction to the tidal flows throughout that region of the domain. There is no immediately obvious trend or pattern to the shape of the "tail" portion of the pathlines.

The third broad group of results involves the three highest noise thresholds, which drastically reduce the regions where the noise avoidance response is triggered. For these simulations (noise thresholds C, D, and E), the porpoise are almost entirely confined to the estuary region of the model. These simulations show similar patterns of movement, with little variation between them that can be obviously linked to the parameters used.

From this set of results, it can be seen that there is a much more obvious variation in behaviours as a result of changing noise tolerance than in equivalent changes in food weighting. Variations in terms of the food weighting can be observed (comparing A-B-HP4 and B-B-HP4 for example), but are less easily explained and far smaller in scope than the noise related changes.

The results for the simulations starting with initial population distribution HP5 have been plotted and divided as described above for the HP4 results, and are shown in Figures 6.7 and 6.8. The results show similar patterns, but with more varied tracks in each result arising from the wider starting distribution. This can be seen clearly in the first column of results in Figure 6.7 (noise threshold A), where two or three main 'escape routes' run across the domain in contrast to the single route traced out in the HP4 results. The results for noise threshold B show a similar 'tail' in the centre of the domain, varying with food weighting in a manner consistent with the HP4 results - although the pattern of that variation is no clearer.

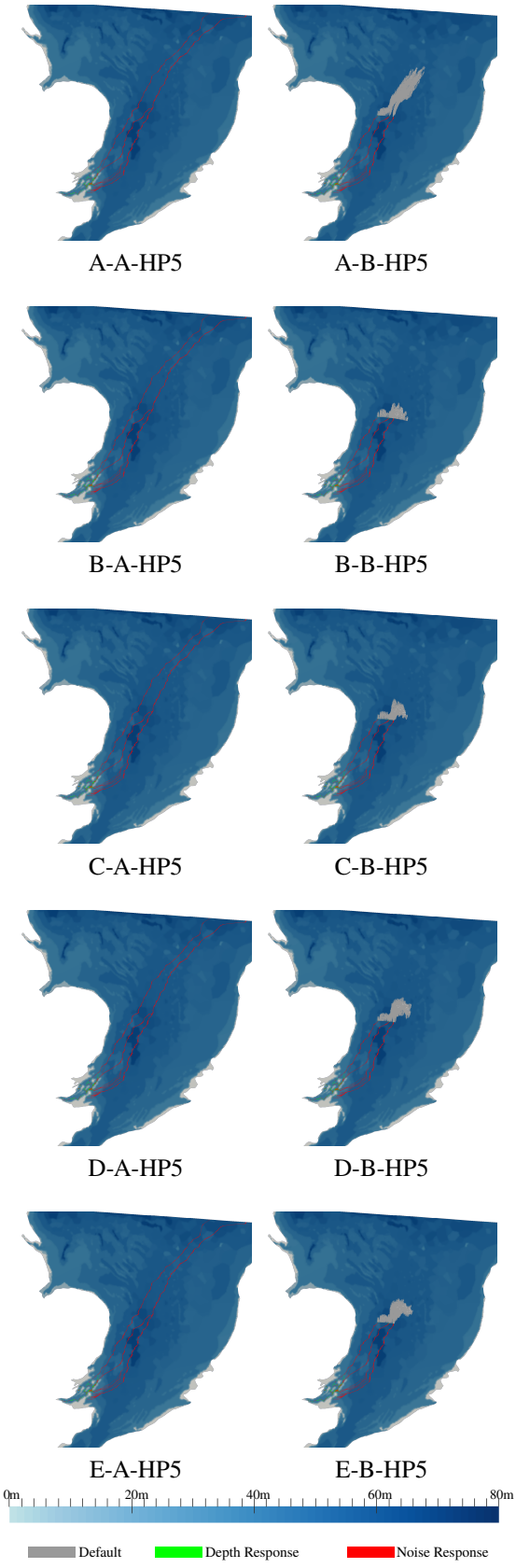

Figure 6.7: Porpoise tracks for HP5 simulations for noise thresholds A and B

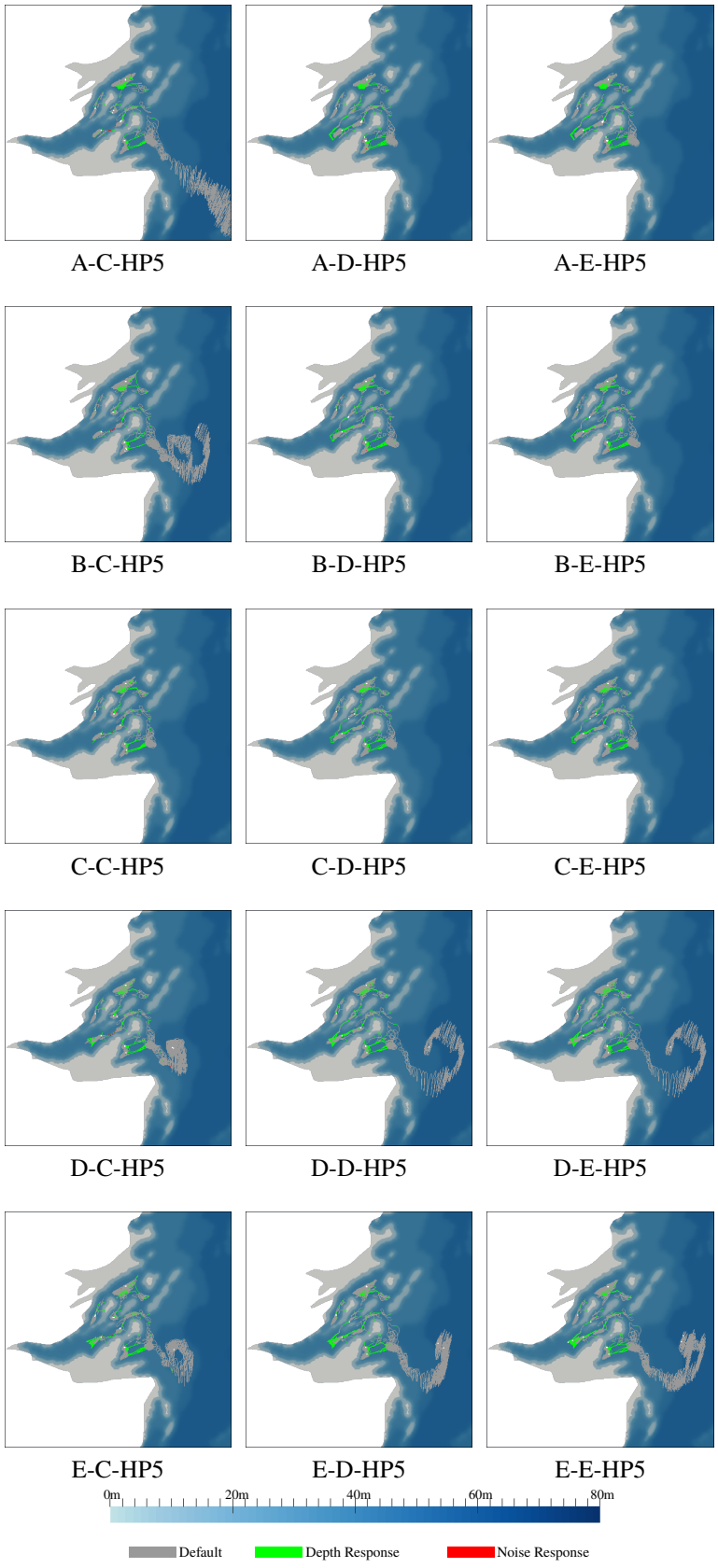

Figure 6.8: Porpoise tracks for HP5 simulations for noise thresholds C, D and E

In contrast to the results from the HP4 based simulations, there are some obvious variations evident between the results using noise thresholds C, D and E (shown in Figure 6.8). These variations can be seen as individuals or small groups of porpoise 'wandering' away from the south east of the estuary area in 8 of those 15 simulations. Investigating these traces more closely shows them to be due to cumulative differences in the tracks followed by individual animals based on the differing weightings and thresholds, which lead those individuals to be exposed to different tidal flows and subsequently different environmental conditions. The appearance and disappearance of these wanderers with changing parameters shows that the parameter values can cause significant changes in the behaviour of otherwise identical individuals, even though the general population behaviour remain otherwise consistent.

6.4.3 Side-by-side comparison

In order to comment further on the behaviours seen, 6 simulations were selected based on the general track patterns seen across both sets of results. These simulations (A-A-HP4, A-A-HP5, C-C-HP4, C-C-HP5, E-E-HP4 and E-E-HP5) are shown in Figure 6.9. The Figures have been cropped to the estuary area - the same area shown in Figures 6.6 and 6.8 but shown to a larger scale. The simulations selected are pairs of simulations using the same food weightings and noise thresholds for each starting porpoise distribution.

Taking the first two Figures (6.9a and 6.9b), it can be seen that the tracks are completely dominated by noise avoidance behaviour (red), with areas of shallow water avoidance behaviour (green). Several traces show an alternating pattern of behaviour - this is likely caused by the rise and fall of the tide, with the occupied areas only exceeding the depth limit towards high tide. Comparing the two sets of results, a greater number of routes can be seen in the HP5 results - due to the wider range in starting positions for that distribution. It should be noted that in neither set of results are 40 distinct tracks visible - the porpoise tend to collect into particular areas or follow similar routes. This is not particularly surprising - the porpoise in these populations are identical and are subject to the same rules. This is also reflected in the same general pattern of behaviour evident in both Figures.

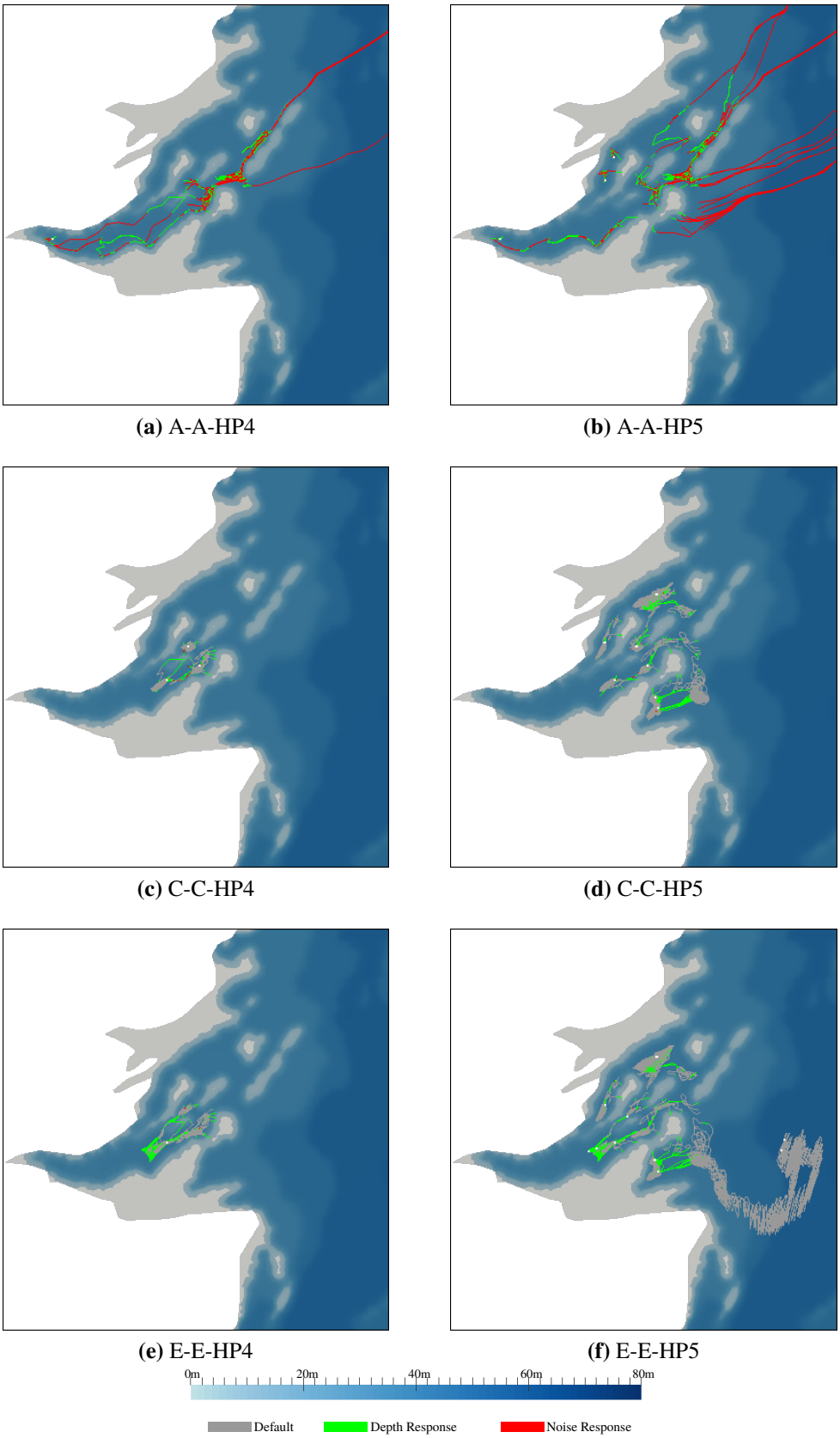

(a) A-A-HP4 **(b)** A-A-HP5

(c) C-C-HP4 **(d)** C-C-HP5

(e) E-E-HP4 **(f)** E-E-HP5

Figure 6.9: Cropped view of selected simulations from Figures 6.5, 6.6, 6.7 and 6.8

The next two Figures (6.9c and 6.9d - depicting simulations C-C-HP4 and C-C-HP5) show a mix of the default behaviour (grey) and shallow water avoidance (green). Although there are more locations in figure 6.9d where the porpoise congregate (due to the wider starting distribution), it can be seen that there all areas where porpoise appear to have congregated in the HP4 case show similar behaviour in the HP5 case. The general pattern of behaviour in this pair of models can be seen as the porpoise gathering in groups in areas where conditions are more favourable (sufficient water depth, tolerable additional noise), but occasionally being forced to move to new areas when caught in shallower water by the changing tidal conditions. Of note is the relative lack of noise avoidance behaviour, due in part due to the location of the noise sources in shallow water in this area of the model. Some small areas of noise avoidance can be found, particularly along the edges of the channels where the water depth is insufficient at some points of the tide. The prioritisation of rules used in the model means that the simulated porpoise will avoid stranding themselves, even where this means exposure to additional noise levels above their threshold.

The final pair of images show traces for simulations E-E-HP4 and E-E-HP5 (Figures 6.9e and 6.9f respectively). These simulations use the strongest food weighting tested and the highest tolerance to additional noise. Comparing E-E-HP4 to the corresponding median simulation (C-C-HP4 - Figure 6.9c) shows an increase in depth avoidance behaviour to the west of the estuary. This is due to the greater food weighting, resulting in more porpoise swimming against the current towards food, and then ending up in shallower water as the tide recedes. As no memory model has been implemented, the porpoise repeat this behaviour until the simulation ends or their movement exposes them to a sufficiently different tidal current to move the individuals further away to deeper water or an area where alternative food sources are close enough to become higher priority. The same pattern can then be seen in Figure 6.9f (E-E-HP5). Comparing this to C-C-HP5 (Figure 6.9d) shows that the congregation area to the north of the estuary appears to enjoy more porpoise activity, which is not seen by the north western site - which appears approximately the same in both simulations.

The most obvious difference observed in E-E-HP5 is the appearance of a small group (3-4 individuals) wandering to the south east of the model before curving back towards the central area as the simulation progressed. These individuals travel significantly

further away than any other individuals in the simulation, and end up further away from food, despite the increased weighting applied. The increased weighting causes the individuals to move into a different tidal current, leading to increasing divergence between the two simulations as time progresses. The increased distance from food sources reduces the influence of food on further motion of these individuals, despite the increased weighting applied to the population as a whole.

6.4.4 Clustering: Why do the porpoise gather where they are?

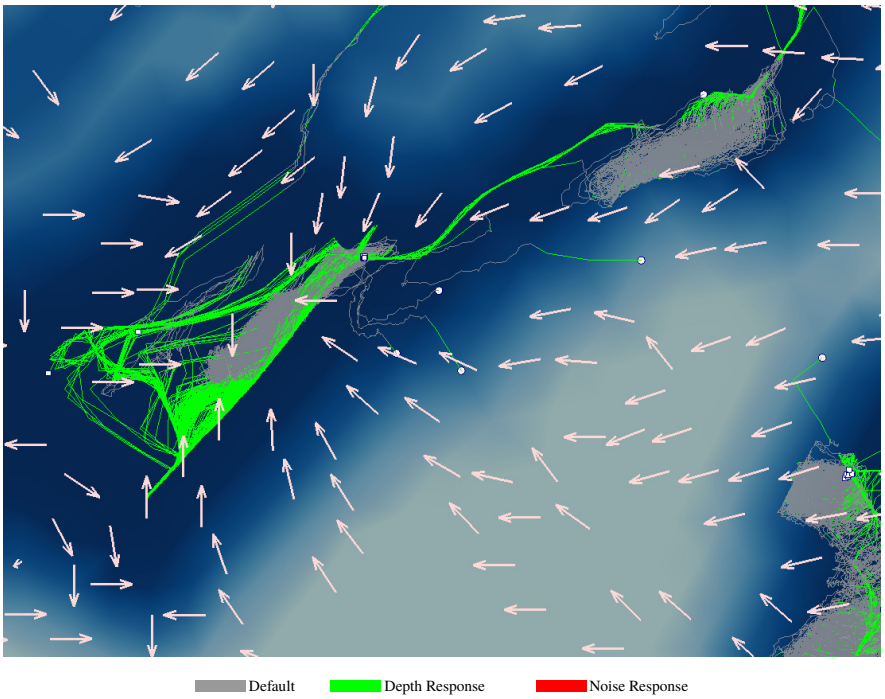

Figure 6.10: Detailed view of a section of Figure 6.9f, showing depth (background colour, exaggerated) and the food availability gradient (white arrows)

As mentioned above, the simulated porpoise have a tendency to collect in particular areas of the simulation. This is not unexpected given the shared behaviour parameters in this implementation of the model. Figure 6.10 shows a close up view of simulation E-E-HP5 (as shown at different scales in Figures 6.8o and 6.9f). The background colouring shows water depth, although the scale has been exaggerated compared to previous figures in order to improve contrast between deeper (dark) and shallower (light) areas. The white arrows represent the gradient of the food availability field, and point in the direction of increased food availability.

Looking at the direction of the arrows around the left hand cluster of tracks, it can be seen how the cluster forms around combinations of deep water and higher food availability, with shallow water avoidance behaviour (green) also limiting the motion of the porpoise. The cluster shown towards the upper right hand corner of the image has formed in an area where the tidal flows reach $1.85 ms^{-1}$, and forms a local balancing point around the motivation to move towards food and the drag minimisation terms of the default behaviour. When porpoise in this region are forced to swim south west (when caught in the shallower regions north of the group, the balance shifts towards the area of the first cluster discussed, which seems stable over the time period and situation simulated. It should be recalled at this point that the food sources here are stationary in space throughout the simulation.

6.5 Statistical Outputs

Visual examination of the paths taken by the porpoise provides an easy method to obtain qualitative information and comparisons between the simulation results, but it is also useful to have measurable quantities associated with the results to allow for quantitative comparisons. Given that the results are the properties of a population, the simple statistical measures of those properties provide a starting point for quantitative analysis. The initial properties of the population in each simulation are independent of the environmental parameters given, and are instead solely dependent on the initial distribution of the porpoise described in section 6.3.2. In order to highlight the differences between simulation results, the results presented show the change in population properties between the start and end of the simulation.

6.5.1 Population position

The results shown in Table 6.4 provide a very clear split between simulations using noise threshold A or B and the remainder, for both starting distributions. This is consistent with the observations described above (section 6.4.2) - the simulations with low noise thresholds showed substantially larger movement in the population which is shown here as a change in mean position between 12 and 168 times larger than corresponding cases with higher noise thresholds (B-B-HP5/B-D-HP5 and A-A-HP4/A-C-HP4 respectively).

		Noise Threshold Multiplier				
		A	B	C	D	E
Food weighting	A	316181	190193	1870	6390	6390
		281625	171982	4425	8356	8356
	B	316181	136088	6677	8610	8610
		281625	121496	7856	9634	9634
	C	316181	142330	6873	8927	8927
		281625	125365	8621	9669	9669
	D	316181	153567	6898	8576	8576
		281625	135150	7995	9171	9171
	E	316181	153666	7078	9116	9116
		281625	135770	7992	7997	8200

Table 6.4: Change in mean population position (in metres) between start and end of simulation. HP4 results presented above HP5 results, as shown in Table 6.3

6.5.2 Population spread

As well as investigating the population position, the spread of that population about the mean can also be examined using the standard deviation. In this instance, the standard deviation in each axis is calculated independently. This is consistent with the initial distribution of porpoise, which was based upon independent random coordinates generated in each axis as described in section 6.3.2. The change in standard deviation of the population's position relative to the initial standard deviation is given in Tables 6.5, 6.6 and 6.7. The sign of the standard deviation change indicates whether the standard deviation has increased (+). implying a more dispersed population, or decreased (-), implying a tighter grouping.

Concentrating on the standard deviations in X and Y, there is the same split based on noise threshold seen in the mean position data (Table 6.4) and track images discussed above. The results for simulations with noise threshold A are have standard deviations in X and Y that only vary with starting distribution. The large values returned for both axes are consistent with the simulated porpoise fleeing for the domain boundary. Moving to the next noise threshold, a variation with the food coupling appears. For both X and Y coordinates, the standard deviation starts high for food weighting A, decreases for B and increases for C and D and decreases again slightly for food weighting E. The trend and magnitude of this variation is consistent with the changes in the shape and size of the 'tail' observed in the track images.

		Noise Threshold Multiplier				
		A	B	C	D	E
Food weighting	A	80510	46142	100	1035	1035
		92876	52341	7457	-1682	-1682
	B	80510	39159	3	-1703	-1703
		92876	42869	1767	-1817	-1817
	C	80510	39579	-159	-2038	-2038
		92876	43402	-1840	-1776	-1776
	D	80510	41649	-182	-1672	-1672
		92876	45817	612	3967	396
	E	80510	41563	-235	-2448	-2448
		92876	46141	-447	2763	2930

Table 6.5: Change in population position standard deviation in X. Results in order shown in Table 6.3

		Noise Threshold Multiplier				
		A	B	C	D	E
Food weighting	A	78334	52541	-16	-706	-706
		94180	60991	3944	-68	-68
	B	78334	35187	930	-715	-715
		94180	38917	1039	4	4
	C	78334	37478	940	-1293	-1293
		94180	40972	468	29	29
	D	78334	40772	901	-659	-659
		94180	44694	503	-29	-29
	E	78334	40700	825	-2389	-2389
		94180	44832	433	759	726

Table 6.6: Change in population position standard deviation in Y. Results in order shown in Table 6.3

Identifying consistent trends in standard deviation for the remaining simulations is less obvious. There is a general trend for an increased food weighting to show a more tightly clustered population compared to other results with the same noise threshold, particularly for the smaller starting distribution (HP4). The trend for the corresponding HP5 simulation is more varied, with the strongest food weighting (E-D-HP5 and E-E-HP5) cases showing a more dispersed population this is likely to be due to the 'wandering' porpoise in the high food weight/high noise threshold results. For the nearby simulations D-C-HP5, D-D-HP5, D-E-HP5 and E-C-HP5, the same wandering tracks are seen, but there is a smaller effect - looking at the tracks it can be seen that the porpoise have looped further back towards the west, reducing the standard deviation of the

		Noise Threshold Multiplier				
		A	B	C	D	E
Food weighting	A	-0.10	+8.45	+2.72	+2.38	+2.38
		+0.00	+7.69	+2.93	+2.56	+2.56
	B	-0.10	+9.77	+2.78	+2.51	+2.51
		+0.00	+9.72	+3.10	+2.68	+2.68
	C	-0.10	+10.42	+2.75	+2.37	+2.37
		+0.00	+9.91	+2.52	+2.23	+2.23
	D	-0.10	+7.95	+2.70	+2.46	+2.46
		+0.00	+9.34	+2.69	+3.17	+3.17
	E	-0.10	+8.13	+2.74	+2.58	+2.58
		+0.00	+8.46	+2.34	+4.37	+3.45

Table 6.7: Change in population position standard deviation in Z. Results in order shown in Table 6.3

population position.

Combining the mean and standard deviation of position at each end of the simulation allows us to represent the change in the populations position and spread graphically. This is shown in Figure 6.11, with the results for noise thresholds C, D and E presented at a larger scale in figure 6.12. In these two figures, the start and end points are plotted, with the corresponding standard deviation shown as error bars. Note that the standard deviation of the starting distribution is too small to be readily identified in Figure 6.11.

The results presented in Figure 6.11 reinforce the previous discussion, and show the clear shift in population mean position and increased population spread for the two lowest noise thresholds (A and B). Figure 6.12 shows that the mean position movement is generally south west (into the estuary). The effect of the food weighting on population spread can also be seen clearly in the HP4 results (shown blue), but not in the HP5 results for the reasons discussed above.

6.6 Conclusions

This chapter has shown the wide variation that can occur based on changes to three of the main parameters of this model - initial positions, additional noise tolerance and the weighting between food seeking and drag minimisation.

In a simulation where the other parameters and internal states of the porpoise were homogeneous, the starting positions of the animals largely dictates the differences between

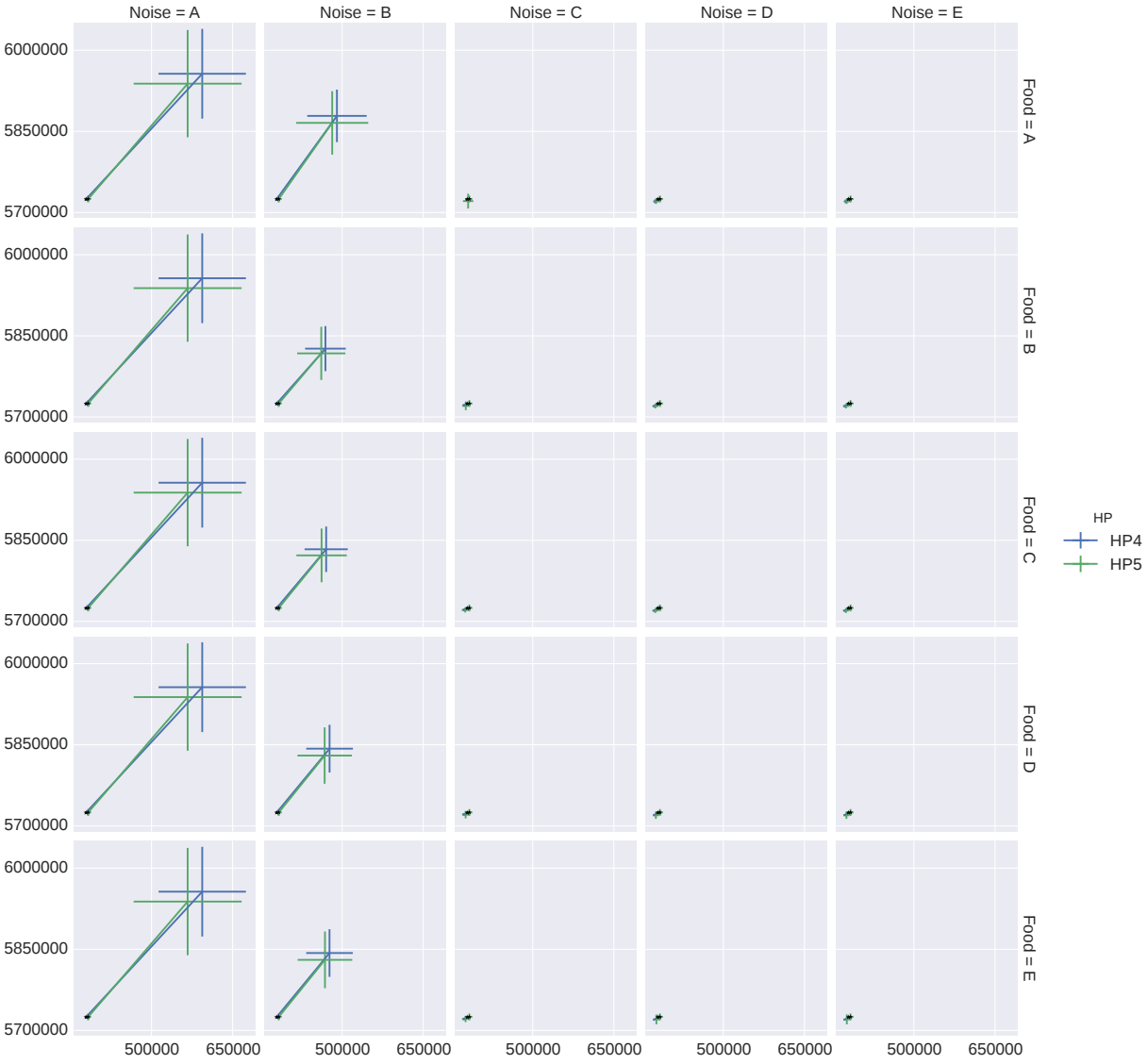

Figure 6.11: Initial and final mean porpoise positions in XY plane $\pm 1\sigma$. Initial timestep marked in black

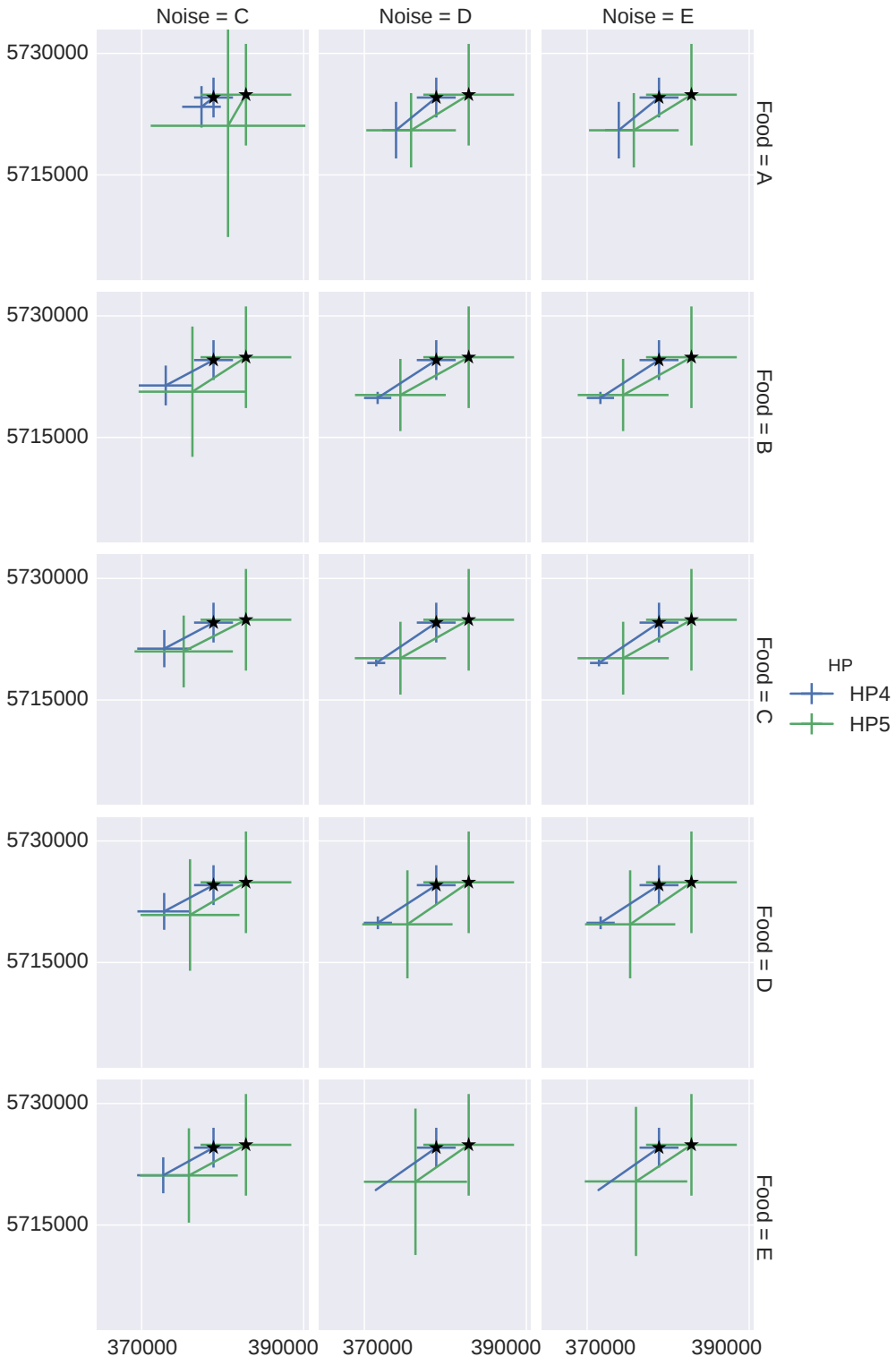

Figure 6.12: Mean porpoise positions in XY plane $\pm 1\sigma$ for Noise thresholds C,D & E. Initial timestep marked in black

individual behaviours and movements over the remainder of the model. This leads to a wider variety in movements and habitat usage for a more widely distributed population, as the more varied placement and local conditions give the individuals more variation. This can also be seen by the wandering porpoise that appear to the eastern edge of some of the results, where small deviations in local position lead to diverging environmental conditions and visibly different movements for a given individual.

Despite the ability for divergent behaviour based on changes in parameters and initial conditions, the results presented here also showed consistent patterns of behaviour and preferred areas where individuals congregated within the model. These areas were formed where local conditions provided a favourable combination of deep enough water and either a source of food or an area where the gradient of food availability was relatively small - such that there was not a significant enough incentive to overcome the local tidal motion.

Taking the information about these effects, the next chapter presents a case study of Ramsey Sound - an energetic tidal area that contains a licensed deployment site for a tidal stream turbine

Part III

Outcomes

Chapter 7

Case Study: Ramsey Sound

"I couldn't get you to the ocean," she said."But there was nothing stopping me bringing the ocean to you. "

Neil Gaiman - The Ocean at the End of the Lane (2013)

7.1 Introduction

One of the aims of this project is to develop a set of tools that allow the potential impact of tidal energy devices on marine mammals to be investigated. This was motivated in part by ongoing commercial developments and other research being carried out within the Marine Energy Research Group at Swansea University during the early stage of this project. This influenced the move to concentrate on tidal stream devices and harbour porpoise specifically.

One of the areas of interest from both a commercial and research perspective is Ramsey Sound[1], located towards the extreme south western extent of Wales. This chapter will introduce the area and results from simulations of the area carried out with the behaviour model described in previous chapters.

7.2 Ramsey Sound

7.2.1 Location

Ramsey Sound is a tidal channel that separates Ramsey Island from the coastline off St David's Head in Pembrokeshire, Wales. The Sound is located at (51° 52' 27" N, 5° 19' 25" W) and shown in Figure 7.1. The channel is approximately 3km long and between 500m and 1.6km wide, with water depths reaching approximately 70m [52, 103]. Ramsey Sound is approximately 40km from the ports at Milford Haven and Fishguard [40].

7.2.2 Physical Features

Ramsey Sound is a highly energetic site, with peak tidal flows up to $4ms^{-1}$, with a mean spring vertical tidal range of 5m [52, 103].Previous studies of the area have shown that the area could provide an estimated extractable power of 74.89GWh/year [40].

The Sound possesses a number of prominent features, including a deeper channel through the centre of the Sound, isolated rock pinnacles and shallower reef areas. These generate complex flows through the area, with Horse rock in the northern Sound and the

[1]For clarity, the geographic area will be rendered as Sound, with the acoustic term kept lower case as sound.

(a) Location of Ramsey Sound relative to Great Britain and Ireland

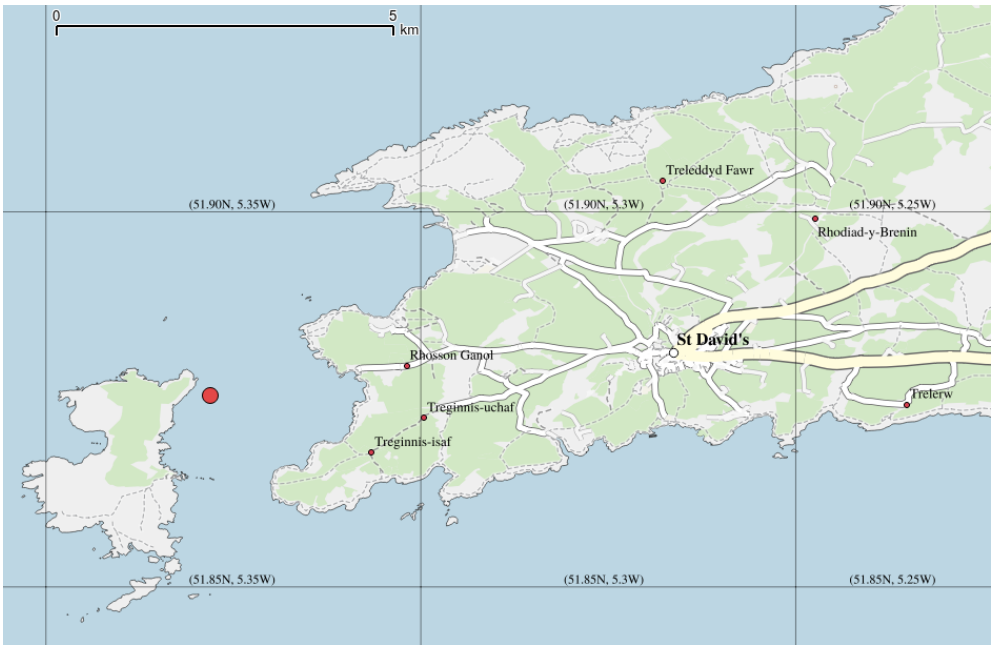

(b) Ramsey Sound area, including Ramsey Island and St David's

Figure 7.1: Location of Ramsey Sound

Bitches reef in the south each associated with distinctive flow patterns. There is also a significant flow asymmetry between flood and ebb tides and areas of recirculation.

The flows throughout the Sound are described and examined in more detail in [104] and [103]. The smaller area around Horse rock and Pony rock was recently subject of a study using CFD simulations and two different turbulence models to investigate the flow in this are in more detail, and these results are presented in [105].

The Sound is also home to a small number of fishing boats, and an RNLI lifeboat station situated on the mainland towards the northern end of the Sound.

7.2.3 Environmental Features

In addition to the varied physical characteristics of the area, Ramsey Sound is also home to a variety of different species and carries a number of protective designations. Ramsey Sound is a National Nature Reserve (NNR), and forms part of the Ramsey and St David's Site of Special Scientific Interest (SSSI). It is also part of the St David's Special Protection Area (SPA), two Special Areas of Conservation (Pembrokeshire marine SAC and the St David's SAC) and sits within the Pembrokeshire Coast National Park [32, 106].

Ramsey Island is also an RSPB nature reserve [32, 106], home to a range of different bird species. A survey carried out in the area identified 21 different species of seabird in and around the Sound, including surface feeding and diving species [32]. The area is also home to grey seals (*Halichoerus grypus*) and harbour porpoise (*Phocoena phocoena*) [30, 102], both protected under the EU Habitats directive [21] and other related regulations and legislation.

7.2.4 Why Ramsey?

The combination of conditions in Ramsey Sound provide favourable conditions for development and testing of tidal stream energy devices, and consent for a single device demonstration was granted to Tidal Energy Ltd. in March 2011 [40]. Environmental surveys and assessments were carried out as part of the development and consenting process for the deployment [30, 32, 102], which provides information that can be used as input for a series of simulations using this model.

The location, status and commercial interest in the site have ensured that it has also been subject to a number of studies, surveys and modelling exercises, providing additional sources of information that have been consulted during the project, and cited throughout this document.

7.3 Tidal Data

The tidal model used to define the simulation area was provided by David Haverson[2] from the Industrial Doctoral Centre for Offshore Renewable Energy at Edinburgh University, and was developed at the Centre for Environment, Fisheries and Aquaculture Science (CEFAS) in Lowestoft.

The model provided is a two dimensional, depth averaged TELEMAC model covering south west Pembrokeshire and the surrounding waters. The model covers a 30 day period, and has been validated against tide gauge and ADCP transect data to confirm the surface elevation and flow speeds respectively. The mesh contains 300948 elements, with edges in the horizontal plane varying between 6m and 5200m in length depending on the position within the domain. The smaller element sizes are required to resolve some of the key features in the Ramsey Sound area of the model that are known to influence flows in the area - such as Horse rock in the northern Sound [119].

7.4 Additional Data

7.4.1 Noise

In order to represent a turbine device, a noise source was added to the domain at coordinates (-592287,331285,0), indicated as the red circle in 7.1b. The noise was represented numerically as a mean square pressure value (MSP), which decays in proportion to $\frac{1}{r^2}$ for linear distance r and can be summed together if multiple sources are present [120]. The MSP value was set to 0.2296 Pa^2 based on the method given in Reference [120], with values approximated to represent a DeltaStream type device.

The threshold value used to enable noise avoidance behaviour in the simulated porpoise was set to 97 dB re 1μPa m, converted to a MSP value of 5.011×10^{-3}i Pa^2

[2] d.haverson@ed.ac.uk

based on the values found in Reference [72]. An alternative criteria considered was an estimated value for Permanent Threshold Shift (PTS, i.e. permanent hearing damage), based on available audiogram data [71, 120]. This would have yielded a higher limit of 108 dB re 1μPa m, but represents physical harm rather than behaviour change. On this basis, the more conservative limit was applied to the model used.

It should be noted that it has been assumed that the sounds emitted by a turbine device would overlap with the hearing range of the harbour porpoise. Given the wide frequency range given in the audiogram data, towards the upper end of the frequencies expected to be emitted by such a device and the lower end of the hearing range of the porpoise. This means that the limit here is likely to be more conservative than the numbers presented above would indicate, although verification of this would require measurements of the noises emitted by a device *in situ*. Similarly, the spreading model used to represent sound propagation is very simplistic, but could be replaced by the output of a more sophisticated model in order to improve that aspect of the simulation.

7.4.2 Food

In ideal circumstances, food sources would have been implemented based on site surveys and studies. In this instance, such information was not readily available, so a number of short simulations were conducted with different food sources implemented. Based on the porpoise sighting densities in [30], a mobile food source was implemented, traversing the Sound based on the tidal state in an attempt to mimic the known porpoise positions. This lead to a strong presence of porpoise to the north of the Sound, but none within it. Reducing the strength of the mobile source made little impact, but better results were obtained using a static source placed in the south of the Sound.

The final set up used includes a food source was placed in the model at (-591971,327430,0) with a radius of 1200m and a strength of 50000 [in arbitrary units] and decay in inverse proportion to distance from the source.

7.5 Scenarios

There are four distinct scenarios that have been simulated as part of this case study:

a. Base - no food or additional noise present within the model

b. Food - the base case, with food availability modelled as in subsection 7.4.2 above

c. Noise - the base case, with additional noise as described above in subsection 7.4.1

d. Both - base case with both food and noise implemented, using the same settings as the separate simulations

A number of smaller scoping simulations were carried out to determine parameter values, but the individual results of these are not presented here.

All four of the main simulations were run using a population of 100 harbour porpoise seeded within the Sound within a 1km $\times$ 1km $\times$ 13m volume, with the depths dictated partially limited by local bathymetry. The starting distribution and domain are shown in Figure 7.2.

All porpoise were initialised with identical parameters apart from their initial position.

7.6 Results

The results of the four simulations are shown in Figure 7.3, which shows pathlines for each porpoise in each simulation for the full duration. The black markers show the final position of each porpoise. In the two simulations which incorporate food as a reference ("Food" - Figure 7.3b and "Both" - Figure 7.3d), a number of porpoise leave the simulation domain through the western boundary towards the end of the simulation.

It can be seen immediately that the results split into two identifiable pairs - Base and Noise, and Food and Both. These are simulations pairs without food incorporated and with food incorporated into the model respectively. This was expected - in the absence of food there would appear to be little reason for the porpoise to remain in and around the immediate area of Ramsey Sound. The westward migration of the porpoise in the two 'with food' cases is distinctive, but not an expected consequence of the inclusion of food within the Ramsey area.

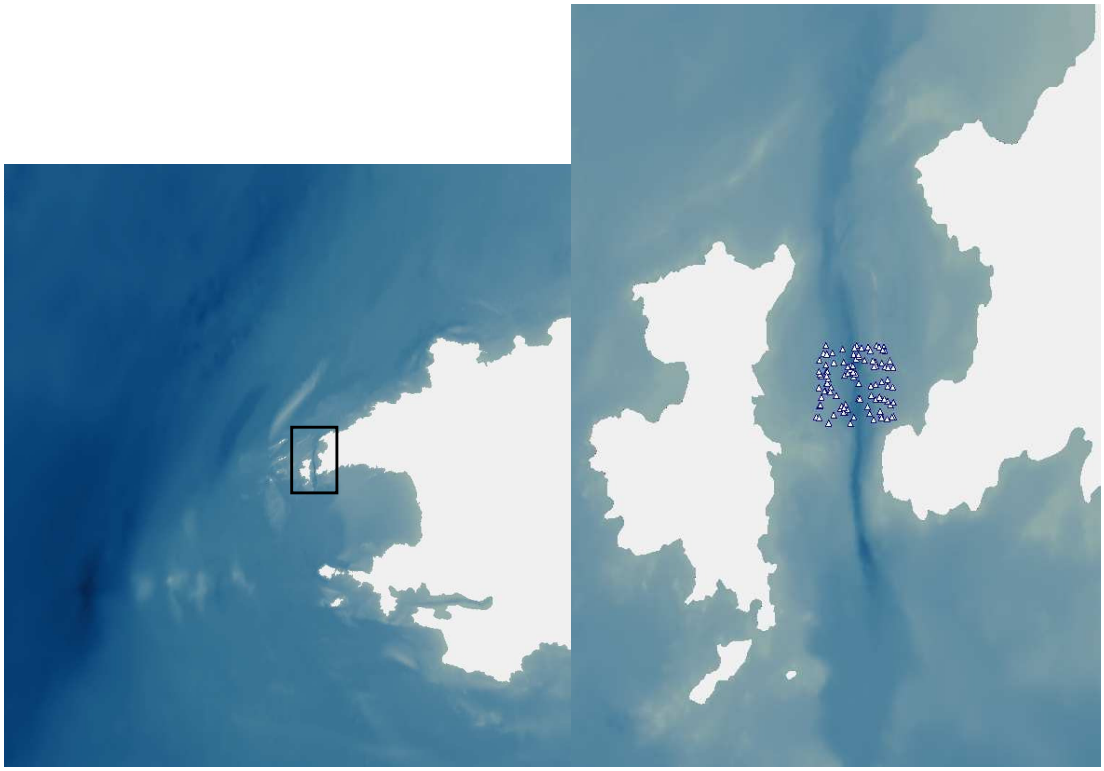

Figure 7.2: Computational domain (left), showing the Ramsey Sound area and starting porpoise distribution (right)

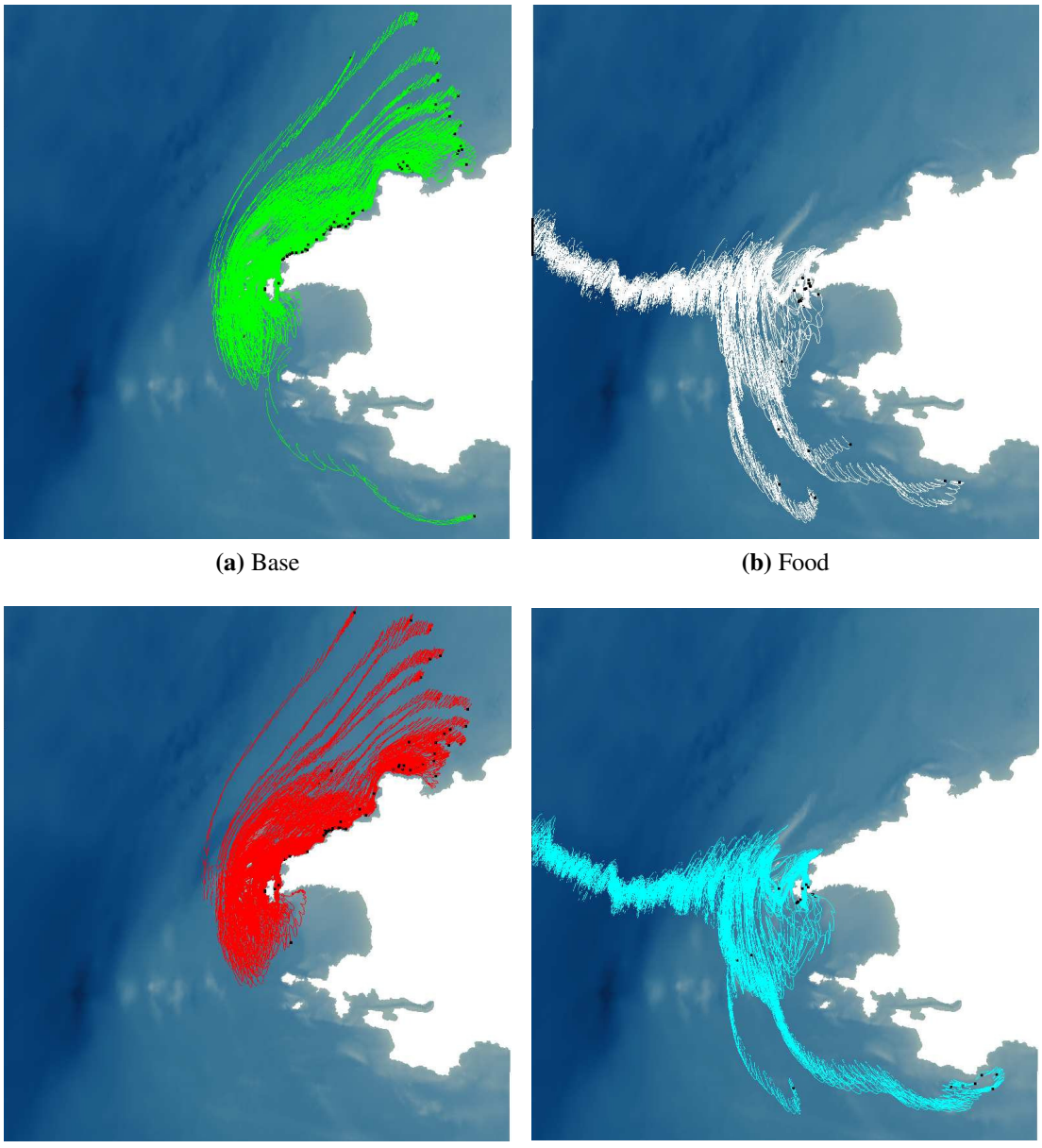

(a) Base **(b)** Food

(c) Noise **(d)** Both

Figure 7.3: Porpoise tracks through Ramsey Sound and surrounding area, based on different combinations of behaviour rules. Black markers show the positions of porpoise at the end of the simulation

7.6.1 Initial comparisons

On visual inspection of the four different simulations, the most significant differences between them are the presence of the westward tracks (in Figures 7.3b and 7.3d) and the corresponding absence of the coast following north eastward tracks (in Figures 7.3a and 7.3c).

Three of the four simulations results show a small amount of activity to the south east of the domain - 1 individual as shown in Figure 7.3a, 7 individuals in Figure 7.3b and 7 individuals in Figure 7.3d. Only the noise only simulation shown in Figure 7.3c shows no porpoise activity in this region.

There is little obvious difference between the base simulation and the noise only simulation at first glance. The tracks in the noise simulation (Figure 7.3c) are positioned slightly further north than the corresponding tracks in the base case. Additionally the lone trail present to the south east in the base case is absent in the noise case, as discussed above. Given that the additional noise within the domain covers such a small area, it is unsurprising that the differences between these two simulations are similarly small.

The substantial westward tracks shown in the simulations with food present is counter-intuitive given the net difference between the base and food cases should have been an attraction to the food source positioned in the south of the Sound. To help explain these results, the residual tide is calculated and discussed in the next section.

7.6.2 Residual tide

As described in subsection 7.4.2, the food source is static and positioned at the southern end of Ramsey Sound and should act as an attractor for the porpoise. The presence of additional porpoise within the Sound area itself would seem to correlate with this, but makes the very prominent westward track unexpected.

The residual tide can be obtained by summing the velocity components over the course of a tide, and represents the net velocity experienced at a fixed location over the duration.

Scaling this by the number of samples (to yield an average velocity) and multiplying this average velocity by the period of the M_2 tidal constituent represents this residual quantity as a distance, *rd*, with units of metres per tide:

$$rd = \frac{1}{N\Delta t} \sum_{i=0}^{N} 44712 \boldsymbol{v}_i \tag{7.1}$$

where N is the number of samples of length Δt over the tidal period, $\boldsymbol{v}_i$ is the velocity at that time. This quantity has been calculated over the domain, and is presented in Figure 7.4. The two plots in that figure show the magnitude, $|rd|$, in Figure 7.4a and the angle between *rd* and North (vertical axis as plotted) is shown in Figure 7.4b.

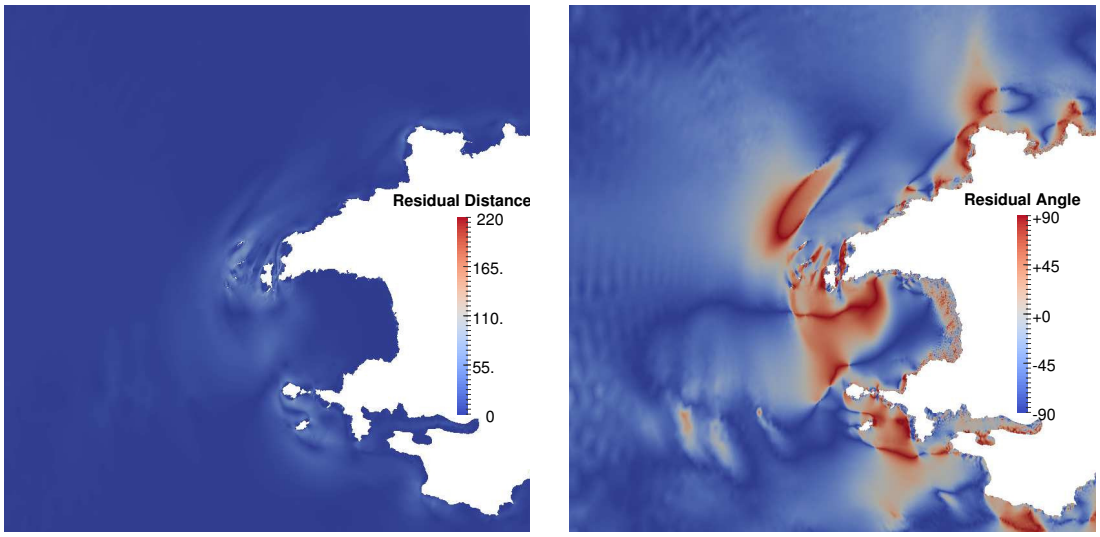

(a) Magnitude **(b)** Angle

Figure 7.4: Residual tidal distance *rd*: magnitude and angle (North = 0°)

The magnitude of this residual distance is generally small, but varies significantly throughout the domain. In particular, high values can be found in and around Ramsey Sound, and Skomer and Skokholm to the south. The angle of this residual indicates the direction of the residual, with blue (negative) areas indicating westward residual flow and red (positive) indicating eastward residual flow.

Figure 7.4b shows the angle of the tidal residual through the domain, and largely shows flow with a westward component (blue). The cumulative effect of the draw towards the food in the Sound may act to keep the porpoise further south than the individual animals in the base case, exposing these individuals to the stronger and more westerly residuals than animals that have followed the tidal flows around the coast to the north east of the Sound with smaller and more varied residuals.

7.6.3 Common features

In addition to the differences described above, there are a number of common features that can be seen in the results as shown in Figure 7.3.

All four simulations show little activity within the confines of St Bride's bay (the larger bay south and east of Ramsey Sound), although all simulations show porpoise present along the boundary of the bay. This avoidance does not relate to the shallow water avoidance behaviours (the 10m depth limit is much closer to shore). Whether this area is used by porpoise is the subject of disagreement in the available literature [29, 31]. There is also lack of porpoise presence within Whitesands bay to the north of Ramsey Sound, but in this instance the water depth is lower and the avoidance of the area is consistent with the shallower water and implemented behaviour rules.

The other notable commonality between the four simulations includes an area of porpoise presence to the south west of Ramsey Island, with tracks leading back towards the Sound - even in the absence of influence from the food source in that region. Comparing the results again to the angle of the residual tide (shown in Figure 7.4b), it can be seen that this corresponds to the region of eastward residual tide, which encourages the return of porpoise to the vicinity of the Sound.

These common features are, however, small compared to the general population distributions shown. The differences between simulations with and without the influence of food are readily apparent when the porpoise tracks are examined visually, and as such it would make sense for these results to be discernible on the basis of statistical measures as well.

	Simulation				
	Initial	Base	Food	Noise	Both
Mean ($\bar{x}$)	-591823	-572525	-625226	-573006	-625495
Mean ($\bar{y}$)	329802	349753	329651	351095	329793
Std. Dev. (σ_x)	303	15632	35255	15144	38123
Std. Dev. (σ_y)	296	17188	16287	16415	15999
$\Delta\bar{x}$	-	19298	-33403	18817	-33672
$\Delta\bar{y}$	-	19951	-151	21293	-9
$\Delta\sigma_x$	-	15329	34951	14841	37820
$\Delta\sigma_y$	-	16892	15991	16119	15703

Table 7.1: Summary statistics for the initial conditions and all four Ramsey Sound simulations. All units are metres. Δ values represent difference from initial conditions shown in the first column of values.

7.6.4 Statistical differences

In addition to the qualitative discussion above, the results can be compared numerically based on statistical measures as described in Chapter 5. The measures discussed in that Chapter have been calculated for the four simulations presented here, and are shown in Table 7.1. Note that the origin of the coordinates used is south east of the domain, leading to negative coordinates in x throughout. This is reflected in the negative values of mean x position, $\bar{x}$, for all simulations described here.

The same pairings of results are visible in these statistical measures as discussed in Section 7.6.1 above. The influence of food leads to a significant shift in mean population position to west and slightly south over the course of the simulation ($\Delta\bar{x} << \Delta\bar{y} < 0$) for the Food and Both cases. Conversely, the north east motion of the Base and Noise results seen in Figure 7.3 is reflected in the mean position and change in mean position values given in Table 7.1.

In terms of the population spread, all four simulations have a larger standard deviation of position in both x and y axes when compared to the initial population distribution - shown, as $\Delta\sigma_i > 0$ for both σ_x and σ_y. This increase is consistent with the populating moving away from the densely packed initial release described in Section 7.5.

The change in standard deviation in x (σ_x) clearly distinguishes between the simulations with and without the influence of food included. The $\Delta\sigma_x$ value for the Food and

Both simulations is more than double the corresponding values for the Base and Noise simulations, indicating a substantially more spread out population.

As a final note in this section, it should be noted that none of the simulations have a greater increase in σ_y than the Base case. This is likely due to the Base case being the only simulation to have particles present at both extremes of the y range of the domain, as shown in Figure 7.3a, and is therefore the most spread population in that direction. Although all three simulations show a positive $\Delta\sigma_y$ value (representing increased spread in the y direction compared to the initial porpoise distribution), this value is smaller than the Base simulation. This would imply that the influence of food and noise (separately or in combination) acts in such a way as to limit the North-South spread of the porpoise during these simulations.

7.7 Impacts

One of the main aims of this model has been to allow the investigation of potential impacts on harbour porpoise due to the influence of tidal stream devices. To that end, we can take the simulation above intended to represent the status quo (Food - as shown in Figure 7.3b) and add a noise source. The results of this simulation are shown in Figure 7.3d - the scenario labelled Both.

Before making that comparison, it is useful to examine two additional questions. First, does the addition of food to the model have the intended effect within the Ramsey Sound area? Secondly, does the resulting data match the behaviour of porpoise based on existing data from the area? These questions are discussed below.

7.7.1 Is Food Significant?

Employing the method described in [30] and in Section 4.5, the results of the simulation can be presented as a grid of cells representing the number of porpoise present per hour in a given location. Using this method to examine simulation results produces an output which can be compared to observational data.

Figure 7.5 shows the results of the of the simulations presented as porpoise presence per hour on a grid of 500m squares. Cells with a value below 0.2 have reduced opacity, with 0 being fully transparent. This allows the underlying domain to be seen, providing context to the results.

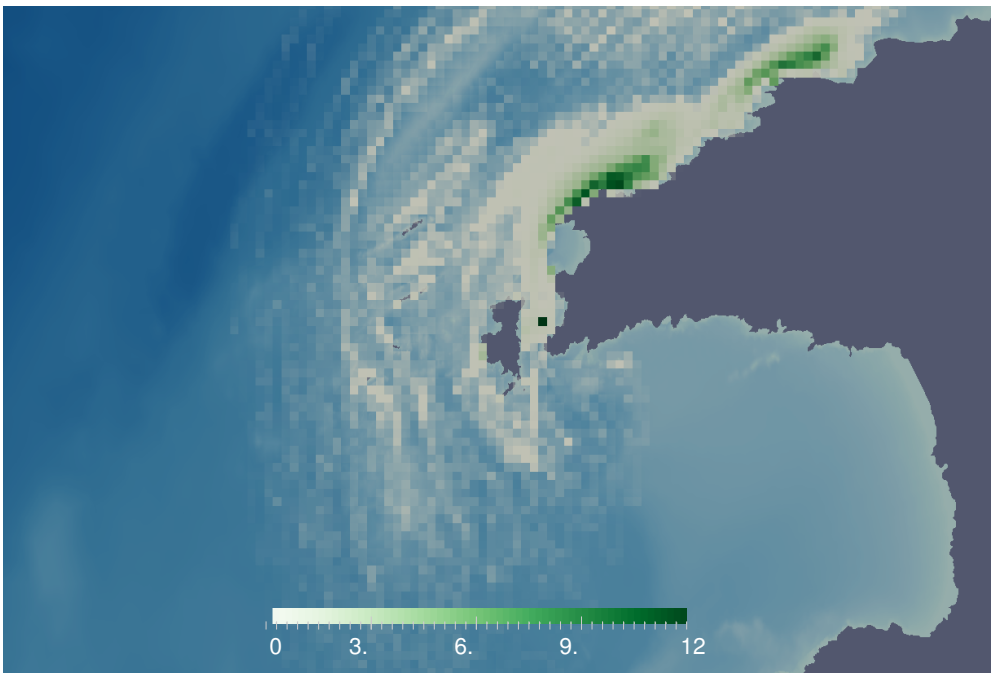

(a) Base

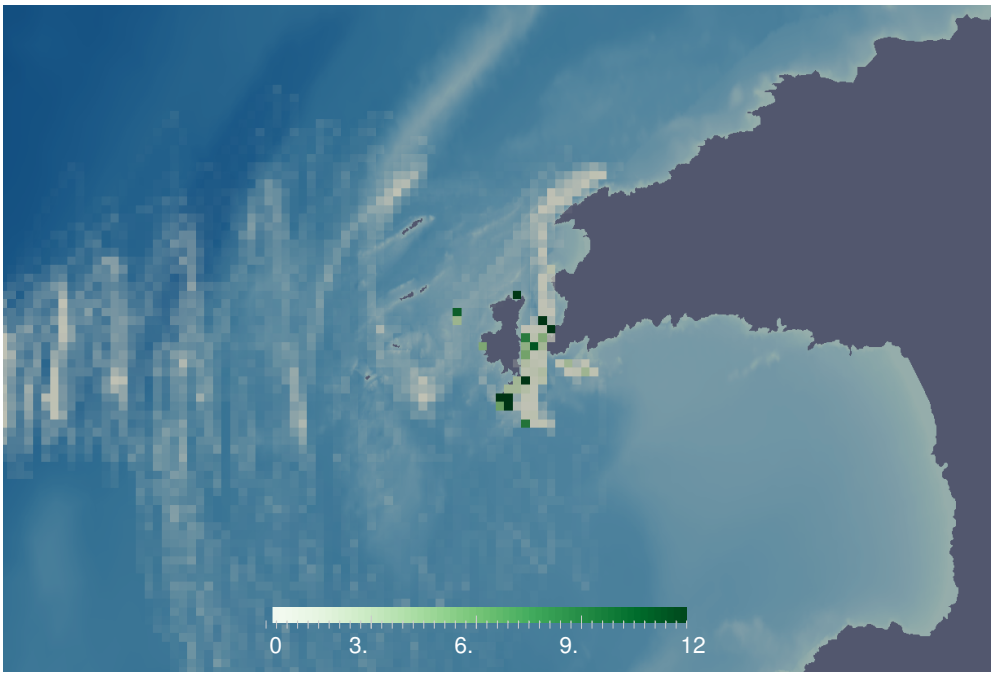

(b) Food

Figure 7.5: Ramsey Sound porpoise presence on a 500m grid

The base simulation (shown in Figure 7.5a) shows a relatively uniform distribution over the area shown, with small patches of increased presence along the coast to the north east of the Sound. The presence of porpoise around Ramsey Island is shown to be reasonably uniform, with reduced presence counts immediately to the south and south east of the Sound itself. With the exception of a single cell, the presence through the Sound is uniformly low, with little presence at the southern end as discussed in [30] or [29].

Adding food to the model gives the results shown in Figure 7.5b. Relative to the Base model, the obvious differences are the lack of any porpoise presence along the coastline to the North East and a larger region of lower presence values to the west (in the area covered by the westward drift shown in Figure 7.3b). The presence immediately around Ramsey is far less uniform, with increased presence in the south of the Sound and substantially reduced presence to the south west and west of Ramsey Island.

This is more consistent with the accounts given in literature for the area in and around the Sound.

7.7.2 Simulated porpoise presence and real porpoise sightings

Plotting the results of the simulations in a normalised grid form as above also allows them to be compared to the equivalent plots made from sightings data in the Ramsey Sound area. There field data results are based on actual sightings, which requires the porpoise to be present at the water surface for long enough to be observed. The plots produced based on the simulation results are based solely on the presence of a porpoise in that area, with no adjustment for depth or detection probability. As such, the values reported for results from the simulations may be 15–50 times higher in value, based on the proportion of time spent by harbour porpoise at the surface, as reported in [45] and described in subsection 2.4.1. No adjustment is made based on detection probability, but it is expected that the overall trends in the results should be comparable.

Figure 7.6 shows simulated and real observational data side by side. The observation data is shown in Figure 7.6b represents porpoise sightings per hour based on four years of observational data, collected over the four year period 2009-2012 and previously discussed in [30]. The surveys were conducted from the three observations points shown, labelled PSJ, PMM, PP.

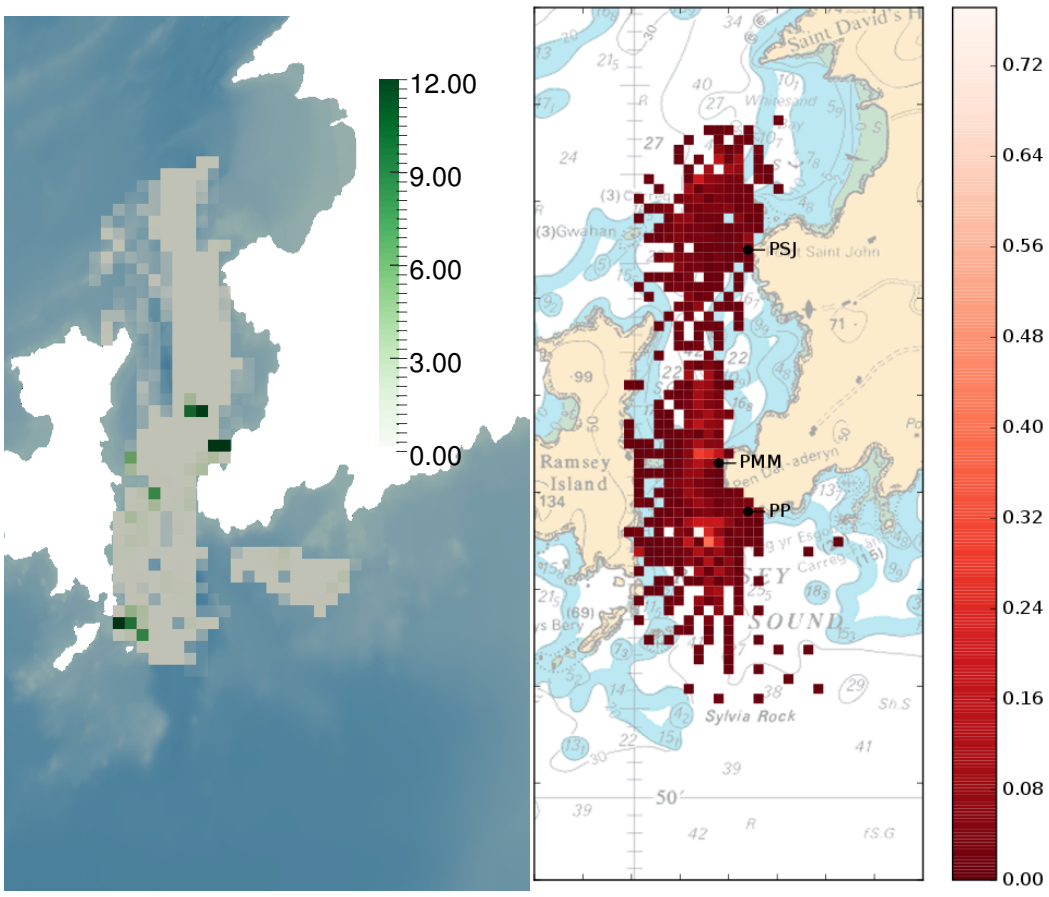

(a) Simulation (Food) **(b)** Field Data

Figure 7.6: Porpoise presence (simulated) and sightings (field) data normalised against time

The simulated data in Figure 7.6a is taken from the Food simulation and has been analysed on a 200m grid, with porpoise presence per hour values below 0.01 rendered transparent. The data has been cropped based on the fields of view used in the analysis of the field data in order to provide a better visual comparison with the field data.

There are a number of features which are visible in both the simulated data and the results of the field data analysis. These include a reduction in presence north of the north eastern tip of the island, level with the point marked PSJ in the field data, followed by a small increase in sightings further north towards the limit of detection. Both images show a lack of porpoise presence in the bay/cove on the eastern side of the Sound (Porthstinian), and an area of porpoise absence immediately south of the point marked

PP.

Some of the variations shown in Figure 7.6b are not clear in the simulation results shown in Figure 7.6a. This may be due to the comparatively small datasets being compared, or due to the increased difficulty sighting porpoise at longer distances, which will reduce the densities shown further from the observation points in the field data results but which the simulated results are not subject to. This could be compensated for by further analysis of the field data (investigating corrections based on work in [55]) or by sampling the simulation data in a fashion closer to that of an observer by incorporating a probability to "miss" the presence of a porpoise on the same basis.

7.7.3 Harbour porpoise changes within Ramsey Sound and the wider area

Figure 7.7 shows the results of the food only source (Figure 7.7a, already shown above as Figure 7.6a) and the "Both" simulation which includes both food and noise as influences. Presented side-by-side in the same form as the existing observation results, it can be seen that there are few differences caused by the presence of the noise source that would be detectable based on observational data.

There is an increase in porpoise presence close to the north eastern shore of Ramsey Island, to the eastern side of the turbine site. This could be interpreted as resulting from porpoise diverting their transits around the turbine vicinity, concentrating the existing presence into a smaller number of grid cells in this location. There are also small changes in the distribution to the southern end of the Sound, which would appear to be due to a slightly increased use of the bay area to the south east of the Sound, as shown in Figure 7.3d.

The statistics presented in Table 7.1 show small differences between the two simulations. The addition of noise as an influence shifts the mean position 269 metres west and 142 metres north, for a total displacement of 304 metres. As a consequence, the change in mean y position relative to the initial conditions is also reduced by the addition of noise compared to the food only case. The change in standard deviation is more notable, with an increase in the standard deviation in x of 2868 metres and a *decrease* in standard deviation in y of 288 metres.

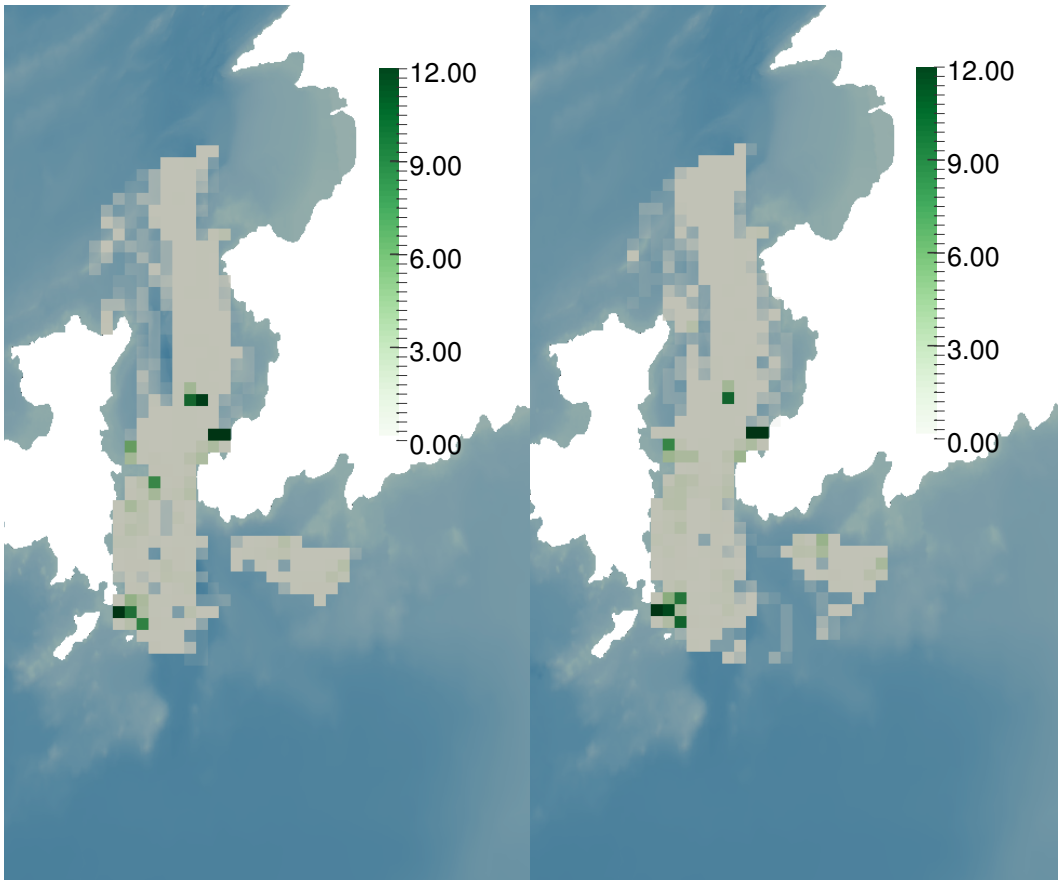

(a) Food **(b)** Both

Figure 7.7: Gridded harbour porpoise presence within the sound before (a) and after (b) a noise source is added

This can be interpreted as the addition of noise partially countering the attraction of the food source at the south end of the Sound, leading to more porpoise ending up outside the effective draw of that food source and wandering to the west or south east of the model under the influence of the underlying tides. It also shows that comparatively small changes in the environment can yield results that should be observable under existing observation methods that have been employed to monitor the presence and movement of harbour porpoise in the real world.

7.8 Conclusions

Ramsey Sound is an important study area for marine and tidal energy, providing an opportunity to examine the interactions between marine life and a tidal stream device. The preliminary results presented here show the ability of the model developed to replicate patterns of movement on a small scale with a comparatively small number of simulated individuals, using the modelled response to food in order to "steer" the simulated population towards the expected behaviour. This would need to be evaluated further if using the model to examine existing observational data, but could also be used as a tool itself to examine how changes in the position of the food source(s) may become visible in observations.

In a similar vein, the model has also shown sufficient sensitivity to present detectable changes in simulated habitat use when a source of disturbance (noise) is introduced into the simulations as shown in Table 7.1 and as discussed further in Section 7.7.

These changes appear to be visible when results are analysed in a manner similar to existing processes for field data suggesting that these changes, though small, may be observable in the field. This is dependent on the responses coded into the model for the stimuli presented in the model, which would need to be investigated further. The lack of existing harbour porpoise movement and presence data for the wider area prevents analysis of the simulated data over the bulk of its range. This means that any results from these simulations need to be viewed cautiously until further validation can be carried out.

Chapter 8

Conclusions

"Universities are truly storehouses of knowledge: students arrive from school confident that they know very nearly everything, and they leave years later certain that they know practically nothing.

Where did the knowledge go in the meantime? Into the university, of course, where it is carefully dried and stored."

Terry Pratchett, Ian Stewart and Jack Cohen - The Science of Discworld (1999)

8.1 Summary

The preceding chapters presented a summarised account of the work and research that has taken place over the course of this project. This chapter will reiterate the conclusions from the previous chapters in the context of the initial aims and motivations behind this project before making recommendations for future work.

8.1.1 Background

Chapter 2 introduced the wide array of possibilities that could be modelled using Individual Based Models and highlighted some of the previous uses of the technique - both within the realms of ecological simulation and in other fields. These included simulating flocks of birds for computer animation [89], the simulation of Moose within a simplified 2D environment [92] and a 3D patch based model of small woodland birds [96]. Some of the computational limitations that might be encountered were also discussed.

The nature of marine mammals was also examined through a description and summary of the properties of harbour porpoise. This included what is known about their use of different habitats and the legal protections afforded to this species under different items of legislation. The difficulties faced obtaining movement and behaviour data from animals were discussed. These included the limitations associated with tagging design and placement [42,43], and limitations due to environmental conditions (on both monitoring equipment [54] and surveys [30, 55]).

8.1.2 Modelling

Given the ability for IBMs to produce plausible results from relatively simple inputs, the technique showed potential for simulating marine mammal behaviours and as an investigative tool.

The discussions moved to the theory behind implementing a simple IBM in a realistic tidal environment in Chapter 3, where the general concepts used in the model were presented. The model has been constructed based on the use of existing tidal models to provide a realistic representation of particular geographic sites. The models used have been mesh based as discussed in section 3.4, and either 3D or converted to 3D from an original depth averaged model as discussed in subsection 3.6.1.

The theoretical underpinnings of the model were then restated in a standardised fashion using the ODD protocol in Section 3.8 towards the end of Chapter 3. This description also included some details of the implementation of this model that has been created as part of this project, which has been described in more detail in Chapter 4.

The final two chapters in this part examine the behaviour of the model on a statistical basis (Chapter 5) and based on its behaviour as different input parameters are varied (Chapter 6). This introduced a number of statistical measures that could be used to describe a simulated population, and illustrated the effect of the population size on convergence of these measures towards stable values, and the effect on relative error in these measures. These results suggested that the statistical properties of a simulated population vary based on the size of that population, depending on the properties being discussed. Exploring this dependence based on 3 different simulations in the North Sea showed that simulations required up to 1700 individuals in order to converge on stable values. Some further exploration of the statistical behaviour of the model may well be required to verify this result.

The parametric exploration carried out in Chapter 6 showed how those measures can vary with comparatively small changes in parameter values, with changes in mean position over a simulation varying between 4m to 94180m depending on the parameter values chosen. There were also unexpected outcomes that appeared to result from the cumulative effect of small scale variations applied over the full duration of the simulation, leading to porpoise "wandering" away from the main population. In contrast, there was also a consistent core behaviour of the simulated population that remained similar across a broad range of parameter values, with the population aggregating in areas of locally favourable conditions in the absence of other stimuli forcing them to move away.

8.1.3 Ramsey

The final substantive chapter of this thesis took the example of Ramsey Sound, an area of social, environmental and scientific interest where a developer has obtained a license to deploy a tidal stream turbine deployment - namely Tidal Energy Limited with a license for their DeltaStream prototype. The results of four main simulations were shown, combining baseline data with the effects of a noise source representing a typical tidal stream turbine and a source of food.

The results showed that the availability of food within the model (which was assumed to be unaffected by the addition of the turbine) was the dominating influence in determining the behaviour of the simulated animals over the duration of the model. There were, however, measurable differences between the simulations with an added source of noise and without.

These differences were detectable numerically in both the mean and standard deviation of the population position values, with the presence of food leading to a mean position 33km west of the initial distribution and 53km west of the final mean position for the baseline simulation. Adding a noise source to the Base and Food simulations shifted the mean population positions to the north and west in both cases, moving the Base case by 1425m and moving the mean position of the Food case by 304m.

The lack of data from the wider area hinders validation of the model, limiting confidence in these final results. Despite this, comparisons made to existing observational data from area showed a promising correlation between the simulated and real data, as well as small but detectable changes between the scenarios with and without noise. Although further work and refinement is required, the model has demonstrated the ability to imitate the statistical usage of an area by harbour porpoise on a fine scale and to show potential changes to that usage as the underlying influences are varied.

8.2 Suggestions for Future Work

As stated at the beginning of this thesis, this project aimed to research, investigate, and implement a behaviour model for harbour porpoise that could be used to investigate the behaviour and habitat use of these animals at a potential tidal site. This model has been developed and presented as described above, but leads to a number of possibilities for future work. The order that points are presented below is in loose order of priority.

8.2.1 Improved behaviour modelling

In the context of the software developed, the most obvious scope for improvement lies in the behaviour rules themselves. These are the key to mimicking the movement and behaviour of the animals, and therefore should be the first area examined for improvement.

Energetics

As mentioned in Section 2.4, harbour porpoise are energetic creatures that forage almost continuously in order to replenish the energy they expend. This means that any harbour porpoise trapped or displaced away from food sources are at risk (ultimately) of starvation. Including this in the model should be done by adding a property to the porpoise data structure to track its internal energy reserves, and replenishing this reserve when in an area with sufficient food. Porpoise with an internal energy reserve at or below zero should then be suspended from the simulation and marked with an appropriate exit code to indicate energy exhaustion.

This will also require improved data representing food availability, either by further research or further modelling exercises.

Improve food and noise responses

The directional response to food and noise was kept simple and predictable during development of the model. This should be expanded to better reflect the likely response of a real organism. Thought should also be given to how rapidly the target direction of the porpoise should change with respect to the simulation timestep - small timesteps are required for the hydrodynamic aspects of the simulation, but it may be unrealistic for the porpoise to alternative rapidly between noise avoidance and resting/foraging behaviour. Consideration could be given to some cool down/persistence of internal state. It may be more accurate to represent the directional response as a weighted vector composed from the intended direction of travel due to each behaviour, combined with some weighting factor. This could be implemented similar to the noise response modelled in [87].

Behaviour trade offs and variations

The next recommendation would be to investigate the possibility of allowing trade offs between behaviours. The current implementation of the model places the three behaviour responses in a strict hierarchy, and all simulated porpoise share the same threshold triggers and priority order for their behaviour. This could be modified to consider "exposure" rather than an instantaneous threshold response (weighting the current level of the behaviour trigger against time spent at that level). The tolerance of each animal

to a particular quantity could also be modified - allowing some animals to be more sensitive to noise than others for example. This would provide a greater spread of triggers for any given situation, allowing a wider range of responses. This would represent the natural variation in behaviours between individuals.

A further refinement of this would be to allow the order of responses to vary between individuals - allowing some simulated porpoise to prioritise water depth over noise level, or to prioritise feeding over a certain exposure to noise. As with the suggested modification above, this would simulate a wider variation in responses.

It should also be noted, however, that a wider range of responses would be likely to require simulation of a larger number of individuals to minimise the statistical errors, as discussed in Chapter 5.

Diving/Surfacing

Harbour porpoise spend a great deal of time foraging/hunting, as discussed above and in [78]. A lot of a porpoise's time is spent below the surface of the water, where it is not visible to land based observers [30, 45]. Implementing some vertical behaviours into the model could allow this to be represented, allowing better comparison to visual survey data and potentially allowing for changes in this data to be investigated or predicted. Further research and review of existing literature would be required in order to formulate a suitable description of this behaviour and implement an appropriate behaviour rule within the model.

8.2.2 Further studies

In addition to possible improvements to the animal behaviour side of the model, there are improvements and recommendations that can be made for the data and software side of the project as well.

Noise propagation

One of the weaknesses of the simulations presented here is the simplistic representation of food and noise. Information on both of these proved hard or impossible to find for specific locations, and is often not available at the fine spatial and temporal resolutions for this sort of model.

In the case of the input noise values, this could be improved by using separate software to calculate the propagation of noise through the tidal domain based on the same underlying bathymetry used to define the tidal environment used in simulations with this model. There are existing pieces of software for this purpose, which should be evaluated for suitability. The output of these models could then be interpolated to the nodes defined in the simulation input data in order to provide noise data for the simulation. The file formats required for this to work are described in Appendix A.

Statistical sensitivity

The sensitivity study presented in Chapter 5 has only been completed for a single simulated environment, for a small selection of conditions. This exercise should be repeated for additional simulated environments in order to determine how sensitive it is to different scenarios. This was intended to be completed for the Ramsey Sound simulations presented here, but was not feasible within the computational resources and timescale of the project.

8.2.3 Implementation specific changes

The algorithms and precomputation steps detailed in Chapter 4 have helped reduce the time taken for the software to complete any given simulation. This could be further improved by loading and processing data in a more conservative fashion. A recommended first step would be to investigate any gains available by only calculating mesh movement and updated Z coordinates for areas of the mesh immediately around the porpoise being simulated at any given time. Although this may add complexity, it should further reduce the computational time required - particularly for larger meshes.

A second recommendation in this category would be to load variable data on demand, so that any simulation data not used is left on disk and not transferred to working mem-

ory at any point. This would reduced the memory (RAM) requirements for any given simulation as well as reducing the time required for file input/output.

8.2.4 Source code

It is intended to document and release the model used in this thesis as a freely available, open source code that can be taken and used by others. This may lead to further opportunities for validation and investigation.

8.3 Final remarks

Investigating the potential environmental impacts of marine energy devices and attempting to minimise it them is one of the challenges the industry is grappling with as it grows and moves towards commercialisation. The model developed, implemented and tested over the course of this project and documented in this thesis represent a small contribution toward reducing the barriers and challenges faced by the marine energy industry. This model has already shown promising correlations with existing data and provides a good starting point for the further work and investigations suggested above.

References

[1] World Commission on Environment and Development, "Our Common Future (Brundtland Report)," 4 August 1987.
Online: http://undocs.org/A/42/427

[2] United Nations General Assembly, "United Nations Millennium Declaration," 8 September 2000.
Online: http://undocs.org/A/RES/55/2

[3] Core Writing Team, "Climate Change 2014: Synthesis Report. Contribution of Working Groups I, II and III to the Fifth Assessment Report of the Intergovernmental Panel on Climate Change," IPCC, Geneva, Switzerland, Tech. Rep., 2014.

[4] P. Pearson and J. Watson, *UK Energy Policy 1980-2010 : A history and lessons to be learnt*. London: Parliamentary Group for Energy Studies, January 2012.
Online: http://www.theiet.org/factfiles/energy/uk-energy-policy-page.cfm

[5] O. Ellabban, H. Abu-Rub, and F. Blaabjerg, "Renewable energy resources: Current status, future prospects and their enabling technology," *Renewable and Sustainable Energy Reviews*, vol. 39, pp. 748 – 764, 2014.
Online: http://www.sciencedirect.com/science/article/pii/S1364032114005656

[6] HM Government, "UK Renewable Energy Roadmap," Department of Energy & Climate Change, Tech. Rep., Jul. 2011.

[7] S. Salter, *Looking Back*. Berlin, Heidelberg: Springer Berlin Heidelberg, 2008, ch. 2, pp. 7–39.

[8] I. MacLeay, K. Harris, and A. Annut, Eds., *Digest of United Kingdom Energy Statistics 2014*. London: TSO, 2014, vol. 1, ch. 6, pp. 157–194, a National Statistics publication from the Department of Energy & Climate Change.
Online: https://www.gov.uk/government/collections/digest-of-uk-energy-statistics-dukes

[9] RenewableUK, "Offshore Wind Project Timelines 2015," http://www.renewableuk.com/en/publications/index.cfm/Offshore-Wind-Project-Timelines-2015, June 2015, rUK15-014-04.
Online: http://www.renewableuk.com/en/publications/index.cfm/Offshore-Wind-Project-Timelines-2015

[10] The Crown Estate, "UK Wave and Tidal Key Resource Areas Project," The Crown Estate, Tech. Rep., Oct. 2012.

[11] D. Krohn, M. Woods, J. Adams, B. Valpy, F. Jones, and P. Gardner, "Wave and Tidal Energy in the UK: Conquering Challenges, Generating Growth," RenewableUK and BVG Associates and GL Garrad Hassan, Tech. Rep. RUK13-008-8, February 2013.
Online: http://www.renewableuk.com/en/publications/index.cfm/wave-and-tidal-energy-in-the-uk-2013

[12] M. Mueller and R. Wallace, "Enabling science and technology for marine renewable energy ," *Energy Policy*, vol. 36, no. 12, pp. 4376 – 4382, 2008, foresight Sustainable Energy Management and the Built Environment Project.
Online: http://www.sciencedirect.com/science/article/pii/S0301421508004539

[13] A. Garrad, "The lessons learned from the development of the wind energy industry that might be applied to marine industry renewables," *Philosophical Transactions of the Royal Society of London A: Mathematical, Physical and Engineering Sciences*, vol. 370, no. 1959, pp. 451–471, 2011.

[14] P. Fraenkel, "Practical tidal turbine design considerations: a review of technical alternatives and key design decisions leading to the development of the SeaGen 1.2mw tidal turbine," in *Proceedings of Fluid Machinery Group - Ocean Power Fluid Machinery Seminar*. London: Institution of Mechanical Engineers, October 2010.

[15] M. Harrold, P. Bromley, D. Clelland, A. Kiprakis, and M. Abusara, "Evaluating the thrust control capabilities of the DeltaStream turbine," in *Proceedings of the 11th European Wave and Tidal Energy Conference*, Nantes, France, September 2015.

[16] MeyGen Limited. (2016) The Project. Online, accessed 2016-05-19.
Online: http://www.meygen.com/the-project/

[17] The Energy and Climate Change Committee, "A Severn Barrage?" House of Commons, Tech. Rep., June 2013.
Online: http://www.publications.parliament.uk/pa/cm201314/cmselect/cmenergy/194/194.pdf

[18] J. Norris and I. Bryden, "European Marine Energy Centre: facilities and resources," *Proceedings of the Institution of Civil Engineers - Energy*, vol. 160, no. 2, pp. 51–58, 2007.
Online: http://www.icevirtuallibrary.com/doi/abs/10.1680/ener.2007.160.2.51

[19] SuperGen Marine Energy Research Consortium, "SuperGen Marine Energy Research: Full Report," Produced by The University of Edinburgh, Tech. Rep., October 2011.
Online: http://www.supergen-marine.org.uk/sites/supergen-marine.org.uk/files/publications/Phase_2_Monograph_Oct_2011.pdf

[20] A. B. Gill, "Offshore renewable energy: ecological implications of generating electricity in the coastal zone," *Journal of Applied Ecology*, vol. 42, no. 4, pp. 605–615, 2005.
Online: http://dx.doi.org/10.1111/j.1365-2664.2005.01060.x

[21] "Council Directive 92/43/EEC of 21 May 1992 on the conservation of natural habitats and of wild fauna and flora, as amended."

[22] "The Infrastructure Planning (Environmental Impact Assessment) Regulations," 2009, as amended.
Online: http://www.legislation.gov.uk/uksi/2009/2263/contents/made

[23] "The Conservation (Natural Habitats, &c.) Regulations," 1994, as amended.

[24] "Council Directive 85/337/EEC of 27 June 1985 on the assessment of the effects of certain public and private projects on the environment," pp. 40–48, o.J. L. 5.7.1985.

[25] "Directive 2011/92/EU of the European Parliament and of the Council of 13 December 2011 on the assessment of the effects of certain public and private projects on the environment," pp. 1–21, o.J. L. 26, 28.1.2012.

[26] S. Benjamins, "Surveying Marine Mammals in Nearby Tidal Energy Development Sites: a Comparison," in *Proceedings of the 11th European Wave and Tidal Energy Conference*, Nantes, France, September 2015.

[27] M. R. Willis, I. Masters, S. Thomas, R. Gallie, J. Loman, A. Cook, R. Ahmadian, R. Falconer, B. Lin, G. Gao, M. Cross, N. Croft, A. J. Williams, M. Muhasilovic, I. Horsfall, R. Fidler, C. Wooldridge, I. Fryett, P. Evans, T. O'Doherty, D. O'Doherty, and A. Mason-Jones, "Tidal turbine deployment in the Bristol Channel: a case study," in *Proceedings of the Institution of Civil Engineers - Energy*, vol. 163, no. 900024, Aug. 2010, pp. 93–105.

[28] "CCW recommendations for research into the environmental effects of wave and tidal stream technologies," 2012.

[29] C. Pierpoint, "Harbour porpoise (Phocoena phocoena) foraging strategy at a high energy, near-shore site in south-west Wales, UK," *Journal of*

the Marine Biological Association of the United Kingdom, vol. 88, pp. 1167–1173, 9 2008.
Online: http://journals.cambridge.org/article_S0025315408000507

[30] P. Strong, M. Barradell, S. Morris, S. Quinton, and T. Lake, "Harbour porpoise (*Phocoena phocoena*) in Ramsey Sound, the three year period, 2009 to 2011. How many, when and where?" Client Confidential, Report, Dec. 2013.

[31] M. G. Barradell, "Fine Scale Use of Ramsey Sound, Pembrokeshire, West Wales, by Harbour Porpoise (*Phocoena phocoena*)," BSc Dissertation, Coastal & Marine Environment Research Unit, Pembrokeshire College/University of Glamorgan, 2009.

[32] Tidal Energy Limited, "DeltaStream Demonstrator Project, Ramsey Sound, Pembrokeshire - Non-Technical Summary," , Tech. Rep., Oct. 2009.

[33] I. Fairley, M. Broudic, R. Malki, M. R. Willis, I. Horsfall, and I. Masters, "Results from a multi-disciplinary survey campaign at a tidal stream site in west Wales," in *Proc 4th International Conference on Marine Research for Environmental sustainability*, 2011.

[34] V. Grimm, U. Berger, F. Bastiansen, S. Eliassen, V. Ginot, J. Giske, J. Goss-Custard, T. Grand, S. Heinz, G. Huse, A. Huth, J. Jepsen, C. Jorgensen, W. Mooij, B. Muller, G. Pe'er, C. Piou, S. Railsback, A. Robbins, M. Robbins, E. Rossmanith, N. Ruger, S. E., S. Souissi, R. Stillman, R. Vabo, U. Visser, and D. DeAngelis, "A standard protocol for describing individual-based and agent-based models." *Ecological Modelling*, vol. 198, pp. 115–126, 2006.

[35] V. Grimm, U. Berger, D. L. DeAngelis, J. G. Polhill, J. Giske, and S. F. Railsback, "The {ODD} protocol: A review and first update," *Ecological Modelling*, vol. 221, no. 23, pp. 2760 – 2768, 2010.
Online: http://www.sciencedirect.com/science/article/pii/S030438001000414X

[36] I. MacLeay, K. Harris, and A. Annut, Eds., *Digest of United Kingdom Energy Statistics 2014*. London: TSO, 2014, a National Statistics publication from the Department of Energy & Climate Change.
Online: https://www.gov.uk/government/collections/digest-of-uk-energy-statistics-dukes

[37] ABPmer, "Atlas of UK Marine Renewable Energy Resources: Atlas," Department for Business, Enterprise & Regulatory Reform, Tech. Rep., Mar. 2008.

[38] ——, "Atlas of UK Marine Renewable Energy Resources: Technical Report," Department for Business, Enterprise & Regulatory Reform, Tech. Rep., Mar. 2008.

[39] Tidal Lagoon Swansea Bay, "Proposed Tidal Lagoon Development in Swansea Bay, South Wales," Tidal Lagoon Swansea Bay Ltd., Environmental Impact Assessment Scoping Report, Oct. 2012.
Online: http://infrastructure.planningportal.gov.uk/projects/wales/tidal-lagoon-swansea-bay/?ipcsection=folder

[40] I. Fairley, S. Neill, T. Wrobelowski, M. R. Willis, and I. Masters, "Potential Array Sites for Tidal Stream Electricity Generation off the Pembrokeshire Coast," in *Proceedings of the 9th European Wave and Tidal Energy Conference (EWTEC)*, 2011.

[41] S. Isojunno, J. Matthiopoulos, and P. G. H. Evans, "Harbour porpoise habitat preferences: robust spatio-temporal inferences from opportunistic data," *Marine Ecology Progress Series*, vol. 448, pp. 155–170, 2012.
Online: http://www.int-res.com/abstracts/meps/v448/p155-170/

[42] D. Thompson, "Assessment of Risk to Marine Mammals from Underwater Marine Renewable Devices in Welsh waters (on behalf of the Welsh Government), Phase 2: Studies of Marine Mammals in Welsh High Tidal Waters, Annex 1 Movements and Diving Behaviour of Juvenile Grey Seals in Areas of High Tidal Energy," http://www.marineenergypembrokeshire.co.uk/publications-resources, Jul. 2012, jER3688.

[43] V. Pavlov, R. Wilson, and K. Lucke, "A new approach to tag design in dolphin telemetry: Computer simulations to minimise deleterious effects ," *Deep Sea Research Part II: Topical Studies in Oceanography*, vol. 54, no. 3–4, pp. 404 – 414, 2007, bio-logging Science: Logging and Relaying Physical and Biological Data Using Animal-Attached TagsProceedings of the 2005 International Symposium on Bio-logging ScienceSecond International Conference on Bio-logging Science.
Online: http://www.sciencedirect.com/science/article/pii/S0967064507000185

[44] S. P. Vandenabeele, E. Grundy, M. I. Friswell, A. Grogan, S. C. Votier, and R. P. Wilson, "Excess Baggage for Birds: Inappropriate Placement of Tags on Gannets Changes Flight Patterns," *PLoS ONE*, vol. 9, no. 3, pp. 1–9, 03 2014.
Online: http://dx.doi.org/10.1371%2Fjournal.pone.0092657

[45] A. Read and A. Westgate, "Monitoring the movements of harbour porpoises (*Phocoena Phocoena*) with satellite telemetry," *Marine Biology*, vol. 130, pp. 315–322, 1997.

[46] R. P. Wilson, N. Liebsch, I. M. Davies, F. Quintana, H. Weimerskirch, S. Storch, K. Lucke, U. Siebert, S. Zankl, G. Müller, I. Zimmer, A. Scolaro,

C. Campagna, J. Plötz, H. Bornemann, J. Teilmann, and C. R. McMahon, "All at sea with animal tracks; methodological and analytical solutions for the resolution of movement ," *Deep Sea Research Part II: Topical Studies in Oceanography*, vol. 54, no. 3–4, pp. 193 – 210, 2007, bio-logging Science: Logging and Relaying Physical and Biological Data Using Animal-Attached TagsProceedings of the 2005 International Symposium on Bio-logging ScienceSecond International Conference on Bio-logging Science.
Online: http://www.sciencedirect.com/science/article/pii/S0967064507000045

[47] F. Daunt, G. Peters, B. Scott, D. Grémillet, and S. Wanless, "Rapid-response recorders reveal interplay between marine physics and seabird behaviour," *MARINE ECOLOGY PROGRESS SERIES*, vol. 255, pp. 283–288, Jun. 2003.

[48] D. W. Johnston, A. J. Westgate, and A. J. Read, "Effects of fine-scale oceanographic features on the distribution and movements of harbour porpoises Phocoena phocoena in the Bay of Fundy," *Mar Ecol Prog Ser*, vol. 295, pp. 279–293, 2005.
Online: http://www.int-res.com/abstracts/meps/v295/p279-293/

[49] C. Booth, C. Embling, J. Gordon, S. V. Calderan, and P. S. Hammond, "Habitat preferences and distribution of the harbour porpoise phocoena phocoena west of Scotland," *Marine Ecology Progress Series*, vol. 478, pp. 273–285, 2013.

[50] A. Gallus, M. Dähne, U. K. Verfuß, S. Bräger, S. Adler, U. Siebert, and H. Benke, "Use of static passive acoustic monitoring to assess the status of the 'critically endangered' baltic harbour porpoise in german waters," *Endangered Species Research*, vol. 18, no. 3, pp. 265–278, Oct. 2012, German Oceanographic Museum.

[51] J. Teilmann and J. Castensen, "Negative long term effects on harbour porpoises from a large scale offshore wind farm in the Baltic—evidence of slow recovery," *Environmental Research Letters*, vol. 7, pp. 045 101+10, 2012.
Online: http://stacks.iop.org/ERL/7/045101

[52] M. Broudic, T. Croft, M. R. Willis, I. Masters, and S.-H. Cheong, "Comparison Of Underwater Background Noise During Spring And Neap Tide In A High Tidal Current Site: Ramsey Sound," in *Proceedings of the 11th European Conference on Underwater Acoustics*, Jul. 2012.

[53] M. R. Willis, M. Broudic, C. Haywood, I. Masters, and S. Thomas, "Measuring Underwater Background Noise in High Tidal Flow Environments," *Renewable Energy*, vol. 49, pp. 255–258, Jan. 2013.

[54] S. Benjamins, A. Dale, N. van Geel, and B. Wilson, "Riding the tide: use of a moving tidal-stream habitat by harbour porpoises," *Marine Ecology Progress Series*, vol. 549, pp. 275–288, 2016.

[55] S. Buckland, D. Anderson, K. Burnham, and J. Laake, *Distance Sampling*, Republished Online by the Research Unit for Wildlife Population Assessment, Ed. Chapman and Hall, 1993.

[56] L. D. Williamson, K. L. Brookes, B. E. Scott, I. M. Graham, G. Bradbury, P. S. Hammond, and P. M. Thompson, "Echolocation detections and digital video ssurvey provide reliable estimates of the relative density of Harbour Porpoises," *Methods in Ecology and Evolution*, 2016.
Online: http://onlinelibrary.wiley.com/doi/10.1111/2041-210X.12538/abstract

[57] P. Berggren, P. Wade, J. Carlström, and A. Read, "Potential limits to anthropogenic mortality for harbour porpoises in the Baltic region," *Biological Conservation*, vol. 103, no. 3, pp. 313 – 322, 2002.
Online: http://www.sciencedirect.com/science/article/pii/S0006320701001422

[58] G. B. Stenson, S. Benjamins, and D. G. Reddin, "Using bycatch data to understand habitat use of small cetaceans: lessons from an experimental driftnet fishery," *ICES Journal of Marine Science: Journal du Conseil*, vol. 68, no. 5, pp. 937–946, 2011.
Online: http://icesjms.oxfordjournals.org/content/68/5/937.abstract

[59] P. Jepson, M. Perkins, A. Brownlow, N. Davison, M. ten Doeschate, B. Smith, R. Lyal, R. Sabin, and R. Penrose, "Annual report for the period 1st january - 31st december 2014," UK Cetatean Strandings Investigation Programme, Report MB0111, 2014.
Online: http://randd.defra.gov.uk/Document.aspx?Document=12562_Final_UK_CSIP_Annual_Report_2014.pdf

[60] L. L. IJsseldijk, K. C. Camphuysen, J. J. Nauw, and G. Aarts, "Going with the flow: Tidal influence on the occurrence of the harbour porpoise (Phocoena phocoena) in the Marsdiep area, The Netherlands ," *Journal of Sea Research*, vol. 103, pp. 129 – 137, 2015.
Online: http://www.sciencedirect.com/science/article/pii/S1385110115300332

[61] H. Weimerskirch, M. Louzao, S. de Grissac, and K. Delord, "Changes in Wind Pattern Alter Albatross Distribution and Life-History Traits," *Science*, vol. 335, pp. 211–214, Jan. 2012.

[62] V. Peschko, K. Ronnenberg, U. Siebert, and A. Gilles, "Trends of harbour porpoise (Phocoena phocoena) density in the southern North Sea ," *Ecological Indicators*, vol. 60, pp. 174 – 183, 2016.
Online: http://www.sciencedirect.com/science/article/pii/S1470160X15003635

[63] C. von Linné and L. Salvius, *Systema naturae per regna tria naturae :secundum classes, ordines, genera, species, cum characteribus, differentiis, synonymis, locis.* Holmiae :Impensis Direct. Laurentii Salvii,, 1758, vol. v.1.
Online: http://www.biodiversitylibrary.org/item/10277

[64] P. S. Hammond, G. Bearzi, A. Bjørge, K. Forney, L. Karczmarski, T. Kasuya, W. F. Perrin, M. Scott, J. Y. Wang, R. S. Wells, and B. Wilson, "*Phocoena phocoena*," *The IUCN Red List of Threatened Species*, 2008, e.T17027A6734992, Accessed 2016-06-03.
Online: http://dx.doi.org/10.2305/IUCN.UK.2008.RLTS.T17027A6734992.en

[65] H. J. Temple and A. Terry, "The Status and Distribution of European Mammals," IUCN, Tech. Rep., 2007.

[66] Summary species assessment: *Phocoena Phocoena*. report under the article 17 of the habitats directive, period 2007-2012. European Environment Agency.
Online: http://bd.eionet.europa.eu/article17/reports2012/static/factsheets/mammals/phocoena-phocoena.pdf

[67] C. Lockyer, "Harbour porpoises (*Phocoena phocoena*) in the north atlantic: Biological parameters," *NAMMCO Scientific Publications*, vol. 5, pp. 71–89, 2013.

[68] W. A. McLellan, H. N. Koopman, S. A. Rommel, A. J. Read, C. W. Potter, J. R. Nicolas, A. J. Westgate, and D. A. Pabst, "Ontogenetic allometry and body composition of harbour porpoises (Phocoena phocoena, L.) from the western North Atlantic," *Journal of Zoology*, vol. 257, no. 4, pp. 457–471, 2002.
Online: http://dx.doi.org/10.1017/S0952836902001061

[69] C. Lockyer, G. Desportes, K. Hansen, S. Labberté, and U. Siebert, "Monitoring growth and energy utilisation of the harbour porpoise (*Phocoena phocoena*) in human care," *NAMMCO Scientific Publications*, vol. 5, pp. 107–120, 2013.

[70] F. E. Fish and J. J. Rohr, "Review of Dolphin Hydrodynamics and Swimming Performance," Space and Naval Warfare Systems Centre, San Diego, SSC San Diego, CA 92152-5001, Technical Report 1801, August 1999.

[71] R. A. Kastelein, P. Bunskoek, M. Hagedoorn, W. W. L. Au, and D. de Haan, "Audiogram of a harbour porpoise (Phocoena Phocoena) measured with narrow-band frequency modulated signals," *The Journal of the Acoustical Society of America*, vol. 112, p. 334, 2002.

[72] R. Kastelein, W. Verboom, M. Muijsers, N. Jennings, and S. van der Heul, "The influence of acoustic emissions for underwater data transmission on the behaviour of harbour porpoises (Phocoena phocoena) in a floating pen

," *Marine Environmental Research*, vol. 59, no. 4, pp. 287 – 307, 2005.
Online: http://www.sciencedirect.com/science/article/pii/S0141113604001965

[73] L. A. Miller and M. Wahlberg, "Echolocation by the harbour porpoise: Life in coastal waters," *Frontiers in Physiology*, vol. 4, no. 52, 2013.

[74] F. Marubini, A. Gimona, P. Evans, P. Wright, and G. Pierce, "Habitat preferences and interannual variability in occurrence of the harbour porpoise *Phocoena phocoena* off northwest Scotland," *Marine Ecology Progress Series*, vol. 381, pp. 297–310, 2009.
Online: http://www.int-res.com/abstracts/meps/v381/p297-310/

[75] H. Skov and F. Thomsen, "Resolving fine-scale spatio-temporal dynamics in the harbour porpoise *Phocoena phocoena*," *Marine Ecology Progress Series*, vol. 373, pp. 173–186, 2008.
Online: http://www.int-res.com/abstracts/meps/v373/p173-186/

[76] S. Sveegaard, J. Nabe-NIelsen, K.-J. Stæhr, T. F. Jensen, K. N. Mouritsen, and J. Teilmann, "Spatial interactions between marine predators and their prey: herring abundance as a driver for the distributions of mackerel and harbour porpoise," *Marine Ecology Progress Series*, vol. 468, pp. 245–253, 2012.

[77] M. Santos and G. Pierce, *The diet of harbour porpoise (*Phocoena phocoena*) in the Northeast Atlantic*. CRC Press, 2003, vol. 41, pp. 355–390.

[78] D. Wisniewska, M. Johnson, J. Teilmann, L. Rojano-Doñate, J. Shearer, S. Sveegaard, L. Miller, U. Siebert, and P. Madsen, "Ultra-High Foraging Rates of Harbor Porpoises Make Them Vulnerable to Anthropogenic Disturbance ," *Current Biology*, 2016.
Online: http://www.sciencedirect.com/science/article/pii/S0960982216303141

[79] B. M. Bolker, D. H. Deutschman, G. Hartvigsen, and D. L. Smith, "Individual-based modelling: what is the difference? ," *Trends in Ecology & Evolution*, vol. 12, no. 3, pp. 111 –, 1997.
Online: http://www.sciencedirect.com/science/article/pii/S0169534797849191

[80] B. Breckling, "Individual-Based Modelling: Potentials and Limitations," *The Scientific World*, vol. 2, pp. 1044–1062, 2002.

[81] A. J. McLane, C. Semeniuk, G. J. McDermid, and D. J. Marceau, "The role of agent-based models in wildlife ecology and management," *Ecological Modelling*, vol. 222, no. 8, pp. 1544–1556, 2011.
Online: http://www.sciencedirect.com/science/article/pii/S0304380011000524

[82] J. Uchmański and V. Grimm, "Individual-based modelling in ecology: what makes the difference?" *Trends in Ecology & Evolution*, vol. 11, no. 10, pp. 437 – 441, 1996.
Online: http://www.sciencedirect.com/science/article/pii/0169534796200916

[83] Oxford English Dictionary. population, n.1.
Online: http://www.oed.com/view/Entry/147922?isAdvanced=false&result=1&rskey=8IyW0f

[84] R. L. Goldstone and M. A. Janssen, "Computational models of collective behavior," *Trends in Cognitive Sciences*, vol. 9, no. 9, pp. 424–430, Sep. 2005.

[85] V. Grimm, "Ten years of individual-based modelling in ecology: what have we learned and what could we learn in the future? ," *Ecological Modelling*, vol. 115, no. 2–3, pp. 129 – 148, 1999.
Online: http://www.sciencedirect.com/science/article/pii/S0304380098001884

[86] R. L. Olson and R. A. Sequira, "Emergent Computation And The Modeling And Management Of Ecological-systems," *Computers And Electronics In Agriculture*, vol. 12, no. 3, pp. 183–209, Apr. 1995.

[87] J. Nabe-Nielsen, R. M. Sibly, J. Tougaard, J. Teilmann, and S. Sveegaard, "Effects of noise and by-catch on a Danish harbour porpoise population," *Ecological Modelling*, vol. 272, pp. 242–251, January 2014.
Online: http://www.sciencedirect.com/science/article/pii/S0304380013004675

[88] V. Grimm, K. Frank, F. Jeltsch, R. Brandl, J. Uchmański, and C. Wissel, "Pattern-oriented modelling in population ecology," *Science of The Total Environment*, vol. 183, no. 1, pp. 151 – 166, 1996.
Online: http://www.sciencedirect.com/science/article/pii/0048969795049665

[89] C. W. Reynolds, "Flocks, herds and schools: A distributed behavioral model," *ACM SIGGRAPH Computer Graphics*, vol. 21, no. 4, pp. 25–34, 1987.
Online: http://www.red3d.com/cwr/boids/

[90] R. A. Stillman, A. D. West, R. W. G. Caldow, and S. Dit Durell, "Predicting the effect of disturbance on coastal birds," *Ibis*, vol. 149, pp. 73–81, 2007.

[91] X. Tu and D. Terzopoulos, "Artificial fishes: Physics, locomotion, perception, behavior," in *Proceedings of the 21st annual conference on Computer Graphics and interactive techniques*. ACM, 1994, pp. 43–50.

[92] H. Saarenmaa, N. D. Stone, L. Folse, J. Packard, W. Grant, M. Makela, and R. Coulsen, "An Artificial-intelligence Modeling Approach To Simulating

Animal Habitat Interactions," *Ecological Modelling*, vol. 44, pp. 125–141, 1988.

[93] R. Stillman, "MORPH - an individual based model to predict the effect of environmental change on foraging animal populations," *Ecological Modelling*, vol. 216(3–4), pp. 265–276, 2008, sTP SEA Topic Paper Annexe, Fish Behaviour and Physiology (2009), DEFRA, UK.

[94] P. C. Cramer and K. M. Portier, "Modeling Florida panther movements in response to human attributes of the landscape and ecological settings," *Ecological Modelling*, vol. 140, pp. 51–80, 2001.

[95] R. J. H. Herbert, J. Willis, E. Jones, K. Ross, R. Hübner, J. Humphreys, A. Jensen, and J. Baugh, "Invasion in tidal zones on complex coastlines: modelling larvae of the non-native Manila clam, *Ruditapes philippinarum*, in the UK," *Journal of Biogeography*, vol. 39, pp. 585–599, 2012.
Online: onlinelibrary.wiley.com/doi/

[96] J. Alderman and S. A. Hinsley, "Modelling the third dimension: Incorporating topography into the movement rules of an individual-based spatially explicit population model," *Ecological Complexity*, vol. 4, no. 4, pp. 169–181, Dec. 2007.

[97] G. Vigueras, M. Lozano, J. Orduña, and F. Grimaldo, "A comparative study of partitioning methods for crowd simulations," *Applied Soft Computing*, vol. 10, no. 1, pp. 225–235, Jan. 2010.
Online: http://www.sciencedirect.com/science/article/pii/S156849460900088X

[98] S. P. Neill, J. R. Jordan, and S. J. Couch, "Impact of tidal energy converter (TEC) arrays on the dynamics of headland sand banks," *Renewable Energy*, vol. 37, no. 1, pp. 387–397, 2012.
Online: http://www.sciencedirect.com/science/article/pii/S0960148111003855

[99] T. Carlson, B. Watson, J. Elster, A. Copping, M. Jones, M. Watkins, R. Jepsen, and K. Metzinger, "Assessment of Strike of Adult Killer Whales by an OpenHydro Tidal Turbine Blade," Pacific Northwest National Laboratory, Tech. Rep. PNNL-22041, Nov. 2012, draft Version.
Online: http://mhk.pnnl.gov/publications/assessment-strike-adult-killer-whales-openhydro-tidal-turbine-blade

[100] C. S. Abernethy, B. G. Amidan, and G. Cada, "Laboratory studies of the effects of pressure and dissolved gas supersaturation on turbine-passed fish," Pacific Northwest National Laboratory. PNNL-13470. Hydropower Program, US Department of Energy, Idaho Falls, Idaho, Tech. Rep., 2001.

[101] Marine Energy Research Group, "Internal Report," Swansea University, Tech. Rep., 2013.

[102] M. Barradell, S. Morris, S. Quinton, and P. Strong, "Ramsey Sound grey seal sightings at sea and hauled out, baseline data analysis, 2009-2012," Client Confidential, Report, Dec. 2013.

[103] P. Evans, S. Armstrong, C. Wilson, I. Fairley, C. Wooldridge, and I. Masters, "Characterisation of a Highly Energetic Tidal Energy Site with Specific Reference to Hydrodynamics and Bathymetry," in *Proceedings of the 10th European Wave and Tidal Energy Conference*, Aalborg, Denmark, September 2013.

[104] P. Evans, A. Mason-Jones, C. Wilson, C. Wooldridge, T. O'Doherty, and D. O'Doherty, "Constraints on extractable power from energetic tidal straits ," *Renewable Energy*, vol. 81, pp. 707 – 722, 2015.
Online: http://www.sciencedirect.com/science/article/pii/S0960148115002761

[105] E. Zangiabadi, M. Edmunds, I. Fairley, M. Togneri, A. J. Williams, I. Masters, and N. Croft, "Computational Fluid Dynamics and Visualisation of Coastal Flows in Tidal Channels supporting Ocean Energy Development," *Energies*, no. 8, pp. 5997–6012, 2015.

[106] I. Fairley, P. Evans, C. Wooldridge, M. Willis, and I. Masters, "Evaluation of tidal stream resource in a potential array area via direct measurements," *Renewable Energy*, vol. 57, no. 0, pp. 70–78, 2013.
Online: http://www.sciencedirect.com/science/article/pii/S0960148113000499

[107] J. Nabe-Nielsen, J. Tougaard, J. Teilmann, K. Lucke, and M. Forchhammer, "How a simple adaptive foraging strategy can lead to emergent home ranges and increased food intake," *Oikos*, vol. 122, no. 9, pp. 1307–1316, Sep. 2013.

[108] M. Dyndo, D. M. Wiśniewska, L. Rojano-Doñate, and P. T. Madsen, "Harbour porpoises react to low levels of high frequency vessel noise," *Scientific Reports*, vol. 5, pp. 11 083–, Jun. 2015.
Online: http://dx.doi.org/10.1038/srep11083

[109] O. C. Zienkiewicz, R. L. Taylor, and J. Z. Zhu, *Finite Element Method : Its Basis and Fundamentals*, 6th ed. Butterworth-Heinemann, April 2005.

[110] J.-M. Hervouet, "TELEMAC modelling system: an overview," *Hydrological Processes*, vol. 14, no. 13, pp. 2209–2210, 2000.

[111] T. O'Doherty, A. Mason-Jones, D. O'Doherty, P. Evans, C. Wooldridge, and I. Fryett, "Considerations of a horizontal axis tidal turbine," in *Proceedings of the Institution of Civil Engineers - Energy*, vol. 163, no. 900024, 2010, pp. 119–130.

[112] M. Lewis, S. Neill, P. Robins, S. Ward, M. Piano, and R. Hashemi, "Observations of Flow Characteristics at Potential Tidal-Stream Energy Sites," in *Proceedings of the 11th European Wave and Tidal Energy Conference*, Nantes, France, September 2015.

[113] T. Ju, S. Schaefer, and J. Warren, "Mean value coordinates for closed triangular meshes," *ACM Transactions on Graphics*, vol. 24, no. 3, pp. 561–566, Jul. 2005.

[114] J. Ahrens, B. Geveci, C. Law, C. Hansen, and C. Johnson, *ParaView: An End-User Tool for Large-Data Visualization*, 2005.

[115] J. D. Hunter, "Matplotlib: A 2D graphics environment," *Computing In Science & Engineering*, vol. 9, no. 3, pp. 90–95, 2007.

[116] T. N. Croft, "Unstructured Mesh - Finite Volume Algorithms For Swirling, Turbulent, Reacting Flows," Ph.D. dissertation, Centre for Numerical Modelling and Process Analysis, School of Computing and Mathematical Sciences, University of Greenwich, London, Jun. 1998.

[117] B. Zhou and S. Zhou, "Parallel Simulation Of Group Behaviors," in *Proceedings of the 2004 Winter Simulation Conference R. G. Ingalls, M. D. Rossetti, J. S. Smith, and B. A. Peters, eds.*, 2004.
Online: http://ieeexplore.ieee.org/xpls/abs_all.jsp?arnumber=1371337&tag=1

[118] K. Chandy, *An introduction to parallel programming*. Boston, MA: Jones and Bartlett, 1992.

[119] D. Haverson, J. Bacon, and H. Smith, "Modelling the far field impacts of a tidal energy development at Ramsey Sound," in *Proceedings of the 21st TELEMAC-MASCARET user conference*, O. Bertrand and C. Coulet, Eds., October 2014.

[120] T. P. Lloyd, S. R. Turnock, and V. F. Humphrey, "Modelling Techniques for Underwater Noise Generated by Tidal Turbines in Shallow Waters," in *Volume 5: Ocean Space Utilization; Ocean Renewable Energy*. ASME International, 2011.
Online: http://dx.doi.org/10.1115/OMAE2011-49994

[121] S. A. Gauthreaux and J. W. Livingston, "Monitoring bird migration with a fixed-beam radar and a thermal-imaging camera," *Journal of Field Ornithology*, vol. 77, no. 3, pp. 319–328, 2006.

[122] T. C. Guilford, J. Meade, R. Freeman, D. Biro, T. Evans, F. Bonadonna, D. Boyle, S. Roberts, and C. M. Perrins, "GPS tracking of the foraging movements of manx shearwaters puffinus puffinus breeding on skomer island, Wales," *Ibis*, vol. 150, no. 3, pp. 462–473, 2008.

[123] J. Willis, "Modelling swimming aquatic animals in hydrodynamic models," *Ecological Modelling*, vol. 222, no. 23–24, pp. 3869–3887, 2011.
Online: http://www.sciencedirect.com/science/article/pii/S0304380011004893

[124] H. Lorek and M. White, "Parallel Bird Flocking Simulation," 1993.
Online: http://citeseer.ist.psu.edu/viewdoc/versions?doi=10.1.1.48.8430

[125] V. I. Nikora, J. Aberle, B. J. F. Biggs, I. G. Jowett, and J. R. E. Sykes, "Effects of fish size, time-to-fatigue and turbulence on swimming performance: a case study of Galaxias maculatus," *Journal of Fish Biology*, vol. 63, no. 6, pp. 1365–1382, 2003.

[126] E. Pirotta, L. New, J. Harwood, and D. Lusseau, "Activities, motivations and disturbance: An agent-based model of bottlenose dolphin behavioral dynamics and interactions with tourism in Doubtful Sound, New Zealand," *Ecological Modelling*, vol. 282, pp. 44–58, 2014.
Online: http://www.sciencedirect.com/science/article/pii/S0304380014001537

[127] R. Solar, R. Suppi, and E. Luque, "High performance distributed cluster-based individual-oriented fish school simulation," in *Proceedings of the International Conference on Computational Science*, ser. Procedia Computer Science, vol. 4, 2011, pp. 76–85.

[128] G. Vigueras, M. Lozano, C. Pérez, and J. Orduña, "A Scalable Architecture for Crowd Simulation: Implementing a Parallel Action Server," in *37th International Conference on Parallel Processing*, Sep. 2008, pp. 430–437.
Online: http://ieeexplore.ieee.org/xpls/abs_all.jsp?arnumber=4625878

[129] A. West and S. l. dit Durell, "Severn Estuary Bird Food Monitoring. Phase 1," Centre for Ecology and Hydrology, Natural Environment Research Council, Tech. Rep., Oct. 2006.

[130] *VTK File Formats for VTK Version 4.2*.
Online: http://www.vtk.org/VTK/img/file-formats.pdf

[131] *Proceedings of the 11th European Wave and Tidal Energy Conference*, Nantes, France, September 2015.

Appendix A

File Formats

A.1 Input Formats: `telemac-parse`

The file formats generated by telemac-parse are described below. For information about the SELAFIN file format, see the TELEMAC documentation or the brief descriptions given in the `tawe-telemac-utils` documentation. Each file has a defined format and naming convention, with all files sharing a common basename and being stored in the same folder. The basename is often the name of the input SELAFIN file.

A.1.1 Coordinates

X and Y coordinates are stored in flat tab separated text files with the following format:

File format:

```
npoin
id0     coordinate0
id1     coordinate1
id2     coordinate2
```

`npoin` represents the total number of nodes in the mesh, `id0`...`idN` are the node ID numbers and `coordinate0`...`coordinateN` are the coordinates for each node in a fixed decimal form.

The files are named *base.x.txt* and *base.y.txt* respectively.

Z coordinates (for 3D simulations) are permitted to vary in time, and are stored as variables. The data is then used to adjust the vertical coordinates of each node during the simulation.

A.1.2 Connectivity

The connectivity file specifies the IDs for nodes making up each element. It also specifies the number of nodes in each element, which determines the element shape.

File format:

```
nelem   ndp
eid0    nid00
eid0    nid01
....    .....
eid0    nid0N
....    .....
eidN    nidNN
```

`nelem` is the total number of elements and `ndp` specifies the number of points per element. There are then `nelem*ndp` entries in the file specifying an element ID and node ID. Each element is finished (all points specified) before the next is started. `eid0`...`eidN` represent the element IDs and `nid00`...`nidNN` represent the corresponding node IDs. All ID numbers are specified as integer values.

The file is named *base.conn.txt*.

A.1.3 Variable names

The variable name file provides the user visible labels associated with each variable number.

File format:

```
numvars
varid0      varname0
varid1      varname1
.....       ........
```

numvars is the total number of variables in the simulation. varidN is the variable number and varname is the name of the variable. The variable names are unquoted - any characters between the tab character and the end of line will be used, up to a limit of 33 characters.

The file is named *base.vars.txt*

A.1.4 Simulation variables

Simulation results or variables are output in either text or binary files, with one file for each variable for each timestep.

Text files are easier to process with other tools - but are typically larger and slower to process. Binary files tend to be smaller and faster to read, and should be portable to any machine using IEEE 754 floating point formats.

Binary format

Binary files are named *base.varI.tN.dat*, where I is the variable number and N is the timestep.

The file contains npoin double values, written with no header, padding or delimiters:

```
int fwcount = fwrite(dd, sizeof(double), results.npoin, datafile);
```

See the source of *telemac-parse.c* in tawe-telemac-utils or the convert_to_dat source for the precise code used.

Text format

Text files are named *base.varI.tN.txt*, where I is the variable number and N is the timestep.

There is no header for these files - each line consists of a node ID and value in fixed decimal form, separated by a tab character.

```
nid0    value0
nid1    value1
....    ......
```

A.1.5 Timestamps

Each simulation timestep has an associated timestamp, representing the seconds elapsed since a given reference point. This reference point is usually (but may not be) the first timestep.

File format:

```
nt
ts0   time0
ts1   time1
...   .....
tsN   timeN
```

`nt` is the number of timesteps included in the simulation. `ts0`...`tsN` are the integer timestep IDs, and correspond to the values used to label variable files. `time0`...`timeN` are the elapsed times, written in fixed decimal form.

The file is named *base.times.txt*

A.2 Input formats: Field Definitions

The fields used to define additional data can be created using any method that produces valid variable files, as described above in subsection A.1.4. The `fieldddata` uses a properties file and one or more source files to define a field. The field strength at each point is given by:

$$\phi = \sum_{\text{sources}}^{i=0} \frac{k.a_i}{\left(\sqrt{\Delta x_i{}^2 + \Delta y_i{}^2}\right)^b} \tag{A.1}$$

where k and i are input parameters, a_i is the value of the i^{th} source and $\Delta x_i, \Delta y_i$ represent the distance from the point to the source centre in x and y axes respectively. The sources defined here have a finite radius and any node lying within the radius of a source has it's contribution from that source set to the source value, independent of where within the radius it falls.

A.2.1 Field properties file

Field properties are specified in an INI format file, with section and parameter names as described in Table A.1

Although parameters for vertical distribution are recognised, at time of writing the software only supports flat (2D) distributions and vertical profiles are ignored. The `fieldddata` tool warns about this and will refuse to run if the `flat` parameter is not set true.

An example property file is given below:

```
[field]
name = Tidal Fish 2016-05-17
```

Name	Values	Meaning
Section: field		
name	string	Name to be used for field
basename	path	File path + prefix used to locate source files
flat	boolean	Define a flat (true) or vertically variable (false) field
constant	boolean	Is field constant (true) or time varying (false)
Section: radial or **vertical**		
multiplier	float	k value, see equation A.1
power	float	b value, see equation A.1

Table A.1: Field property file parameters

```
basename = /opt/Ramsey/RS_FISH/f2
flat = true
constant = 0
[radial]
multiplier = 1
power = 1
```

A.2.2 Field source files

In addition to a properties file specifying the general characteristics of the field to be generated, it is also necessary to specify the position, size and strength (value) of the sources creating the field. These sources are defined in flat text files - either a single file for a constant field or one file per mesh timestep for a time varying field. The files are named *base.txt* and *base.tN.txt* for a constant field or timestep `N` respectively.

Each source file has the following format:

```
ns          coordsys
x0,y0,z0    r0          v0
x1,y1,z1    r1          v1
........    ..          ..
xN,yN,zN    rN          vN
```

The header line sets the number of sources (`ns`) and the coordinate system in use (`coordsys`). Two coordinate systems are supported:

1. Universal Transverse Mercator (UTM)
2. Latitude, Longitude, Elevation

These are specified by number.

Each of the remaining `ns` lines contains the coordinates - either x, y, x or $lat, lon, elev$, followed by the radius (`rN`) and value (`vN`). Tabs are used to separate the radius, value and coordinates block with the individual coordinates being separated by commas as shown.

A.3 Input formats: Porpoise properties

Porpoise are defined using an INI format file, with sections and properties as described in Table A.2. In addition to the info and defaults sections, numbered sections can be used to override the properties of any individual porpoise. The ordering of sections in this file is important: there must be one `info` section, followed by an optional `defaults` section, followed optionally by numbered sections overriding properties for individual porpoise. If a property is not specified in a numbered section then it is set to the value given in the defaults section, or to the compiled in default values (usually zero).

Name	Values	Meaning
Section: info		
comment	string	Descriptive text displayed at run time
np	integer	Number of porpoise to include in the simulation
Section: defaults or **id**		
position	float[3]	Porpoise release coordinates
velocity	float[3]	Initial release velocity (ms^{-1})
orientation	float[3]	Initial orientation angles (α, β, γ)
drag	float[3]	Drag coefficients
area	float[3]	Reference areas

Table A.2: Porpoise definition file parameters [Identical to Table 4.2]

A.4 Input formats: Case files

Case files form the core configuration for the programs developed as part of this project, and provide settings for the main simulation as well as common core settings that should not be varied between program invocations. Case files are also defined as an INI format, with sections and properties as described below in Table A.3.

An example case file is shown below:

```
[paths]
basename = /opt/Ramsey/RS3D/RS_30d_mesh_v15_tpxo8_basecase.slf
output = /opt/Ramsey/RS3D_out/
particles = /opt/Ramsey/RSHP1.txt

[settings]
dimensions = 3
particle_steps = 60
threshold = 10

[indexes]
z = 5
u = 0
v = 1
w = 6
```

```
depth = 7
fish = 8
noise = 9
```

In this case, the gradients for variables 7,8 and 9 would then be searched for using the default prefix ('GRAD').

A.5 Output formats: Track files

Track files form the main output from the model, and can be recorded in two forms: Long or short. The files are written as tab separated text files, with an initial header containing the number of porpoise (`np`) and the maximum possible timestep (`nt`). The remainder of the file consists of porpoise state data, written in time and porpoise ID order such that all porpoise are read sequentially for one timestep before reading porpoise 0 of the following timestep.

The general file structure for both long and short format files is as follows:

```
np   nt
0    0    [state of porpoise 0 at timestep 0]
1    0    [state of porpoise 1 at timestep 0]
...  ...  ...
n    0    [state of porpoise n at timestep 0]
0    1    [state of porpoise n at timestep 1]
...  ...  ...
n    T    [state of porpoise n at timestep T]
```

The state section consists of tab separated values for each porpoise, with the properties and ordering detailed below.

It should be noted that it is not guaranteed that a file starts with timestep zero or finishes at the maximum timestep specified, but the maximum timestep will not be exceeded. A timestep is only considered complete and well formed if it contains state data for `np` porpoise specified.

Track files in either format are stored in *output/base.tracks.txt*.

A.5.1 Long format

The long format state section consists of the following properties, written as tab separated values. Vectors are written in component order, with each component separated by tabs:

- Position (vector)
- Velocity in local frame (vector)
- Velocity in global frame (vector)
- Orientation angles (yaw, pitch, roll)
- Force (vector)
- Local flow velocity (vector)

- Target (vector)
- Orientation random offset
- Velocity random offset
- Mass
- Last occupied element (-1 if out of domain)
- Current behaviour state
- Exit time (-1 if still in simulation)
- Exit status

A.5.2 Short format

The state section in short format files consists of the following tab separated values, with vectors written in component order and each component separated by tabs:

- Position (vector)
- Last occupied element (-1 if out of domain)
- Current behaviour state
- Exit time (-1 if still in simulation)
- Exit status

A.6 Output formats: Resume files

A resume file contains the full state for all porpoise at a given timestep, and is used to resume an interrupted simulation. The format is very similar to a long format track file (described above in subsection A.5.1). The header specifies the total number of porpoise (`np`) and the simulation timestep number (`t`). The long format state of each porpoise then follows.

File format:

```
np   t
0    t    [long state of porpoise 0 at timestep t]
1    t    [long state of porpoise 1 at timestep t]
...  ...  ...
n    t    [long state of porpoise n at timestep t]
```

The resume file is stored in *output/base.resume*

A.7 Output formats: VTK formats

In order to facilitate the visualisation of results from the model, the VTK file format was selected as a suitable output format. The format (in it's different variants described below) is a well defined and open format, described in [130], that is compatible with Paraview [114].

VTK specifies two different families of file formats - an older, flat text format and a newer XML based standard. The latter has been used here, and is further divided into different types based on the data contained and whether the data has been prepared for parallelisation or not. All the descriptions that follow are for single XML format files, not the parallel versions. The reference text ([130]) should be referred to for details, with this document providing supplemental information.

A.7.1 VTU Files - unstructured mesh data

The first of these formats is used for unstructured mesh data, and is used to visualise the computational domain and its physical and environmental properties. These files are produced using the `vtkexport` utility, with one file produced for each selected timestep. These files are named *base.ti.vtu*, where `i` represents the simulation timestep τ_i for the file.

The general structure of each file is as follows:

```
<?xml version="1.0" encoding="UTF-8"?>
<VTKFile type="UnstructuredGrid">
 <UnstructuredGrid>
  <Piece NumberOfPoints="npoin" NumberOfCells="nelem">
   <Points>
    <DataArray Name="Coordinates" type="Float64" format="binary"
     NumberOfComponents="3">[Base64 Encoded Data]</DataArray>
   </Points>
   <Cells>
    <DataArray Name="connectivity" type="Int32" format="binary">
     [Base64 Encoded Data]
    </DataArray>
    <DataArray Name="types" type="Int32" format="binary">
      [Base64 Encoded Data]</DataArray>
    <DataArray Name="offsets" type="Int32" format="binary">
      [Base64 Encoded Data]</DataArray>
   </Cells>
   <PointData>
    <DataArray Name="Z" type="Float64" format="binary">
      [Base64 Encoded Data]</DataArray>
    <DataArray Name="Velocity" type="Float64" format="binary"
     NumberOfComponents="3">
     [Base64 Encoded Data]
    </DataArray>
   </PointData>
  </Piece>
 </UnstructuredGrid>
</VTKFile>
```

The data is provided as a single <Piece>, with the number of points (npoin) and number of cells (elements, npoin) specified for the full mesh. VTK defines shapes based on nodes and connectivities, with the node coordinates provided as a sequence. In ASCII format, the points are specified as whitespace separated triplets $(x_0\, y_0\, z_0\, x_1\, y_1\, z_1 \ldots x_n\, y_n\, z_n)$. In binary form, the data is provided as Base64 encoded doubles in the same order (see below for details about Base64 encoded data. Coordinates must always be specified in three dimensions, even for two dimensional data. The z component can be fixed to zero in these cases.

Connectivities are specified as per subsection A.1.2 as space separated integers in ASCII format or as a sequence of Base64 encoded integers. The offsets field specifies which connectivities correspond to each element by specifying the position of the first ID of the next element, e.g. for an element with 6 points, element 0 has offset 6, element 1 has offset 12, element 2 has offset 18 etc. The offset values are provided as space separated integers of as a Base64 encoded sequence as above.

Variables are provided as <DataArray> elements in the <PointData> section. Cell centred values would be specified similarly in a <CellData> section, but are not used in this instance. Each variable is provided as floating point values in ASCII or Base64 encoded form. Vector quantities can be provided by setting the NumberOfComponents property appropriately and specifying values in the same manner as the point coordinates.

Base64 Encoded data and compression

Base64 encoding allows arbitrary data to be transferred in a compact and portable manner. Each block of data (marked [Base64 Encoded Data] above) consists of a Base64 encoded integer specifying the length of the data to be read, followed by the data itself. The data can be integers or floating point values, and is specified in the type attribute of the <DataArray> element. Within this project, data has either been 32 bit integers ("Int32") or double precision floating point values ("Float64")

To produce correctly encoded data for a <DataArray> element, perform the following steps:

- Take input data ϕ
- Base64 encode ϕ into a new string φ
- Calculate number of characters of φ and store as an unsigned 32 bit integer λ
- Base64 encode λ into a new string Λ.
- Concatenate Λ and φ and output

In this project, the Base64 encoding itself was performed using a 3rd party library available from http://libb64.sourceforge.net/ and made available by its authors as a Public Domain work.

A.7.2 VTP Files - point data

The VTK PolyData (VTP) format has been used to provide particle position data without linking the points into any other structures. Due to the usually smaller nature of these files, the `vtkparticles` tool provided outputs all data in unencoded ASCII format rather than using the Base64 encoding described above. A minimal example file for 2 points is shown below:

```
<?xml version="1.0" encoding="UTF-8"?>
<VTKFile type="PolyData">
 <PolyData>
  <Piece NumberOfPoints="2">
   <Points>
    <DataArray Name="Coordinates" type="Float32"
      format="ascii" NumberOfComponents="3">
     +196766.4925 +146232.1125 +6.7544
     +196769.1619 +146232.8293 +6.1225
    </DataArray>
   </Points>
   <Verts>
   <DataArray Name="connectivity" type="Int32" format="ascii">0 1</DataArray>
    <DataArray Name="offsets" type="Int32" format="ascii">1 2</DataArray>
   </Verts>
   <PointData>
    <DataArray Name="Vector Velocity" type="Float32"
      format="ascii" NumberOfComponents="3">
     +0.0000 +0.0000 +0.0000
     +0.0000 +0.0000 +0.0000
    </DataArray>
    <DataArray Name="Last Element" type="Int32"
      format="ascii" NumberOfComponents="1">
     +41137
     +41137
    </DataArray>
   </PointData>
  </Piece>
 </PolyData>
</VTKFile>
```

Connectivities and offsets are specified as for data in the VTU files. Note that as each point is isolated, it is only connected to itself and the offset for point n is simply $n + 1$.

A.7.3 VTS Files - structured grid data

Structured grid files are simpler files that allow point or cell data to be specified at locations on a regularly spaced grid laid over a particular area. In this model, they are used to provide output from the `gridstats` tool, which normalises porpoise position data onto a regular grid.

The size of the grid is specified giving the number of cells in each direction Assuming a two dimensional grid starting from $0, 0$, this `WholeExtent` would be written as $0nx0ny00$. It can also be viewed as the ID of the first and last point in each direction (this is consistent, as 4 points are required to define 3 cells). For the outputs here, each

grid is presented as a single <Piece>, which should have an Extent property matching the WholeExtent of the <StructuredGrid> element.

Points are defined by their coordinates, specified as space separated coordinates as described above. Point should be ordered in rows (x) then columns (y) as shown in the example below. This ordering defines the cells. Data can then be specified in the <CellData> section in this order.

A 3x3 example grid with values in the middle and top rows when viewed with the origin towards the lower left of the grid. Note that the entire grid is offset from the origin:

```
<?xml version="1.0" encoding="UTF-8"?>
<VTKFile type="StructuredGrid">
<StructuredGrid WholeExtent="0 3 0 3 0 0">
<Piece Extent="0 3 0 3 0 0">
 <CellData>
  <DataArray Name="Count" type="Int32" format="ascii">
   0 0 0
   1736 8608 533
   3526 4713 15
  </DataArray>
 </CellData>
 <Points>
  <DataArray Name="coordinates" type="Float32"
    NumberOfComponents="3" format="ascii">
   184123.0 136035.0 0 185123.0 136035.0 0 186123.0 136035.0 0 187123.0 136035.0 0
   184123.0 137035.0 0 185123.0 137035.0 0 186123.0 137035.0 0 187123.0 137035.0 0
   184123.0 138035.0 0 185123.0 138035.0 0 186123.0 138035.0 0 187123.0 138035.0 0
   184123.0 139035.0 0 185123.0 139035.0 0 186123.0 139035.0 0 187123.0 139035.0 0
  </DataArray>
 </Points>
</Piece>
</StructuredGrid>
</VTKFile>
```

Note that no connectivities or offsets are required as the cells are implied by the WholeExtent and the points themselves.

The file names used for the VTS files generated by gridsstats take the form *base.grid.sS.vts* for data covering the entire simulation duration and *base.grid.sS.tI-J.vts* for data covering the period between simulation timesteps τ_I and τ_J (inclusive). The S value in both formats gives the cell edge length in metres. For example, *base.grid.s100.t0-1199.vts* represents data covering simulation timesteps between 0 and 1199, calculated over a grid of 100m$\times$100m cells.

A.7.4 PVD Files - Paraview data

PVD files are a little different to the previous three formats in that they don't describe any simulation input or output data directly. PVD files are specific to Paraview, and are used to group data series together. The vtkexport, vtkparticles, and gridstats tools all produce PVD files. Each file in a series is listed in a <DataSet/> element as shown below, along with a timestep value for each file. The timestep value here is set to the clock time (see Chapter 3) at the start of the interval represented by the file.

```
<?xml version="1.0" encoding="UTF-8"?>
<VTKFile type="Collection">
 <Collection>
  <DataSet timestep="0.00" part="0" file="base.t0.vtu"/>
  <DataSet timestep="9000.00" part="0" file="base.t5.vtu"/>
 </Collection>
</VTKFile>
```

Each PVD file can contain an arbitrary number of files. The following naming conventions are used for PVD files:

- `vtkexport`
  - *base-mesh.pvd*:
    Time series of exported mesh data, representing the full simulation duration
  - *base-mesh-N.pvd*:
    File *N* of a sequence of PVD files as above, each representing part of the simulation duration.
- `vtkparticles`
  - *base-tracks.pvd*:
    Time series of porpoise positions, covering the full simulation duration
  - *base-tracks-N.pvd*:
    File *N* of a sequence of PVD files as above, each representing part of the simulation duration.
- `gridstats`
  - *base.grid.sS.pvd*:
    Time series of gridded data, with cell size `S`, covering the full simulation duration
  - *base.grid.sS.tI-J.pvd*:
    Partial time series of gridded data, covering the period τ_I to τ_J using cell size `S`

Name	Values	Meaning
Section: paths		
basename	path	File path + prefix used to locate input data
output	path	Output folder
particles	path	File containing particle (porpoise) definitions - see section A.3
Section: settings		
dimensions	2 or 3	Select 2D or 3D simulation
longoutput	boolean	Output full track information (larger, slower output)
prefix	string	Prefix applied to/searched for gradient information
particle_steps	integer	Split each mesh timestep into this many simulation timesteps
food_weight	float	Weighting applied to food seeking vs drag reduction behaviour
foodrule	0 or 1	Weight food behaviour by gradient (0) or field value (1)
noise_threshold	float	Maximum tolerated additional noise.
threshold	float	Minimum tolerated water depth
Section: indexes		
u	variable index	Variable number to use for velocity components (u, v, w), vertical coordinates (z), depth, food availability (fish) and additional noise.
v		
w		
z		
depth		
fish		
noise		
Section: speeds		
default	float	Mean swimming speed for default, depth avoidance and noise avoidance cases
depth		
noise		
defaultrange	float	Standard deviation of speed for default, depth avoidance and noise avoidance cases
depthrange		
noiserange		

Table A.3: Case file parameters

Appendix B

Computer Specification

B.1 Performance comparisons

Although the simulation results used in this thesis were produced across a range of machines, all performance comparisons listed in the document (principally in Chapter 4) were carried out on a single desktop machine. The hardware specification of this machine is listed below for reference purposes.

B.1.1 Operating System and Compilers

Although the same underlying hardware was used throughout the project, the operating system and compilers used varied. Initial development and testing was carried out using a 64 bit installation of Cygwin running under Windows 7. The GNU Compiler Collection (GCC) was used, with the last versions of the code tested under Windows using version 4.9 of GCC. This configuration was used to generate the Windows result in Table 4.3.

The bulk of the simulations and development were performed on the same hardware running the Fedora GNU/Linux distribution. The exact versions varied over the course of the project, with the final performance figures in Chapter 4 generated under Fedora 25, Kernel `4.9.12-200.fc25.x86_64`, with GCC `6.3.1 20161221 (Red Hat 6.3.1-1)`.

The following information was adapted from the output of the `lshw` command:

- Dell XPS 8500
- 256KiB L1-Cache
- 1MiB L2 cache
- 8GiB DDR3 Synchronous RAM, 1600 MHz clock speed
- Intel(R) Core(TM) i7-3770 CPU. 4 physical cores, 3.40GHz clock speed. Hyperthreading enabled.
- AMD Radeon HD 7770/8760 / R7 250X graphics card
- Storage:
  - System Disk: Seagate ST2000DM001-9YN1 (2TB)
    Windows install, Linux `/home`, `/var` and swap space
  - System Disk: Samsung SSD PM83 (32GB)
    Linux `/` and `/boot`
  - Storage: Western Digital WDC WD3003FZEX-0 (3TB)
  - Storage: Western Digital WDC WD40EZRX-00S (4TB)